DETAILED CHEMICAL AND SPECTROSCOPIC PROBES OF THE MULTICOPPER ACTIVE SITES IN RHUS LACCASE

by

DARLENE JOY SPIRA

B.S. STANFORD UNIVERSITY

1980

SUBMITTED IN PARTIAL FULFILLMENT OF THE REQUIREMENTS FOR THE DEGREE OF DOCTOR OF PHILOSOPHY

at the

MASSACHUSETTS INSTITUTE OF TECHNOLOGY

August, 1984

Signature of Author Signature redacted

Department of Chemistry, August, 1984

Certified by Signature redacted

Edward I. Solomon, Thesis Co-Supervisor

Certified by Signature redacted

William Orme-Johnson, Thesis Co-Supervisor

Accepted by Signature redacted

Dietmar Seyferth, Chairman, Department Committee

This doctoral thesis has been examined by a Committee of the Department of Chemistry as follows:

Professor Alan Davison — Signature redacted

Chairman

Professor Edward I. Solomon — Signature redacted

Thesis Co-Supervisor

Professor William H. Orme-Johnson — Signature redacted

Thesis Co-Supervisor

Professor Mark S. Wrighton — Signature redacted

DETAILED CHEMICAL AND SPECTROSCOPIC PROBES OF THE MULTICOPPER ACTIVE SITES IN *RHUS* LACCASE

by

DARLENE JOY SPIRA

Submitted to the Department of Chemistry
on August 20, 1984, in partial fulfillment of the
requirements for the degree of Doctor of Philosophy in
Chemistry

ABSTRACT

Chapter I.

Through study of copper sites in different metalloenzymes with comparison to relevant copper model complexes, correlations between active site electronic structure and biological function can be developed. The multicopper oxidase laccase is the subject of this thesis research; hence, an overview of the spectral properties and reactivity of copper in biological systems is presented. The Blue, Normal and Coupled Binuclear Copper Proteins and the Multicopper Oxidases are each discussed, with emphasis on how the oxidase T1, T2 and in particular, T3 sites relate to their analogues in the relatively simple copper proteins.

Chapter II.

Through normalized x-ray absorption edge difference spectra, a procedure is developed for the quantitative determination of Cu(I) content in protein samples of mixed Cu(I) and Cu(II) composition. Type 2 Depleted (T2D) laccase contains 70 $\pm$ 15% Cu(I), and while ferricyanide does not alter this [Cu(I)], aqueous peroxide and nitrite oxidize the cuprous T3 site and generate met T2D forms. A visible-UV - x-ray absorption peroxide titration of T2D laccase indicates that peroxide oxidizes but does not bind to the T3 site in T2D laccase. This correlation is used to determine that native laccase, as isolated, contains ~25% reduced T3 sites and that all spectral changes observed upon peroxide addition can be accounted for by oxidation of these reduced sites. The importance of these results to previous reports of peroxide binding at the laccase active site is discussed.

Chapter III.

A detailed examination of the chemistry and spectroscopy of deoxy {T1:[Cu(II)]; T3:[Cu(I)Cu(I)]}, half met {T1:[Cu(II)]; T3[Cu(I)Cu(II)]}, and met {T1:Cu(II); T3:[Cu(II)Cu(II)]} T2D laccase is presented, and these results are compared to related studies of the coupled binuclear copper site in the

hemocyanins and tyrosinase. From these studies, strong similarities - as well as important differences - are observed which provide insight into correlations of binuclear copper active site structure with biological reactivity. Whereas deoxy T2D is stable to oxygen, deoxy hemocyanin readily oxidizes to oxyhemocyanin. Chemical and spectral studies of deoxy T2D show that this is not due to an inaccessibility of the binuclear cuprous site to neutral small molecules. In contrast to met hemocyanin, met T2D undergoes facile one-electron reduction to yield half met T2D laccase and chemical and spectral studies of this derivative have demonstrated an inability of exogenous ligands to bridge the binuclear copper site in laccase. EXAFS studies have excluded S ligation at the laccase T3 site, and in general, studies of the met derivatives indicate that the coupled binuclear copper site is very similar in hemocyanin and met T2D laccase. Finally, in studies of met-N_3^- T2D at low pH, N_3^- and H^+ are found to competitively displace and protonate the endogenous protein at the T3 site in laccase, turning off the superexchange pathway and generating EPR detectable dipolar interacting Cu(II)'s. From these studies, a spectroscopically effective model for the binuclear copper site in T2D laccase is presented and contrasted to that in hemocyanin and tyrosinase.

Chapter IV.

Structural changes induced in the T1 Cu(II) by the T3 copper site in T2D and native laccase are studied through a combination of EPR and resonance Raman techniques. A spectral comparison between deoxy and met T2D and native laccase shows that there are changes in the T1 site associated with the reduction of the T3 site in deoxy T2D; these results are extended to peroxide reactions of the reduced copper present in native laccase. Effects of exogenous anion coordination to the T3 site on the spectral features of the Blue site are also presented and these are found to be different from those induced by oxidation. These T3-T1 intersite interactions appear to correlate to intramolecular electron transfer in this multicopper enzyme.

Chapter V.

Variable temperature magnetic circular dichroism demonstrates that low affinity N_3^- is bridging the paramagnetic T2 and diamagnetic T3 copper sites in native laccase. This assignment is confirmed by a perturbation of the MCD spectrum which uncouples the antiferromagnetically coupled T3 coppers and renders the T3-N_3^- spectral features paramagnetic. The utility of this "three copper active site" in laccase for the multi-electron reduction of dioxygen to water is discussed.

Edward I. Solomon, William H. Orme-Johnson, Professors of Chemistry, Thesis Co-Supervisors.

To my parents, grandmother, and the memory of my uncle.

TABLE OF CONTENTS

LIST OF FIGURES

LIST OF TABLES

LIST OF SCHEMES

PAGE

ABBREVIATIONS

EPR	electron paramagnetic resonance
CD	circular dichroism
MCD	magnetic circular dichroism
XAS	x-ray absorption spectroscopy
EXAFS	extended x-ray absorption fine structure
AA	atomic absorption
rR	resonance Raman
OR^-	endogenous protein ligand at the active site
L,X	ligand
K, K_{eq}	equilibrium binding constant
BCP	Blue copper protein
EDTA	ethylene diamine tetraacetic acid
DMG	dimethylglyoxime
PPB	potassium phosphate buffer
T1,T2,T3	Type 1, Type 2, Type 3
T2D	Type 2 Depleted

I. THE INORGANIC CHEMISTRY OF COPPER AND ITS OXYGEN REACTIVITY IN BIOLOGICAL SYSTEMS

A. Introduction

A number of important proteins[1] contain copper ions at their active sites. These copper active sites are associated with a variety of biological functions including electron transfer, superoxide dismutation, and the transport, activation, and reduction of molecular oxygen (see Table 1.1). In each of these metalloenzyme systems, the protein ligand imposes a unique geometry and electronic structure at the copper site which determines the detailed structure of the active site and enables biological function of the protein. Consequently, the spectral features and chemical reactivity of copper in biological systems are often very different from what one normally observes in aqueous small molecule copper complexes. Hence, by studying the copper sites in different metalloenzymes with comparison to relevant copper model complexes, one can begin to see correlations between active site electronic structure and biological function; that is, the relative contributions of specific geometric and electronic structural features to active site reactivity.

The simplest of the multicopper oxidases, laccase[2], will be the subject of this dissertation. In particular, studies will focus on the coupled binuclear copper site in Rhus vernicifera laccase and its unique features which are responsible for the irreversible binding and four-electron

Table 1.1 Copper in Biological Systems

Normal Copper Proteins	Source	Total Cu	Total Subunits	Reactivity
Cu-Zn superoxide dismutase	Bovine erythrocytes	2	2	$2O_2^- + 2H^+ \rightarrow O_2 + H_2O_2$
Galactose oxidase	Dactylium dendroides	1	1	$RCH_2OH + O_2 \rightarrow RCHO + H_2O_2$
Diamine oxidase	Bovine plasma, pig kidneys Pea seedlings	2	2	$R'CH_2NHR + O_2 + H_2O \rightarrow R'CHO + HNR_2 + H_2O_2$
Dopamine β-monooxygenase	Bovine adrenal glands	4	4	Dopamine + ascorbate + O_2 ---> noradrenaline + dehydroascorbate + H_2O
Blue Copper Proteins				
Azurin	Pseudomonas denitrificans	1	1	
Plastocyanin	Spinach and French bean chloroplasts	1	1	electron transfer
Stellacyanin	Rhus vernifera latex	1	1	
Coupled Binuclear Copper Proteins				
Mollusc hemocyanin	Snail, octopus serum	2 copper/1 active site		
Arthropod hemocyanin	Lobster, crab serum	"bipolymer" of active sites		reversible O_2 transport
Tyrosinase	Neurospora crassa	2	1	
Multicopper Oxidases				
Tree laccase	Rhus vernicifera (Asian lacquer trees)		4	
Fungal laccase	Polyporus versicolor (white rot)		4	$O_2 + 4H^+ + 4e^- \rightarrow 2\ H_2O$
Ceruloplasmin	Human blood plasma		5-7	
Ascorbic acid oxidase	Green zucchini squash		6-8	

reduction of oxygen to water at this copper site compared to the reversible binding of oxygen in the relatively simple and well-understood coupled binuclear copper[3] containing proteins, the hemocyanins and tyrosinase. This understanding of the electronic and geometric structure of the laccase active site will be obtained through the development of

(1) systematic chemical variations of the copper active site, and

(2) appropriate spectroscopic techniques for their detailed study.

Ultimately, these studies will generate a "spectroscopically effective model" for the laccase active site and its oxygen reactivity. However, before this understanding can be developed and assimilated into correlations of binuclear copper active site structure and oxygen reactivity in related copper proteins, it is important to briefly summarize the biological reactivity, electron paramagnetic resonance (EPR) and electronic absorption features associated with copper active site structure in the simpler protein systems. Before addressing the unique spectral features of copper in proteins, however, it is necessary to consider the spectral features normally associated with the geometric and electronic structure of copper in aqueous inorganic complexes.

B. Inorganic Chemistry of Copper

In aqueous solutions, copper is normally found in two oxidation states, copper(I) and copper(II). Copper(I) is commonly coordinated by four ligands in a tetrahedral geometry with the d-energy orbital splitting shown in Figure 1.1. As Cu(I) is in a $^1A_1$ ground state and diamagnetic, it cannot be probed by EPR spectroscopy. Because of its d^{10} closed shell electron configuration, Cu(I) complexes also exhibit no ligand field nor ligand to metal charge transfer transitions; thus, Cu(I) is said to be inaccessible to study by conventional spectroscopic techniques.

Alternatively, and fortunately for spectroscopists interested in copper and copper containing proteins, Cu(II) contains nine d- electrons in a range of coordination geometries. In an octahedral environment, the cupric ion would possess the degenerate ^2E_g electronic ground state diagrammed in Figure 1.2A. However, in accordance with the Jahn-Teller theorem, a geometric distortion removes this degeneracy to produce a more stable electronic structure. Consequently, Cu(II) is most commonly found in a tetragonal ligand environment with four strongly bound equatorial ligands and one or two weakly bound axial ligands. As is apparent from the d-orbital splitting shown in Figure 1.2B, the tetragonal distortion of the Cu(II) complex results in the non-degenerate $^2B_{1g}$ ground state in which the dx^2-y^2 orbital is highest in energy and half-occupied.

Figure 1.1 Qualitative coordination geometry and d orbital splitting for Cu(I) in a tetrahedral ligand environment.

(Symmetry properties of the d orbitals are indicated in parentheses)

Figure 1.2 Qualitative coordination geometry and d orbital splitting for Cu(II) in (A) octahedral and (B) tetragonal ligand environments.

(Symmetry properties of the d orbitals are indicated in parentheses)

CU (I)

d^{10}

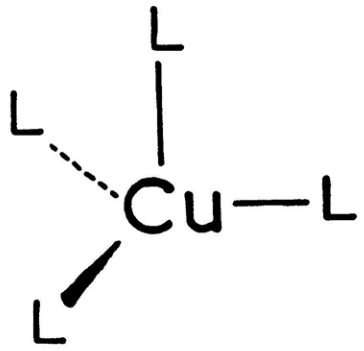

TETRAHEDRAL

↑↓ ↑↓ ↑↓ d_{xy}, d_{xz}, d_{yz} (t_2)

↑↓ ↑↓ $d_{x^2-y^2}, d_{z^2}$ (e)

CU(II)

d^9

OCTAHEDRAL TETRAGONAL

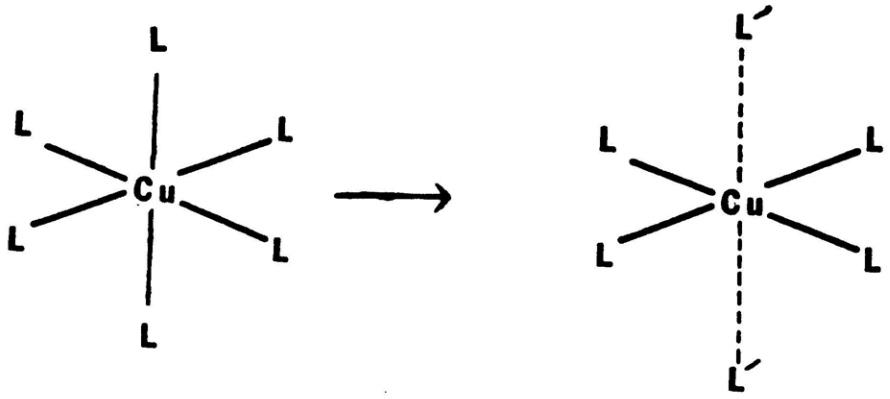

(e_g) $d_{x^2-y^2}$, d_{z^2}

(t_{2g}) d_{xz}, d_{yz} d_{xy}

A.

$d_{x^2-y^2}$ (b_{1g})

d_{z^2} (a_{1g})

d_{xy} (b_{2g})

d_{xz}, d_{yz} (e_g)

B.

It should be noted that Cu(II) may also exist in square pyramidal and trigonal bipyramidal ligand geometries, but for simplicity, only the spectroscopic properties of square planar Cu(II) will be considered. Reciprocally, from EPR and optical analyses, the electronic ground state geometry of the Cu(II) complex can often be determined.

The unpaired electron in the dx^2-y^2 orbital allows the Cu(II) complex to be studied by EPR spectroscopy. Application of a magnetic field (Figure 1.3) to a tetragonal Cu(II) complex induces a Zeeman splitting = $\pm$ 1/2gβH of the energy of the dx^2-y^2 electron, depending upon its spin orientation with respect to the magnetic field. When the applied microwave energy $h\nu$ = 1/2gβH-(-1/2gβH)) = gβH, an EPR transition will occur. As shown in Figure 1.4, the g value is anisotropic and two EPR transitions are observed (plotted as the first derivative) according to whether the magnetic field is oriented along the axial ligand direction ($g_{||}$) or in the equatorial plane ($g_{\perp}$). From ligand field theory and allowing for spin orbit coupling, $g_{||} > g_{\perp} > 2$ for tetragonal Cu(II) complexes. In a frozen solution, g values for all possible orientations of the complex will be observed. In addition, the copper nucleus has a nuclear spin I = 3/2 which couples to the unpaired electron and produces a hyperfine splitting of the transition into 2I + 1 = 4 components. This splitting is usually apparent in the parallel region ($A_{||}$)

Figure 1.3 Magnetic field induced Zeeman splitting of the tetragonal Cu(II) ground state for EPR spectroscopic probe.

Figure 1.4 EPR spectroscopy: g value anisotropy and hyperfine interaction.

(A) The magnetic field is applied parallel ($H_{||}$) or perpendicular ($H_{\perp}$) to the L'-Cu-L' axis of the tetragonal Cu(II) complex with EPR transitions characterized by $g_{||}$ and $g_{\perp}$;

(B) Hyperfine interaction of the electron with the copper nucleus as characterized by $A_{||}$.

ELECTRON PARAMAGNETIC RESONANCE

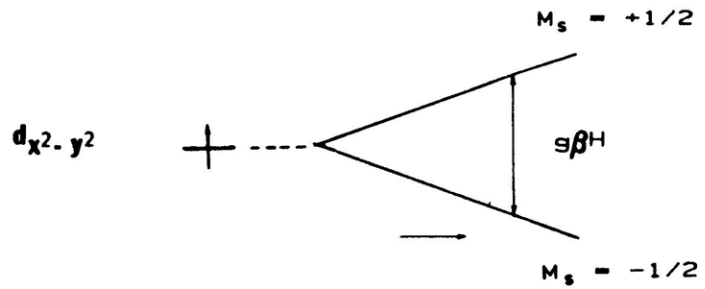

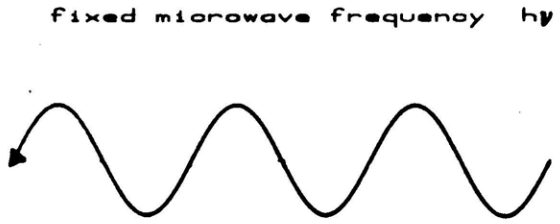

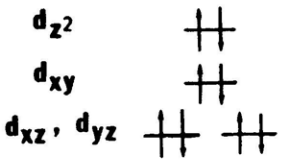

H = 0 H⟶

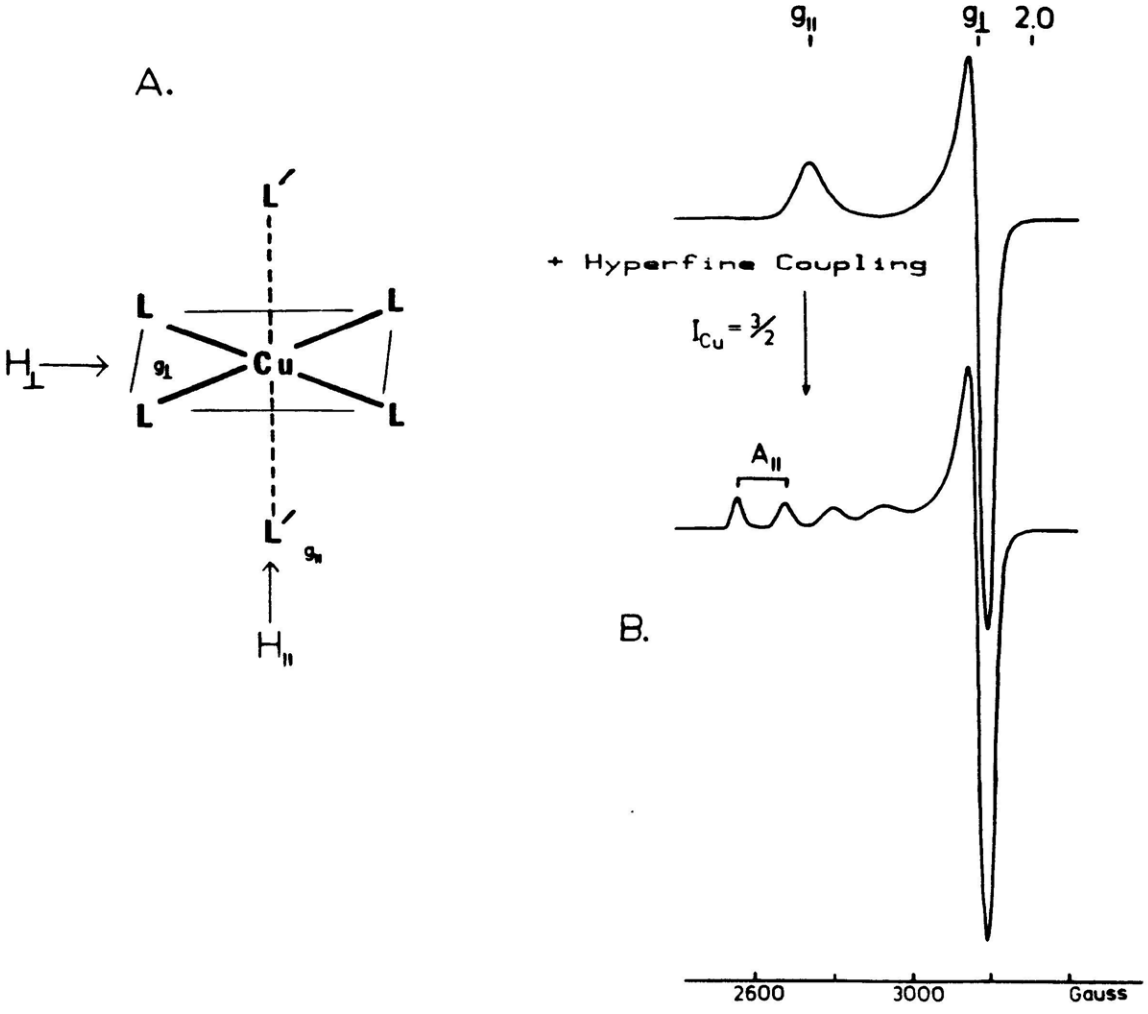
A.
L'
L
L
L
L
Cu
$g_\perp$
L'
$g_\parallel$
$H_\perp$
$H_\parallel$
$g_\parallel$
$g_\perp$ 2.0
+ Hyperfine Coupling
$I_{Cu} = 3/2$
$A_\parallel$
B.
2600
3000
Gauss

but is often smaller and unresolved in the perpendicular region ($A_{\perp}$). For tetragonal Cu(II) complexes, 140×10^{-4} $cm^{-1} \leq A_{||} \leq 200 \times 10^{-4}$ cm^{-1}.

The electron hole in the dx^2-y^2 orbital also generates low energy electronic excited states which can be studied through optical spectroscopy. With energy in the red spectral region (1000 - 600 nm), one can excite electrons from lower lying metal-centered d orbitals to the half-empty dx^2-y^2 orbital (Figure 1.5). In a tetragonal ligand field, these d-d transitions are LaPorte forbidden but gain some intensity (ε's up to $\approx$200 $M^{-1}cm^{-1}$) through vibronic coupling and ground state distortions which remove the centrosymmetry. Higher energy radiation into the UV ($\approx$350 - 200 nm) may also excite electrons from filled ligand-centered orbitals to the dx^2-y^2 orbital, generating Ligand to Cu(II) charge transfer (L ---> Cu(II) CT) transitions (Figure 1.5). These transitions are electronic dipole allowed and therefore exhibit much greater intensities (ε's $\approx$1,000 - 10,000 $M^{-1}cm^{-1}$) than do the lower energy d-d transitions. Thus, whereas Cu(I) is spectroscopically inaccessible, the ground state magnetism and low energy electronic excited states of Cu(II) give its inorganic complexes characteristic EPR and optical spectral features. With this background, the spectral features associated with copper coordination in biological systems can now be investigated.

Figure 1.5 Ligand field and Ligand to Cu(II) charge transfer transitions for Cu(II) in a tetragonal environment.

ABSORPTION SPECTROSCOPY

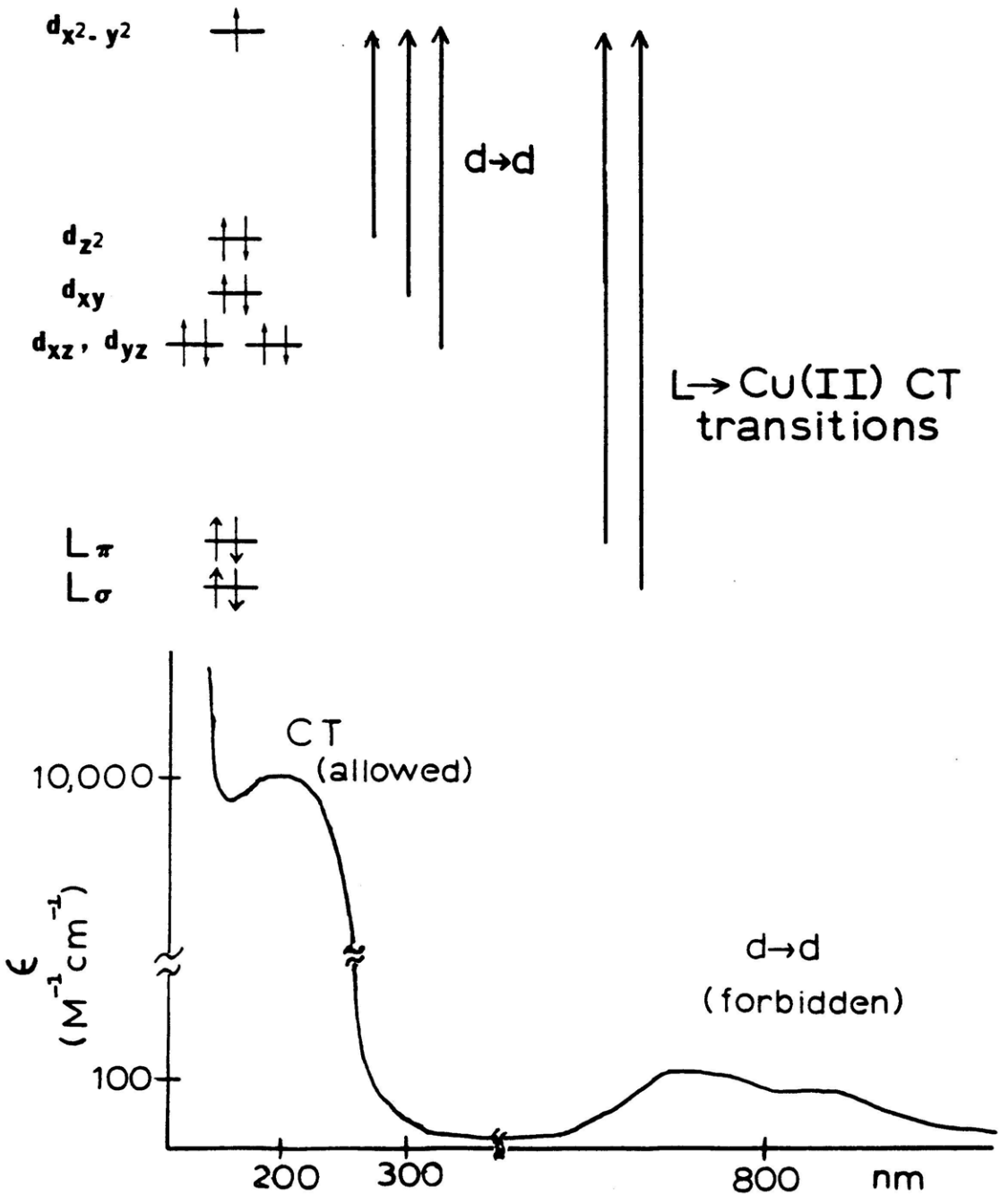

C. Copper Containing Proteins and Their Oxygen Reactivity

1. Normal Copper Proteins

Several copper proteins exhibit spectral features similar to those of inorganic complexes; these are summarized in Table 1.2. The Cu(II) EPR parameters are quite similar in these metalloenzymes and suggest pseudo-square planar geometries. To date, only simple nitrogen, oxygen (N,O) ligations have been indicated, and in addition, each of the normal proteins appears to possess at least one exchangeable position for coordination by exogenous ligands. However, these enzymes differ significantly from one another with respect to quaternary structure, prosthetic groups and reactivity, and it is therefore more appropriate to consider them as individual classes of copper sites.

Only Cu-Zn Superoxide Dismutase (SOD)[4] has been defined by x-ray crystallography.[5] As indicated by the EPR parameters, the Cu(II) coordination is tetragonal and consists of three imidazoles and an imidazolate, which bridges to a tetrahedral Zn(II). Similar to Cu(II) model complexes, the ligand field transitions are observed at ≈680 nm.[6] The large molar extinction coefficient, however,

Table 1.2 Spectroscopic Properties: Normal Copper Proteins

Protein:	Cu_2Zn_2SOD	GALACTOSE OXIDASE	DIAMINE OXIDASE	DOPAMINE β-MONOOXYGENASE
Prosthetic Groups:	2 Cu, 2 Zn	Cu	2 Cu + organic cofactor	4 Cu
EPR: $g_{\|\|}$	2.26	2.28	2.28	2.26
$g_{\perp}$	2.09, 2.03	2.05	2.06	2.08, 2.05
$A_{\|\|}$ ($10^{-4}cm^{-1}$)	142	186	172	180
Absorption: $\lambda max(nm)/\varepsilon(M^{-1}cm^{-1})$	650/~300 330/≤1000 430/≤400	775/900 630/1000 445/1150 314/1370	600/~100 500/~500 400/~600	--- --- ---
Cu Coordination Geometry:	tetragonal	tetragonal	tetragonal	tetragonal
Ligation (partial):[a]	N_4O	N_2O_2X	N_3O_2X	N
Exogenous Anions:	N_3^-, CN^-, SCN^-, Cl^-	N_3^-, CN^-, F^-, SCN^-	N_3^-, CN^-, SCN^-	---

[a] Spectroscopically defined for all but SOD

indicates that the site is of lower symmetry. At higher energy are the L ---> Cu(II) CT transitions.[6] The band at 330 nm has been assigned as a Histidine (his) ---> Cu(II) CT transition, while the shoulder at 430 nm is probably associated with the bridging imidazolate.

Galactose oxidase[7] is the only normal copper protein known to contain no other prosthetic group. Interestingly, it catalyzes a two-electron redox process using a single copper site; one proposed turnover mechanism is therefore based on a Cu^{3+}/Cu^{+} redox cycle.[8] The optical spectrum[9] of galactose oxidase is quite rich compared to that of the other normal proteins, and as no other prosthetic groups are present, these transitions have all been associated with the Cu(II) ion. At ≈600 - 800 nm, and again surprisingly intense, are the d-d transitions, while those to higher energy have been suggested as endogenous imidazole (his) or phenolate (tyrosine) ---> Cu(II) CT transitions.[10] From spectroscopic studies,[9,11] the Cu is thought to be equatorially coordinated by two equivalent histidine imidazoles, one exchangeable water (or OH^{-}) and a fourth undefined ligand which is likely to be a tyrosine phenolate (or carboxylate);[12] an axial H_2O has also been indicated.

Copper containing amine oxidases[13] are widely distributed in nature and have been purified from microorganisms, plants, and mammals. These amine oxidases

have many common features, but exhibit minor spectral and structural differences as well as variation in substrate specificities. Each enzyme appears to be composed of two similar subunits (each contains one copper) held together by disulfide bonds.[14] The stoichiometry and identity of the organic prosthetic group are not well determined, but a pyridoxal phosphate[15] or a modified flavin[16] appears likely. The EPR[17] and absorption[18] data again indicate tetragonal coordination; the d-d bands likely contribute to the 600 nm absorption and endogenous (N,O) ---> Cu(II) CT to that at 400 nm; the organic cofactor is believed to absorb at 500 nm. Evidence has been presented for one axial and one equatorial water, and inorganic anions do compete for one exchangeable equatorial position on the Cu(II).[19] Imidazole N's (and perhaps the organic cofactor) are postulated to complete the coordination of the site.

Dopamine β-monooxygenase[20] contains four copper ions in four subunits and is the least defined of the normal copper proteins to be addressed. The EPR spectrum is tetragonal, although its optical spectrum and exogenous anion reactivity have not been characterized. Experiments with various chelating agents would suggest that the copper has at least one and possibly two exchangeable ligands, one of which may be H_2O.[21] Superhyperfine structure in the EPR spectrum indicates that nitrogen may also be coordinated at the site.

2. Blue Copper Proteins

Stellacyanin, the plastocyanins, and the azurins are the most widely studied of the Blue copper proteins (BCP's).[2a,22] These proteins are all involved in redox chemistry, and with the exception of stellacyanin, exhibit unusually high redox potentials. Moreover, each of the BCP's displays spectral features which are clearly different from those of normal copper complexes (Table 1.3 and Figure 1.6). While $g_{||} > g_{\perp} > 2$ as in the normal copper proteins, the Blue copper sites exhibit a significantly smaller $A_{||} < 70 \times 10^{-4}$ cm^{-1}. In the perpendicular region, a strong rhombic splitting ($g_x \neq g_y$) is observed in stellacyanin, whereas the plastocyanins and azurins are almost axial. The most striking feature about these proteins, however, is their deep blue color; intense absorption features at ≈600 nm (ε's ≈5000 $M^{-1}cm^{-1}$) characterize each of the BCP's, where normal copper complexes exhibit only weak d-d transitions in this region.

Through extensive spectroscopic studies[23] (especially IR-CD) these distinctively different spectral properties of the BCP's have been attributed to a tetrahedral distortion of the Cu(II) active site which leaves the Blue copper in an effectively D_{2d} symmetry. Near the tetrahedral limit, all of the electronic transitions are predicted to be much lower in

Table 1.3 Spectroscopic Properties: Blue Copper Proteins[2a,22]

Protein:	Plastocyanin	Azurin	Stellacyanin
EPR: $g_{\|\|}$	2.226	2.26	2.287
$g_{\perp}$	2.053	2.05	2.077, 2.025
$A_{\|\|}$ ($10^{-4}cm^{-1}$)	63	60	35 (29, 57)
Absorption:			
λmax-600 nm	597	625	608
ε ($M^{-1}cm^{-1}$)	4900	3500	4030
Cu Coordination Geometry:	distorted Td	distorted Td	distorted Td
Ligation:[a]	N_2S_2	N_2S_2	N_2SX
E° (mV)	370	300-328	184

[a] Spectroscopically defined for azurin, stellacyanin

Figure 1.6 (A) Electronic absorption and

(B) EPR spectra: Blue copper proteins compared to a tetragonal copper site.

(——) Blue copper; (---) tetragonal copper(II)

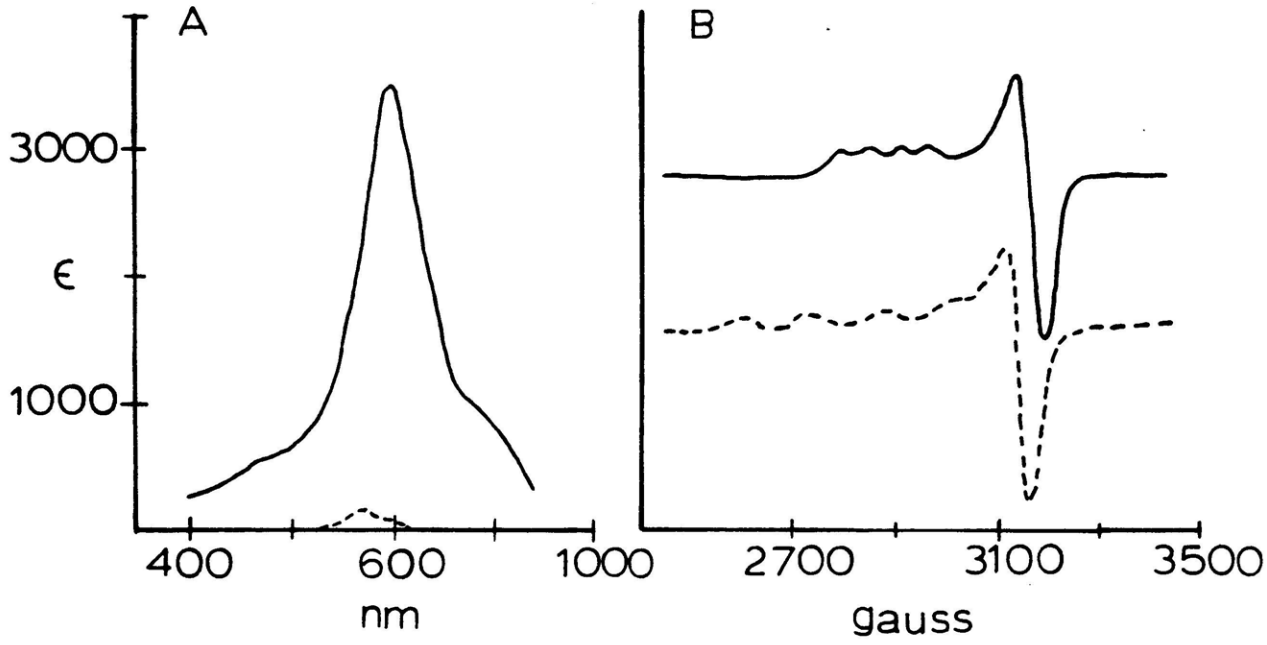
A
B
3000
ε
1000
400
600
1000
nm
2700
3100
3500
gauss

Table 1.4 Spectroscopic Properties: Coupled Binuclear Copper Proteins

Protein:	Oxyhemocyanin	Oxytyrosinase
EPR:	Non-detectable	Non-detectable
Optical:		
λmax (nm)/ε ($M^{-1}cm^{-1}$)	~700/200	~700/200
	570/1000	600/1000
	345/20,000	345/18,000
Cu coordination geometry:	Tetragonal	Tetragonal
Ligation:[a]	N_2O_3	N_2O_3

[a] Spectroscopically defined

energy than in the square planar complex. This shifts the d-d transitions from the visible to the near-IR and the L ---> Cu(II) CT transitions out of the UV and into the visible spectral region. In particular, all known Blue copper proteins contain a cysteine[24] residue coordinated at the active site, and the intense optical feature at ≈600 nm has been assigned[25] primarily as a cysteine(S) ---> Cu(dx^2-y^2) CT transition. In the case of plastocyanin, this spectroscopically effective model for the Blue copper site has been confirmed by x-ray crystallography.[26] Two imidazole N's (histidine) and, in the azurins and plastocyanins, a thioether S (methionine) complete the Blue copper coordination sphere. It is interesting to note the lack of exchangeable H_2O at this site, and in fact, in strong contrast to the normal copper proteins, there is no evidence for exogenous ligand binding or perturbation of any of the BCP's.[27] Two questions which still remain, however, are the origin of the reduced hyperfine splitting and the identification of the fourth, non-methionine ligand in stellacyanin.

3. Coupled Binuclear Copper Proteins

The arthropod and mollusc hemocyanins,[3] and tyrosinase,[3,28] are the coupled binuclear copper proteins (Table 1.4). All of these proteins function as biological

oxygen carriers, a property which will be discussed in greater detail in section 2.4. Parallel to the previous two sections, however, only the spectroscopic properties and structure of the coupled copper site will now be considered. Each of these proteins contains two tetragonal copper ions at its active site, but their spectral features are very different than what is observed in copper model complexes and in normal copper proteins. Whereas Cu(II) complexes are predicted to exhibit four line parallel and perpendicular EPR intensity at g≈2, oxyhemocyanin and oxytyrosinase (Figure 1.7) are EPR non-detectable, and in fact, diamagnetic to the most sensitive superconducting quantum interference detector magnetometers.[29] Moreover, in contrast to the weak, low-energy ligand field bands associated with normal Cu(II), two intense absorption spectral features dominate the visible-UV spectrum of the coupled binuclear copper proteins. Extensive research[3] has led to a detailed understanding of the origins of these unique spectroscopic features. Resonance Raman spectroscopy of the 570 nm and 350 nm optical bands of oxyhemocyanin reveals[30] a peak at ≈750 cm^{-1} which shifts on $^{18}O_2$ substitution, allowing its assignment to the O-O stretch of the oxygen bound in oxyhemocyanin. Further, the energy of this vibration indicates that the oxygen is bound as peroxide, ($\nu\ O_2$ = 1580 cm^{-1}, $\nu\ O_2^-$ ∿1100 cm^{-1}, $\nu\ O_2^{2-}$ ∿800 cm^{-1}). That is, two Cu(I)'s in the deoxy [Cu(I)Cu(I)] state of the protein are formally oxidized by O_2 which is thereby

Figure 1.7 (A) Electronic absorption and

(B) EPR spectra: Oxyhemocyanin compared to a tetragonal copper(II) complex

(——) oxyhemocyanin; (---) tetragonal copper(II)

OXYHEMOCYANIN ——
NORMAL COPPER ------

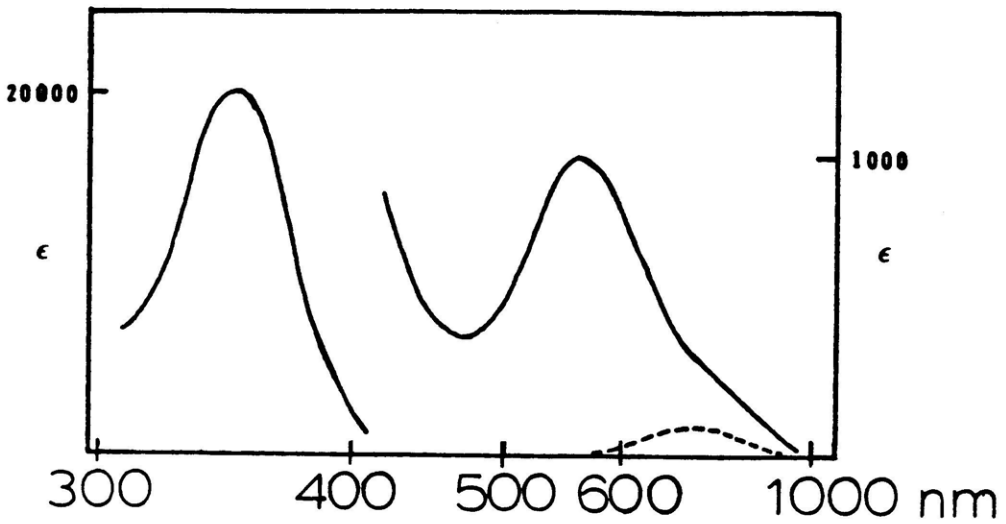

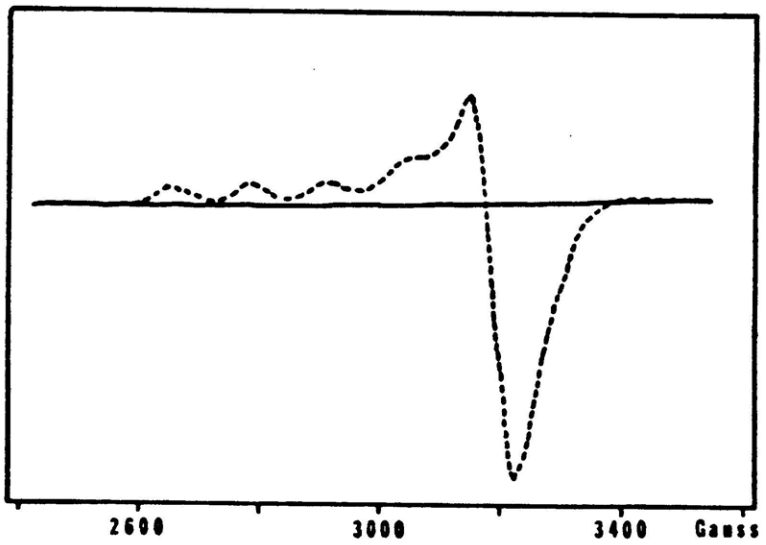

reduced by two electrons and bound as peroxide. In order to further define the structure of the binuclear copper active site, a series of systematically varied binuclear copper derivatives[3,31] were prepared (Figure 1.8). Detailed studies of their spectroscopic properties and perturbations on binding exogenous ligands generated the "spectroscopically effective model"[3] for the oxyhemocyanin and oxytyrosinase active site pictured in Figure 1.9A. This model explains the unusual spectral properties of the site which were previously raised. Two tetragonal copper(II)'s are bridged by a protein residue (likely phenolate, OR^-). This endogenous bridge mediates antiferromagnetic superexchange through its overlap with the unpaired electrons in the Cu(II) dx^2-y^2 orbitals (Figure 1.9B), resulting in a diamagnetic oxyhemocyanin ground state and no EPR signal. Exogenous ligands also bridge the exchange coupled Cu(II)'s, and the intense absorption features at 570 and 350 nm (and CD at 450 nm) have all been assigned[31] as O_2^{2-} ---> Cu(II) CT transitions of a peroxide bound in a 1,2 bridging geometry (Figure 1.9B). Four imidazole N's from histidine residues complete the equatorial coordination of the Cu(II)'s and exchangeable axial water molecules permit ligand substitution chemistry of the active site to occur.

4. Multicopper Oxidases and Structure Function Correlations to the Simpler Copper Containing Proteins

Figure 1.8 Representations of the binuclear copper active site derivatives of hemocyanin and tyrosinase.

Figure 1.9 (A) Spectroscopically effective active site picture of oxyhemocyanin and oxytyrosinase and

(B) its unique properties: (Left) electronic absorption spectra (~15 K) of oxy (——) and met (---) hemocyanin and CD spectrum (298 K) of oxy (—·—·—) with assignment features; (Right) antiferromagnetic superexchange interaction between the dx^2-y^2 orbitals of the tetragonal cupric centers through the endogenous protein bridge (R).

DEOXY

Cu^{+1} Cu^{+1}

HALF APO

Cu^{+1} —

MET APO

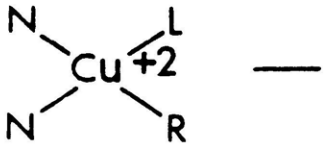

—

HALF MET – 1

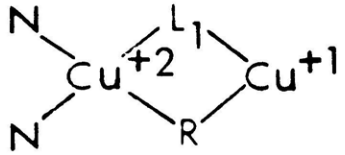

HALF MET – 2

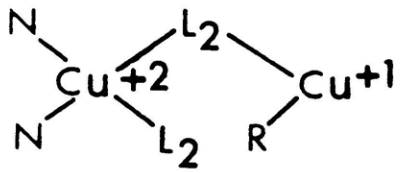

MET

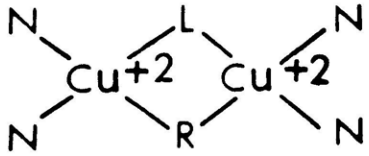

DIMER

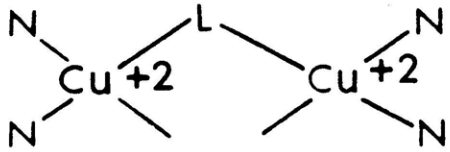

OXY

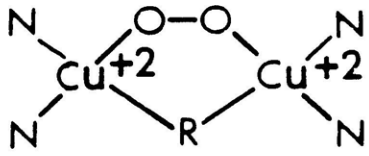

A. OXYHEMOCYANIN

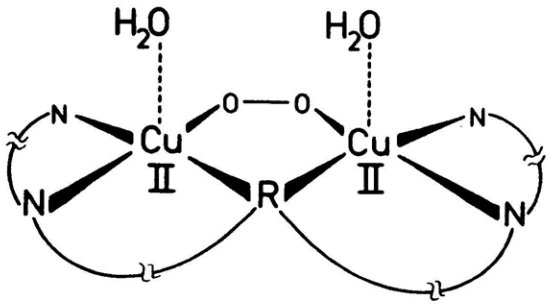

B. UNIQUE PROPERTIES

OPTICAL

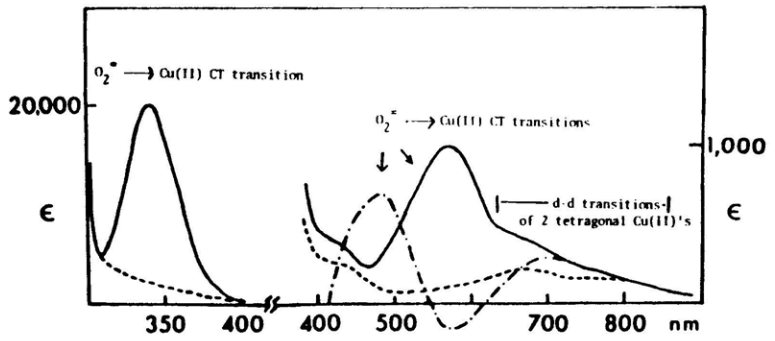

EPR

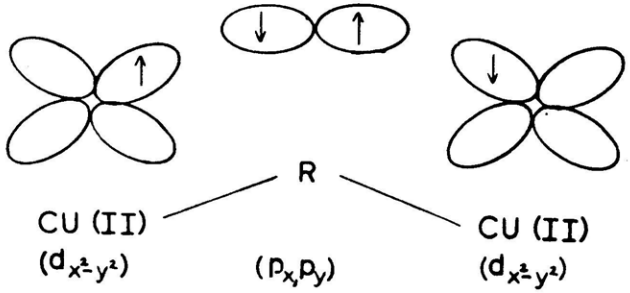

The multicopper oxidases[2,32-34] (Table 1.5) contain a combination of sites analogous to the three copper coordination environments previously discussed. Hence, all of these enzymes contain at least four copper ions at their active site and are significantly more complicated than the copper proteins in Tables 1.2 - 1.4. Together, these copper centers couple four one-electron oxidations of substrates to the four-electron reduction of dioxygen to water. In the case of laccase,[35] the substrate phenols urishiol and laccol, as well as the oxidase, are dissolved in the latex of Asian lacquer trees and serve a protective function for the trees. When the tree is damaged, it bleeds this latex; aerobic oxygen and laccase then oxidize the phenols to free radicals which polymerize to form a natural polyphenolic plastic which essentially seals the injured area.

For simplicity in the oxidases, the Blue, normal, and coupled binuclear coppers are designated[2b,36] as Type 1 (T1), Type 2 (T2) and Type 3 (T3) copper sites, respectively. The laccases contain one T1, one T2, and one T3 copper center and are the simplest and most clearly defined of the multicopper oxidases; even the number of copper ions is still uncertain in both ceruloplasmin (5-7) and ascorbic acid oxidase (6-8). As shown in Figure 1.10, the T1 copper is observed in both the optical (λ max = 614 nm = 5700 $M^{-1}cm^{-1}$) and EPR ($A_{||}$ = 43 X 10^{-4} cm^{-1}) spectra of native tree laccase. While the

Table 1.5 Spectroscopic Properties: Multicopper Oxidases

Protein:	Laccases		Ceruloplasmin		Ascorbic Acid Oxidase	
	Tree	Fungal				
Distribution of Copper:						
T1	1	1	2		3	
T2	1	1	1		1	
T3	1	1	1-2		1-2	
EPR:						
T1 $g_{\|\|}$	2.30	2.19	2.215	2.206	2.227	2.242
$g_{\perp}$	2.06, 2.03	2.09	2.05	2.05	2.058, 2.036	2.053
$A_{\|\|}$ ($10^{-4}cm^{-1}$)	43	90	95	74	58	199
T2 $g_{\|\|}$	2.24	2.24	2.247			
$g_{\perp}$	2.05	2.04	2.06			
$A_{\|\|}$ ($10^{-4}cm^{-1}$)	206	194	189			
Absorption:						
λmax (nm)/ε ($M^{-1}cm^{-1}$)	614/5700	610/4900	610/11,000		610/1210 $m[Cu]^{-1}cm^{-1}$	
	330/2800	330/2700	330/3300		330/490 $m[Cu]^{-1}cm^{-1}$	

Figure 1.10 (A) Electronic absorption and

(B) EPR spectra of the multicopper oxidase, Rhus vernicifera laccase.

The spectral features associated with each of the cupric centers is indicated.

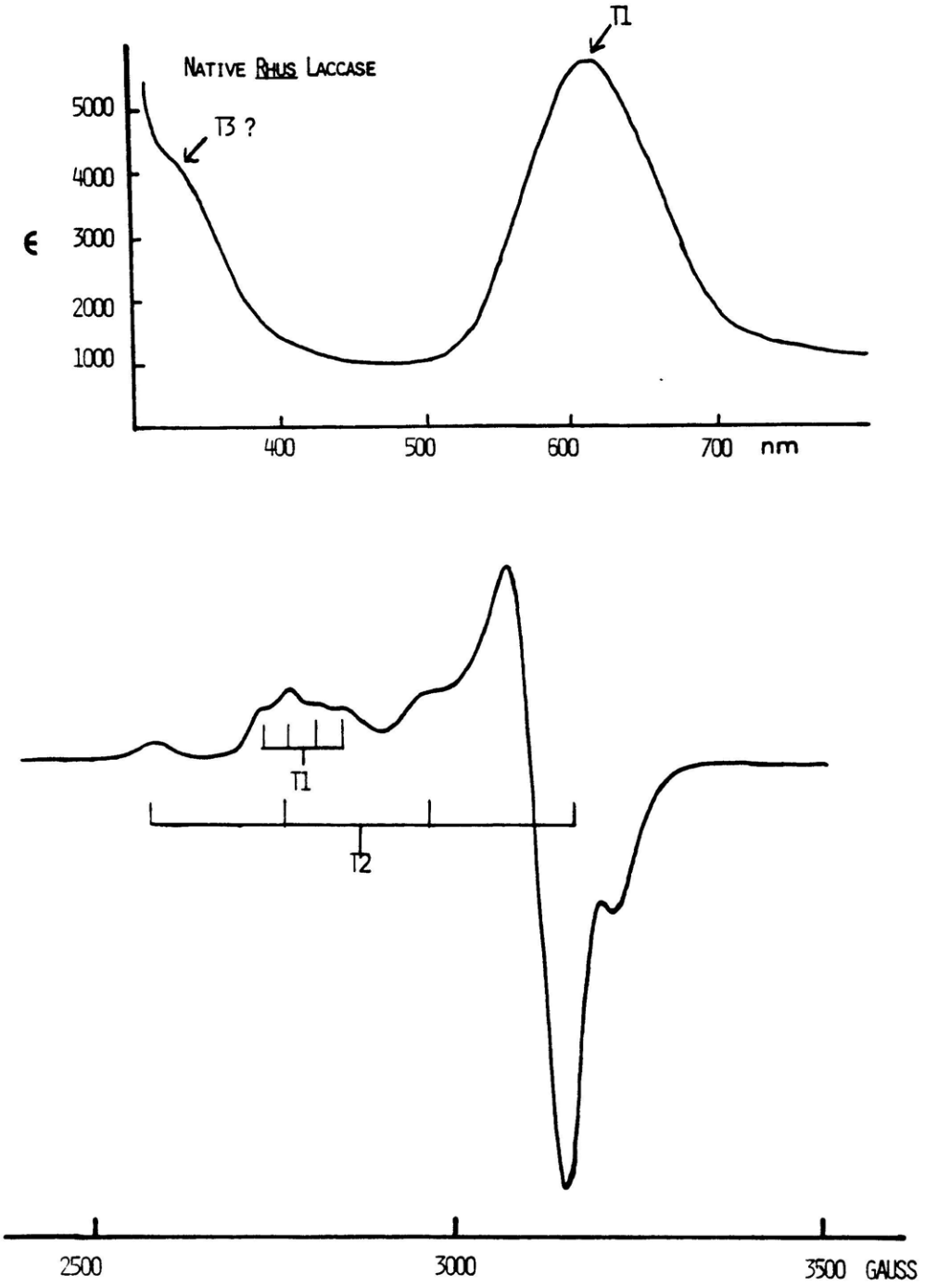
NATIVE RHUS LACCASE
T1
T3 ?
5000
4000
3000
2000
1000
ε
400
500
600
700 nm
T1
T2
2500
3000
3500 GAUSS

optical features due to the T2 copper are weak and dominated by the intense, overlapping T1 charge transfer bands, the T2 Cu(II) EPR contribution is clear ($A_{||}$ = 206 X 10^{-4} cm^{-1}). The T3 site is antiferromagnetically exchange coupled (-2J > 550 cm^{-1})[29] and EPR nondetectable; however, based on reductive titration studies[37], the binuclear copper site has been associated with the absorption band at 330 nm (ε = 2800 M^{-1} cm^{-1}) which reduces as a two electron acceptor.

Thus, spectroscopically, in native laccase are observed optical and EPR contributions due to the individual types of copper which comprise its active site and which are similar to those observed in the simpler copper proteins. More specifically, the T1 Cu(II) in laccase is more like the Blue copper in the plastocyanins and azurins (axial EPR, higher E°, possible methionine coordination) than in stellacyanin (rhombic EPR, lower E°, no methionine). While the T2 Cu(II) is thought to contain simple, tetragonal N,O coordination and two exchangeable positions, it has no organic prosthetic group; thus it appears similar to galactose oxidase, but no absolute correlation to any of the normal copper proteins can be made. Finally, aside from the intense CT features associated with the exogenous O_2^{2-} bound to the copper active site in oxyhemocyanin and oxytyrosinase, the spectral features of the T3 site in laccase would appear very similar to those of the hemocyanins and tyrosinase copper centers.

How the structure and function of each of these sites in the oxidases relate to its analogous site in the simpler copper containing proteins is a more complicated but extremely important question. The T1 copper, as in the Blue copper proteins, is suggested[38] to be the center of electron transfer in laccase and is believed to be the copper site which first accepts electrons from reducing substrates. The function of the T2 copper is still quite controversial, but this research indicates an important role for the T2 center in effecting reactivity at the T3 copper site (Chapter 5). As in the hemocyanins and tyrosinase, the oxidase T3 site is believed to be the site of O_2 interaction.[39] However, whereas O_2 binds reversibly in the simpler copper proteins, it is irreversibly bound and reduced to water in the oxidases. This difference in oxygen reactivity might suggest the existence of important differences as well as similarities between these coupled binuclear sites.

Looking more closely at the coupled binuclear copper proteins and their oxygen reactivity (Figure 1.11), the simplest are the arthropod hemocyanins which just reversibly bind O_2. Next in complexity are the mollusc hemocyanins which, in addition to reversible oxygen binding, dismutate peroxide to oxygen and water (catalase acitivity).[40] Tyrosinase functions as do mollusc hemocyanins, but in addition,[41] is able to hydroxylate phenols to orthodiphenols

Figure 1.11 Oxygen reactivity at coupled binuclear copper active sites.

Coupled Binuclear Copper Proteins

Hemocyanin

Arthropod

$$\text{deoxy} + O_2 \rightleftharpoons \text{oxy}$$

Mollusc

$$\text{deoxy} + O_2 \rightleftharpoons \text{oxy}$$
$$2H_2O_2 \rightleftharpoons O_2 + 2H_2O$$

Tyrosinase

$$\text{deoxy} + O_2 \rightleftharpoons \text{oxy}$$
$$2H_2O_2 \rightleftharpoons O_2 + 2H_2O$$
$$\text{phenol} + 2e^- + O_2 + 2H^+ \rightleftharpoons \underline{o}\text{-diphenol} + H_2O$$
$$2\underline{o}\text{-diphenol} + O_2 \rightleftharpoons 2\underline{o}\text{-quinone} + 2H_2O$$

Laccase
Ceruloplasmin
Ascorbic Acid Oxidase

$$4AH + O_2 \rightarrow 4A + 2H_2O$$

(monooxygenase activity) and oxidize the resulting diphenol to the orthoquinone (diphenolase activity).

As previously mentioned, extensive research has led to a fairly detailed understanding of the mollusc hemocyanin active site (Figure 1.9A). Extension of these studies[42] to a series of mollusc and arthropod hemocyanins demonstrates a strong similarity between the coupled binuclear copper sites in these phyla; rather, the lack of catalase activity in arthropods seems to relate to a structural distortion of the arthropod site which affects the exogenous ligand bridge and interferes with peroxide binding at this site.

Much of this research has been extended toward understanding copper-oxygen reactivity in tyrosinase.[28,42] Here, it would again appear that the tyrosinase coupled binuclear copper site is very similar to that found in the hemocyanins. The enhanced reactivity of tyrosinase, rather, appears to relate to increased substrate accessibility to the active site which is provided by the orientation of the protein pocket around the binuclear copper site. Thus, while the protein ligand imposes unique effects on the active site, in all these proteins the geometric and electronic structure of the coupled binuclear copper sites are very similar, and moreover, all of these proteins function to reversibly bind oxygen.

The purpose of this research has been to extend this understanding of coupled binuclear copper active site structure and biological function to the multicopper oxidases, and in particular, the tree laccase, Rhus vernicifera. As summarized in Table 1.5, oxygen does not reversibly bind to the oxidases, but rather binds irreversibly and undergoes a four-electron reduction to water. Thus, we return to the initial question of how differences in geometric and electronic structure of the active site determine differences in biological function, that is, the reversible compared to the irreversible binding of dioxygen. In extending this research toward understanding the more complicated oxidases in Table 1.5, it is unlikely that spectroscopically effective models for the tree laccase active site will directly relate to those for ceruloplasmin and ascorbic acid oxidase which contain additional copper ions at their active sites. However, knowledge of the multicopper active site in laccase will certainly be important to a fundamental understanding of how the T1, T2, and in particular the T3 copper sites in the oxidases relate to their counterparts in the simpler copper containing proteins. Moreover, through study of the laccase active site, one can in the simplest way begin to develop insight into the allosteric interactions of the T3 copper with the T1 and T2 centers (Chapters 4 and 5) which are clearly critical to the intramolecular four-electron transfer required for

reduction of dioxygen to water. This research indicates that these intersite interactions are essential to a comparison of the oxidase binuclear unit with that of the simpler binuclear copper containing proteins.

References and Notes

1. Solomon, E.I.; Penfield, K.W.; Wilcox, D.E. Struct. Bonding (Berlin) **1983**, 53, 1-57.
2. a. Fee, J.A. Struct. Bonding (Berlin) **1975**, 23, 1-60.
   b. Malkin, R.; Malmstrom, B.G. Adv. Enzymol. **1970**, 33, 177-244.
3. Solomon, E.I. in Copper Proteins (**1981**) Spiro, T.G., Ed. (Wiley Interscience: New York) Ch. 2.
4. Valentine, J.S.; Pantoliano, M.W. in Copper Proteins (**1981**) Spiro, T.G., Ed. (Wiley Interscience: New York) Ch. 8.
5. Richardson, J.S.; Thomas, K.A.; Rubin, B.A.; Richard, D.C. Proc. Natl. Acad. Sci. USA **1975**, 72, 1349-1353.
6. a. Weser, U.; Bunnenberg, E.; Cammack, R.; Djerassi, C.; Flohe, L.; Thomas, G.; Voelter, W. Biochim. Biophys. Acta **1971**, 243, 203-213.
   b. Weser, U. Struct. Bonding (Berlin) **1973**, 17, 1-65.
7. Ettinger, M.J.; Kosman, D.J. in Copper Proteins (**1981**) Spiro, T.G., Ed. (Wiley Interscience: New York) Ch. 6.
8. a. Hamilton, G.; Libby, R.; Hartzell, C. Biochem. Biophys. Res. Comm. **1973**, 55, 333-340.
   b. Dyrkacz, G.R.; Libby, R.D.; Hamilton, G.A. J. Am. Chem. Soc. **1976**, 98, 626-628.
9. a. Bereman, R.D.; Kosman, D.J. J. Am. Chem. Soc. **1977**, 99, 7322-7326.

b. Bereman, R.D.; Ettinger, M.J.; Kosman, D.J.; Kurland, R.J. Adv. Chem. **1977**, 162, 263-280.

c. Kosman, D.J.; Peisach, J.; Mims, W.B. Biochem. **1980**, 19, 1304-1308.

10. Ettinger, M.J. Biochem. **1974**, 13, 1242-1247.

11. a. Blumberg, W.; Horecker, B.L.; Kelly-Falcoz, F.; Peisach, J. Biochim. Biophys. Acta **1965**, 96, 336.

b. Giordano, R.S.; Bereman, R.D. J. Am. Chem. Soc. **1974**, 96, 1019-1023.

12. a. Amundsen, A.; Wherlan, J.; Bosnich, B. J. Am. Chem. Soc. **1977**, 99, 6730-6739.

b. Solomon, E.I.; Hare, J.W.; Gray, H.B. Proc. Natl. Acad. Sci. USA **1976**, 73, 1389-1393.

13. Hamilton, G.A. in Copper Proteins (**1981**) Spiro, T.G., Ed. (Wiley Interscience: New York) Ch. 5.

14. Suzuki, H.; Ogura, Y.; Yamada, H.; Arima, K. Biochim. Biophys. Acta, **1975**, 403, 23-31.

15. a. Blaschko, H.; Buffoni, F. Proc. Roy. Soc. (London) Ser. B **1965**, 163, 45-60.

b. Olsson, B.; Olsson, J.; Pettersson, G. Eur. J. Biochem. **1976**, 71, 375-382.

16. Veryovkina, I.V.; Abdel Samed, M.M.; Gorkin, V.Z. Biochim. Biophys. Acta **1972**, 258, 56-70.

17. Suzuki, S.; Sakurai, T.; Nakahara, A.; Oda, O.; Manabe, T.; Okuyama, T. FEBS Lett. **1980**, 116, 17-20. (Bovine serum)

18. Finazzi-Agro, A.; Guerrieri, P.; Costa, M.T.; Mondovi, B. Eur. J. Biochem. **1977**, 74, 435-440.

19. Barker, R.; Boden, N.; Cayley, G.; Charlton, S.C.; Henson, R.; Holmes, M.C.; Kelly, I.D.; Knowles, P.F. Biochem. J. **1979**, 177, 289.

20. Rosenberg, R.C.; Lovenberg, N. Essays in Neurochem. and Neuropharm. **1980**, 4, 163-209.

21. Blumberg, W.E.; Goldstein, M.; Lauber, E.; Peisach, J. Biochim. Biophys. Acta **1965**, 99, 187-190.

22. Gray, H.B.; Solomon, E.I. in Copper Proteins (**1981**) Spiro, T.G., Ed. (Wiley Interscience: New York) Ch. 1.

23. a. Solomon, E.I.; Hare, J.W.; Gray, H.B. Proc. Natl. Acad. Sci. USA **1976**, 73, 1389-1393.

    b. Solomon, E.I.; Hare, J.W.; Dooley, D.M.; Dawson, J.H.; Stephens, P.J.; Gray, H.B. J. Am. Chem. Soc. **1980**, 102, 168-178.

24. a. Katoh, S.; Takamiya, S. J. Biochem. (Tokyo) **1964**, 55, 378-387.

    b. Solomon, E.I.; Clendening, P.J.; Gray, H.B.; Grunthaner, F.J. J. Am. Chem. Soc. **1975**, 97, 3878-3879.

    c. McMillan, D.R.; Holwerda, R.A.; Gray, H.B. Proc. Natl. Acad. Sci. USA **1974**, 71, 1339-1341.

25. Penfield, K.W.; Gay, R.R.; Himmelwright, R.S.; Eickman, N.C.; Norris, V.A.; Freeman, H.C.; Solomon, E.I. J. Am. Chem. Soc. **1981**, 103, 4382-4388.

26. Colman, P.J.; Freeman, H.J.; Guss, J.M.; Murata, M.; Norris, V.A.; Ramshaw, J.A.M.; Venkatappa, M.P. Nature (London) **1978**, 272, 319-324.

27. A small but significant reversible change in the EPR and optical spectra of stellacyanin has been observed at pH 10.6; Penfield, K.P.; Solomon, E.I. to be published.

28. Himmelwright, R.S.; Eickman, N.C.; LuBien, C.D.; Lerch, K.; Solomon, E.I. J. Am. Chem. Soc. **1980**, 102, 7339-7344.

29. a. Solomon, E.I.; Dooley, D.M.; Wang, R.H.; Gray, H.B.; Cerdonio, M.; Mogno, F.; Romani, G.L. J. Am. Chem. Soc. **1976**, 98, 1029-1031.

b. Dooley, D.M.; Scott, R.A.; Ellinghaus, J.; Solomon, E.I.; Gray, H.B. Proc. Natl. Acad. Sci. USA **1978**, 75, 3019-3022.

30. a. Freedman, T.B.; Loehr, J.S.; Loehr, T.M. J. Am. Chem. Soc. **1976**, 98, 2809-2815.

b. Larrabee, J.A.; Spiro, T.G.; Ferris, N.S.; Woodruff, W.H.; Maltese, W.A.; Kerr, M.S. J. Am. Chem. Soc. **1977**, 99, 1979-1980.

31. Eickman, N.C.; Himmelwright, R.S.; Solomon, E.I. Proc. Natl. Acad. Sci. USA **1979**, 76, 2094-2098.

32. Reinhammar, B.; Malmstrom, B.G. in Copper Proteins (**1980**) Spiro, T.G., Ed. (Wiley Interscience: New York) Ch. 3.

33. Laurie, S.H.; Mohammed, E.S. Coord. Chem. Rev. **1980**, 33, 279-312.

34. Marchesini, A.; Kroneck, P.M.H. Eur. J. Biochem. **1979**, 101, 65-76.

35. Levine, W.G. in The Biochemistry of Copper (**1966**) Peisach, J.; Aisen, P.; Blumberg, W.E., Eds. (Academic Press: New York) p. 371.

36. Malmstrom, B.G.; Andreasson, L.E.; Reinhammar, B. in The Enzymes, Vol. XII (**1975**) Boyer, P.D., Ed. (Academic Press: New York)

37. Reinhammar, B. Biochim. Biophys. Acta **1972**, 275, 245-259.

38. a. Andreasson, L.E.; Reinhammar, B. Biochim. Biophys. Acta **1979**, 568, 145-156.

b. Holwerda, R.A.; Gray, H.B. J. Am. Chem. Soc. **1974**, 96, 6008-6022.

39. a. Aasa, R.; Branden, R.; Deinum, J.; Malmstrom, B.G.; Reinhammar, B.; Vanngard, T. Biochem. Biophys. Res. Comm. **1976**, 70, 1204-1209.

b. Andreasson, L.E.; Branden, R.; Reinhammar, B. Biochim. Biophys. Acta **1976**, 438, 370-379.

40. Ghiretti, F. Arch. Biochem. Biophys. **1956**, 63, 165-176.

41. Makino, N.; Mason, H.S. J. Biol. Chem. **1973**, 248, 5731-5735.

42. a. Himmelwright, R.S.; Eickman, N.C.; LuBien, C.D.; Solomon, E.I. J. Am. Chem. Soc. **1980**, 102, 5378-5388.

b. Eickman, N.C.; Solomon, E.I.; Larrabee, J.A.; Spiro, T.G.; Lerch, K. J. Am. Chem. Soc. **1978**, 6529-6531.

43. Winkler, M.E.; Lerch, K.; Solomon, E.I. J. Am. Chem. Soc. **1981**, 103, 7001-7003.

II. X-RAY ABSORPTION EDGE STUDIES OF TYPE 2 DEPLETED AND NATIVE LACCASE

A. Introduction

An important simplification for study of the coupled binuclear or type 3 site in laccase is the reversible preparation[1] of a type 2 copper depleted (T2D) protein derivative, first reported in 1976. In the EPR spectrum (Figure 2.1), one observes that the features due to the T2 Cu(II) have been selectively removed leaving only the Cu(II) signal associated with the T1 Cu(II) center. The optical spectrum is more complicated, however, as the T2D protein form exhibits no 330 nm absorption band, this feature in the native enzyme having been shown to reduce as a two electron acceptor[2] and therefore associated with the T3 site. Further, this T2D derivative was reported[3] not to exhibit any N_3^- binding to type 3 copper, also in contrast to native laccase for which N_3^- ---> Cu(II) CT features are observed -at 400 and 500 nm.[4] These anomalous properties of T2D laccase were further complicated by several conflicting literature reports[1,3,5,6] by different research laboratories in characterizing the chemical and spectroscopic properties of the, in principle, simplified T2D form.

An important reaction of T2D laccase with H_2O_2 was discovered by LuBien and coworkers in 1981.[7] As shown in Figure 2.2, treatment of T2D laccase with 30X[protein] of H_2O_2 restores 330 nm absorption ($\Delta\varepsilon 330 \approx 2000\ M^{-1}cm^{-1}$) and

Figure 2.1 Electronic absorption and EPR spectra of

(A) Native and

(B) T2D Rhus laccase.

(Left) absorption; (Right) EPR

The spectral features associated with each of the cupric centers is indicated.

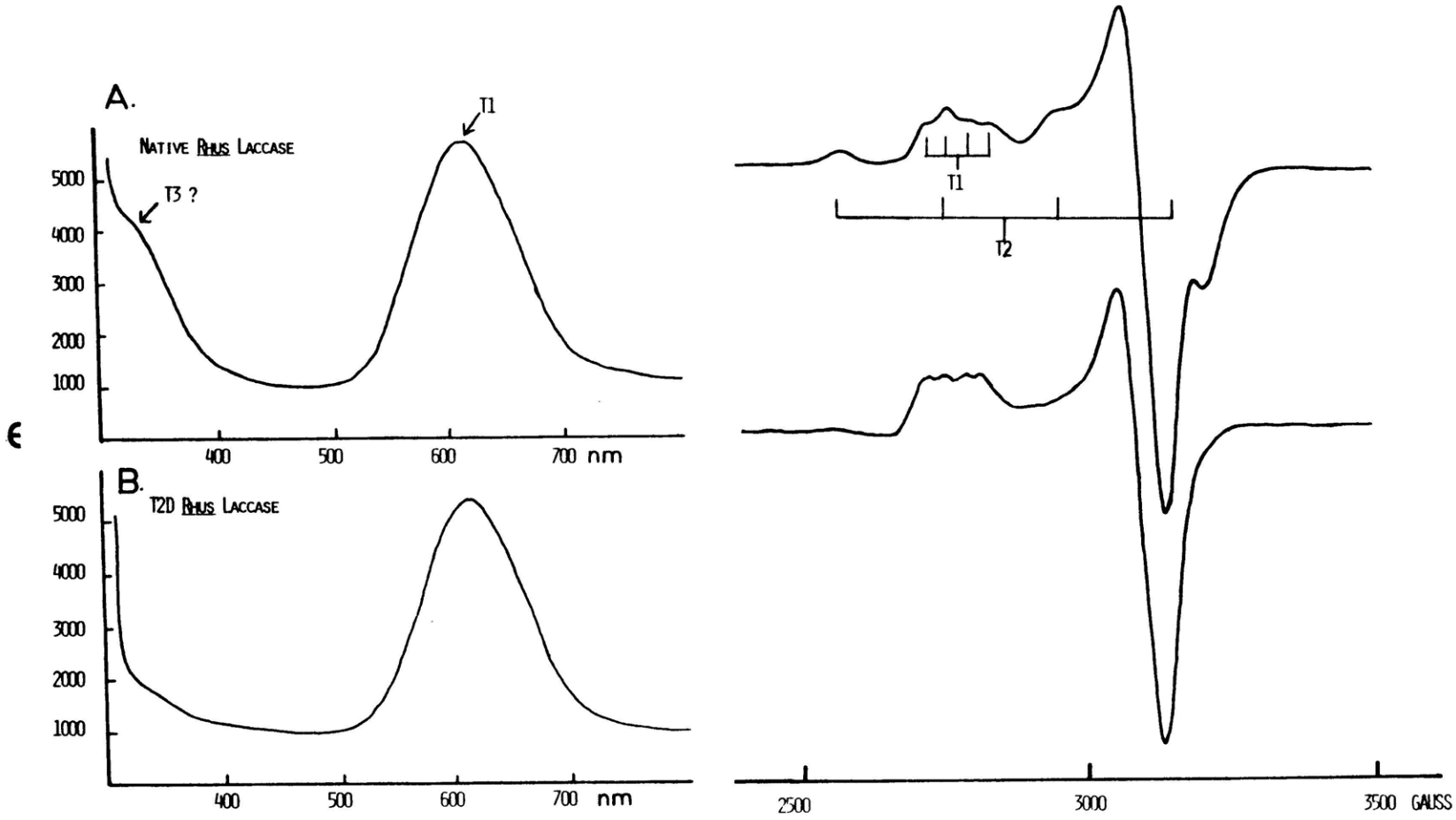
A.
NATIVE RHUS LACCASE
T1
T3 ?
5000
4000
3000
2000
1000
400
500
600
700 nm
B.
T2D RHUS LACCASE
5000
4000
3000
2000
1000
400
500
600
700 nm
ε
T1
T2
2500
3000
3500 GAUSS

generates a feature very similar to that of native laccase (Δ 330, oxidized-reduced = 2800 $M^{-1}cm^{-1}$)[2]. An increase in absorption is also observed in the ligand field region at ≈745 nm (Δε 745 ≈150 $M^{-1}cm^{-1}$); the 614 nm band is only slightly perturbed (Δε614 ≥ -600 $M^{-1}cm^{-1}$). Azide addition to T2D laccase after reaction with H_2O_2 (Figure 2.2) generates a new absorption band at 450 nm[7] which, through resonance Raman spectroscopic studies, has been assigned as an N_3^- ---> Cu(II) CT feature. Thus, it appeared that T2D contained a reduced T3 site which could be reoxidized by H_2O_2 to yield a new T2D protein form displaying the spectroscopic and chemical properties which are normally associated with the coupled binuclear cupric site.

Determination of copper ion oxidation state in both T2D and native laccase is difficult, however, as both a binuclear cuprous site and an antiferromagnetically exchange coupled binuclear cupric site lack characteristic optical and EPR spectral features. Copper ions do, however, have x-ray absorption edge spectra which change dramatically with metal ion oxidation state. For a range of inorganic Cu(I) and Cu(II) complexes[8] the K-edges appear similar in position and shape to those shown for Cu(I) and Cu(II) imidazole solutions in the inset to Figure 2.3. (The nature of these edge structures and their differences will be discussed in section 2B). In preliminary x-ray absorption spectroscopic (XAS)

Figure 2.2 Electronic absorption spectra at 298 K: Peroxide reaction of T2D laccase

(——) Native; (---) T2D;

(····) T2D reacted with 30 protein equivalents H_2O_2;

(—·—·—) T2D + 30X H_2O_2, reacted with 100 protein equivalents NaN_3

(0.1 M potassium phosphate, pH 6.0, [protein] = 0.15 mM)

Figure 2.3 X-ray absorption edges at ~210 K: Native and T2D Laccase

(——) Native; (—·—·—) T2D;

(·····) T2D reacted with 30 protein equivalents H_2O_2

Insert: X-ray absorption edges of Cu(II) (——) and Cu(I) (—·—·—) imidazole complexes.

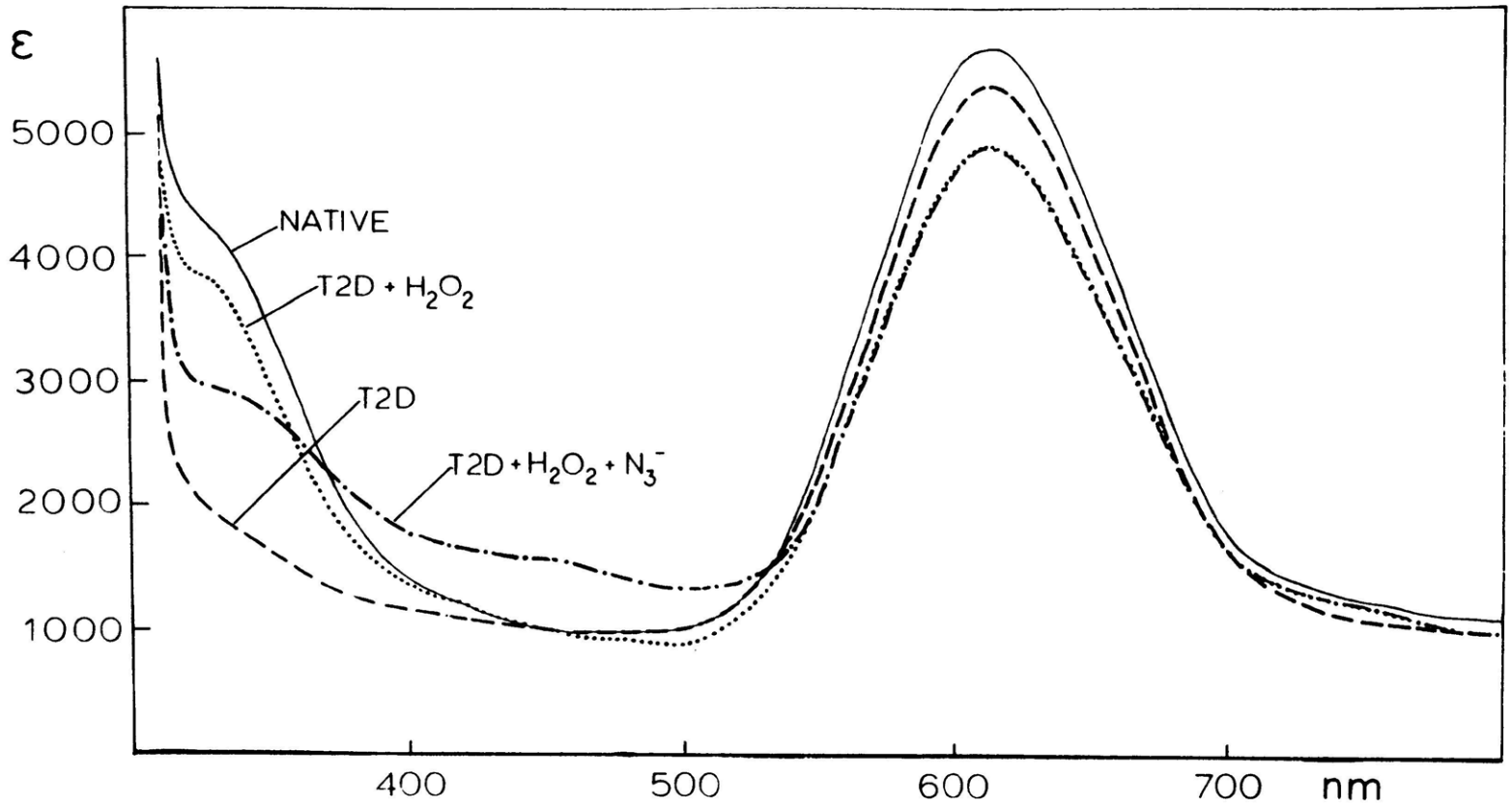
ε
5000
4000
3000
2000
1000
NATIVE
T2D + H_2O_2
T2D
T2D + H_2O_2 + N_3^-
400
500
600
700
nm

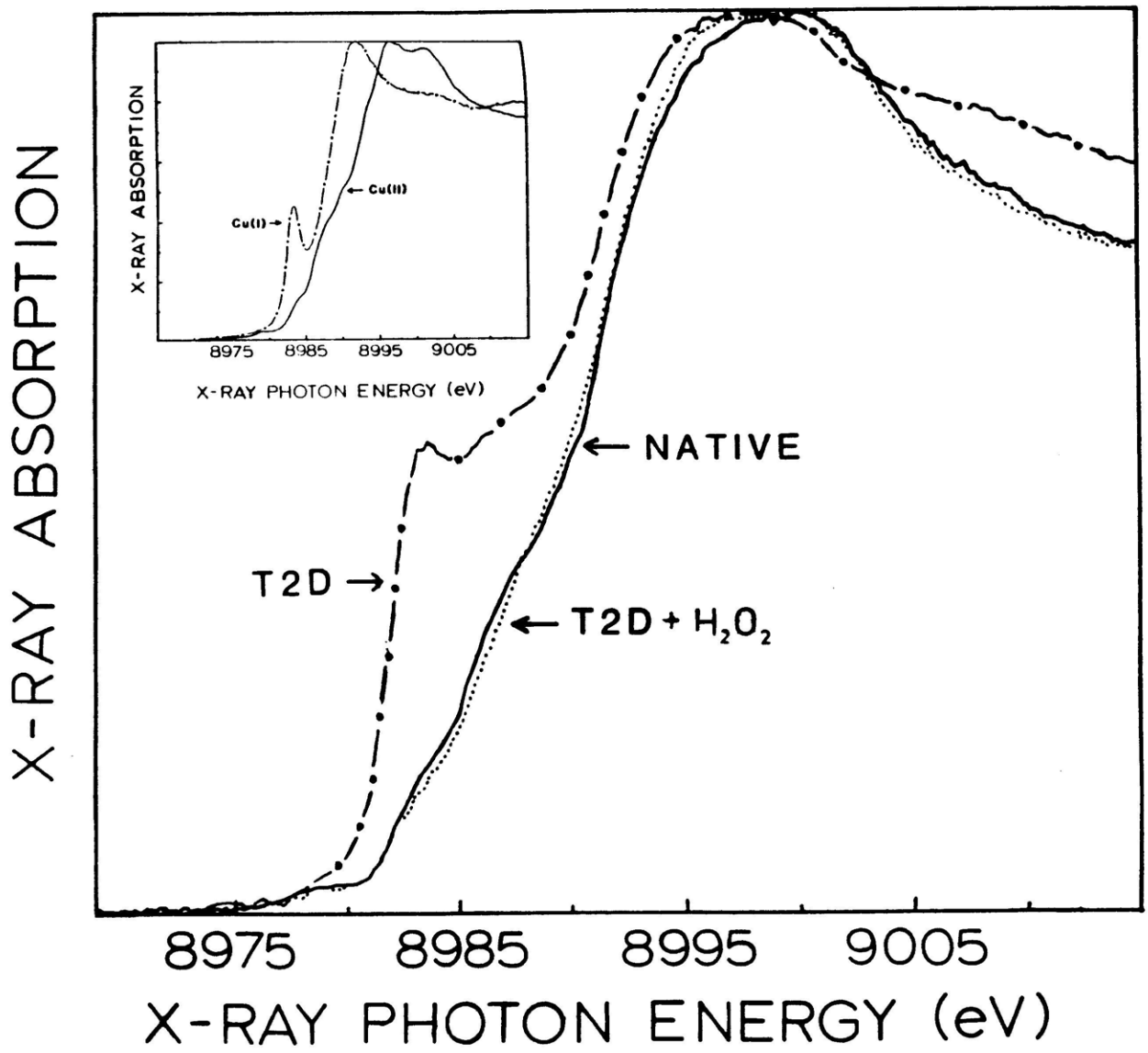
X-RAY ABSORPTION
X-RAY PHOTON ENERGY (eV)
8975
8985
8995
9005
NATIVE
T2D
T2D + H_2O_2
Cu(I)
Cu(II)

studies[7] (Figure 2.3), this fact was used to demonstrate that T2D laccase, as prepared, has an edge structure very similar to that of Cu(I) imidazole and contains a large amount of cuprous copper. Further, peroxide was shown to change the edge spectrum of T2D laccase into one similar to Cu(II) imidazole and essentially identical to that of native laccase, directly demonstrating its ability to oxidize the reduced T3 site in T2D laccase.

Despite the preliminary qualitative XAS studies, significant controversy over the chemical and spectroscopic properties of T2D laccase was still being addressed in the literature. Procedural variations in preparing the T2D derivative which apparently relate to pH[9] and perhaps to extent of metal removal[3,9,10] resulted in T2D forms reported to display different physical properties and chemical reactivity,[1,3,5,6,9-13] the incomplete characterization of which was further complicating the problem. The geographic dependence of the properties of T2D are summarized in Table 2.1.

As determination of copper ion oxidation state is a critical point in understanding these initial differences in T2D, it was necessary to develop an analytical method for

Table 2.1 Type 2 Depleted Laccase - International Chemical and Spectral Properties

Optical Properties of T2D Compared to Native	Rome[3]	Stanford[7]	Israel[11,12]	Sweden[5,10]
$\Delta\varepsilon_{750}$ ($M^{-1}cm^{-1}$)	-300	--200		-500
$\Delta\varepsilon_{614}$ ($M^{-1}cm^{-1}$)	0 (assumed)	0	0	-1000
$\Delta\varepsilon_{330}$ ($M^{-1}cm^{-1}$)	-2000	-2800	-1400[a]	-0
Electrons Accepted in Reductive Titration Studies				
n	3	1.5	3.1	---
Ascorbic Acid Reduction Kinetics	slow	slow	fast	slow
H_2O_2 Reactivity				
$-\Delta\varepsilon_{330}$ ($M^{-1}cm^{-1}$)	+2000 (30X)[b]	+2200 (30X)	+660 (70X)	essentially no spectral changes[c]
$-\Delta\varepsilon_{614}$ ($M^{-1}cm^{-1}$)	300	-300	-900	
Interpretation:	T3 reduced but reoxidized by H_2O_2 in agreement with Stanford	T3 reduced, as prepared, but reoxidized by H_2O_2	T3 oxidized by $O_2/Fe(CN)_6^{3-}$ H_2O_2 is binding	T3 already oxidized by O_2
Buffer:	0.05 M NaOAc pH 5.2	0.1 M PPB pH 6.0	0.05 M NaOAc pH 5.0	0.1 M PPB pH 7.4

[a] Calculated from 12 ; [b] Morpurgo, L. personal communication; [c] Reinhammar, B. personal communication

quantitating Cu(I) concentrations in protein samples of mixed Cu(I) and Cu(II) composition. X-ray absorption spectroscopy can be used to directly probe copper ion oxidation state, and in collaboration with Professor Keith Hodgson and Dr. James Penner-Hahn at Stanford University, an appropriate quantitation technique[14] has been developed, tested on copper model systems, and then used to quantitate Cu(I) content in a number of important reactions of T2D laccase. By examining the binary difference comparison of normalized x-ray absorption edge spectra, we have been able to unambiguously define the oxidation state composition of the T2D laccase prepared at Stanford and its reactivity with potential exogenous oxidants. In addition, accurate determination of the copper ion oxidation state composition has been important to the complete characterization of the binuclear copper active site derivatives which will be discussed in Chapter 3. Finally, through a careful combination of UV-Vis and x-ray absorption spectroscopic studies, clear understanding of peroxide reactivity of the coupled binuclear site in T2D and native laccase has been achieved.

B. Experimental

Laccase was purified from the acetone powder (Saito and Company, Osaka) of the Japanese lacquer tree Rhus vernicifera to a ratio of $A_{280}:A_{614}$ = 15.0 - 16.5 in 0.1 M

potassium phosphate buffer (PPB), pH 6.0, as described in references 5 and 15. Two modifications to the procedure were the centrifugation (5000 g for 12 minutes using an RC-5 superspeed centrifuge) of the stirred acetone powder suspension in 0.01 M PPB, pH 6.0, and its filtering over celite prior to its filtering through filter paper for its batch extraction by Sephadex CMC-50. T2D laccase was prepared as in Morpurgo, et al.[1] Routinely, ≈0.1 mM protein is dialyzed anaerobically in 2 L of 0.05 M sodium acetate, pH 5.2. To the $N_2(g)$ purged dialysate is added 2.0 mM dimethylglyoxime (0.43 g) and 2.0 mM potassium ferrocyanide (1.69 g). After 24 hours of dialysis against the solution, 1 mM ethylene diamine tetraacetic acid disodium salt (0.74 g) is added to this reaction vessel and dialysis continues for an additional 24 hours (48 hours total dialysis). Reagents are removed by anaerobic dialysis against 0.05 M sodium acetate, pH 5.2, followed by two dialyses against anaerobic 0.1 M PPB, pH 6.0, followed by several dialysis changes of aerobic 0.1 M PPB, pH 6.0.

Water is purified to a resistivity of 15 - 18 MΩ-cm through a Sybron-Barnstead Nanopure deionizing system. All studies utilized reagent grade chemicals without further purification. Reagent grade peroxide (30% aqueous solution) was standardized as described in reference 16. Protein samples were concentrated to ≈1 mM by Amicon (Amicon Corporation, Lexington, MA) using a PM-10 or YM-10 membrane.

Atomic absorption analyses for total copper present were routinely performed on a Perkin Elmer 2380 AA spectrophotometer equipped with an HGA-400 graphite furnace. A copper AAS standard solution (Alfa, 1000 μg/mL) was diluted in the appropriate buffer matrix for each run. The maximum intensity for Cu is observed at 324.7 nm with a slit width of 0.7 nm. The programmable controller conditions used were as follows: drying temperature was 110°C with a ramp time of 10 seconds and a hold time of 20 seconds. Charring temperature was 600°C with a ramp time of 10 seconds and a hold time of 20 seconds. Atomization was at 2600°C with a 4 second ramp time and a 4 second hold time.

Optical absorption spectra were measured at room temperature, before and after x-irradiation, in 1 mm quartz cells on a Cary 14 spectrophotometer. CD spectra for diluted aliquots of protein were recorded on a Jasco J-500C spectropolarimeter; positive ($\Delta\varepsilon$) values refer to Left-Right polarization. A Bruker ER 220 D-SRC EPR spectrometer (operating at 10 mW microwave power and 20 G modulation amplitude) was used to examine the frozen protein solutions at 77 K in the x-ray sample cells immediately prior to and after x-irradiation.

All x-ray absorption edge data were collected at the Stanford Synchrotron Radiation Laboratory using a Si[220] double crystal monochromator. They were measured as fluorescence excitation spectra, using an array of NaI(Tl) scintillation detectors with Ni filters. Multiple scans (dedicated beam, 2 scans; parasitic beam, 10-20 scans) per sample were measured at ~210 K. To ensure consistent energy determinations, the scans were calibrated using the internal calibration method[17] and averaged. To allow proper normalization, the absorption was measured for at least 300 eV below and 200 eV above the Cu K-edge. After averaging the calibrated scans, the pre-edge region was fitted with a second-order polynomial which was subtracted from the data to correct for residual absorption. Since the data are normalized to a Cu K-edge jump of 1.0, the results are independent of concentration.

C. Results and Discussion

1. Quantitative X-ray Absorption Edge Analysis: Technique and Application to Model Complexes

Whereas Cu(II) possesses an open shell d^9 electron configuration with d-d and L ---> Cu(II) CT transitions in the near-IR and UV-Vis region of the electronic spectrum (1500 - 250 nm, <25 eV), Cu(I) contains

ten d electrons in a closed shell and therefore exhibits no such transitions. To spectroscopically probe Cu(I), one must excite transitions to electronic vacancies in higher energy orbitals; in particular, the x-ray K-edge (Figure 2.4) corresponding to excitation of the deeply buried Cu 1s core electron to the open Cu 4s and Cu 4p atomic orbitals occurs at ≈9000 eV and is accessible through the intense, tunable synchrotron radiation available at the Stanford Linear Accelerator.

A typical x-ray absorption spectrum is illustrated in Figure 2.5. To lower energy is the pre-edge region which has monotonically decreasing absorption due to the absorption fall-off of the lower energy edges of the atoms in the sample (e.g. the L-edges for Cu). The x-ray absorption edge region refers to the structure which is superimposed on the discontinuous increase in absorption; both bound (e.g. atomic-type 3d, 4s, 4p orbitals) and non-bound (multiple-scattering of the photoelectron) states contribute to this structure. To higher energy is the extended x-ray absorption fine structure (EXAFS) region of the spectrum which corresponds to excitation of the 1s electron beyond the edge and into the continuum. While some EXAFS results will be discussed in Chapter 3, the following studies focus only on the edge itself.

Figure 2.4 X-Ray absorption K-edge spectroscopy for copper complexes.

The solid arrows represent electrons in a tetragonal Cu(II) d^9 environment. In Cu(I) complexes (different d-orbital splitting) the d orbitals are fully occupied (dashed arrow).

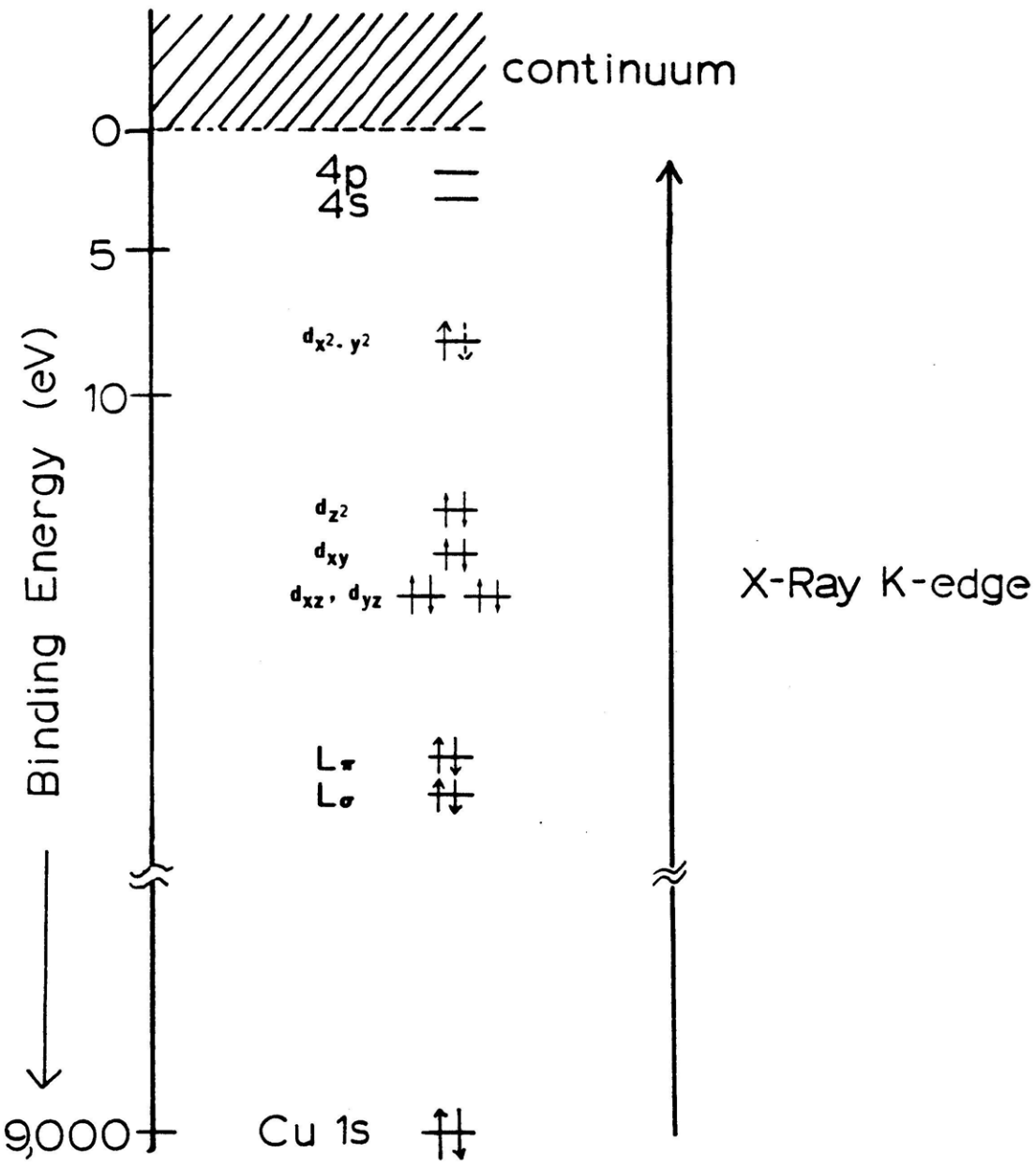
continuum
0
4p
4s
5
$d_{x^2-y^2}$
10
d_{z^2}
d_{xy}
d_{xz}, d_{yz}
L_π
L_σ
Binding Energy (eV)
9,000
Cu 1s
X-Ray K-edge

Figure 2.5 A typical x-ray absorption spectrum.

The pre-edge, edge, and EXAFS spectral regions are each illustrated. The dashed line is the smoothly varying absorption that would be observed in the absence of edge and EXAFS structure.

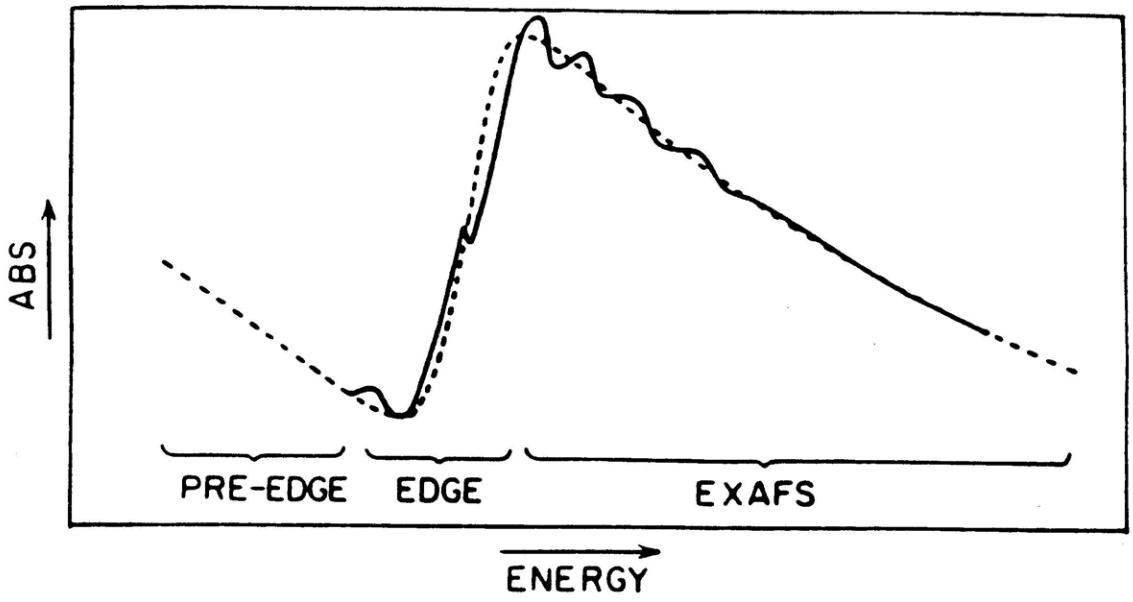
ABS
PRE-EDGE
EDGE
EXAFS
ENERGY

Copper(II) complexes also display x-ray absorption transitions upon excitation of the 1s core electron, but because of differences in charge, geometric and electronic structure, Cu(I) and Cu(II) complexes have distinguishing XAS edge spectra, as illustrated for their respective imidazole complexes in Figure 2.6.

Cu(I) imidazole is characterized by an intense transition at 8984 eV and an edge maximum at ≈8992 eV. Cu(II) imidazole exhibits a weak pre-edge transition at 8979 eV corresponding to the 1s ---> 3d transition accessible only in Cu(II), no 8984 eV transition, and an edge maximum at ≈9000 eV, consistent with its higher effective nuclear charge.

Of particular interest is the 8984 eV transition[18] which is present for copper complexes in the +1 oxidation state but absent for complexes in the +2 oxidation state. While this change in edge shape relates to geometric and electronic structural differences which are yet to be fully elucidated, it can be used as a qualitative indicator of the presence of Cu(I) in a variety of metalloproteins.[8,20,21] However, due to difficulties in normalization, background removal, and effects of instrumental resolution on edge structure, there have been few attempts to use x-ray absorption edges quantitatively.[22]

Figure 2.6 X-ray absorption edge spectra for Cu(I) and Cu(II) imidazole complexes.

(— — —) Cu(I); (———) Cu(II) imidazole

The distinguishing spectral features are summarized.

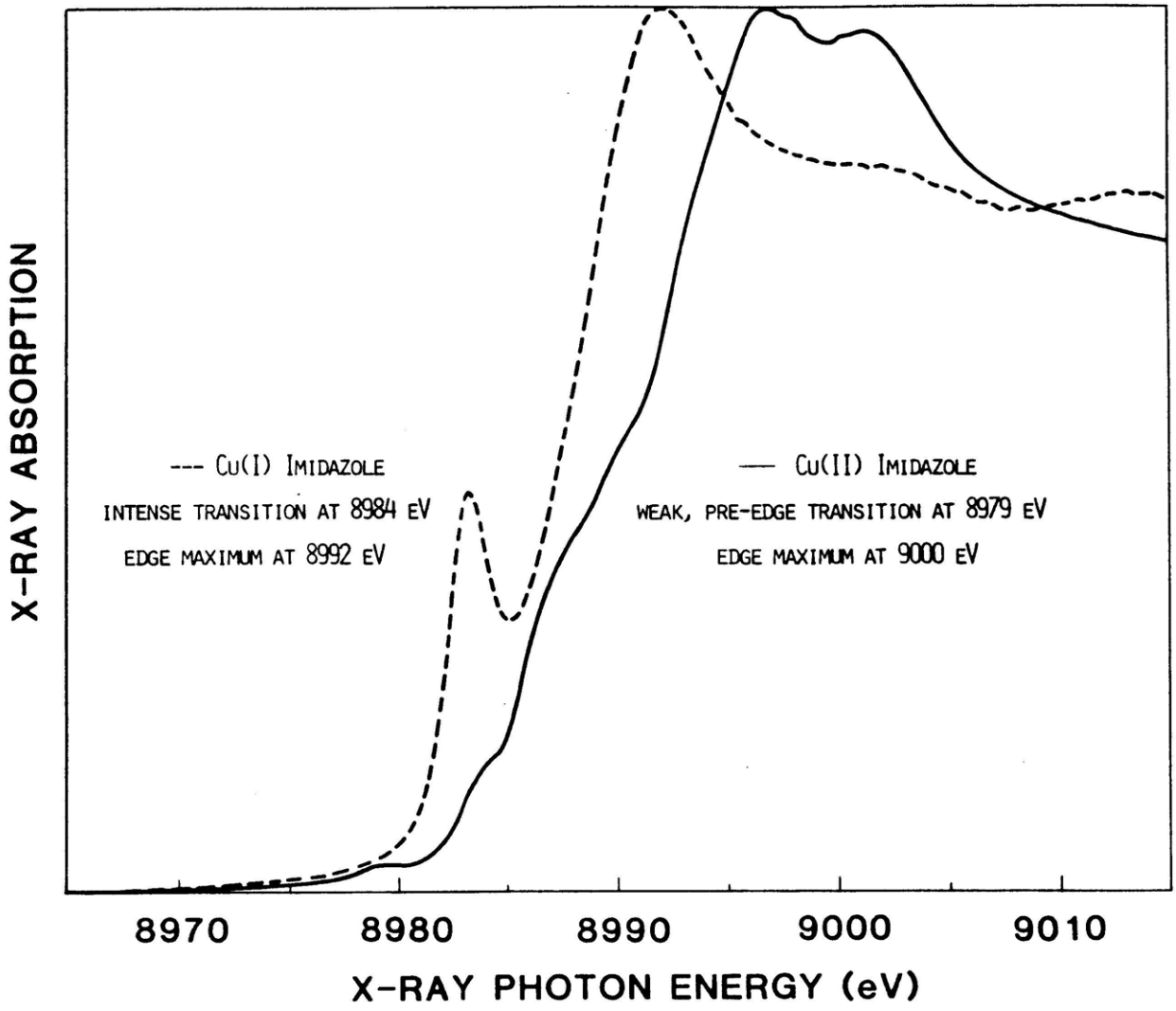
X-RAY ABSORPTION
--- Cu(I) IMIDAZOLE
INTENSE TRANSITION AT 8984 eV
EDGE MAXIMUM AT 8992 eV
— Cu(II) IMIDAZOLE
WEAK, PRE-EDGE TRANSITION AT 8979 eV
EDGE MAXIMUM AT 9000 eV
8970
8980
8990
9000
9010
X-RAY PHOTON ENERGY (eV)

In the absence of EXAFS effects, the absorbance above the edge would be proportional to [Cu] in a sample and could be used to normalize edge spectra.[20] Rather than normalizing the absorbance at a single energy, we fit a straight line to the EXAFS region (starting at ≈9050 eV) and extrapolate this line to 9000 eV to avoid any error caused by incomplete background removal. The data are normalized by scaling the pre-edge subtracted data to give an extrapolated absorbance of 1.0 at 9000 eV. This linear fit removes any potential normalization errors due to EXAFS modulations.

Background removal is necessary since the 8984 eV transition is not resolved, but occurs as a shoulder on a rapidly increasing absorption background. The apparent area of the 8984 eV transition thus depends on the background which is used to model the intense transition. The difference technique (vide infra) avoids this difficulty by not requiring calculation of this area.

Resolution has been suggested as being responsible for apparent differences in the edge structure of nominally identical samples.[23] In general, the data reported were all collected with significantly better resolution (≈2 eV) than the width of the 8984 eV transition (FWHM ≈5 eV), so small resolution differences between data sets should not affect the results.

Examination of the properly normalized edges reveals that in addition to the 8984 eV transition, Cu(I) edges differ from Cu(II) edges by having a weaker peak absorption at ≈9000 eV. Subtraction of a typical Cu(II) edge from a Cu(I) edge thus yields the characteristic derivative pattern shown in Figure 2.7.

The values ε_1 and ε_2 are defined to be the normalized absorbance of Cu(I) and Cu(II), respectively. A sample containing mole fraction f of Cu(I) will thus have a normalized absorbance ε given by $f\varepsilon_1 + (1-f)\varepsilon_2$. For samples X and Y with mole fraction Cu(I) of f_X and f_Y respectively, the normalized difference of X-Y, $\Delta\varepsilon$, will be given by

$$\Delta \varepsilon = (f_X - f_Y)(\varepsilon_1 - \varepsilon_2) \qquad (1)$$

Thus, from a knowledge of $(\varepsilon_1 - \varepsilon_2)$ one can determine change in % Cu(I), $(f_X - f_Y)$, from a measurement of $\Delta\varepsilon$. Although expression (1) will be valid for all points on the absorption edge, the most accurate results will be obtained for the maximum values of $(\varepsilon_1 - \varepsilon_2)$, e.g. at ≈8984 eV and ≈9000 eV (Figure 2.7).

This analysis implicitly assumes that ε_1 is a constant for all Cu(I) edges (and similarly for ε_2). Although this is not strictly true, examination of a wide variety of Cu(I) and

Figure 2.7 Normalized difference edge spectra: one Cu(I) model minus a variety of Cu(II) models.

The Cu(I) model has (N_2, S) coordination, and the Cu(II) complexes illustrated have (——, —·—·—) (N_4, O_1); (- — —) (N_2, O_2); and (———) (N_2, O_2, S) coordinations. Similar shapes and amplitudes were obtained for several Cu(I) and Cu(II) coordinations.

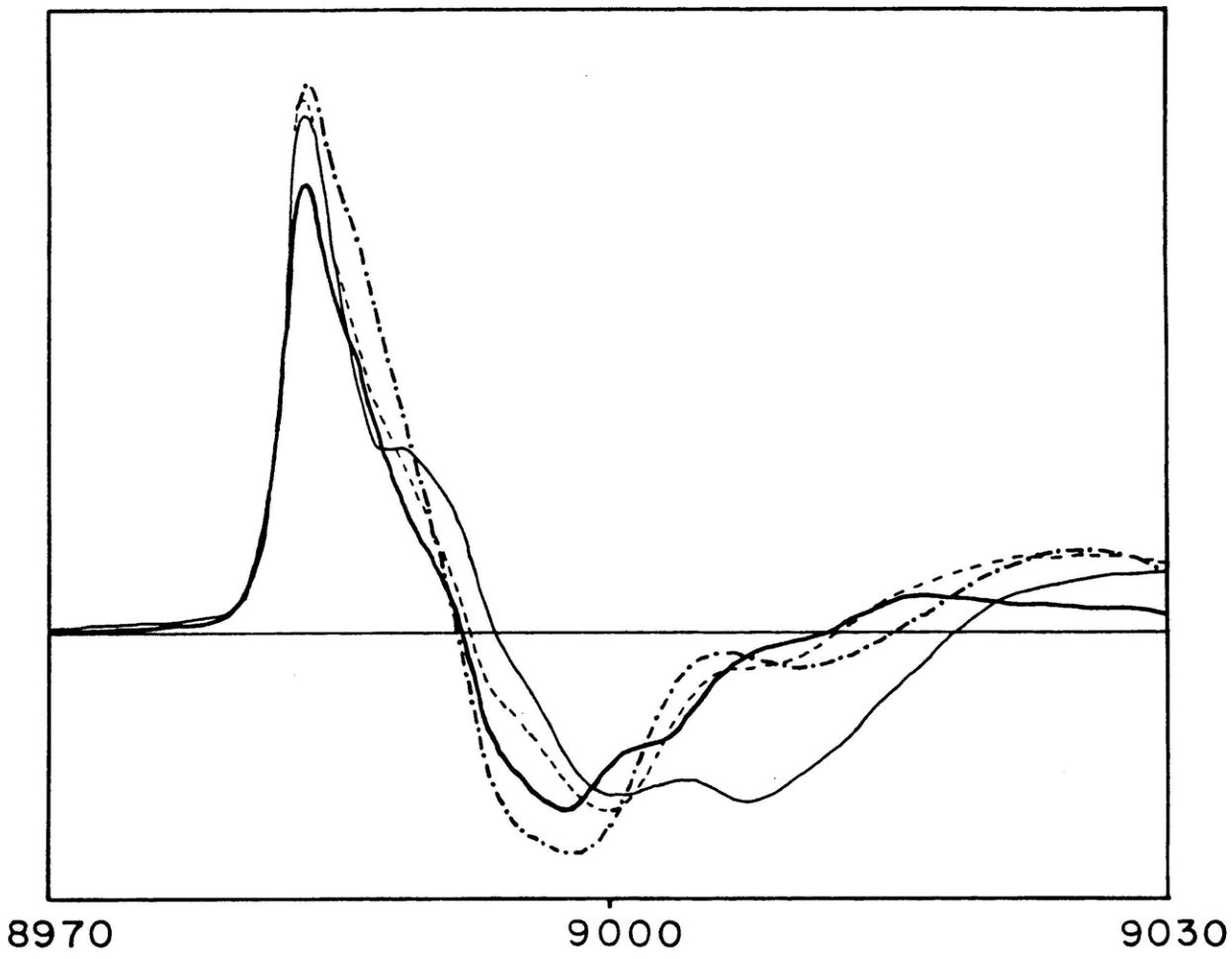
8970
9000
9030
ENERGY (eV)

Cu(II) ligation and site structures indicates the differences ($\varepsilon_1 - \varepsilon_2$) at ≈8984 and ≈9000 eV are surprisingly constant, the relative variation being ≈10%.

As shown in Figure 2.8, the absorption edges are nearly identical for two samples, each containing an ≈1:4 mixture of Cu(I):Cu(II). The difference edge (see inset), however, clearly reveals the different compositions. This sensitivity suggests that an important application may be the detection of photo-reduction or photo-oxidation. It is estimated that single scans of ≈1 mM protein samples have a sufficiently large signal/noise ratio to allow detection, by comparing the first and last scans, of a 5% change in [Cu(I)] during data collection.

2. T2D Laccase and Its Reactivity with Potential Exogenous Oxidants

Through difference edge analysis, comparing protein edges to those of Cu(II) model compounds, the untreated T2D form is clearly defined to contain 70 ± 15% Cu(I). As EPR and optical data indicate that the T1 copper is oxidized, this requires that >90% of the T3 centers are reduced in the prepared T2D. Thus, O_2 does not reoxidize the binuclear coppers in the T2D laccase form (as prepared in references 1, 3, 6, 7, and 9). However, >95% of the cuprous

Figure 2.8 Normalized edge spectra: two different oxidation state mixtures of a Cu model complex.

Inset shows the difference edge spectrum (upper edge - lower edge), indicating Δ% Cu(I) = 6%. Using Equation 1 and a Cu(II) reference, the upper spectrum represents a 26:74 mixture of Cu(I): Cu(II), the lower, a 20:80 mixture.

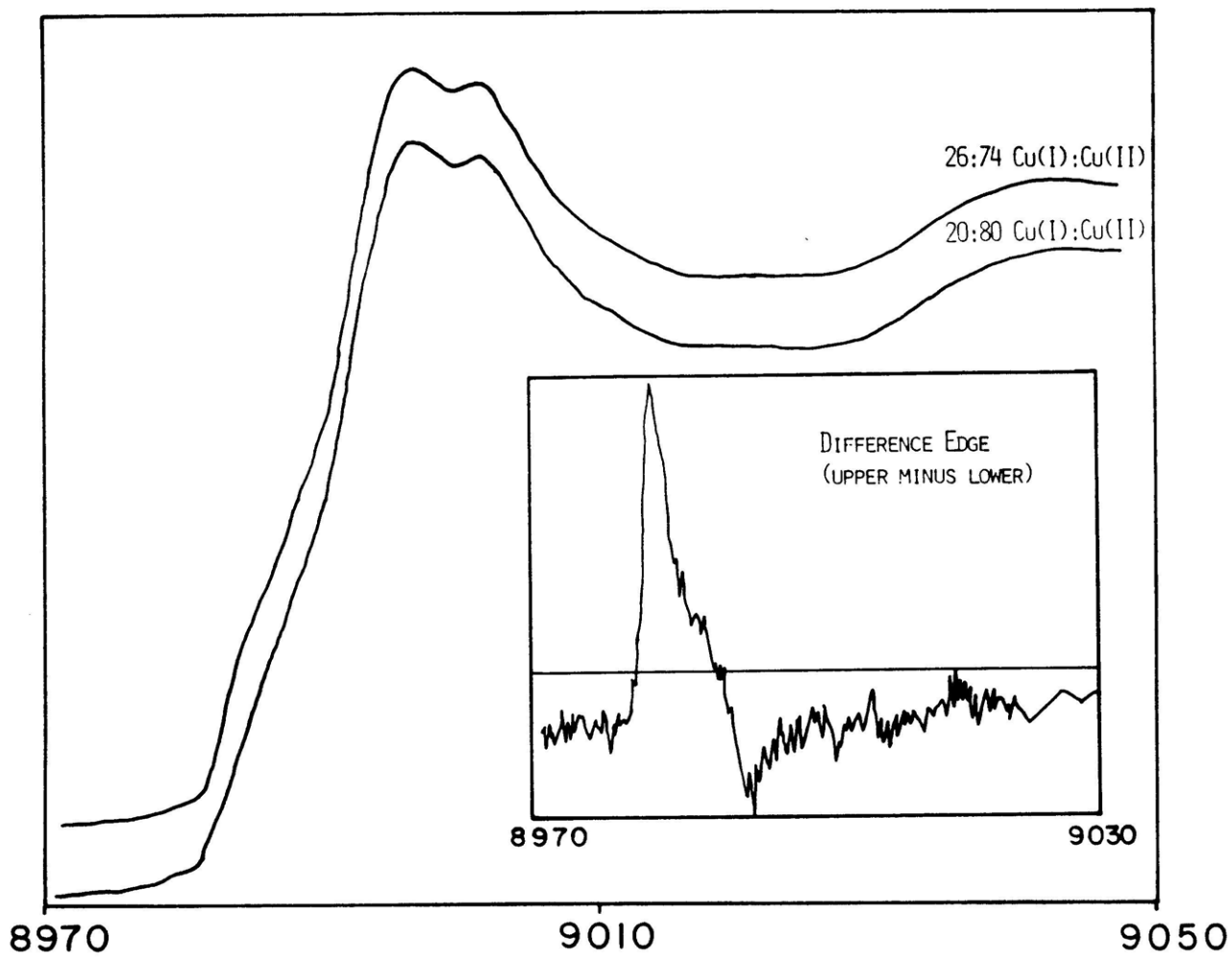
26:74 Cu(I):Cu(II)
20:80 Cu(I):Cu(II)
DIFFERENCE EDGE
(UPPER MINUS LOWER)
8970
9030
8970
9010
9050
ENERGY (eV)

binuclear copper is reoxidized by peroxide as also demonstrated in the initial qualitative x-ray absorption edge work.[7]

Having defined the oxidation state composition of T2D laccase and its peroxide treated derivative, one can define T2D nomenclature analogous to that of the hemocyanins.[24] T2D containing a reduced T3 site {T1:[Cu(II)]; T3:[Cu(I)Cu(I)} is referred to as deoxy T2D, and T2D laccase which has been oxidized by peroxide {T1:[Cu(II)]; T3:[Cu(II)Cu(II)]} will hereafter be referred to as met T2D.

Before presenting further quantitation of Cu edge results, it is important to consider conditions under which the difference edge technique could be in error. Extremely covalent Cu(II) complexes have features at ≈8984 eV which resemble those found in Cu(I) edges.[20] As there is no apparent Cu(I) signal in the peroxide treated T2D sample, none of the Cu(II) sites in laccase appear to be sufficiently covalent to cause interference. A 2-coordinate Cu(I) complex is also known which exhibits an unusually intense 8984 eV transition.[25] While complications due to very low coordination number at the T3 site in T2D cannot be conclusively excluded, the presence of 2-coordinate Cu(I) would at most reduce the estimate of Cu(I) percentages to 70% of the calculated values.[25] Since edge structure does depend

on absorber geometry,[26] unusual geometries (e.g. tetrahedral Cu(II)) must be tested before applying this technique. In the absence of other information regarding coordination geometry, this problem can be addressed by examining the fully oxidized and fully reduced forms of a given sample in order to "fine-tune" $\Delta\varepsilon$ to that particular sample. The difference edge method is expected to achieve highest accuracy when the samples being compared have nearly identical structures, although this is not essential (c.f. Figure 2.7).

When excess ferricyanide is reacted with T2D laccase, the intense absorption of the free oxidant at 420 and 330 nm precludes determination of any potential change in the protein absorbance in this region. However, difference edge analysis (Figure 2.9A) of the reaction of 25X ferricyanide with the untreated T2D indicates 70 $\pm$ 15% Cu(I) and shows no significant change in Cu(I):Cu(II) composition relative to that of the untreated T2D. Thus, the binuclear cuprous site is inert to ferricyanide oxidation. Peroxide addition to this ferricyanide-treated T2D, however, does yield an exclusively cupric edge spectrum (Figure 2.9C), difference analysis of which indicates <5% Cu(I), consistent with our results for peroxide on untreated T2D. These results are in disagreement with research accounts from Frank, et al.[11,12] (see Table 1) which claim that dialysis against aerobic

Figure 2.9 Normalized difference edge spectra at 210 K: exogenous oxidant reactivity of T2D laccase.

The laccase edges are referenced to a Cu(II) (N_2, O_2, S coordination) model complex.

(A) Untreated T2D + 25 protein equivalents $K_3Fe(CN)_6$;

(B) untreated T2D + 100 protein equivalents $NaNO_2$, preincubated 20 hours at 4°C;

(C) sample A, in ferricyanide + 30 protein equivalents H_2O_2. Analysis at the marked energies indicates that these difference edges correspond to 70 $\pm$ 15, 11 $\pm$ 5, and 0 $\pm$ 5% Cu(I), respectively. (0.1 M potassium phosphate, pH 6.0; [protein] ~1.2 mM).

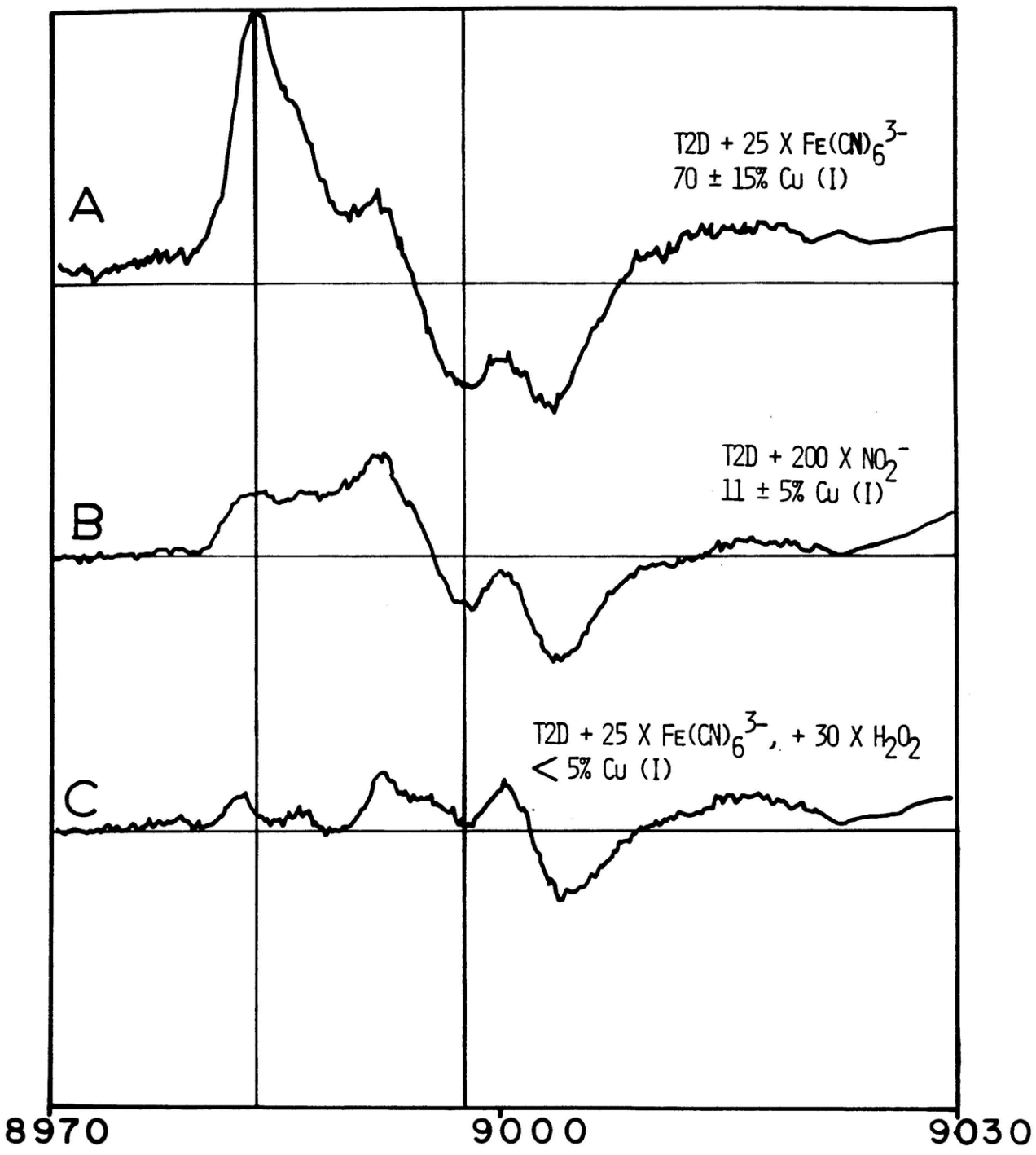
A
T2D + 25 X $Fe(CN)_6^{3-}$
70 ± 15% Cu (I)
B
T2D + 200 X NO_2^-
11 ± 5% Cu (I)
C
T2D + 25 X $Fe(CN)_6^{3-}$, + 30 X H_2O_2
< 5% Cu (I)
8970
9000
9030
ENERGY (eV)

ferricyanide results in a T2D protein form containing an oxidized T3 site but which displays no 330 nm absorption feature.

Excess nitrite also oxidizes the untreated T3 site, but whereas no detectable Cu(I) was found in the peroxide oxidized samples, Figure 2.9B represents 11 $\pm$ 5% Cu(I) which we attribute to ≈40% of the binuclear sites being [Cu(I)Cu(II)] through one electron reduction subsequent to the two electron oxidation (vide infra).

Direct reduction of the oxidized T3 site in met T2D by nitrite[27] or by ferrocyanide[28] produces 45 $\pm$ 5% half-met T2D, as determined from difference edge analysis (data not shown) and double integrated EPR intensities. Furthermore, difference edge analyses of deoxy and met T2D derivatives treated with excess nitrite show identical Cu(I) compositions (Figure 2.9B), which combined with relevant chemical and spectroscopic studies (Chapter 3), indicate that NO_2^- reacts with deoxy T2D and met T2D to generate indistinguishable half met-NO_2^- {T1:[Cu(II)]; T3:[Cu(I)Cu(II)]-NO_2^-} protein derivatives.

Parallel to the reactivity of the coupled binuclear copper site in hemocyanin,[24] $2e^-$ oxidation of T2D to form met T2D and the $1e^-$ reduction of met T2D to generate half met T2D

presumably occur via the NO derived from aqueous nitrite at pH <7.0. This suggests that the lack of T3 reoxidation by O_2 in the prepared T2D derivative is not due to neutral, small molecule inaccessibility as is further indicated by reversible CO binding studies to the reduced T3 site in the prepared T2D laccase (Chapter 3).

3. Peroxide Reactions of Type 2 Depleted and Native Laccase

Of the exogenous oxidants characterized in Section 2, peroxide is especially important to an understanding of the binuclear copper site in laccase because of its additional role as a potential exogenous ligand and as an intermediate in the 4-electron reduction of oxygen to water. While the XAS edge studies unambiguously showed that peroxide formally oxidizes the binuclear copper site, it was further possible that excess peroxide might bind to the oxidized T3 site and form a peroxy T2D laccase complex exhibiting an O_2^{2-} ---> Cu(II) CT transition at 330 nm. Thus, the question which remained for T2D laccase was whether the Δ 330 = 2000 $M^{-1}cm^{-1}$ represented endogenous protein ligand ---> Cu(II) CT which was absent in T2D laccase but reappeared upon oxidation of the Cu(I) by peroxide, or whether a significant portion of this absorption intensity was due to exogenous O_2^{2-} ---> Cu(II) CT of peroxide bound at the T3 site.

Several studies[29,30] have indicated that during catalytic function, it is the binuclear copper site in the native enzyme which initially binds O_2 for its reduction to water via a 2-electron reduced peroxide intermediate. Moreover, addition of peroxide to native laccase is reported to generate spectral changes at ≈330 nm ($\Delta\varepsilon 325 = 800\ M^{-1}cm^{-1}$, absorption and $\Delta(\Delta\varepsilon, 320) = -3.15\ M^{-1}cm^{-1}$ CD)).[31] From the reported studies, it was concluded that H_2O_2 binds to the native T3 site and forms a peroxylaccase complex,[31,32] producing the above spectral features in analogy to oxyhemocyanin, the peroxide bound derivative of met hemocyanin.[24] However, the chemical and spectroscopic studies of native and T2D laccase herein reported indicate significant differences between the hemocyanin and laccase coupled binuclear copper site, including significantly different optical changes for these proteins on reaction with peroxide. In contrast with the weak optical changes in laccase, unique and very different spectral features characterize peroxide binding to the hemocyanins[33] and tyrosinase[34] ($\Delta\varepsilon 345$ ≈20,000 $M^{-1}cm^{-1}$, $\Delta(\Delta\varepsilon, 320)$ ≈-30 $M^{-1}cm^{-1}$) (Figure 2.10).

Alternatively, the similarity of the spectral changes at 330 nm for H_2O_2 treated native laccase to those associated with the oxidation of the T3 site in T2D laccase suggests they might also be due to oxidation. We have therefore,

Figure 2.10 Electronic absorption and CD spectra: peroxide reactions of laccase and hemocyanin

(Left) laccase: 298 K (——) absorption and (– – –) CD difference spectra of [(native + 30X H_2O_2) - (native)] laccase (0.1 M potassium phosphate, pH 6.0; [protein] ~0.2 mM)

(Right) hemocyanin: 15 K absorption of (——) oxy and (•••••) met derivatives and 298 K CD spectrum (– – –) of oxy.

PEROXIDE REACTIONS

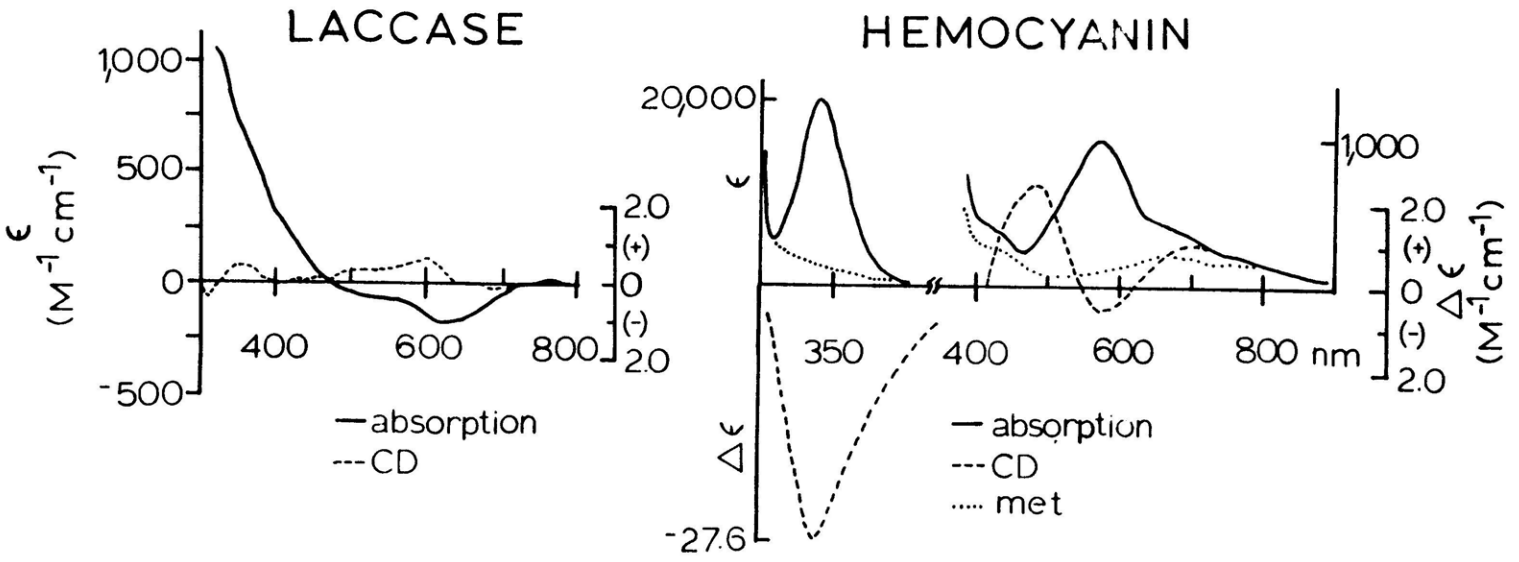

through XAS difference edge analysis, further investigated[35] the nature of the changes in the 330 nm absorption which are associated with O_2^{2-} reactions in both T2D and native laccase. First, we will correlate the quantitative x-ray technique with optical spectroscopy, and probe the effects of sequential H_2O_2 addition to T2D laccase. The dependence of the T2D XAS edge structure on added H_2O_2 is shown in Figure 2.11A. With increasing H_2O_2 concentration, the intensity of the 8984 eV transition decreases and that at 9000 eV increases, demonstrating that Cu(I) is being oxidized to Cu(II). The isosbestic point at 8994 eV indicates that change is occuring in only two absorbing species. No detectable change is observed in the integrated EPR intensity, establishing that the redox state of the remaining (T1) copper in T2D laccase in unaffected by H_2O_2. The difference edges (inset, Figure 2.11A) thus accurately reflect changes in only the T3 copper site.[36] In the optical spectrum (Figure 2.11B) the peroxide reaction results in a new 330 nm absorption feature[7] which is similar to that observed in native laccase as previously discussed; no significant change occurs in the CD. Within experimental error, the increase in intensity of the absorption band at 330 nm correlates linearly to the decrease in the x-ray absorption feature at 8984 eV (Figure 2.12). Reaction with 60X H_2O_2 yields an overall $\Delta\varepsilon 330 \approx 2000\ M^{-1}cm^{-1}$ and a 70 $\pm$ 15% change in Cu(I); higher $[H_2O_2]$ leads to irreversible protein

Figure 2.11 X-ray/vis-UV absorption spectra: peroxide titration of T2D laccase.

(A) Normalized x-ray absorption edge spectra (210 K) of T2D laccase in the presence of: 0, 5, 25, and 60 protein equivalents H_2O_2. Data have been smoothed with a Gaussian-weighted running average (Gaussian width = 1.6 eV). Arrows indicate direction of change on treatment with H_2O_2.

Inset: Unsmoothed, normalized difference edge spectra of these samples, relative to 60X H_2O_2.

(B) (Upper) 298 K electronic absorption spectra for the same T2D samples (1 mm pathlength); (Lower) CD spectra of T2D laccase before (——) and after (– – –) treatment with 50X H_2O_2 (1 cm pathlength); (0.1 M potassium phosphate, pH 6.0; [protein] ~1 mM, x-ray; Absorption; ~0.15 mM CD).

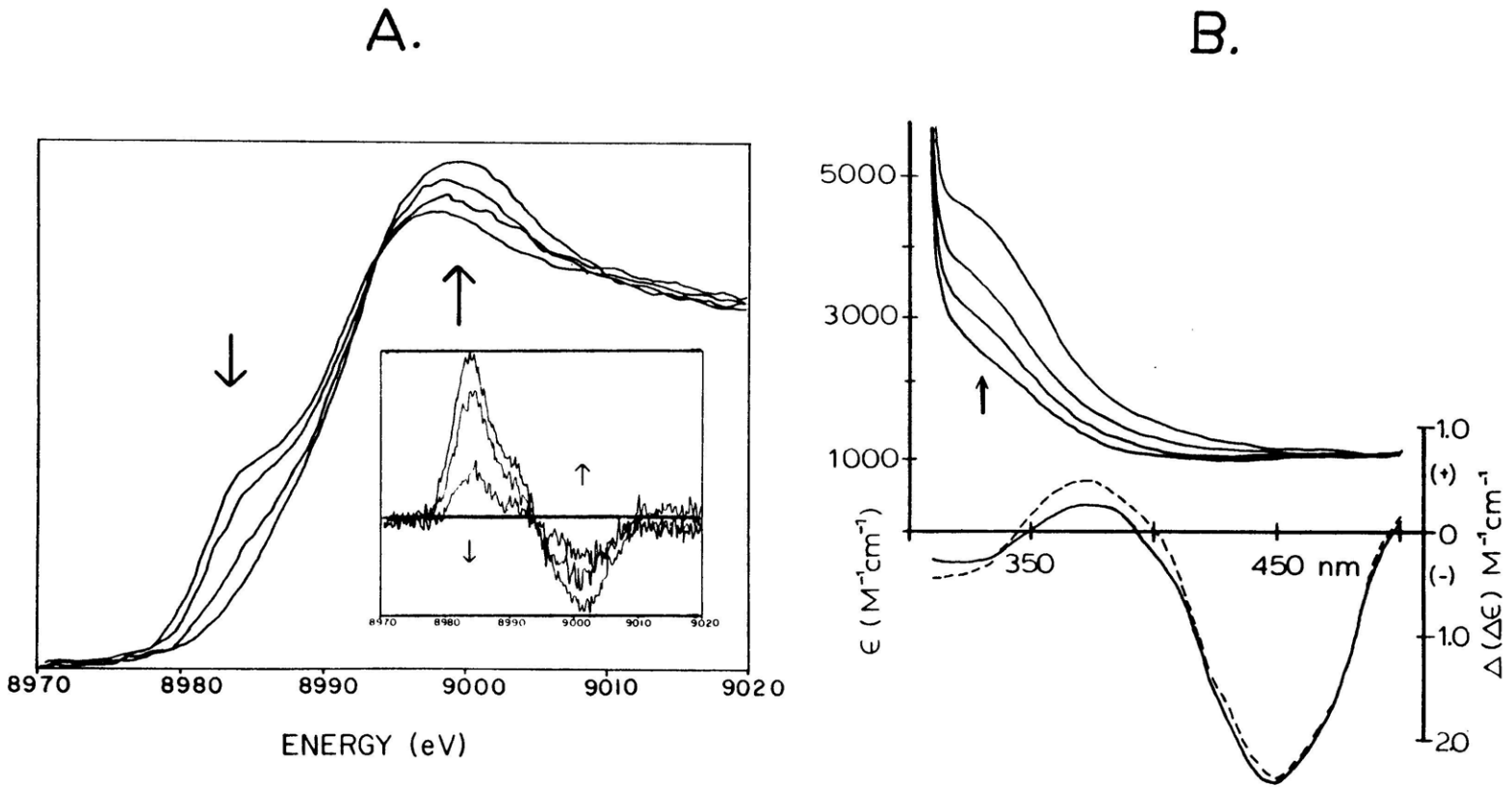
A.
B.
8970
8980
8990
9000
9010
9020
ENERGY (eV)
5000
3000
1000
350
450 nm
1.0
(+)
0
(-)
1.0
2.0

Figure 2.12 Correlation: $\Delta\varepsilon_{8984}$ and $\Delta\varepsilon_{330}$ for T2D laccase samples on treatment with H_2O_2.

All absorbance changes are referenced to the fully oxidized (60X H_2O_2) sample.[36] The stoichiometric excess of [H_2O_2] is indicated for each data point (X).

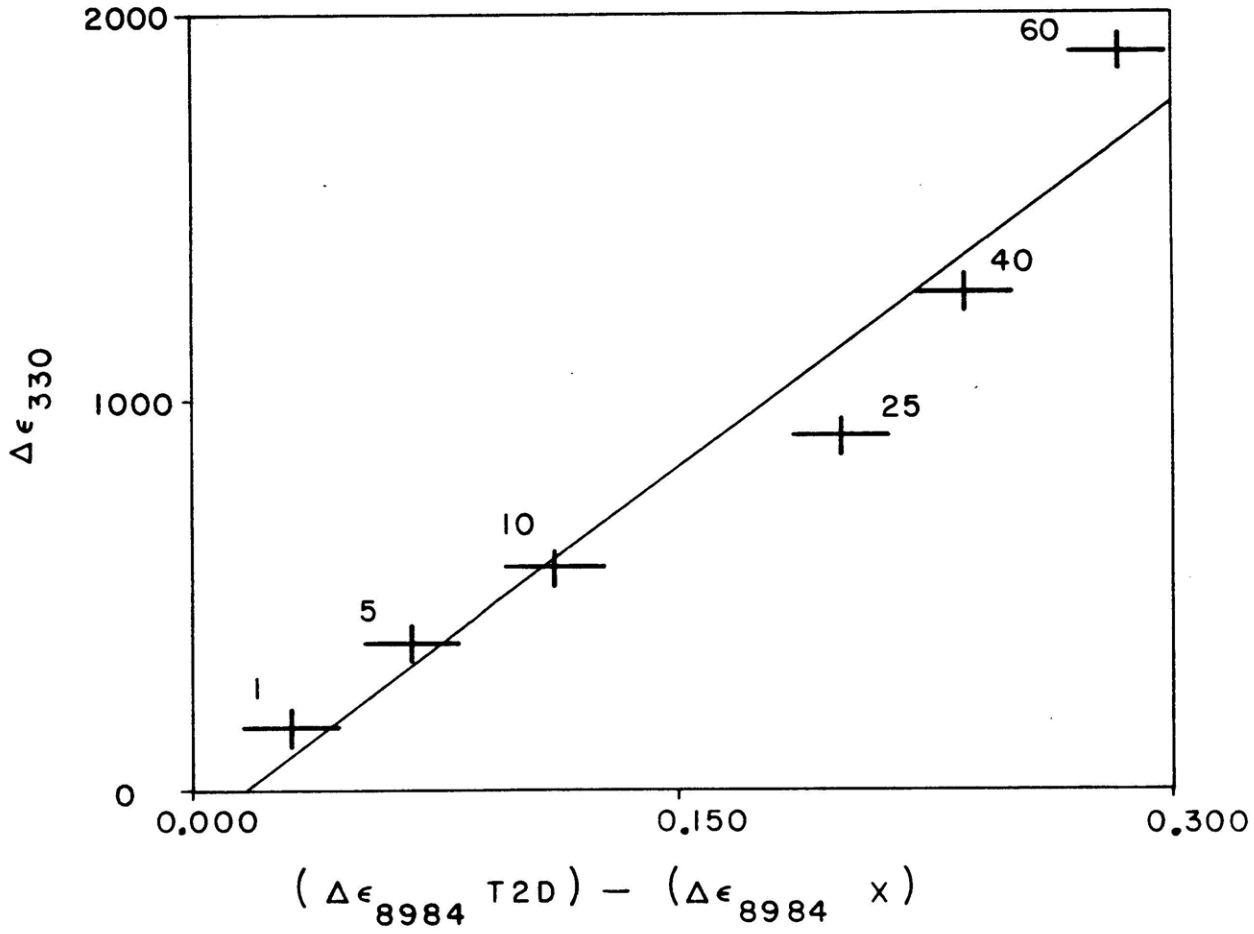
2000
1000
0
$\Delta\epsilon_{330}$
60
40
25
10
5
1
0.000
0.150
0.300
$(\Delta\epsilon_{8984\ T2D}) - (\Delta\epsilon_{8984\ X})$

damage. The linear correlation of these changes indicates that H_2O_2 is acting as an oxidant throughout the titration; no new spectral features are observed. If peroxide further bound to the oxidized T3 site, (as has been proposed by Frank, P., Farver, O., and Pecht, I. **1983** J. Biol. Chem. 258, 11112-11117), 330 nm intensity would continue to increase even after all of the T3 sites were reoxidized. Moreover, one would expect significant additional spectral features, based on the intense O_2^{2-} ---> Cu(II) CT transitions observed upon peroxide binding to the coupled binuclear copper sites in hemocyanin and tyrosinase (Figure 2.10).[24] Such transitions are not observed.

The presence of binuclear cuprous sites in T2D and their stability to oxidation by O_2 but not H_2O_2 suggested that the similar, although weaker, optical changes (Figures 2.10 and 2.13 B) observed in peroxide reactions of the native enzyme might also be due to oxidation. We therefore extended our XAS edge studies to native laccase, both as isolated and after treatment with excess H_2O_2. EPR and optical spectra demonstrate that the T1 and T2 copper sites are fully oxidized. The difference of their XAS edges (Figure 2.13A, inset) must therefore again reflect a change at only the T3 site. Calibrated to a fully reduced T3 site in the untreated T2D laccase (but corrected for the additional T2 Cu(II) absorber present in native laccase), the difference edge

Figure 2.13 X-ray/vis-UV absorption spectra: peroxide reaction of native laccase.

(A) Comparison of normalized x-ray absorption edge spectra at 210 K of native laccase (dark) and native laccase treated with 30 protein equivalents of H_2O_2 (light).

Inset: Difference spectrum of [native - (native + 30 X H_2O_2)] laccase edges, smoothed with a gaussian-weighted running average 1.6 eV wide.

(B) (Upper) 298 K electronic absorption and (Lower) CD spectra for the same laccase samples before (——) and after (— — —) treatment with 30X H_2O_2. (1 mm pathlength; pH 6.0; [protein] ~1.2 mM).

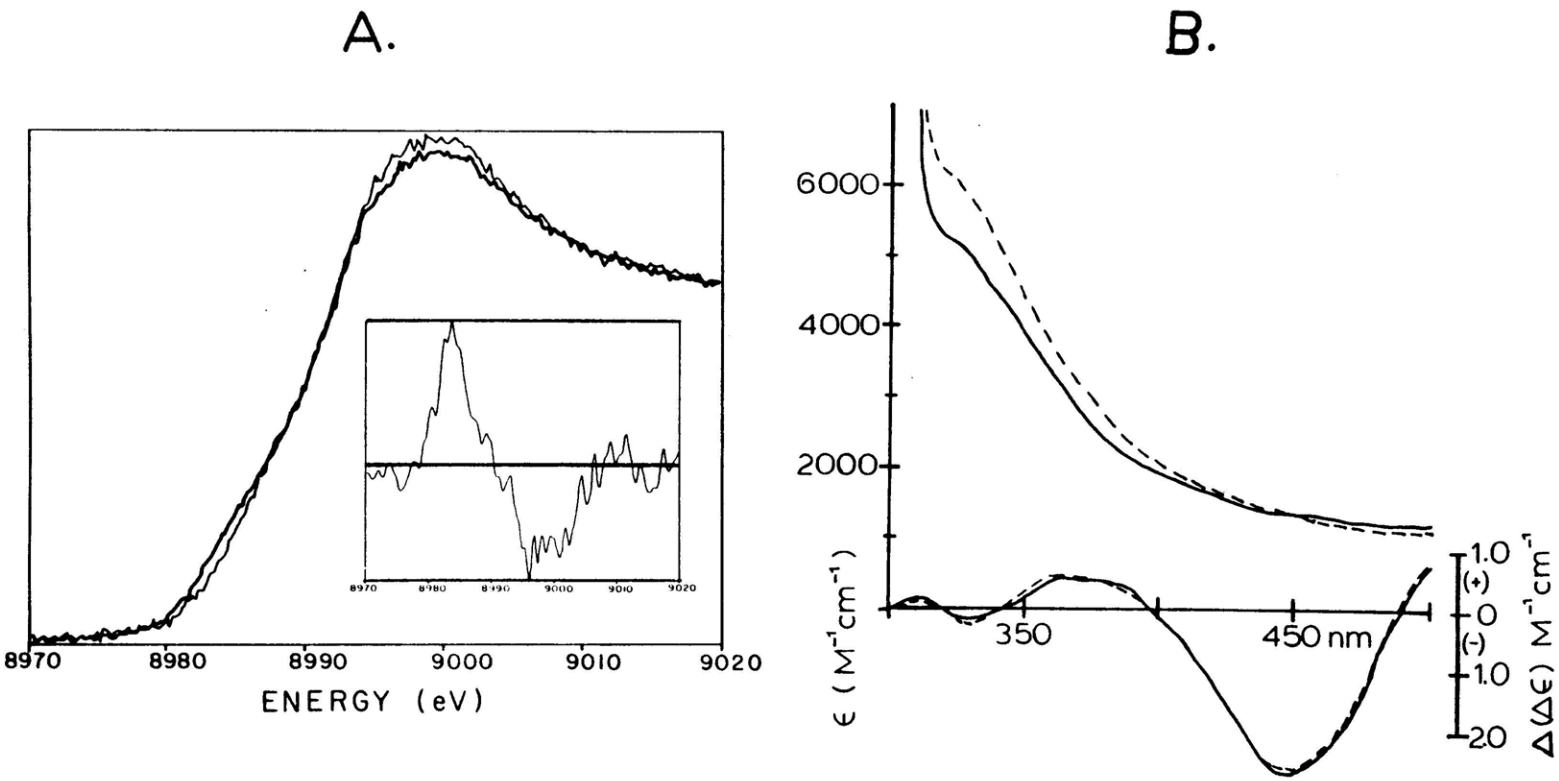
A.
B.
8970
8980
8990
9000
9010
9020
ENERGY (eV)
6000
4000
2000
350
450 nm
1.0
(+)
0
(-)
1.0
2.0

corresponds to 12 ± 3% overall Cu(I), or reduction of ~25% of the T3 sites in the native, as isolated, laccase.

Using the linear relationship between $\Delta\varepsilon 330$ and $\Delta\varepsilon 8984$ in T2D laccase (Figure 2.12), we calculate that at least $\Delta\varepsilon 330 = 440 \pm 100$ is expected when H_2O_2 is reacted with native laccase solely as a result of oxidation of reduced type 3 sites. This calculation depends only on the $\Delta\varepsilon$ values, and is independent of the precise extent of T3 reduction in T2D laccase. Previous studies[31,32] have used $\Delta\varepsilon 325 = 800\ M^{-1}cm^{-1}$ absorption and $\Delta(\Delta\varepsilon, 320) = -3.15\ M^{-1}cm^{-1}$ CD features to conclude that peroxide binds to native laccase. After correcting for T3 oxidation, no absorption features remain which could reasonably reflect peroxide ---> Cu(II) CT. Titration studies[30a,38] further indicate that the increase at 330 nm represents a single, continuous reaction. The CD change ($|\Delta(\Delta\varepsilon 320)| < 0.3\ M^{-1}cm^{-1}$) observed in our[37] and other[38] laboratories is also accounted for by the oxidation of ≈25% of the binuclear copper sites.

We can use the observed $\varepsilon 330 = 2000 \pm 200\ M^{-1}cm^{-1}$ for the T3 site in T2D and the ratio of the observed ($800\ M^{-1}cm^{-1}$) and calculated ($440 \pm 100\ M^{-1}cm^{-1}$) ε 330 in native laccase to estimate an $\varepsilon 330 = 3600 \pm 900\ M^{-1}cm^{-1}$ for the fully oxidized native enzyme. A similar value results when the reported $\varepsilon = 2800\ M^{-1}cm^{-1}$ is corrected for T3 oxidation ($\Delta\varepsilon 800\ M^{-1}cm^{-1}$).

In conclusion, the increase in intensity of the 330 nm absorption feature which results from peroxide titration of T2D laccase correlates linearly with the percent of oxidation of the binuclear copper site. This indicates that peroxide oxidizes, but does not bind to the T3 site. This correlation has been used to determine that native laccase as isolated contains ≈25% reduced binuclear copper sites and that all spectral changes observed upon peroxide addition to native laccase can be accounted for by oxidation of these reduced sites. The lack of additional intense spectral features upon peroxide addition to both T2D and native laccase indicate that peroxide binding is not observed, contrary to all previous literature reports. This is extremely important to the interpretation of many of the chemical and spectroscopic studies which follow.

References and Notes

1. Graziani, M.T.; Morpurgo, L.; Rotilio, G.; Mondovi, B. FEBS Lett. **1976**, 70, 87-90.
2. Reinhammar, B. Biochim. Biophys. Acta **1972**, 275, 245-259.
3. Morpurgo, L.; Graziani, M.T.; Finazzi-Agro, A.; Rotilio, G.; Mondovi, B. Biochem. J. **1980**, 187, 361-366, in 0.05 M NaOAc, pH 5.2 and 0.1 M PPB, pH 6.0.
4. Morpurgo, L.; Rotilio, G.; Finazzi-Agro, A.; Mondovi, B. Biochim. Biophys. Acta **1974**, 336, 324-328.
5. Reinhammar, B.; Oda, Y. J. Inorg. Biochem. **1979**, 11, 115-127, in 0.25 M PPB, pH 7.4.
6. Morpurgo, L.; Graziani, M.T.; Desideri, A.; Rotilio, G. Biochem. J. **1980**, 187, 367-370.
7. LuBien, C.D.; Winkler, M.E.; Thamann, T.J.; Scott, R.A.; Co, M.S.; Hodgson, K.O.; Solomon, E.I. J. Am. Chem. Soc. **1981**, 103, 7014-7016.
8. a. Brown, J.M.; Powers, L.; Kincaid, B.; Larrabee, J.A.; Spiro, T.G. J. Am. Chem. Soc. **1980**, 102, 4210-4216.
   b. Hu, V.W.; Chan, S.I.; Brown, G.S. Proc. Natl. Acad. Sci. USA **1977**, 74, 3821-3825.
   c. Eccles, T.K. Ph.D. Dissertation, **1977**, Stanford University, Stanford, CA.

9. Morpurgo, L.; Desideri, A.; Rotilio, G.; Mondovi, B. FEBS Lett. **1980**, 113, 153-156.

10. Reinhammar, B. J. Inorg. Biochem. **1983**, 18, 113-121.

11. Farver, O.; Frank, P.; Pecht, I. Biochem. Biophys. Res. Comm. **1982**, 108, 273-278, in 0.1 M HEPES, pH 7.4.

12. Frank, P.; Farver, O.; Pecht, I. J. Biol. Chem. **1983**, 258, 11112-11117.

13. Frank, P.; Farver, O.; Pecht, I. Inorg. Chim. Acta **1984**, 91, 81-88.

14. Hahn, J.E.; Co, M.S.; Hodgson, K.O.; Spira, D.J.; Solomon, E.I. Biochem. Biophys. Res. Comm. **1983**, 112, 737-745.

15. Reinhammar, B. Biochim. Biophys. Acta **1970**, 205, 35-47.

16. Kolthoff, I.M.; Sandell, E.B.; Meehan, E.J.; Bruckenstein, S. Quantitative Chemical Analysis **1969** (Macmillan Co.: N.Y.).

17. Scott, R.A.; Hahn, J.E.; Doniach, S.; Freeman, H.C.; Hodgson, K.O. J. Am. Chem. Soc. **1982**, 104, 5364-5369.

18. This transition has been assigned as 1s ---> 4s with the corresponding (weak) 1s ---> 4s transition in (approximately square planar) Cu(II) complexes being assigned as a shoulder at ≈ 8987 eV[8b,19]. Recent calculations [Kutzler, F.W. Ph.D. Thesis, **1981**, Stanford University] demonstrate that such atomic descriptions are overly simplistic. To avoid future confusion, we will refer to this transition only as the "8984 eV transition".

19. Hu, V.W.; Chan, S.I.; Brown, G.S. FEBS Lett. **1977**, 84, 287-290.

20. a. Powers, L.; Blumberg. W.E.; Chance, B.; Barlow, C.; Leigh, J.S., Jr.; Smith, J.C.; Yonetani, T.; Vik, S.; Peisach, J. in Frontiers of Biological Energetics **1978**, Dutton, P.L.; Leigh, J.S.; Scarpa, A., Eds. (Academic Press) Volume 2, pp. 863-871.

b. Powers, L.; Blumberg. W.E.; Chance, B.; Barlow, C.; Leigh, J.S., Jr.; Smith, J.C.; Yonetani, T.; Vik, S.; Peisach, J. in Cytochrome Oxidase **1979**, King, T.E.; Orii, Y.; Chance, B.; Okunuki, K., Eds. (Elsevier) pp. 189-195.

c. Powers, L.; Blumberg, W.E.; Chance, B.; Barlow, C.; Leigh, J.S., Jr.; Smith, J.C.; Yonetani, T.; Vik, S.; Peisach, J. Biochim. Biophys. Acta **1979**, 546, 520-538.

21. Blumberg, W.E.; Peisach, J.; Eisenberger, P.; Fee, J.A. Biochem. **1978**, 17, 1842-1846.

22. Tullius, T.D.; Gillum. W.O.; Carlson, R.M.K.; Hodgson, K.O. J. Am. Chem. Soc. **1980**, 102, 5670-5676.

23. Brudvig, G.W.; Bocian, D.F.; Gamble, R.C.; Chan, S.I. Biochim. Biophys. Acta **1980**, 624, 78-89.

24. Solomon, E.I. in Copper Proteins **1981**, Spiro, T.G., Ed. (Wiley-Interscience: New York) Chapter 2.

25. Co, M.S.; Hodgson, K.O., unpublished results.

26. Shulman, R.G.; Yafet, T.; Eisenberger, P.; Blumberg, W.E. Proc. Natl. Acad. Sci. USA **1976**, 73, 1384-1388.

27. Spira, D.J.; Solomon, E.I. Biochem. Biophys. Res. Comm. **1983**, 112, 729-736.

28. Spira, D.J.; Winkler, M.E.; Solomon, E.I. Biochem. Biophys. Res. Comm. **1982**, 107, 721-726.

29. Aasa, R.; Branden, R.; Deinum, J.; Malmstrom, B.G.; Reinhammar, B.; Vanngard, T. Biochem. Biophys. Res. Comm. **1976**, 70, 1204-1209.

30. Andreasson, L.E.; Branden, R.; Reinhammar, B. Biochim. Biophys. Acta **1976**, 438, 370-379.

31. a. Farver, O.; Goldberg, M.; Lancet, D.; Pecht, I. Biochem. Biophys. Res. Comm. **1976**, 73, 494-500.

    b. Farver, O.; Goldberg, M.; Pecht, I. FEBS Lett. **1978**, 94, 383-386.

32. a. Farver, O.; Goldberg, M.; Pecht, I. Eur. J. Biochem. **1980**, 104, 71-77.

    b. Farver, O.; Pecht, I. in Copper Proteins **1981**, Spiro, T.G., Ed. (Wiley-Interscience: New York) Chapter 4.

33. Eickman, N.C.; Himmelwright, R.S.; Solomon, E.I. Proc. Natl. Acad. Sci. USA **1979**, 76, 2094-2098.

34. Himmelwright, R.S.; Eickman, N.C.; LuBien, C.D.; Lerch, K.; Solomon, E.I. J. Am. Chem. Soc. **1980**, 102, 7339.

35. Hahn, J.E.; Hedman, B.; Hodgson, K.O.; Spira, D.J.; Solomon, E.I. Biochem. Biophys. Res. Comm. **1984**, 119, 567-574.

36. Note that referencing all samples to fully oxidized T2D precludes errors due to inappropriately chosen model compounds, differences in resolution, or T1 copper contributions to the T2D edge structure.

37. a. Winkler, M.E.; Spira, D.J.; LuBien, C.D.; Thamann, T.J.; Solomon, E.I. Biochem. Biophys. Res. Comm. **1982**, 107, 727-734.

b. LuBien, C.D.; Spira, D.J.; Winkler, M.E.; Solomon, E.I., to be published.

38. a. Dooley, D.M.; Gray, H.B., private communication.

b. Morpurgo, L. International Conference on Bio-Inorganic Chemistry, Florence, Italy, June, 1983.

III. CHEMICAL AND SPECTROSCOPIC STUDIES OF THE COUPLED BINUCLEAR COPPER SITE IN TYPE 2 DEPLETED LACCASE: COMPARISON TO THE HEMOCYANINS AND TYROSINASE

A. Introduction

In this chapter, detailed studies of the electronic and geometric structure of the coupled binuclear copper site in T2D laccase will be presented and compared to the coupled binuclear copper site in the hemocyanins and tyrosinase. Having fully characterized the prepared T2D and devised a method for copper ion oxidation state determination, the chemistry of T2D can now be developed. Through this research, a series of active site derivatives have been prepared in which the oxidation and/or ligation state of the T3 site has been systematically varied. In the presence of an oxidized T1 center, protein forms are now accessible wherein the T3 coppers are reduced, mixed valence and oxidized, which are defined, in analogy to hemocyanin and tyrosinase chemistry,[1,2] as deoxy, half met, and met T2D, respectively. These derivatives, while prepared by different chemical paths, directly parallel the well-characterized hemocyanin and tyrosinase active site derivatives and hence allow systematic comparison of the oxidase T3 site to the hemocyanin and tyrosinase coupled binuclear sites in a variety of protein forms. Similarities and important differences exist in these derivatives and provide significant insight into how differences in binuclear copper active site structure relate to differences in biological function, that is, the reversible *vs.* irreversible binding of O_2 and reduction to H_2O in these systems.

Summarized in Scheme 3.1 is an overview of the chemistry of T2D; in part 1 of this chapter a detailed examination of the chemistry and spectroscopy of each derivative is presented, and in part II, these results will be compared to related studies on the hemocyanins and tyrosinase. The prepared, or deoxy T2D {T1:[Cu(II); T3:[Cu(I)Cu(I)]} is oxidized by either peroxide or the nitric oxide generated from aqueous nitrite at pH < 7.0 to form the met T2D {T1:[Cu(II)]; T3:[Cu(II)Cu(II)]} derivative. Met can then undergo a one-electron reduction upon reaction with either ferrocyanide or an additional molecule of aqueous NO to generate the half met-aquo {T1:[Cu(II)]; T3[Cu(II)Cu(I)]} or half met-NO_2^- protein forms, respectively. The half met derivatives can undergo further ligand substitution chemistry or oxidation by peroxide to yield met T2D laccase.

B. Experimental

Native and T2D laccase were prepared as described in Chapter 2. In later samples, T2D laccase was additionally run through a short column of DEAE-A50 to remove nearly 100% of the residual $Fe(CN)_6^{3-}$ from the preparative procedure. This resulted in T2D protein in which 330/614 ≈0.350-0.400.

Water is purified to a resistivity of 15-18 MΩ-cm through a Sybron Barnstead Nanopure deionizing system. All

SCHEME 3.1. CHEMISTRY: TYPE 2 DEPLETED LACCASE

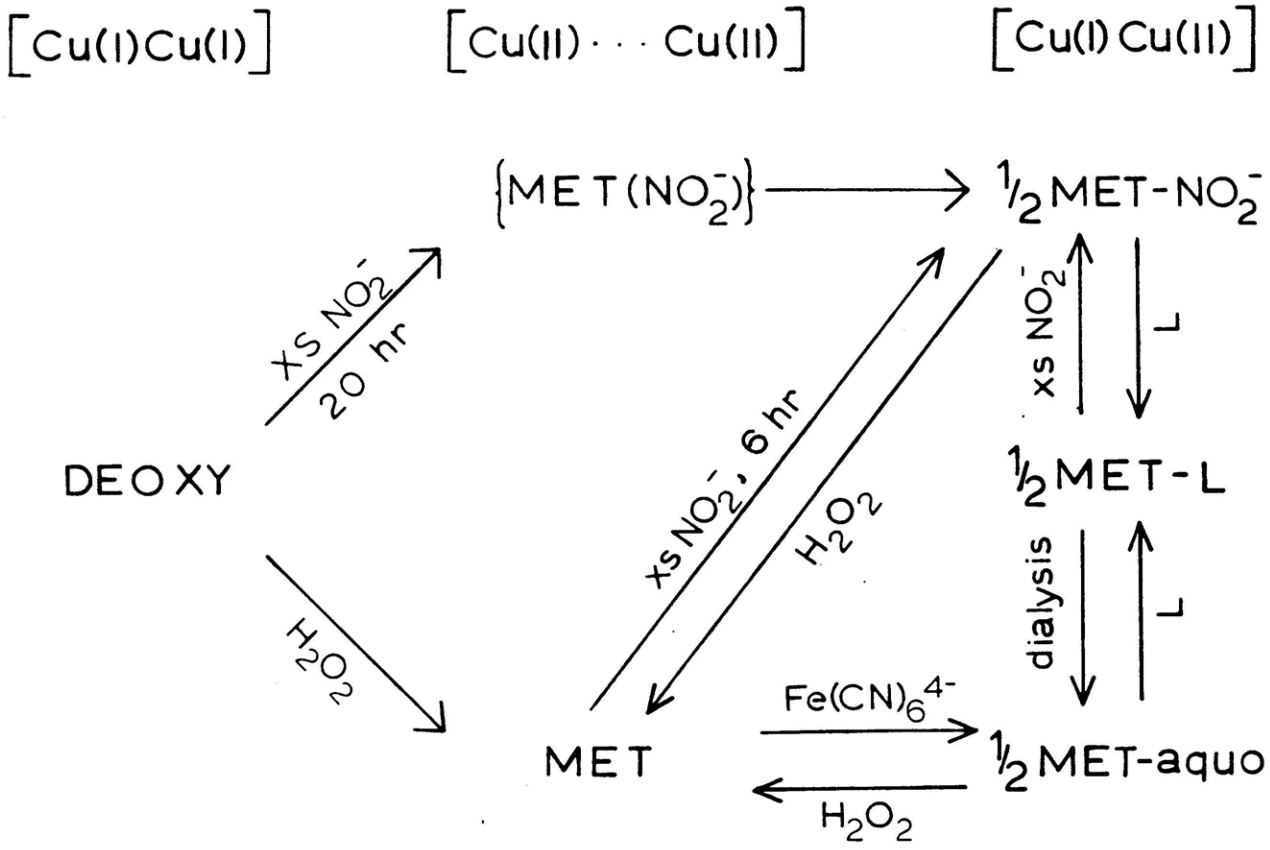

studies are in 0.1 M PPB, pH 6.0 unless otherwise stated and utilized reagent grade chemicals without further purification. Protein solutions were made anaerobic by repeated vacuum pump/N_2 purge cycling on an N_2 Schlenk line equipped with a chromous[3] perchlorate bubbler. Typically, exogenous anion reactivity studies were performed by direct addition of the anion (in a 5-10 μL aliquot of appropriate concentration) followed by 24-40 hour incubation at 4°C. Equilibrium binding constants were calculated as described by Byers.[4] Reagent grade peroxide (30% aqueous solution) was standardized by permanganate.[5]

99.5% CO(g) was purchased from Matheson. Experiments under ≈1 atm CO were performed in 2 mL serum stoppered disposable test tubes by first evacuating T2D laccase solutions to remove oxygen and then replacing it with CO gas; equilibration was routinely 45-60 minutes. For higher pressures of CO (≈2 atm), protein solutions were placed in a 20 mL high pressure glass reaction vessel (Lab glass, Vineland, New Jersey). 298 K absorption spectra under 1 atm CO were recorded in a 1 cm quartz cell with an 0.5 L gas reservoir on a Cary 17 spectrophotometer.

Sodium nitrite(s) was added directly to the aerobic protein solutions in 5 mL reaction vials. These were

lightly sealed so as to generally prevent protein spillage but to allow slow gas exchange. These vials were then stored in 300 mL centrifuge bottles which were tightly sealed to prevent escape of toxic gases over the extended reaction time at 4°C.

Optical absorption spectra at 298 K were measured in 1 cm quartz cells on a Cary 14 spectrophotometer. Spectra at 77 K were recorded in 50% v/v glycerol/0.1 M potassium phosphate, pH 6.0 between quartz disks with typical pathlengths of ≈1.4 mm. For these spectra, an Air Products LTD-3-110 Heli tran liquid helium transfer refrigerator and temperature controller were used in combination with a cryotip sample holder mounted to a Cary 17 spectrophotometer. CD spectra were recorded in 1 cm cells on a Jasco J-500C spectropolarimeter operating with an S1 and S20 photomultiplier tube for the near-IR and visible-UV spectral regions, respectively. CD calibration was with camphor sulfonic acid and positive ($\Delta\varepsilon$)'s correspond to Left-Right circularly polarized light. CD data were digitized in 5 nm increments and baseline corrected using a Houston Instruments Hipad digitizer. The digitized intensities were entered into a DEC PDP-1124 computer for conversion to molar extinction coefficients (from millidegree values obtained from the spectrometer), data manipulation, and spectral plotting on a Hewlett Packard 7225 B Plotter.

Total copper ion concentrations in T2D derivatives were routinely determined by atomic absorption spectroscopy using a Perkin-Elmer model 2380 AA spectrophotometer equipped with an HGA 400 graphite furnace; conditions were as described in Chapter 2. A Bruker ER 220 D-SRC EPR spectrometer (operating at 100 KHz modulation, at 10 mW incident power and 20 G modulation amplitude, unless otherwise stated) was used to examine frozen protein solutions at a microwave frequency ≈9.27 GHz at 77K; sample temperatures between 7 and 60 K were obtained at ≈9.40 GHz with an Air Products LTD-3-110 Heli-Tran liquid helium transfer refrigerator and a Lake Shore Cryotronics, Inc. cryogenic temperature controller, model DTC-500. Computer EPR simulation was performed with the program GNDIMER obtained from Professor John Pilbrow at Monash University, Australia. EPR difference spectra were calculated on a Nicolet Instrument Corporation NIC-1180E Data Processor which was interfaced to the Bruker EPR spectrometer.

X-ray absorption edge data were collected at the Stanford Synchrotron Radiation Laboratory (SSRL), as described in Chapter 2. All EXAFS data were also collected at SSRL using Si[220] monochromator crystals, and were recorded (at -60° C) as fluorescence excitation spectra by using an array of NaI(Tl) scintillation counters with Ni filters. The energy scale was calibrated relative to a Cu

foil, with the first preedge inflection of the Cu K-absorption edge being assigned to 8980.3 eV. EXAFS data reduction and analysis are described in reference 6. EXAFS data are normalized per copper atom and are reported as average values per atom present. First and final scan comparison of the X-ray spectra, as well as optical and EPR characterization after irradiation ascertained protein integrity.

C. Results and Discussion

1. Chemical and Spectroscopic Studies of Type 2 Depleted Laccase Derivatives

a. Deoxy T2D Laccase

i. Spectroscopic Properties

The prepared,[7] or deoxy T2D contains a [Cu(I)Cu(I)] type 3 site[8] (see Chapter 2) and is the simplest of the coupled binuclear copper active site derivatives of T2D laccase. As the T3 site is reduced and the T2 copper is removed, the optical and EPR features are primarily those of the T1 cupric center. In the electronic absorption spectrum (Figure 3.1) the T1 copper absorbs strongly at 614 nm, ε = 5700 $M^{-1}cm^{-1}$ and weakly at ≈450 nm, ε < 200 $M^{-1}cm^{-1}$. The

Figure 3.1 Electronic absorption spectra at 77 and 298 K: deoxy T2D laccase.

(———) 298 K; (– – –) 77 K. 50% v/v glycerol/ 0.1 M potassium phosphate, pH 6.0; [protein] = 0.95 mM, pathlength = 1.5 mm).

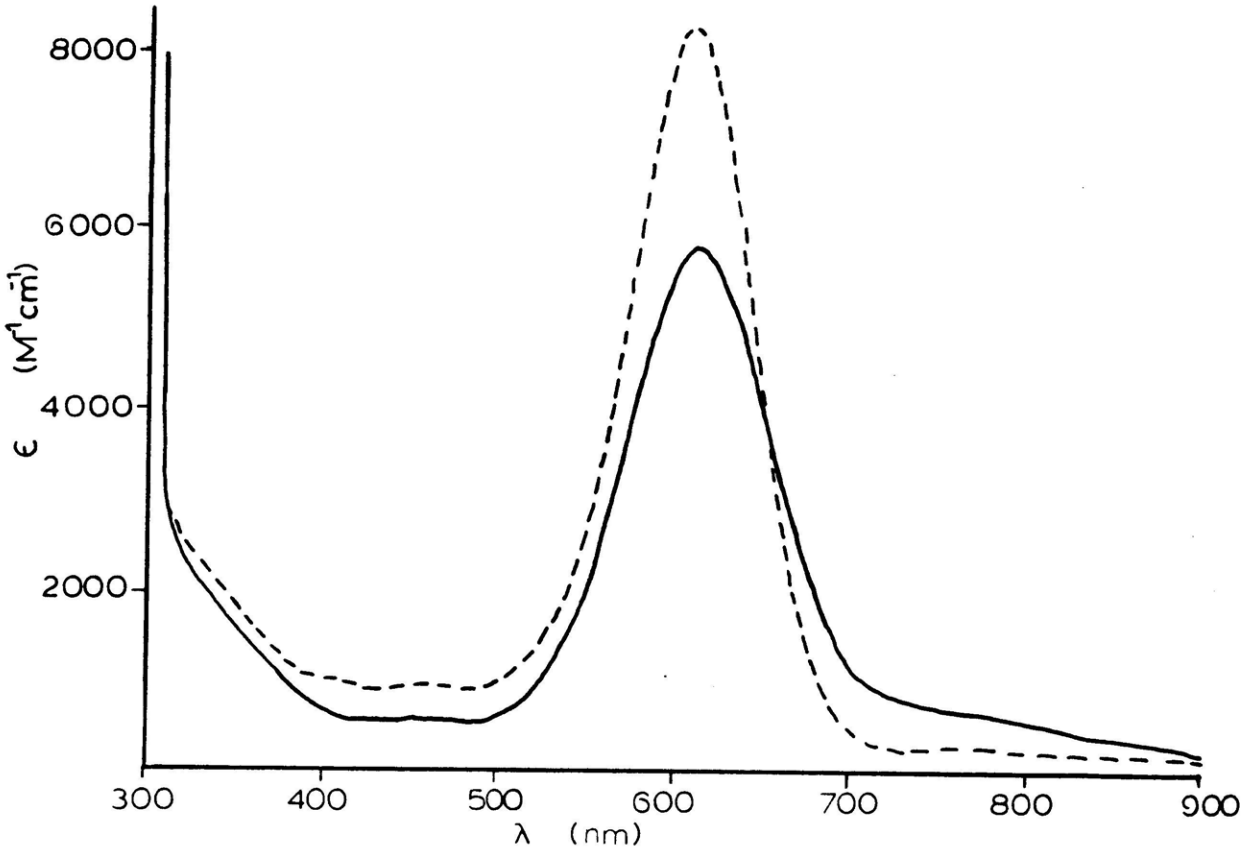
8000
6000
4000
2000
ε (M⁻¹cm⁻¹)
300
400
500
600
700
800
900
λ (nm)

shoulder at ≈400 nm is not copper-related but rather appears to be due to extraneous (less than 0.1 protein equivalent) but specifically bound ferricyanide which is an artifact of the T2D preparative procedure.[9] Upon cooling deoxy T2D to 77K, no new features appear in the 900-300 nm absorption spectrum. As shown in Figure 3.1, the Blue band sharpens by ≈40% (no new integrated intensity), and the aforementioned CT bands at 450 and 400 nm are more clearly defined.

Transitions of the T1 Cu(II) also dominate the CD spectrum of deoxy T2D. In the near-IR (Figure 3.2A), two transition envelopes are centered at ≈840 nm ($\Delta\varepsilon$) = -2.4 $M^{-1}cm^{-1}$) and 730 nm ($\Delta\varepsilon$) = -2.8 $M^{-1}cm^{-1}$). In the visible region (Figure 3.2B), the blue absorption feature is split into at least two CD transitions which maximize at 600 nm ($\Delta\varepsilon$) = +1.5 $M^{-1}cm^{-1}$ and at 535 nm ($\Delta\varepsilon$) = +1.4 $M^{-1}cm^{-1}$, and similar to the Blue copper proteins,[10] an intense CT transition is observed at 450 nm ($\Delta\varepsilon$) = -2.9 $M^{-1}cm^{-1}$. In the 77 K EPR spectrum (Figure 3.3), the T1 Cu(II) is characterized by $g_{||}$ = 2.300, $g_{\perp}$ = 2.06 and $A_{||}$ = 37.8 X 10^{-4} cm^{-1}. The broad, weak feature at ≈2650 G derives primarily from an impurity in the cavity of our EPR spectrometer but also contains an additional component which does not saturate as mononuclear copper and would therefore also appear to be ferricyanide-related. This signal is not perturbed by reaction with exogenous oxidants or ligands and will not be

Figure 3.2 CD spectra at 298 K: deoxy T2D laccase

(A) near IR and,

(B) visible-UV spectral regions

(0.1 M potassium phosphate, pH 6.0; [protein] = 0.271 mM).

Figure 3.3 EPR spectrum at 77 K: deoxy T2D laccase

(9.26 GHz; 50% v/v 0.1 M potassium phosphate, pH 6.0; [protein] = 0.95 mM).

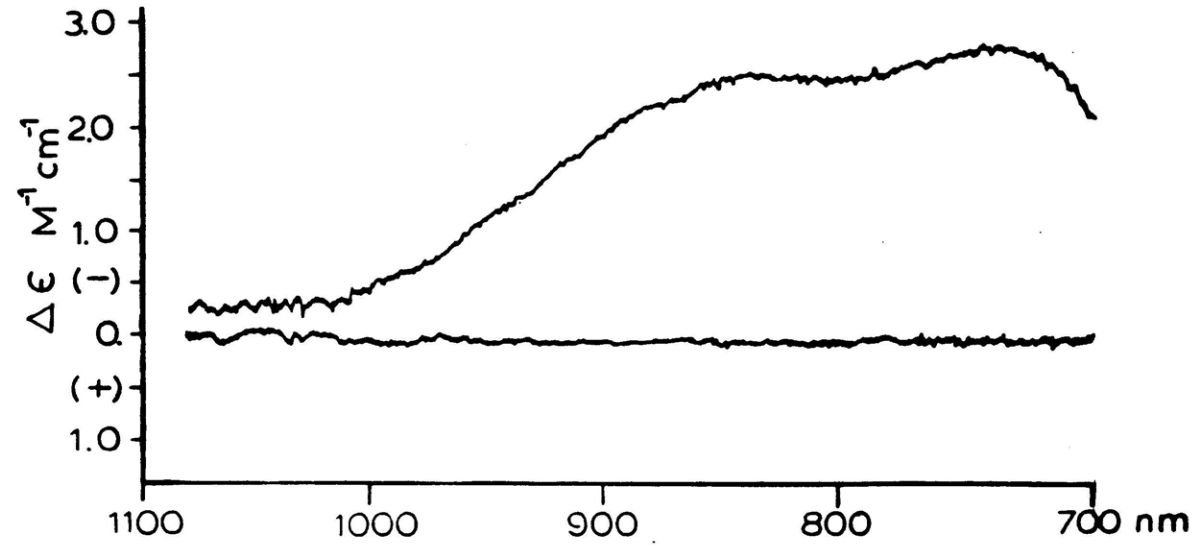
3.0
2.0
1.0
(−)
0.
(+)
1.0
Δε M⁻¹ cm⁻¹
1100
1000
900
800
700 nm

A

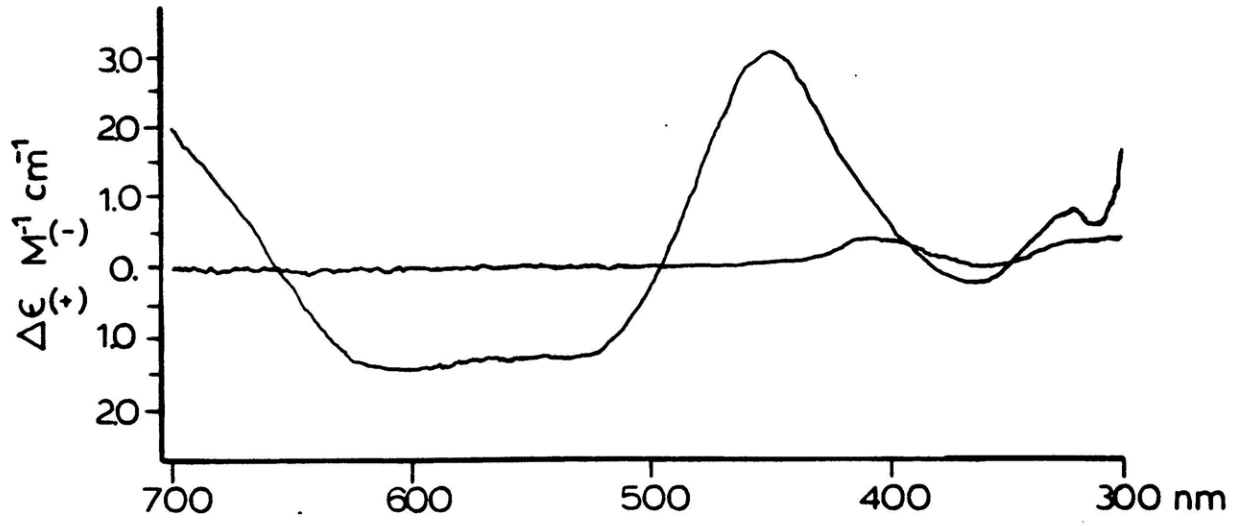
3.0
2.0
1.0
0.
1.0
2.0
Δε M⁻¹ cm⁻¹
(−)
(+)
700
600
500
400
300 nm

B

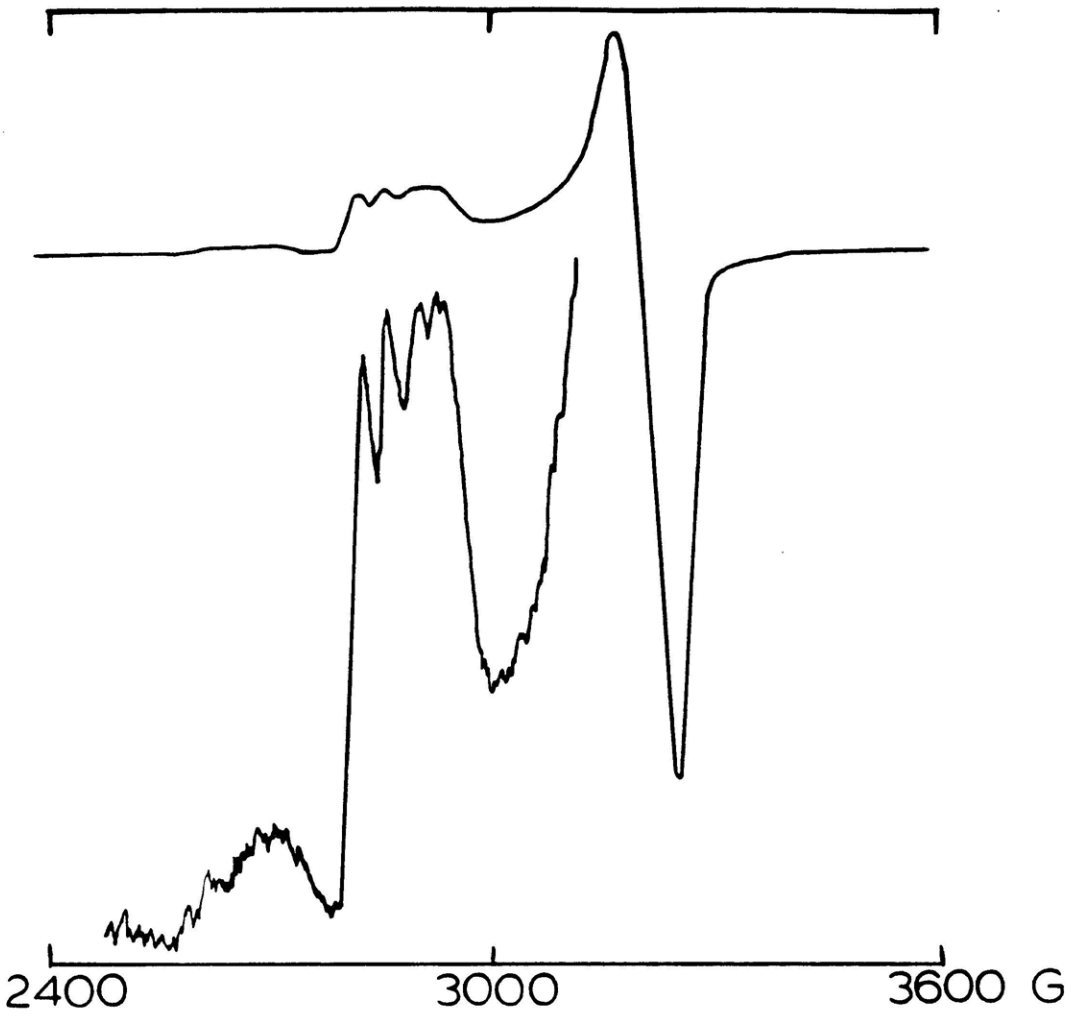
2400
3000
3600 G

further discussed in the chemical studies which follow.

ii. Chemical Properties

As the d^{10} electron configuration of deoxy T2D renders it inaccessible to spectroscopic probe, the direct characterization of its potential reactivity with exogenous ligands is not possible. However, through allosteric interactions of the T3 cuprous site with the T1 cupric site which is also present at the active site, reactivity at the deoxy T3 site can be indirectly probed. While this T3-T1 intersite interaction will be further discussed in Chapter 4, we can for now analytically use these features to indicate chemical perturbation of the binuclear cuprous site.

In Figure 3.4 are shown the 77 K EPR spectra of (A) deoxy T2D laccase at equilibrium with the halide ions, (B) bromide and (C) iodide; chloride only very weakly perturbs the T1 Cu(II) features and fluoride, at 200X protein excess and 40 hour preincubation, does not modify the deoxy T2D EPR spectrum. From Figure 3.4 and the T3-X^- EPR parameters summarized in Table 3.1, these anions all bind in a similar mode which results in a more axial T1 Cu(II) whose g transition occurs at a slightly higher field with an increased hyperfine coupling constant. As the T1 Cu(II) is

Figure 3.4 EPR Spectra at 77 K: deoxy T2D laccase reacted with Br^- and I^-.

(A) original deoxy T2D laccase;

(B) after reaction with 150 protein equivalents Br^-; and

(C) with 150 protein equivalents I^-.

In the primed spectra, the g parallel regions are at 6.3X higher gain (9.27 GHz; 0.1 M potassium phosphate, pH 6.0; [protein] = 0.311 mM).

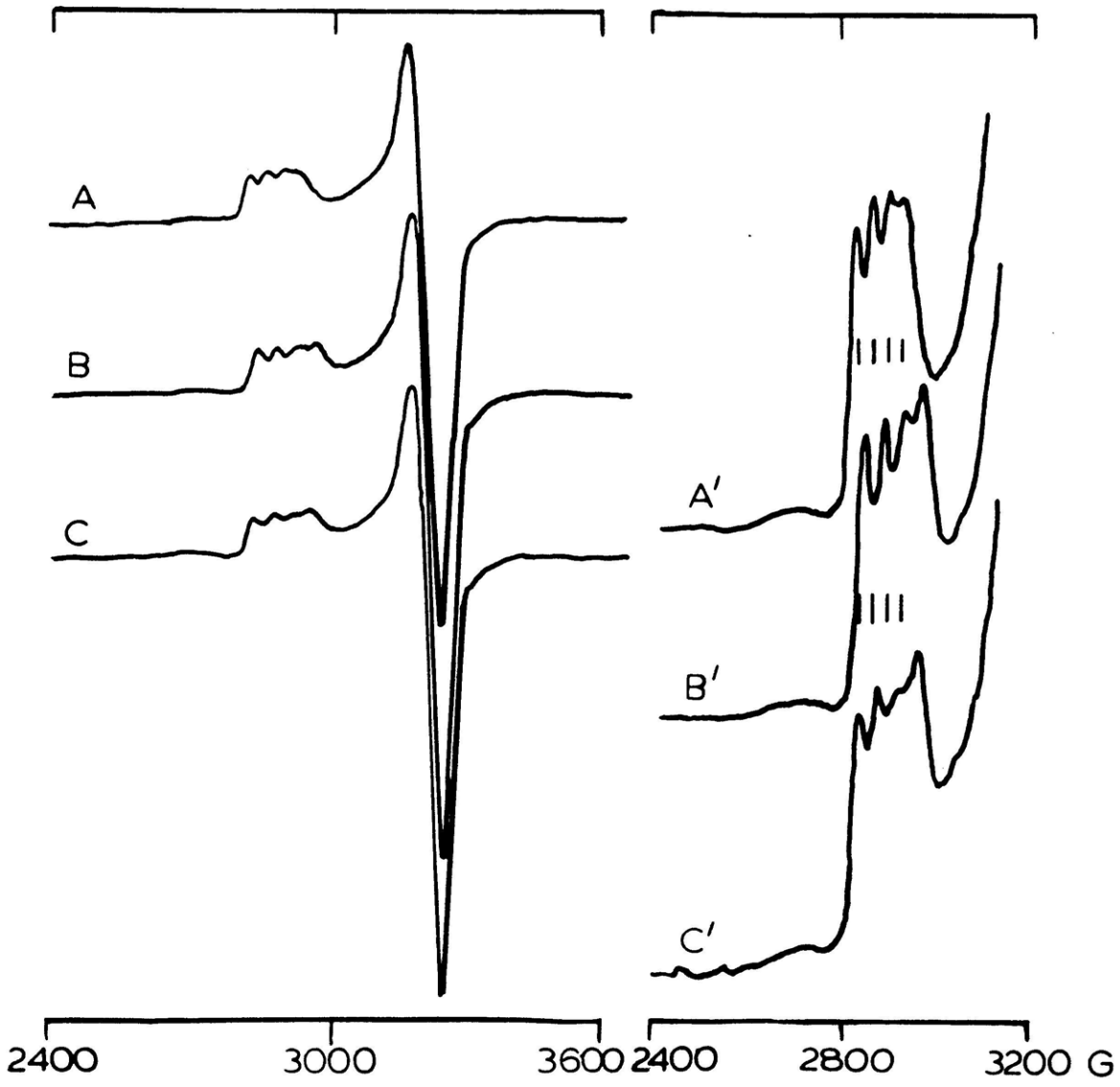
A
B
C
A′
B′
C′
2400
3000
3600
2400
2800
3200 G

believed to possess no exchangeable coordination positions (see Chapter 1), these EPR changes are interpreted as changes in the electronic structure of the cupric T1 site which have been induced by ligands binding at the cuprous T3 site. CO binding and competition studies (vide infra) further corroborate this model. EPR titration studies indicate that only one ligand binds per site. In the optical absorption spectra (data not shown), only slight decreases in the intensity of the T1 Cu(II) ($\Delta\varepsilon_{614} < |-300|\ M^{-1}cm^{-1}$) are observed which could be due to either intersite interaction or T1 reduction at high anionic strength.

Azide and thiocyanate also bind to the T3 site in deoxy T2D, as indicated by the EPR spectra in Figure 3.5B and C. The observed changes in the T1 Cu(II) EPR parameters (Table 3.1) are more extensive than those observed for the halides; their removal upon short term dialysis, however, indicates that no irreversible T1 site disruption has occurred. Similar to the halide reactions, only slight decreases in the T1 spectral features are observed in the absorption and CD spectra of deoxy $+N_3^-$ or SCN^-, but from EPR titration studies, monitoring the increase in $A_{||}$(T1) Cu(II), only one exogenous anion binds per T1 site; for N_3^-, $K_{eq} \sim 100\ M^{-1}$ at 77 K.

Reaction of deoxy T2D with 1 atm CO(g) for 1 hour also leads to perturbation of the T1 EPR signal. (Figure 3.6). On

Figure 3.5 EPR spectra at 77 K: deoxy T2D laccase reacted with N_3^- and SCN^-.

(A) original deoxy T2D laccase;

(B) after reaction with 150 protein equivalents N_3^-, and

(C) with 150 protein equivalents SCN^-.

In the primed spectra, the g parallel regions are recorded at 8X higher gain (9.26 GHz; 0.1 M potassium phosphate, pH 6.0; [protein] = 0.156 mM).

Figure 3.6 EPR spectra at 77 K: deoxy T2D laccase reacted with CO.

(A) original deoxy T2D laccase;

(B) after 1 hour reaction with 1 atm CO;

(C) sample B after 45 minutes equilibration in air at 4°C.

In the primed spectra, the g parallel regions are expanded at 8X higher gain (9.26 GHz; 0.1 M potassium phosphate, pH 6.0; [protein] = 0.22 mM).

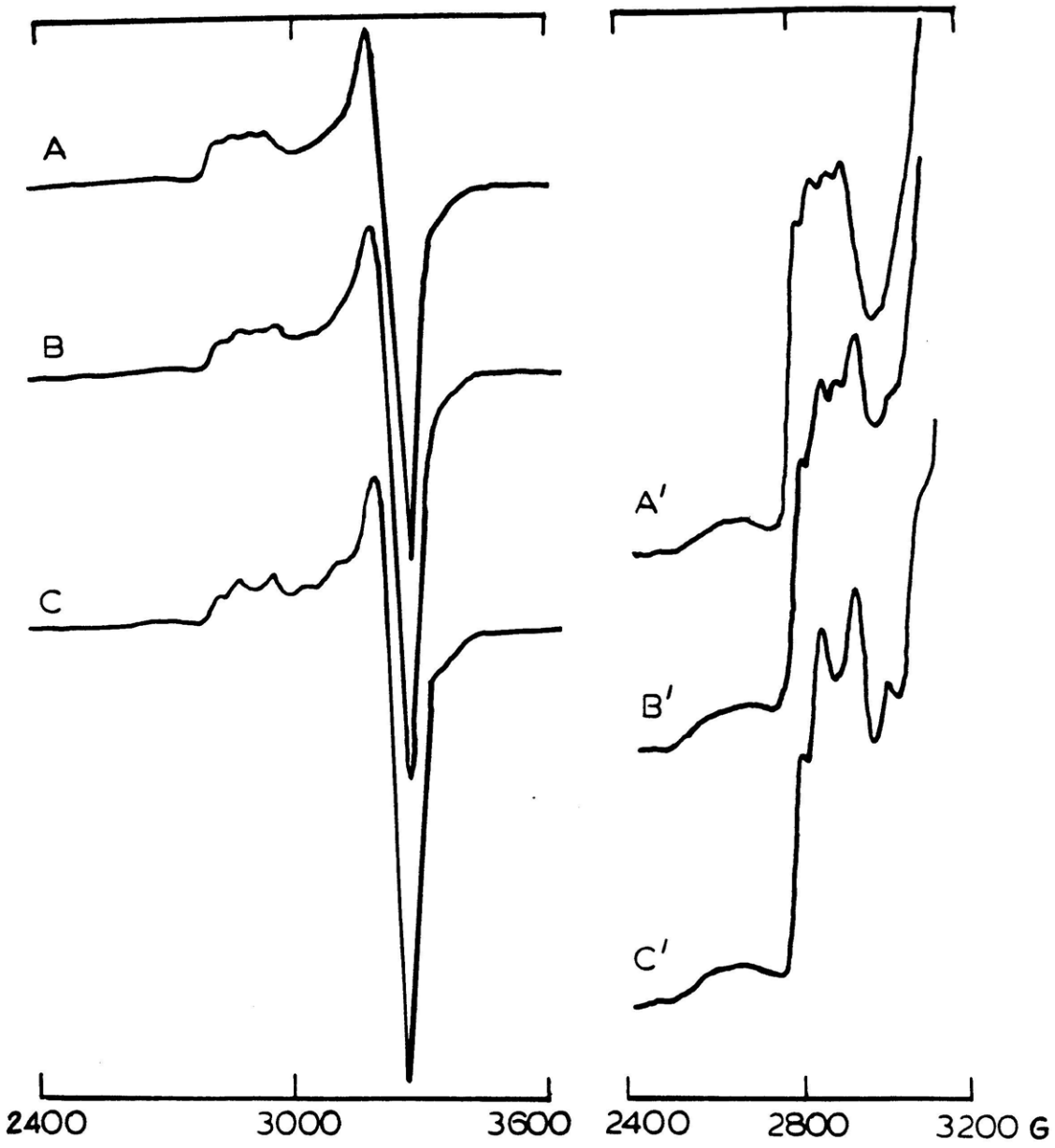
A
B
C
A′
B′
C′
2400
3000
3600
2400
2800
3200 G

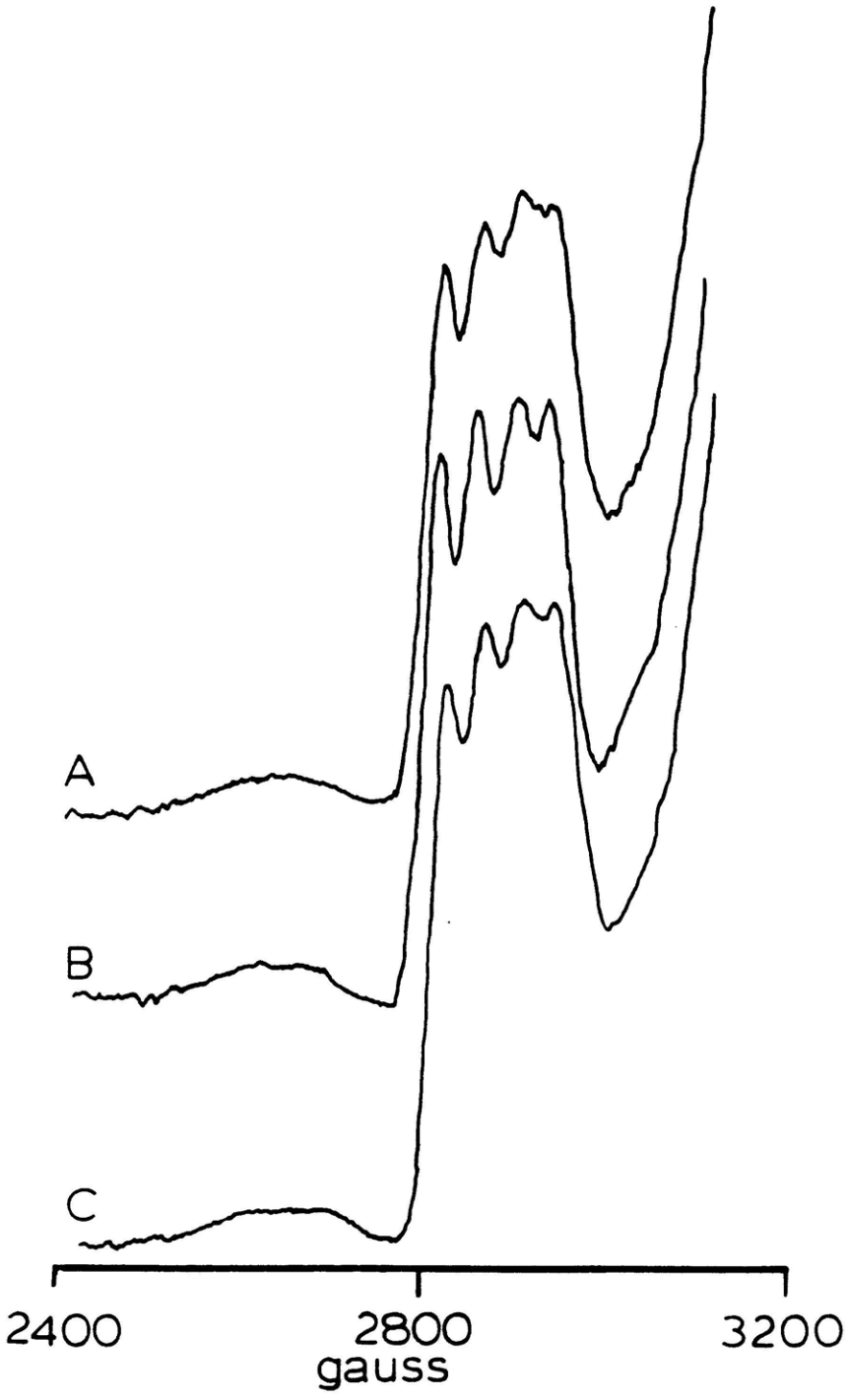
A
B
C
2400
2800
3200
gauss

Table 3.1 EPR Parameters: Deoxy T2D Laccase

[Cu(I)Cu(I)]-X	$g_{\|\|}$	$g_{\perp}$	$A_{\|\|}$ ($\times 10^{-4}$ cm^{-1})
aquo	2.30	2.06	37.8
F^-	no reaction		
Cl^-	2.28	2.05	44.0
Br^-	2.28	2.06	44.5
I^-	2.29	2.06	43.2
N_3^-	2.26	2.06	72.6
SCN^-	2.21	2.04	83.6

binding CO (Figure 3.6B), the $A_{||}$ of the T1 center increases from ≈109 to 120-125 G and the relative intensities of the T1 peaks change. While the magnitude of the change is limited, it is reproducibly observed, and moreover, upon mixing in air (Figure 3.6C) the original EPR spectrum of deoxy T2D is regained. No perturbation of the Blue copper absorption features was observed with 1 atm CO, and increasing the CO pressure to 2 atm results in no further EPR spectral perturbation.

That CO binds to the reduced T3 site in deoxy T2D has two major implications. First, it demonstrates that the lack of oxygen reactivity in T2D is not due to an inaccessibility of the active site to neutral small molecules. This point will later be further addressed, but basically, removal of the T2 Cu(II) does not result in a conformational change of the protein which renders its active site inaccessible to uncharged diatomics such as CO and O_2. Second, whereas the anions discussed previously can potentially bind to Cu(II) as well as to Cu(I), CO is normally a high affinity ligand only for Cu(I). Thus, while it could be argued that in T2D laccase, the T1 Cu(II) was experiencing direct anion perturbation, it is clear that the CO is binding to the binuclear cuprous site and modifying the electronic structure of the T1 site. Through CO/anion competition studies we can now confirm that all of these ligands are binding to the

reduced T3 site. In Figure 3.7 are shown the 77 K EPR spectra of deoxy-I^- T2D (A) before and (B) after treatment with 1 atm CO. The observed increase and sharpening of the T1 hyperfine in the CO treated spectrum is very similar to that of deoxy + CO indicating that CO and I^- are competing for the same binding site; thus, I^- must also be binding to the T3 copper. As for deoxy T2D, exposure to air (Figure 3.7C) removes the CO perturbation and regenerates the original deoxy-I^- spectrum. Similar results have been obtained in Cl^-/CO competition studies and are shown in Figure 3.8.

Competition studies between CO and N_3^- are shown in Figure 3.9. While 10X N_3^- (Figure 3.9 A-C) has essentially no effect on the deoxy-CO spectrum, higher N_3^- concentrations (Figure 3.9 D-F) effectively compete for the CO binding site such that a mixture of both deoxy-N_3^- and deoxy-CO spectral features are observed. The lack of additional spectral features indicates that a deoxy-CO/N_3^- ternary complex is not being formed. SCN^- appears to be the most strongly bound anion, as no change in the deoxy-SCN^- spectrum is achieved by even 2 atm of CO.

Thus, from the single anion studies, it appears that Cl^-, Br^- and I^- all coordinate similarly to the deoxy active site. The EPR perturbations by N_3^- and SCN^- are different

Figure 3.7 EPR spectra at 77 K: deoxy-I T2D laccase reacted with CO.

(A) $g_{||}$ region of deoxy T2D laccase pre-incubated 20 hours in 100 protein equivalents KI;

(B) after 40 minute equilibration with 1 atm CO;

(C) sample B after 6 hour equilibration in air at 4°C.

(9.26 GHz; 0.1 M potassium phosphate, pH 6.0; [protein] ~0.22 mM).

Figure 3.8 EPR spectra at 77 K: deoxy-Cl T2D laccase reacted with CO.

(A) g|| region of original deoxy T2D laccase;

(B) after 3 hour reaction in 150 protein equivalents Cl^- at 4°C;

(C) after 40 minute equilibration with 1 atm CO;

(D) sample C after 8 hour equilibration in air at 4°C.

(9.26 GHz; 0.1 M potassium phosphate, pH 6.0; [protein] = 0.15 mM).

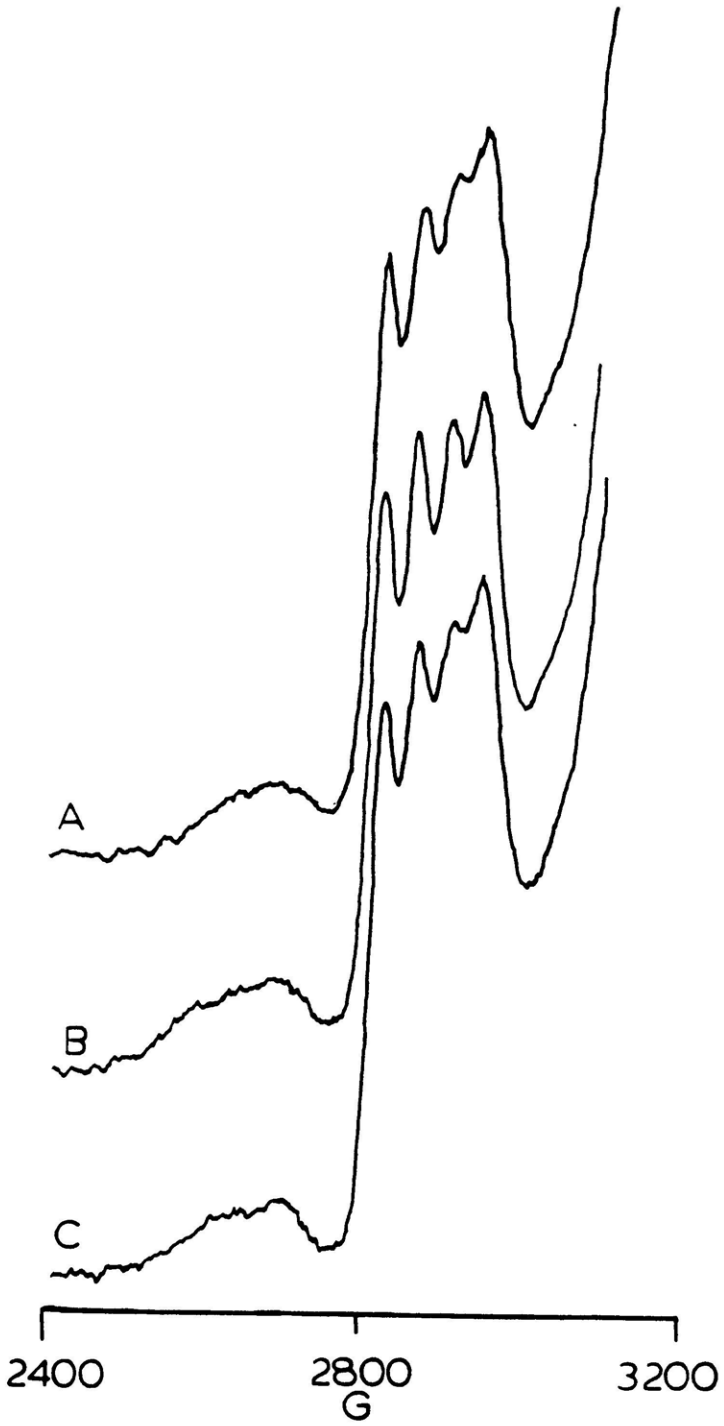
A
B
C
2400
2800
3200
G

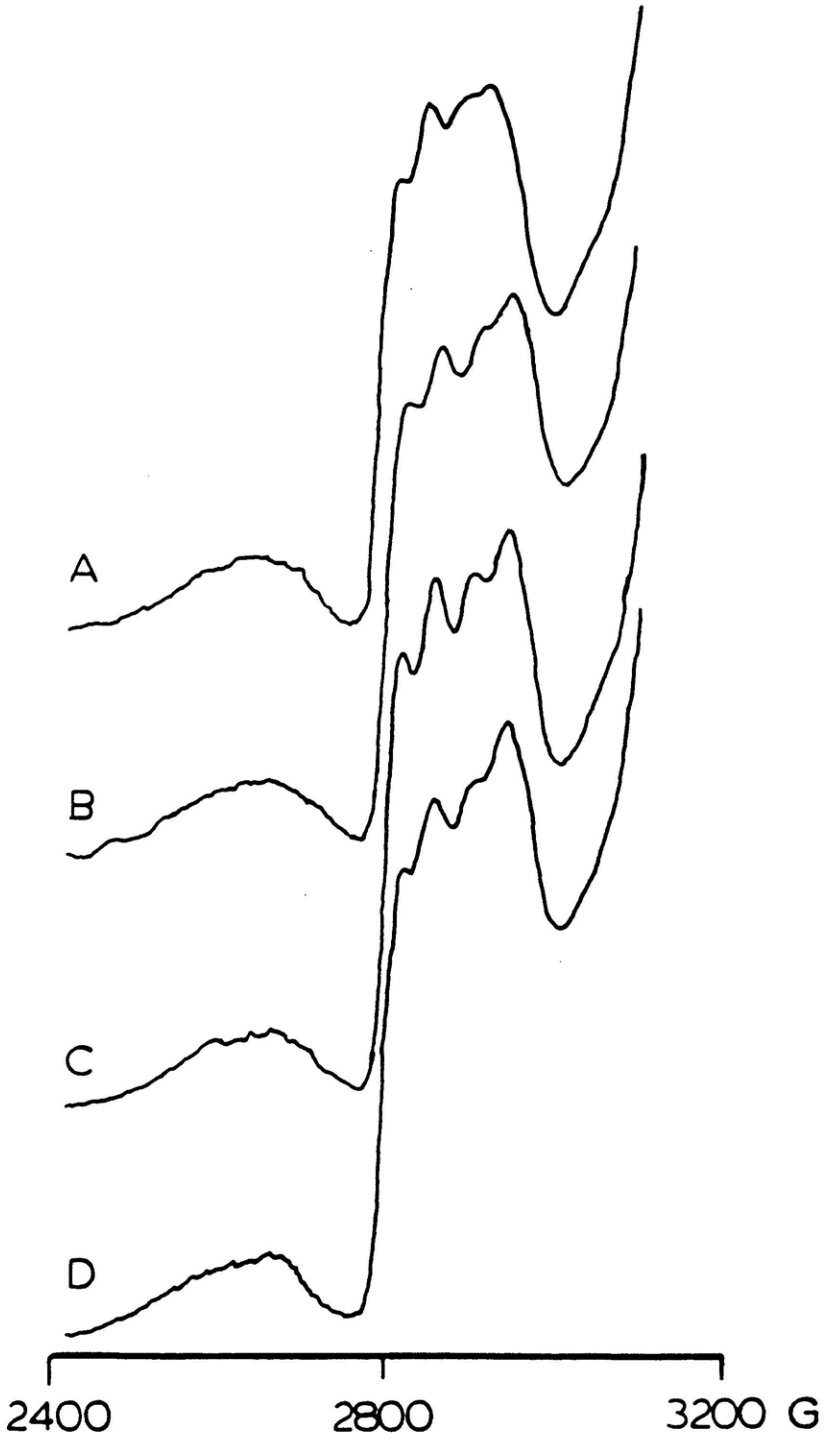
A
B
C
D
2400
2800
3200 G

Figure 3.9 EPR spectra at 77 K: deoxy-N_3^- T2D laccase reacted with CO.

(A) $g_{||}$ region of deoxy T2D laccase pre-incubated 3 hours with 10 protein equivalents NaN_3;

(B) after 30 minute equilibration with 1 atm CO;

(C) sample B after 3 hour equilibration in air at 4°C;

(D) deoxy T2D laccase pre-incubated with 200 protein equivalents NaN_3;

(E) after 60 minute equilibration with 1 atm CO;

(F) sample E, after 10 hour equilibration in air at 4°C.

Spectra A-C are at 9.26 GHz and the [protein] = 0.22 mM; spectra D-F are at 9.27 GHz and the [protein] = 0.311 mM. (0.1 M potassium phosphate, pH 6.0)

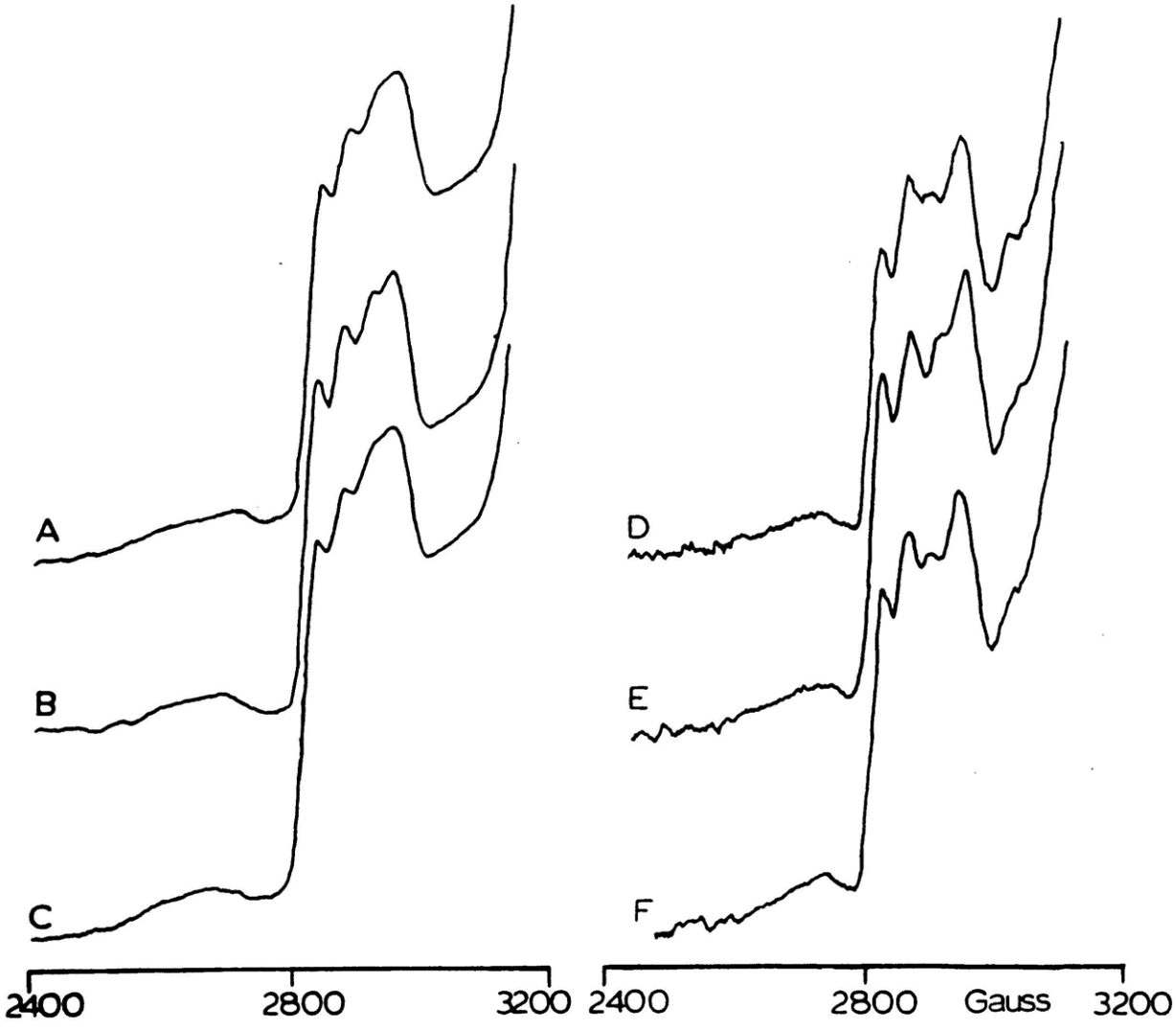
A
B
C
D
E
F
2400
2800
3200
2400
2800
Gauss
3200

from those of the halides (Table 3.1) but are quite similar to one another. The significantly dissimilar electronic and geometric structures of these anions compared to the halide ions could be responsible for these differences, or alternatively, SCN^- and N_3^- could be binding to a different coordination position than do the halides at the binuclear cuprous site.

Through CO competition studies, it is clear that all of these ligands are indeed binding to the T3 site. CO readily displaces the halide ions but competes less effectively with N_3^- and SCN^- at this site. That no new spectral features are observed in these CO competition studies, especially with N_3^- and SCN^-, suggests that a ternary complex is not being formed and that N_3^- and SCN^- are not binding to a different coordination position but are more effectively competing with the CO. Thus, from these studies it would appear that exogenous ligand affinity at the deoxy T3 site decreases over the series $SCN^- > CO \approx N_3^- > Br^- \quad I^- > Cl^- >> F^-$.

Cyanide is also a strong ligand for Cu(I), and in fact, its complexation can often result in metal removal from a protein site. For this reason, cyanide reactivity is being addressed separately from that of the aformentioned more innocent anions. The immediate spectrum of one protein equivalent of NaCN reacted with deoxy T2D (at pH = 7.2) is

shown in Figure 3.10B. A new feature is observed at ≈3350 G, which, after 2 1/2 hours reaction at 4°C, converts to spectrum 3.10C. The new perpendicular feature and the additional peak intensity at ~2675 G, 2850 G, and 3050 G are suggestive of mononuclear tetragonal Cu(II). These EPR changes continue with additional CN^- equivalents until after reaction wtih 3X CN^-, an EPR spectrum (3.10D) very similar to that of native laccase is obtained, suggesting that CN^- has reincorporated copper into the T2 site. In the electronic absorption spectra (Figure 3.11) 1X CN^- causes an immediate increase in the 750-850 nm region, a decrease at 614 nm and a large broad increase from ~500-300 nm, maximizing at ~330 nm. These changes continue until ~2-3X CN^- have been added, at which point $\Delta\varepsilon_{750} \sim 190\ M^{-1}cm^{-1}$, $\Delta\varepsilon_{614} \sim -400\ M^{-1}cm^{-1}$, and $\Delta\varepsilon_{330} \sim 2000\ M^{-1}cm^{-1}$. The energy, intensity, and shape of the increase at 330 nm, as well as the increase in the ligand field region suggest that the T3 copper site is being oxidized through reaction with CN^-. Combined with the EPR data, it appears that copper is slowly removed from the T3 site and reincorporated into the T2 site via its reaction with exogenous CN^-. The presence of the T2 copper then allows reoxidation of the T3 copper active site

Figure 3.10 EPR spectra at 77 K: deoxy T2D laccase reacted with CN^-.

(A) original deoxy T2D laccase;

(B) after addition of one protein equivalent, NaCN, 10 minutes;

(C) sample B, after 2 1/2 hour reaction time;

(D) after total addition of three protein equivalents NaCN, 3 hour reaction time.

Primed spectra of the $g_{||}$ regions are recorded at 6.5X higher gain. (9.26 GHz; 0.1 M potassium phosphate, pH 7.2; [protein] = 0.161 mM)

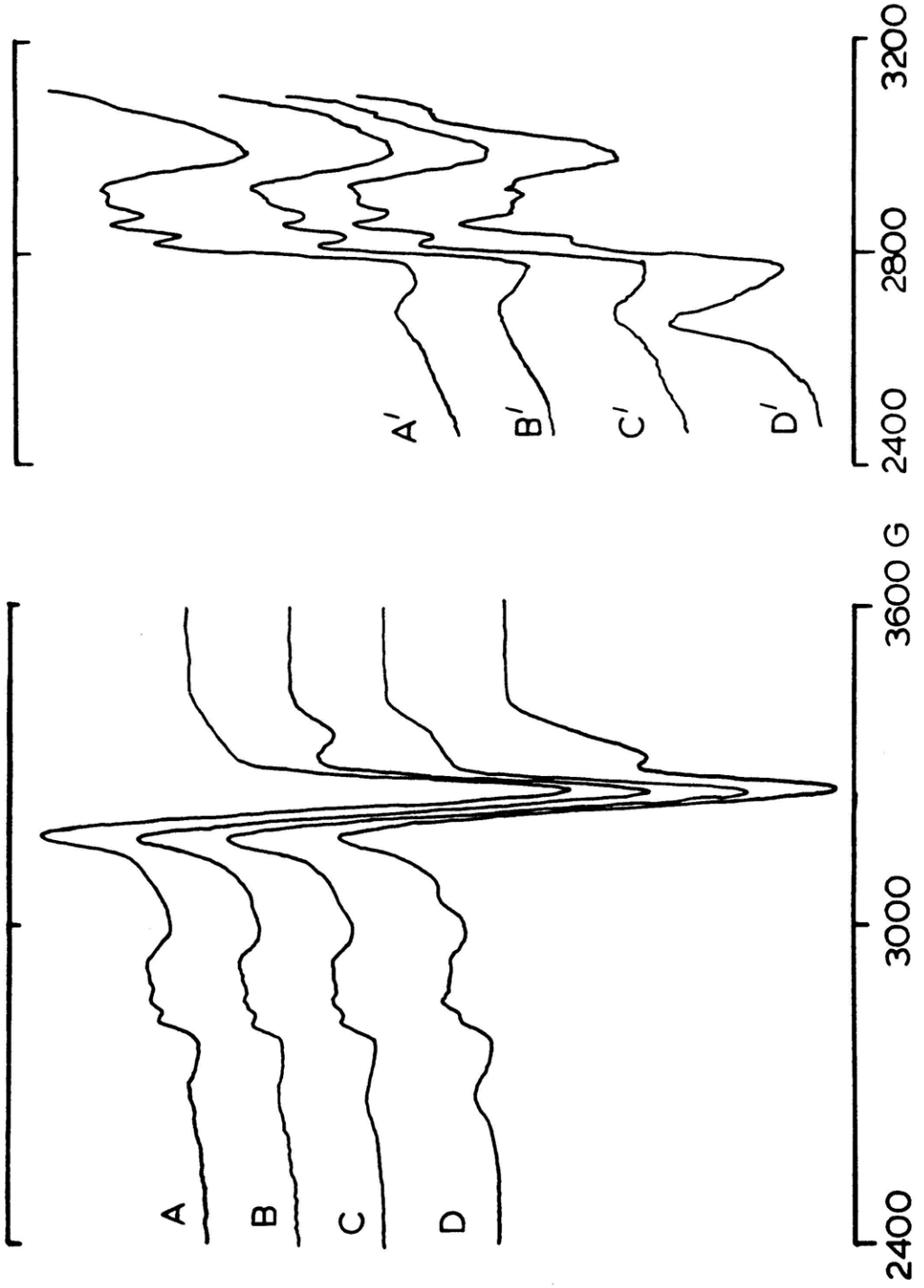
A
B
C
D
A'
B'
C'
D'
2400
3000
3600 G
2400
2800
3200

Figure 3.11 Electronic absorption spectra at 298 K: deoxy T2D laccase reacted with CN^-.

(a) (———) original deoxy T2D laccase;

(b) (——) after addition of one protein equivalent NaCN, 10 minutes;

(c) (– – –) sample B after 2 hour reaction time;

(d) (——) after total addition of three protein equivalents NaCN, 3 hour reaction time.

Arrows indicate direction of change with CN^- and time. (0.1 M potassium phosphate, pH 7.2; [protein] = 0.161 mM).

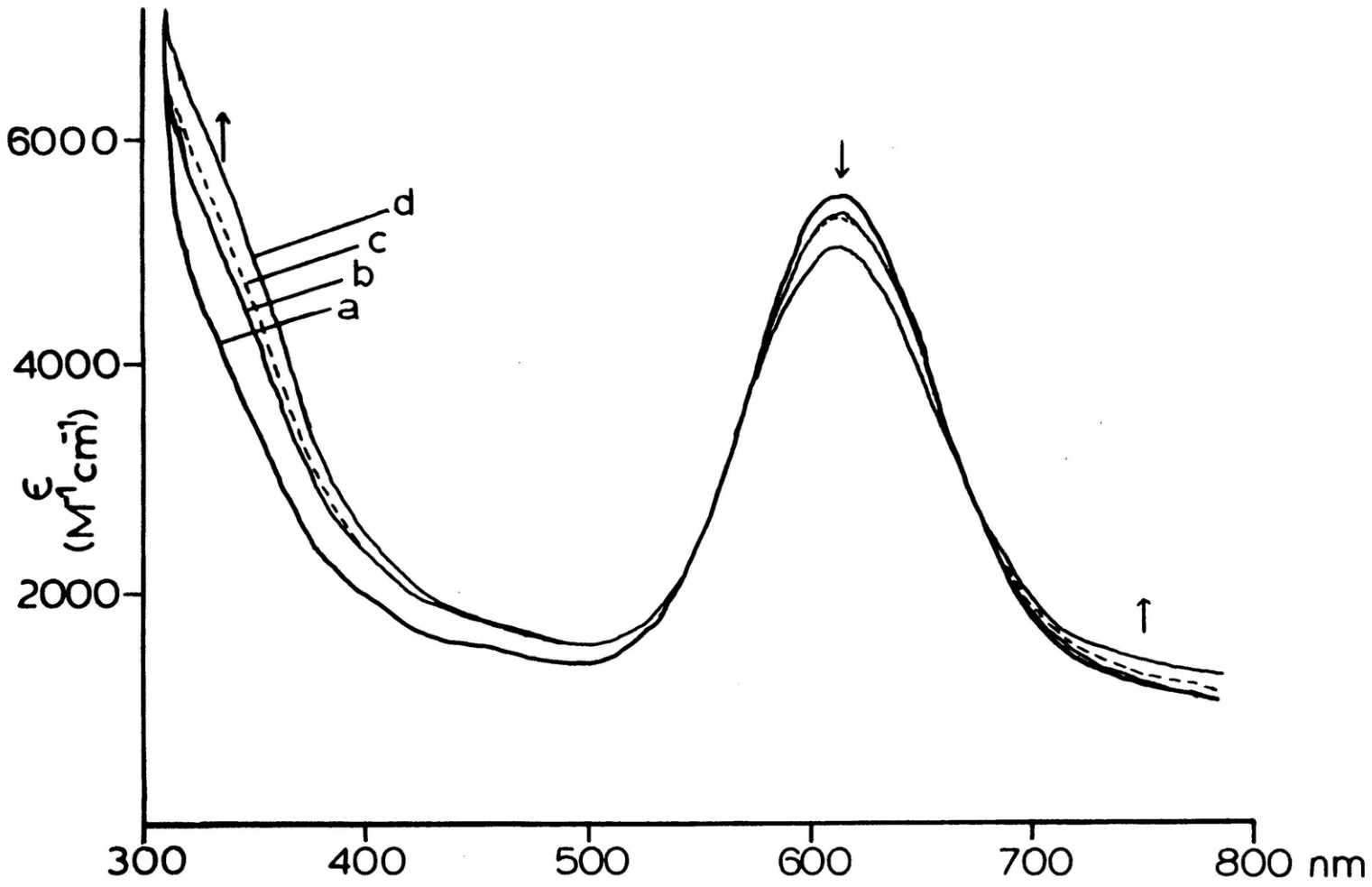
6000
4000
2000
ε
(M⁻¹cm⁻¹)
d
c
b
a
300
400
500
600
700
800 nm

(Chapter 5) by molecular oxygen and the reappearance of the 330 nm absorption feature to approximately two-thirds of its value in native laccase. At this point, cyanide binding[11] to the cupric copper could, of course, also modify its charge transfer spectrum. Finally, peroxide addition to the cyanide treated T2D laccase causes essentially no further increase in 330 nm absorption, consistent with the oxidation of the T3-T2 site by oxygen.

b. Half Met T2D Laccase

Next in complexity of the binuclear copper active site derivatives is half met T2D which contains a formally [Cu(I)Cu(II)] T3 site. As this derivative is paramagnetic and directly accessible to EPR spectroscopic probe, significant insight into the binuclear copper site in T2D laccase has been achieved through its spectral-chemical study.

i. Preparation and Spectroscopic Properties

When oxidized T2D (met) laccase is anaerobically reduced with ferrocyanide, (Figure 3.12A) a new cupric EPR signal results whose intensity maximizes with 0.7-1.0 protein equivalents of reductant and which has been associated with a mixed valence [T3:Cu(II)Cu(I)] or half met

Figure 3.12 EPR spectra at 77 K: half met T2D laccase

(A) original met T2D laccase;

(B) after anaerobic addition of 0.7 protein equivalents $Fe(CN)_6^{4-}$, aerobically dialyzed;

(C) sample B, reacted with 30 protein equivalents H_2O_2.

Primed spectra are recorded at ~5X higher gain. (9.25 GHz; 0.1 M potassium phosphate, pH 6.0; [protein] = 0.20 mM).

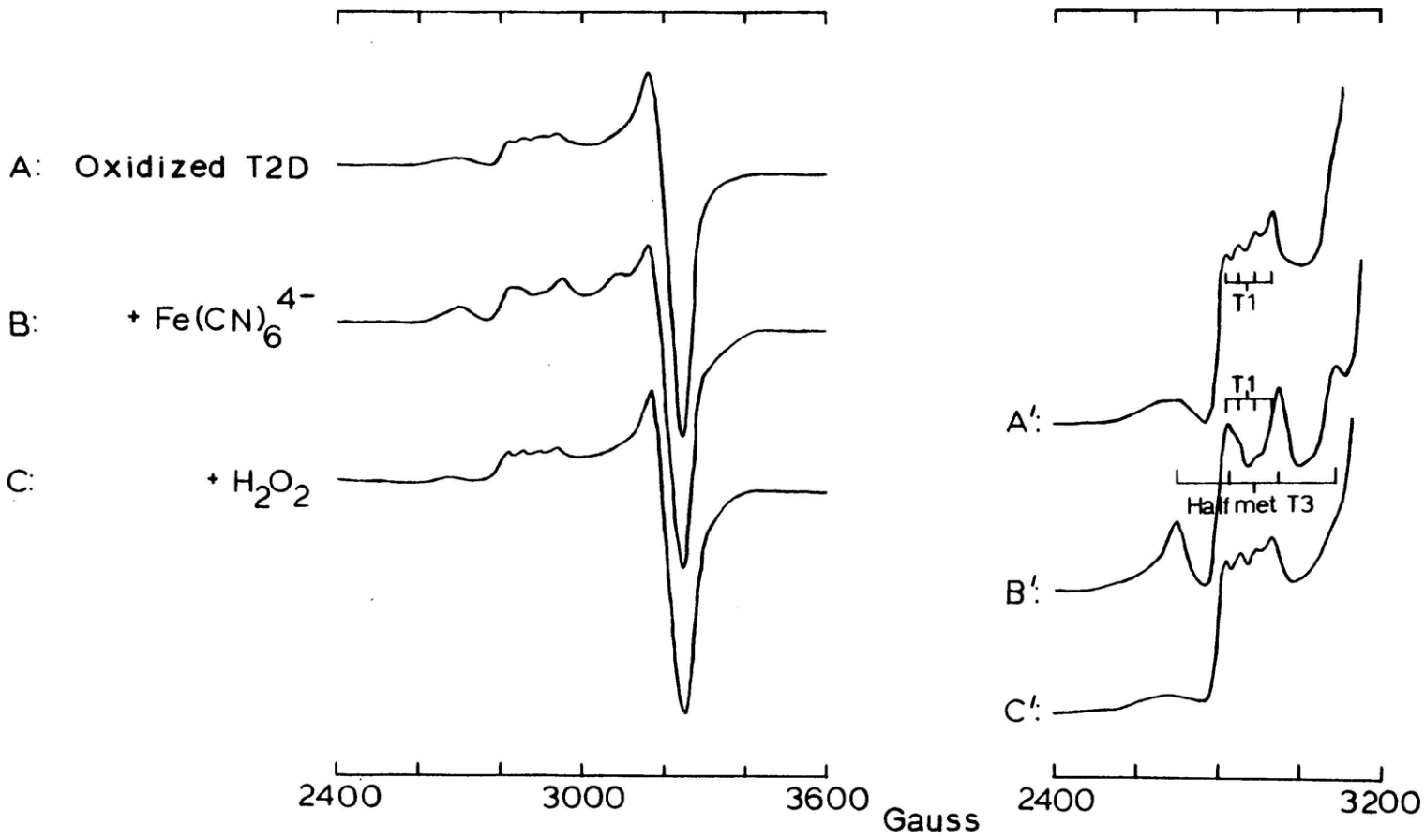
A: Oxidized T2D
B: + $Fe(CN)_6^{4-}$
C: + H_2O_2
2400
3000
3600
Gauss
A′:
B′:
C′:
T1
T1
Half met T3
2400
3200

T2D derivative. Exposure to air reoxidizes any reduced T1 copper for a final double-integrated EPR intensity of ~1.6 spin/mole (Figure 3.12B). The signal is clearly cupric in nature, with four discernable hyperfine lines ($A_{||}$ = 138 X 10^{-4} cm^{-1}, $g_{||}$ = 2.28, $g_{\perp}$ = 2.07, suggesting no delocalized mixed valence character. That $g_{||} > g_{\perp} > 2$ indicates that the T3 cupric center is tetragonal with a dx^2-y^2 or dxy ground state. Removal of the ferricyanide by dialysis against a buffer or anion exchange chromatography does not alter the half met cupric spectral features. These signals are also stable to dialysis against EDTA and chromatography on Chelex 100. In the optical absorption spectrum (ferricyanide removed), the 614 nm band is unperturbed while 330 nm absorption is decreased relative to that of met T2D (Figure 3.13). Addition of peroxide, however, regenerates the fully oxidized met T2D, restoring the optical and EPR features associated with this form (Figures 3.12C and 3.13). Half met T2D therefore is a reversible and thus valid protein derivative. While a related T3 cupric EPR signal may have been observed in T2D Polyporus versicolor laccase,[12] only half met T3 kinetic intermediates during reoxidation have been previously reported for T2D tree laccase.[13] As shown in Figure 3.14, x-ray absorption spectroscopy confirms the presence of cuprous copper in half met T2D ([Cu(I)]/[Cu(II)] ~1/6). This ratio, together with the double-integrated EPR intensity of ~1.5 spin/mole, characterizes this new

Figure 3.13 Electronic absorption spectrum at 298 K: Half met T2D laccase

(———) met T2D laccase

(— — —) half met T2D laccase

(—•—•—) deoxy T2D laccase

Absorption spectra were digitized, computer baseline corrected and are not smoothed (0.1 M potassium phosphate, pH 6.0; [protein] = 0.271 mM).

Figure 3.14 X-ray absorption edge spectra: T2D laccase derivatives.

(———) deoxy T2D laccase;

(•••••) half met T2D laccase;

(— — —) met T2D laccase

(0.1 M potassium phosphate, pH 6.0; [protein] ~1.0 mM)

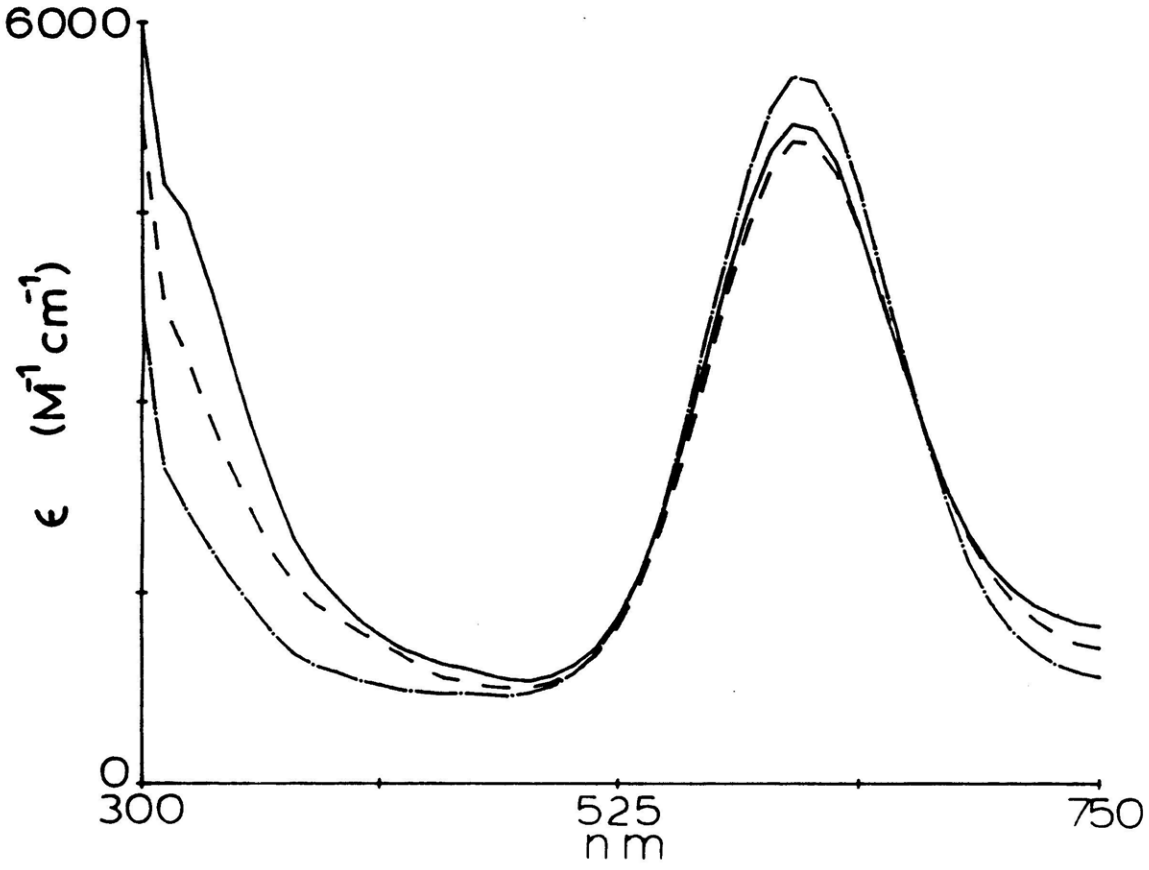
6000
0
ε (M⁻¹cm⁻¹)
300
525
750
nm

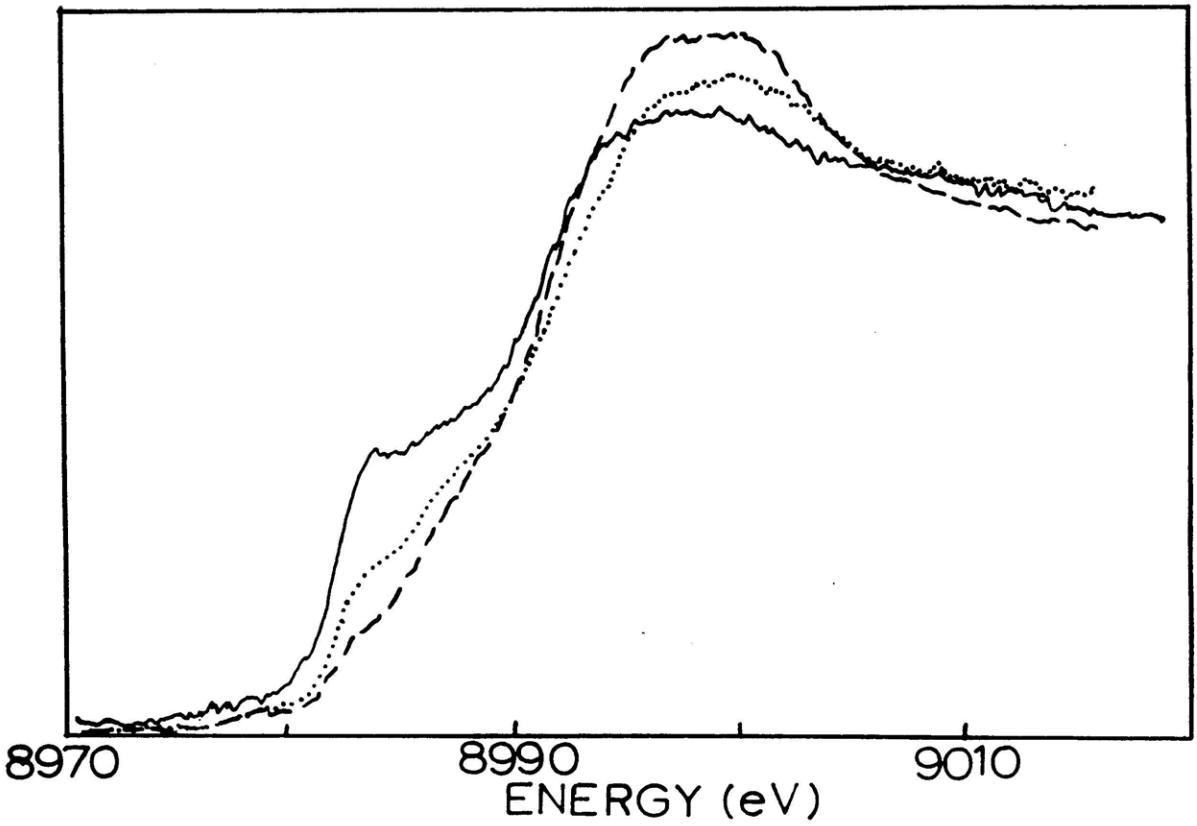
8970
8990
9010
ENERGY (eV)

derivative as containing T2D laccase in which 50% of the protein contains binuclear sites which are mixed valent and the remaining 50% contains fully oxidized T3 sites.

Spectroscopic (and chemical) study of the stable mixed valent site in half met T2D laccase is therefore complicated by the additional presence of an approximately equimolar concentration of fully oxidized T3 centers. This is readily apparent when probing the ligand field bands of half met T2D by CD spectroscopy. In Figure 3.15 are shown the CD transitions of met T2D after treatment with ferrocyanide, dialyzed compared to those of deoxy T2D. If the reduction to half met T2D went to completion, the differences between these spectra would represent the ligand field and charge transfer transitions associated with the half met T3 Cu(II). However, the ~60% met T3 sites present are also contributing to this half met spectrum; therefore, subtraction of the met spectral features and appropriate scaling is necessary before the transitions relating to the mixed valence sites can be ascertained. The resulting spectra are shown in Figure 3.16 and indicate transitions at ~995 nm ($\Delta(\Delta\varepsilon) = +1.29\ M^{-1}cm^{-1}$ and at 645 nm $\Delta(\Delta\varepsilon) = +0.971\ M^{-1}cm^{-1}$ which are likely[14] the d-d transitions of the site.

Finally, it is noted that complications due to the met

Figure 3.15 CD spectra at 298 K: half met and deoxy T2D laccase.

(———) met T2D laccase, anaerobically reduced with one protein equivalent ferrocyanide, dialyzed;

(– – –) deoxy T2D laccase, for comparison.

CD spectra were digitized, computer baseline corrected and are not smoothed. (0.1 M potassium phosphate, pH 6.0; [protein] = 0.244 mM)

Figure 3.16 Theoretical CD spectrum at 298 K: "met corrected" half met T2D laccase.

(———) half met T2D laccase (from Figure 3.15) minus 60% met T2D laccase (Figure 3.33), scaled to 100% half met protein sites (unsmoothed data);

(– – –) deoxy T2D laccase is shown for comparison.

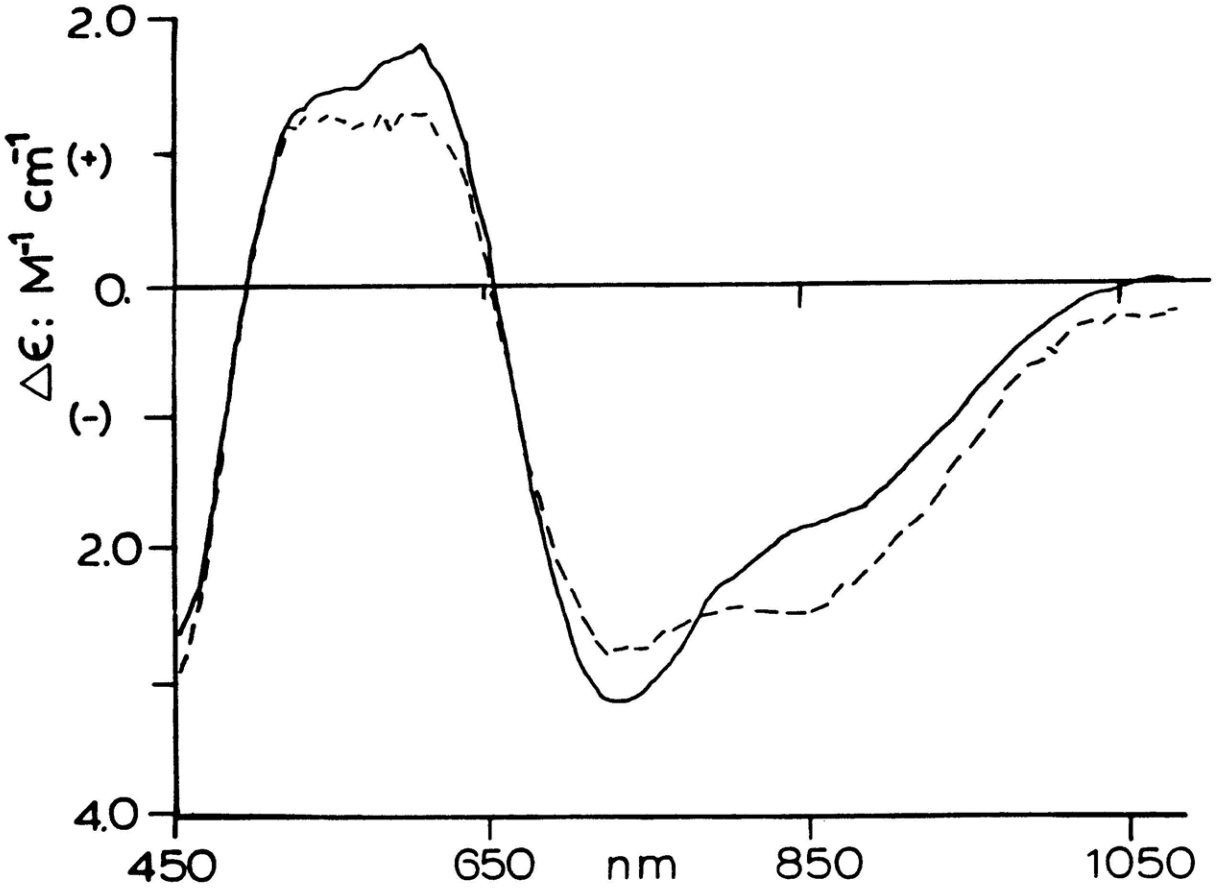
2.0
(+)
0.
(-)
2.0
4.0
$\Delta\epsilon$: M^{-1} cm^{-1}
450
650
nm
850
1050

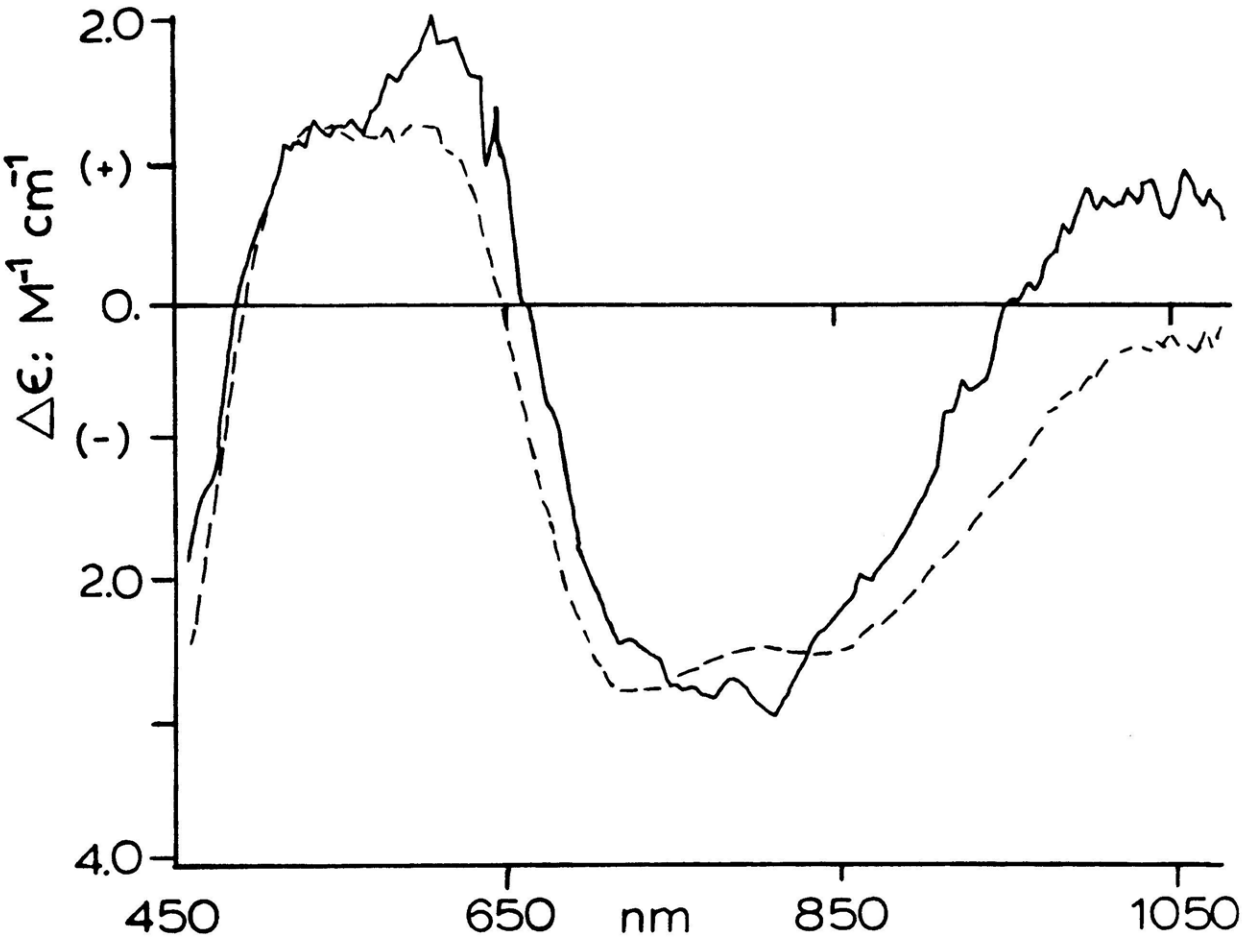
2.0
(+)
0.
(-)
2.0
4.0
$\Delta\epsilon$: M^{-1} cm^{-1}
450
650
nm
850
1050

T2D can also arise in the EPR spectra of half met T2D. Even though the T3 sites in met T2D are diamagnetic and therefore EPR non-detectable, perturbations of the underlying T1 Cu(II) EPR spectrum due to exogenous anion reactivity at the fully oxidized T3 site (analogous to the T3-T1 interaction described for deoxy T2D) can complicate the interpretation of the EPR properties of the half met sites, which themselves already contain two paramagnetic centers.

ii. Chemical Properties

Ligand binding to this stable, half met T2D laccase has been investigated for a series of exogenous ligands. The effects of Br^- on the T3 Cu(II) EPR spectrum are shown in Figure 3.17(A-C). While the broadening of the third half met hyperfine peak at ~2950 G may relate only to an underlying T1 Cu(II) EPR perturbation (Section c), the narrowing of the T3 peak at ~2830 G clearly indicates that X^- is also binding at the mixed valent copper sites. Compared to the other halide complexes (data not shown), the [Cu(I)Cu(II)]-Br^- EPR spectrum most strongly differs from that of [Cu(I)Cu(II)]-OH_2 suggesting that it has the strongest interaction at the half met site. At 77 K, a single equilibrium binding constant K ~3000 M^{-1} can be calculated from the decrease in the full width at half maximum of the hyperfine peak at 2830 G. For all of the

Figure 3.17 EPR spectra at 77 K: Br^- titration of half met T2D laccase.

(A) $g_{||}$ region of original half met T2D laccase;

(B) + 5 protein equivalents NaBr;

(C) + 150 protein equivalents NaBr;

(D) sample C, dialyzed.

(0.1 M potassium phosphate, pH 6.0; [protein] = 0.09 mM for spectra A-C, 0.075 mM for spectrum D)

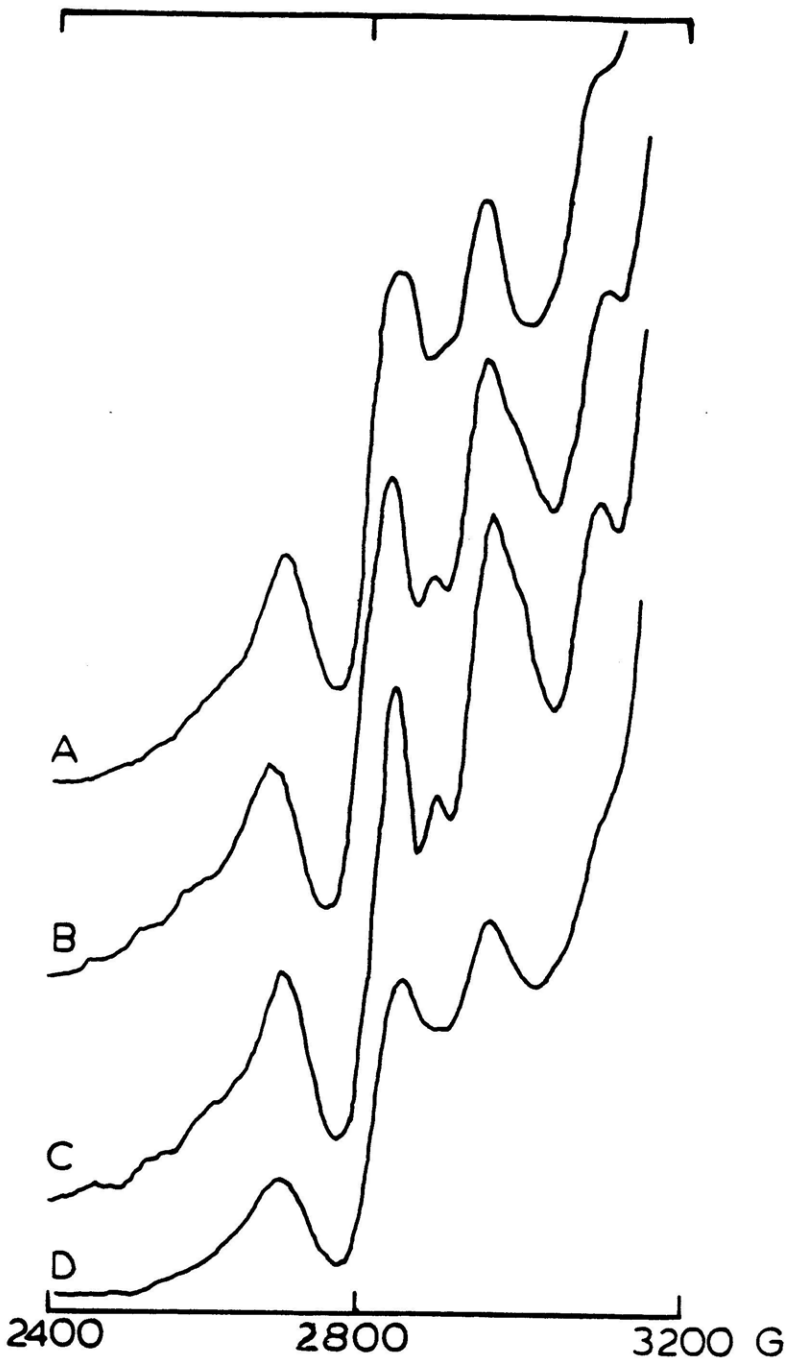
A
B
C
D
2400
2800
3200 G

halide ions, a total of four T3 Cu(II) hyperfine peaks are observed indicating that there is little, if any, delocalization of the unpaired electron onto the Cu(I) nucleus (2I + 1 = 7 hyperfine lines would be expected). Finally, short term (< 5 hour) dialysis removes all anion effects and restores the original half met-aquo EPR features (Figure 3.17D).

Similar results are obtained in SCN^- titrations of the half met T2D EPR signal (Figure 3.18); here, however, detailed spectral analysis is complicated by the simultaneous and more significant T1 Cu(II) perturbation which also occurs with binding to the met (and perhaps half met) T2D binuclear copper sites. The lower field shift of the first T3 aquo peak (Figure 3.18 B and C) does indicate perturbation of the T3 Cu(II), however, and from this spectral change a single binding constant $K_{eq} \sim 500\ M^{-1}$ is estimated at 77 K. Optical studies of half met T2D in excess SCN^- show no SCN^- ---> Cu(II) CT transitions ($\Delta\varepsilon < 200\ M^{-1}cm^{-1}$) and only very weak changes in the ligand field region. Short term dialysis again removes SCN^--related EPR features to regenerate half met aquo T2D (Figure 3.18D). That cysteamine ($NH_2CH_2CH_2SH$) and β-mercaptoethanol ($HOCH_2CH_2SH$) show no perturbation of the half met EPR signal suggests that SCN^- may be coordinating through its nitrogen.

Figure 3.18 EPR spectra at 77 K: SCN^- titration of half met T2D laccase.

(A) $g_{||}$ region of original half met T2D laccase;

(B) + 25 protein equivalents NaSCN;

(C) + 150 protein equivalents NaSCN;

(D) sample C, dialyzed.

(0.1 M potassium phosphate, pH 6.0; [protein] = 0.155 mM for spectra A-C, 0.140 mM for spectrum D)

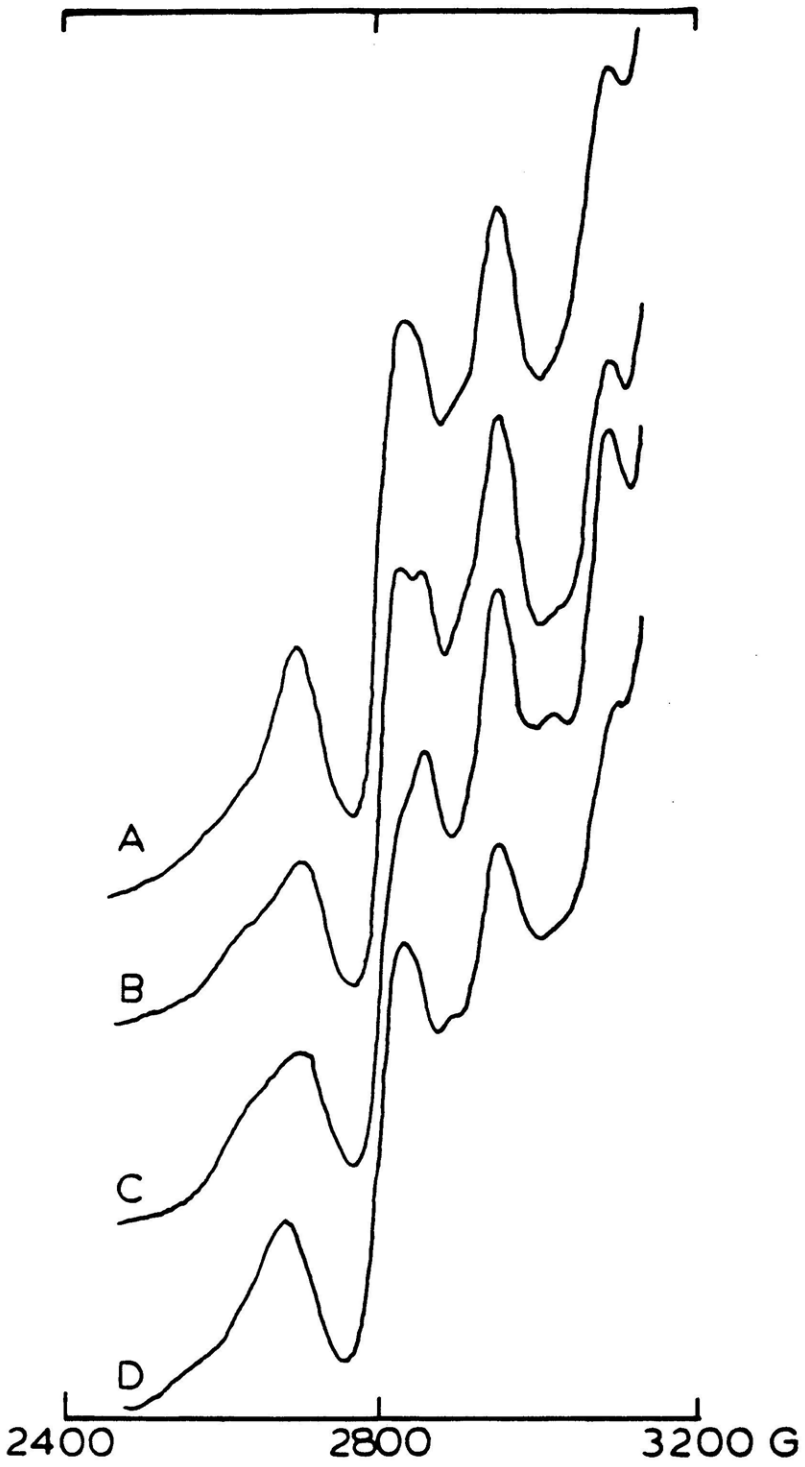
A
B
C
D
2400
2800
3200 G

Azide has been an especially effective ligand for probe of the half met T3 site. With 20 protein equivalents of N_3^-, a significant change in the T3 EPR spectrum is observed (Figure 3.19B). $A_{||}$ decreases to 101 X 10^{-4} cm^{-1} and g shifts to 2.280, still exhibiting little, if any, delocalized character; met T2D shows no EPR perturbation at these N_3^- concentrations. With additional azide, the intensities of these features continue to increase, although perturbations of the underlying met T1 features complicate their discernation. From the 77 K EPR changes, $K_{eq} \sim 6000\text{-}8000\ M^{-1}$.

In the electronic absorption spectrum (Figure 3.20), a broad increase in intensity is observed between 550 and 320 nm. After correcting the optical spectrum for the N_3^- ---> Cu(II) CT intensity (K_{eq} = 200 $M^{-1}cm^{-1}$, $\Delta\varepsilon_{450}$ = 900 $M^{-1}cm^{-1}$, cf. Figure 3.37) associated with the met-N_3^- T2D which is also present, significant intensity ($\varepsilon \sim 1000\text{-}1500\ M^{-1}cm^{-1}$) remains at ~480 and 400 nm which must reflect N_3^- ---> Cu(II) CT transitions at the mixed valent T3 site. 77 K optical studies of half met-N_3^- (Figure 3.21) greatly improve the resolution of the 480 nm feature and confirm its assignment as an N_3^- ---> Cu(II) CT transition present only in half met-N_3^- and not met-N_3^- T2D; the validity of the 400 nm feature as an additional CT transition in half met-N_3^- is still ambiguous at 77 K.[15] From the room temperature titration studies (Figure 3.20), values of $K_{eq} \sim 10^2\ M^{-1}$ are

Figure 3.19 EPR spectra at 77 K: N_3^- titration of half met T2D laccase.

(A) g $||$ region of original half met T2D laccase;

(B) + 20 protein equivalents NaN_3;

(C) + 100 protein equivalents NaN_3;

(D) sample C, dialyzed.

(0.1 M potassium phosphate, pH 6.0; [protein] = 0.114 mM)

Figure 3.20 Electronic absorption spectra at 298 K: N_3^- titration of half met T2D laccase.

Arrows indicate direction of change with 10, 25, 100, and 250 protein equivalents NaN_3. (0.1 M potassium phosphate, pH 6.0; [protein] = 0.184 mM)

Figure 3.21 Electronic absorption spectra at 77 and 298 K: half met-N_3^- T2D laccase

Half met T2D + 20 protein equivalents NaN_3;
(——) 298 K; and (– – –) 77 K.
(1.45 mm pathlength; 50% v/v glycerol/0.1 M potassium phosphate, pH 6.0; [protein] ~0.85 mM)

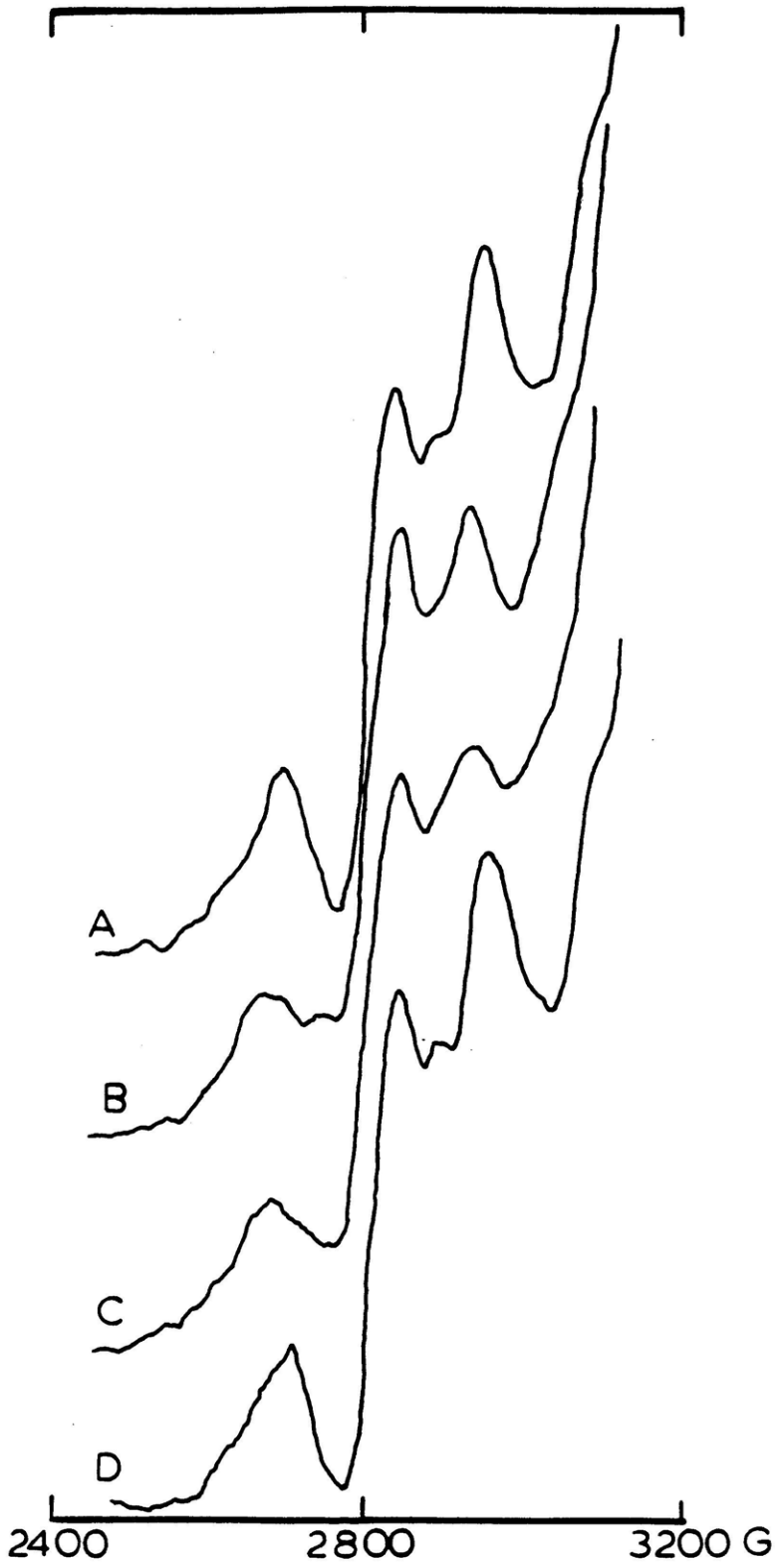
A
B
C
D
2400
2800
3200 G

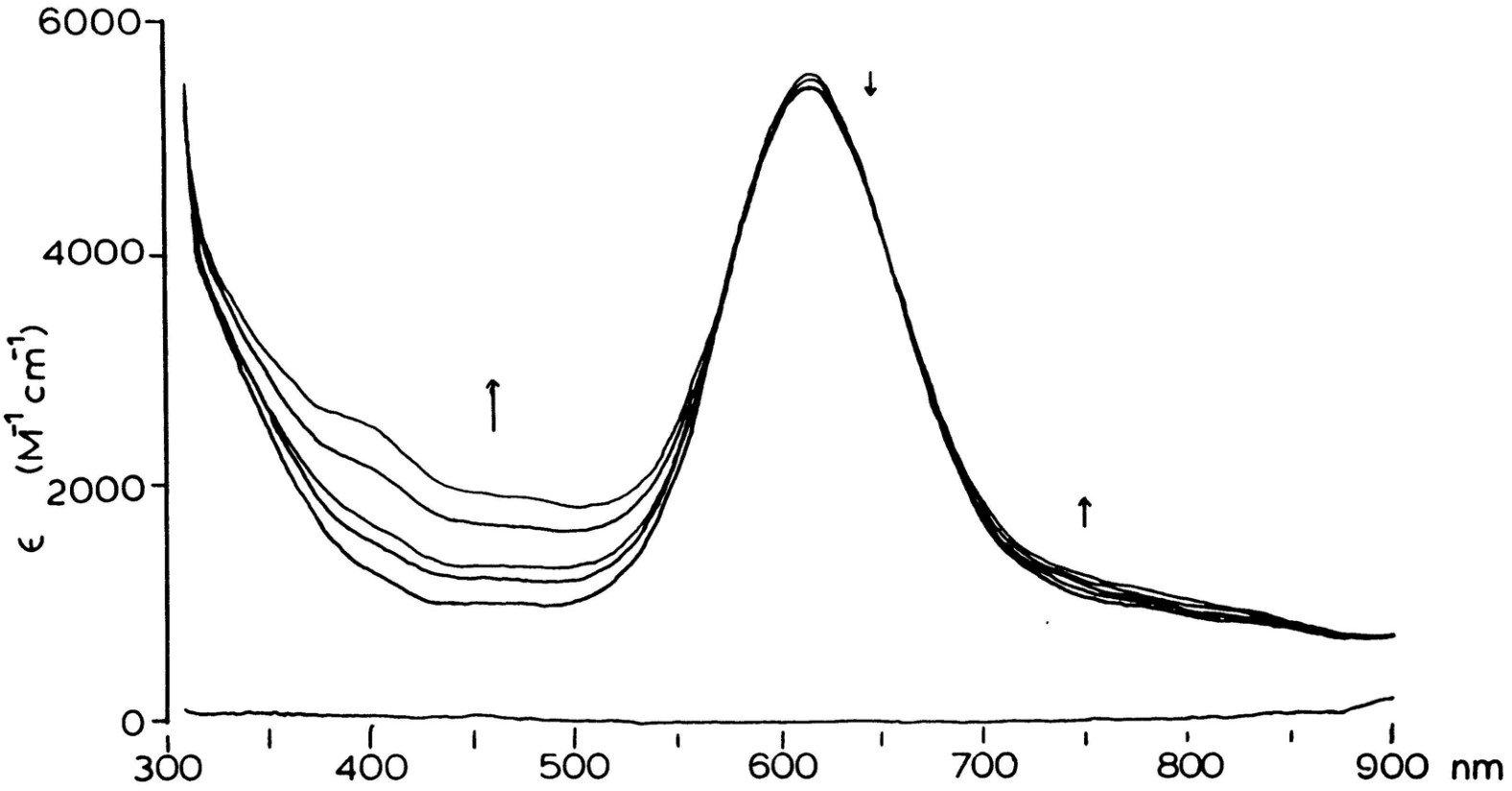
6000
4000
2000
0
ε (M⁻¹cm⁻¹)
300
400
500
600
700
800
900 nm

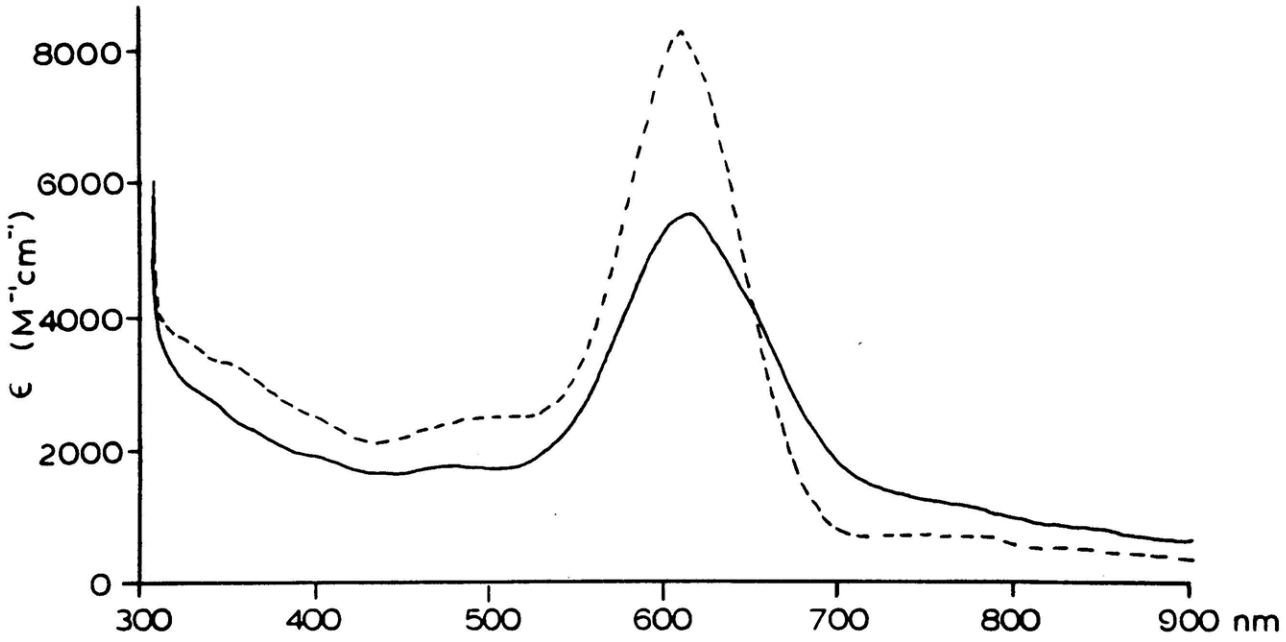
8000
6000
4000
2000
0
ε (M⁻¹cm⁻¹)
300
400
500
600
700
800
900 nm

calculated throughout the N_3^- ---> Cu(II) CT region. Due to the overlapping met-N_3^- and half met-N_3^- spectral features, it can only be concluded that N_3^- is binding with similar affinities at each of these T3 sites. The presence of both titratable absorption and EPR changes with N_3^- demonstrates the importance temperature can have in affecting exogenous anion reactivity ($K_{N_3^-}$ 298 K ~100-200 M^{-1}; $K_{N_3^-}$, 77K ~6000-8000 M^{-1}).

Two additional absorption changes (Figure 3.20) are noted in the N_3^- titration of half met T2D. First, absorption intensity at 330-350 nm is somewhat increased over that of the original half met T2D but significantly increased over that of met-N_3^- which shows a large intensity decrease ($\Delta \varepsilon \sim$-600 $M^{-1}cm^{-1}$) in this region. Correcting for the offsetting met-N_3^- effect, a significant increase in 330-350 nm absorption intensity must result when N_3^- binds to half met T2D. Whether this intensity derives from N_3^- ---> Cu(II) CT or a perturbation of the 330 nm feature which is associated with endogenous L ---> Cu(II) CT at the T3 site cannot be concluded. Second, N_3^- reaction of half met T2D results in a large increase ($\Delta\varepsilon_{750} \sim 400$ $M^{-1}cm^{-1}$, extrapolating to 100% half met-N_3^-) in the ligand field region; the calculated K ~130 M^{-1} demonstrates that this change is associated with the increase in CT intensity at higher energy, and suggests the assignment of the 750 nm

absorption as the shifted d-d bands of half met-N_3^-. Further insight into the changes which occur in this spectral region derives from parallel CD studies of half met-N_3^- T2D.

The near-IR CD titration of half met T2D with N_3^- is shown in Figure 3.22. From the broad decrease centered at ~840 nm, K = 100 M^{-1} and $\Delta(\Delta\varepsilon)$ = 0.934 $M^{-1}cm^{-1}$. However, a very different set of spectral changes is obtained when the half met and half met-N_3^- spectra are corrected for their respective met and met-N_3^- contributions which are also present and affecting the titration data in Figure 3.22. The resultant met-corrected half-met data (normalized to 100% half met T3 sites) are shown in Figure 3.23. (Note that comparison to the analogous titration data of N_3^- on met T2D (Figure 3.38) is necessary to rationalize the half met-N_3^- spectrum in Figure 3.23 compared to that of 3.22. From the difference spectrum in the inset to Figure 3.23, half met-N_3^- T2D would appear to contain a negative feature at ~995 nm and a positive feature at ~810 nm relative to half met-OH_2 T2D. However, in CD spectroscopy, it is not possible to differentiate the gain of a new spectral feature from the loss of a preexisting feature of opposite sign. This problem is surmounted in half met-N_3^- T2D through comparison to deoxy T2D which can serve as a baseline for the original half met aquo ligand field transitions. Referring back to Figure 3.16, it is clear that the negative band in half met-N_3^-

Figure 3.22 Near-IR CD spectra at 298 K: N_3^- titration of half met T2D laccase.

Arrows indicate the direction of change with 10, 25, 100, and 250 protein equivalents NaN_3. (0.1 M potassium phosphate, pH 6.0; [protein] = 0.184 mM)

Figure 3.23 Theoretical CD spectrum at 298 K: "met-N_3^- corrected" half met N_3^- T2D laccase.

(— — —) half met-N_3^- T2D laccase (from Figure 3.22) minus 60% met-N_3^- T2D laccase (Figure 3.38), scaled to 100% half met-N_3^- protein sites (unsmoothed data);

(——) the analogous 100% half met-aquo T2D spectrum is shown for comparison.

Inset: Theoretical CD difference spectrum: half met N_3^- - half met aquo T2D laccase.

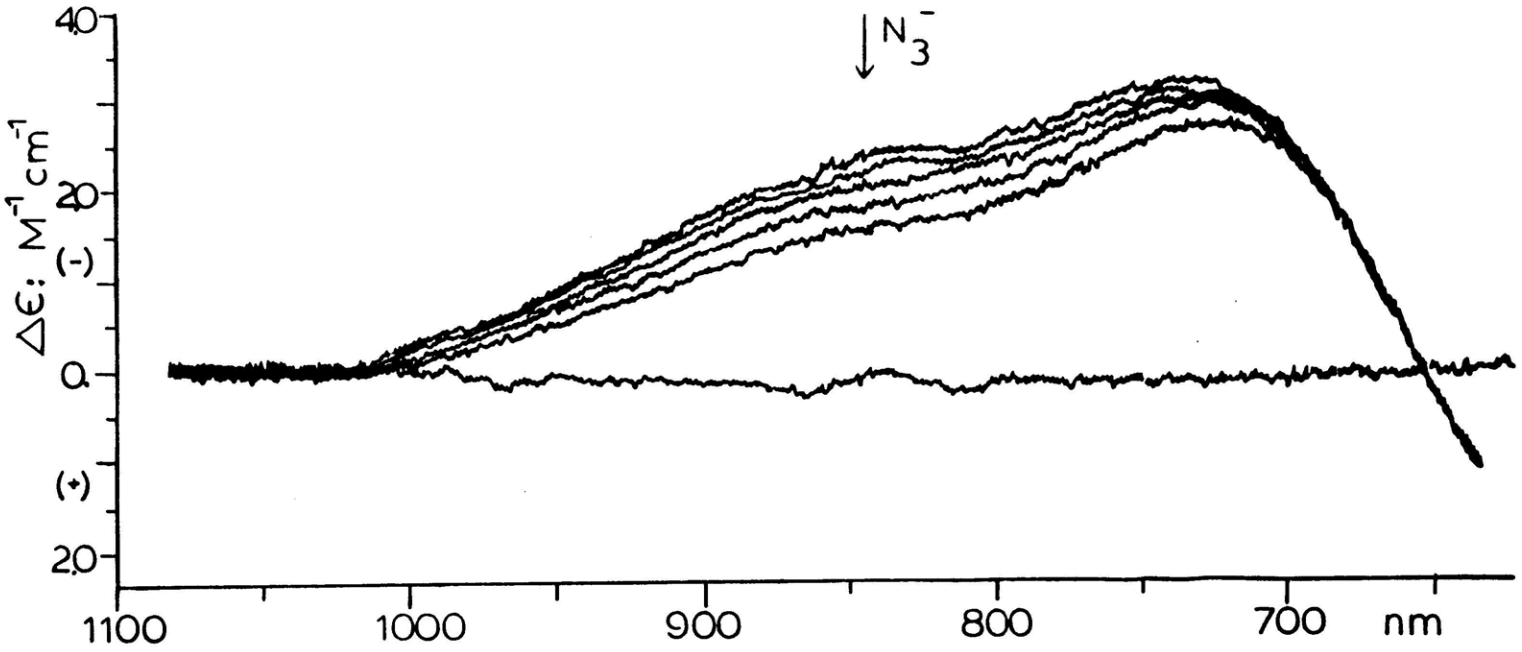
40
20
0
20
(-)
(+)
$\Delta\epsilon$; $M^{-1}cm^{-1}$
$\downarrow N_3^-$
1100
1000
900
800
700
nm

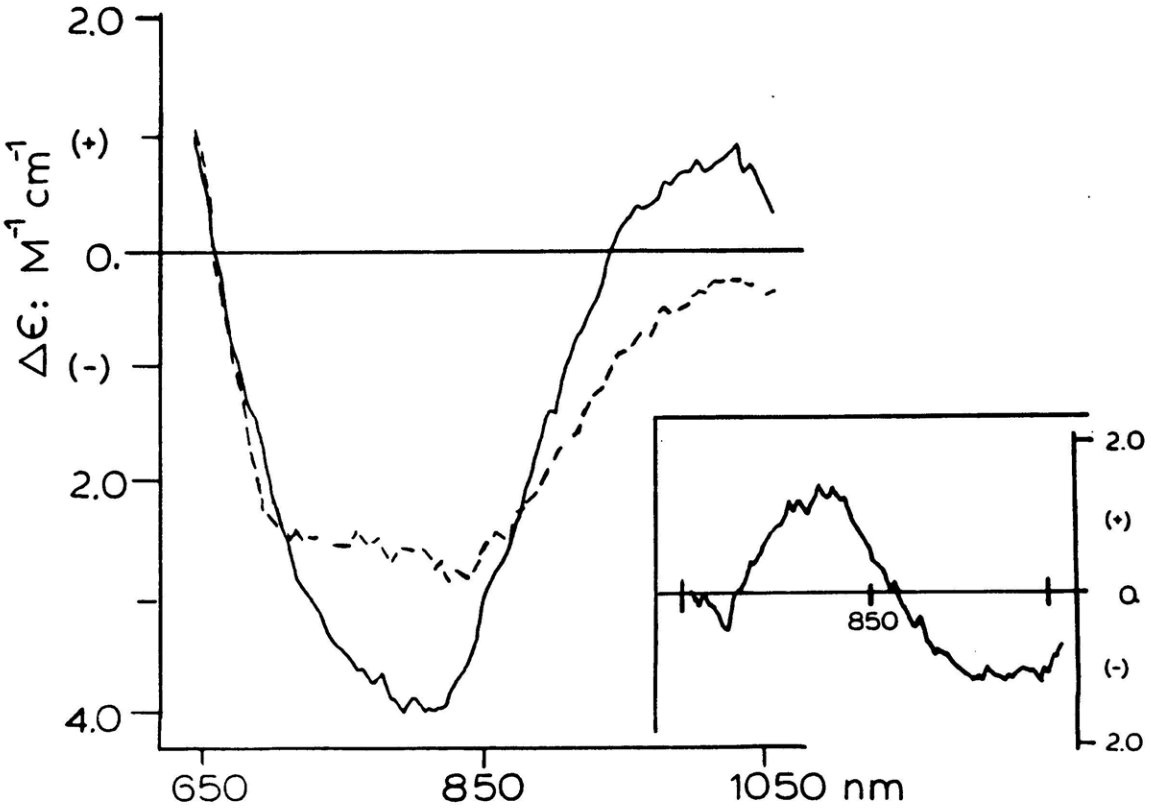
2.0
(+)
0.
(-)
2.0
4.0
ΔE: M⁻¹cm⁻¹
650
850
1050 nm
850
2.0
(+)
0
(-)
2.0

represents a disappearance of the original half met ligand field transition and that the positive intensity at ~800 nm must arise from a new transition. Thus, coordination of N_3^- to half met T2D shifts the ~1000 nm transition ($\Delta(\Delta\varepsilon) = -1.29\ M^{-1}cm^{-1}$) to ~800 nm; ($\Delta(\Delta\varepsilon) = +1.36\ M^{-1}cm^{-1}$); the second half met ligand field band at ~650 nm is unaffected by N_3^-.

It should be noted that the energy of the new CD feature at ~800 nm (12,500 cm^{-1}) is quite consistent with the increased intensity at ~750 nm (13,300 cm^{-1}) in the absorption spectrum, where in general, the CD transition is often found to lower energy.[16] The actual shift of the band when coordinating N_3^- is unusually large and corresponds to ~2300 cm^{-1}; this undoubtedly represents a major change at the half met site on binding N_3^- and will be further discussed in part 2 of this chapter.

Investigation of the nitrite reactivity of T2D laccase has led to the development of new routes for (i) oxidation of the reduced T3 site in deoxy T2D to form met T2D and (ii) generation of half met T2D laccase forms. In contrast to the anaerobic $Fe(CN)_6^{4-}$ reduction of met T2D to prepare half met T2D laccase, half met hemocyanin[17,18] is accessible only through the action of nitric oxide.[1]

(i) deoxy [Cu(I)Cu(I)] + 2 NO ---> met [Cu(II)...Cu(II)] + NO_2

(ii) met [Cu(II)...Cu(II)] + NO ---> half met-NO_2^- [Cu(I)Cu(II)]NO_2^-

and in the presence of O_2

(iii) half met-NO_2^- [Cu(I)Cu(II)]-NO_2^- + NO ---> dimer-N_xO_y [Cu(II)Cu(II)]N_xO_y

as can be derived from aqueous nitrite chemistry at pH < 7.0:

(iv) $3\ NO_2^- + 2\ H^+ \rightarrow 2\ NO + NO_3^- + H_2O$

The extension of this reactivity to the T2D laccase derivatives follows.

The EPR signal of deoxy T2D laccase treated with excess sodium nitrite is shown in Figure 3.24; overlapping the peaks normally associated with the T1 copper center are four additional hyperfine lines characteristic of isolated tetragonal Cu(II) $g_{||} = 2.31$, $g_{\perp} = 2.06$, $A_{||} = 160 \times 10^{-4}$ cm^{-1}). As the T2 center is ≥ 90% removed and double integrated EPR intensity is 1.4 spin/mole, the new cupric

Figure 3.24 EPR spectra at 77 K: nitrite reactivity of deoxy T2D laccase.

(A) original T2D laccase;

(B) after reaction with 100 protein equivalents $NaNO_2$, 20 hours;

(C) sample B, dialyzed;

(D) sample C, after 45 minute reaction with 30X H_2O_2.

Primed spectra were recorded at ~6X higher gain. (9.26 GHz; 0.1 M potassium phosphate, pH 6.0; [protein] = 0.15 mM for spectra A,B, 0.14 mM for spectra C,D)

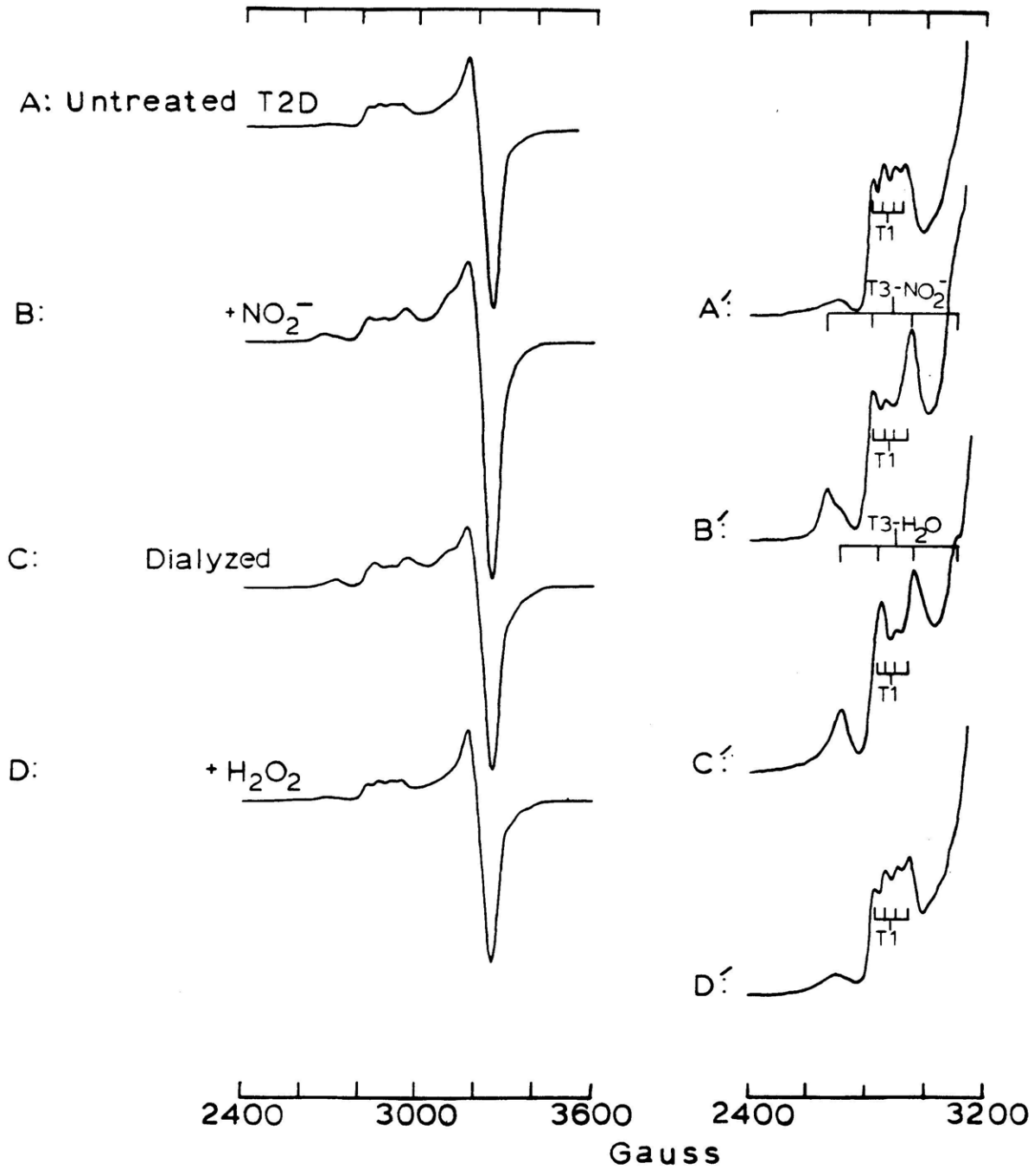
A: Untreated T2D
B: +NO2−
C: Dialyzed
D: +H2O2
A′:
B′:
C′:
D′:
T1
T3-NO2−
T3-H2O
2400
3000
3600
2400
3200
Gauss

signal must originate from the binuclear copper site. Increased [NO_2^-]'s (up to 1000X NO_2^-), lower temperatures (≈10 K) and higher microwave powers (197 mW) result in no apparent g~4, Δm_s = 2 signal nor broad g≈2, Δm_s = 1 signal indicating that, in contrast to hemocyanin chemistry,[20] an N_xO_y uncoupled derivative[19,20] has not been formed. Short term dialysis (< 5 hour) alters the T3-related signal and results in an EPR spectrum (Figure 3.24C) which is identical to that of half met-aquo T2D, as generated through ferrocyanide reduction of met T2D. The 330 nm absorption, associated with the T3 site in met T2D,[8] is increased relative to the original deoxy T2D but less than that normally observed in the peroxide-oxidized T2D; little or no perturbation in the 600 nm region is observed. As is found for the $Fe(CN)_6^{4-}$-generated half met T2D derivative, peroxide removes the T3 EPR signal, decreases the integrated EPR intensity to ~1.0 spin/mole and increases 330 nm absorption, indicating oxidation to met T2D (Figure 3.24D) and assuring that the NO_2^- treated deoxy T2D is a regenerable protein form. X-ray absortion edge studies (Chapter 2) show 11 $\pm$ 5% Cu(I) in the NO_2^--treated deoxy T2D protein, consistent with the double-integrated EPR intensity and a mixture of met and half met-NO_2^- binuclear copper sites (optical and EPR data demonstrate the Blue copper is fully oxidized). Thus, the significantly decreased percentage of Cu(I) and increased 330

nm absorption in the NO_2^--treated protein indicate that, analogous to hemocyanin and tyrosinase nitrite chemistry,[1] NO oxidizes the cuprous T3 site in deoxy T2D. Further, the new T3 EPR signal associated only with a $\Delta m_s = 1$ transition, its conversion to half met-aquo T2D upon simple dialysis, the Cu(I) in the x-ray absorption edge, and related nitrite studies on met T2D (vide infra) together demonstrate that this met intermediate reduces by one electron to generate a stable half met-NO_2^- protein form.

Parallel nitrite reactions on met T2D {T3: [Cu(II)Cu(II)]; T1: [Cu(II)]} also result in the 1.4 spin/mole EPR spectrum (Figure 3.25B); the spectral and chemical properties associated with this protein are essentially indistinguishable from those of the NO_2^- treated deoxy T2D derivative. As some $Fe(CN)_6^{3-/4-}$ is inevitably present in the T2D protein prior to NO_2^- addition and this reductant has been shown to generate half met-aquo from met T2D, control experiments monitored the oxidation state stability of met T2D in the absence of nitrite and confirmed the direct involvement of NO/NO_2^- in the one-electron reduction of the binuclear cupric site.[21] Short term dialysis of the NO_2^- treated met T2D again removes the weakly coordinated NO_2^- ligand to produce half met-aquo T2D (Figure 3.25C).

Figure 3.25 EPR spectra at 77 K: nitrite reactivity of met T2D laccase.

(A) $g_{||}$ region of original met T2D laccase;

(B) after reaction with 100 protein equivalents $NaNO_2$, 20 hours;

(C) sample B, dialyzed;

(D) half met-aquo T2D laccase;

(E) sample D, reacted with 200 protein equivalents $NaNO_2$;

(F) sample B reacted with 10 protein equivalents NaN_3.

(9.25-9.26 GHz; 0.1 M potassium phosphate, pH 6.0; [protein] = 0.186 mM for spectra A-C, F, 0.107 mM for spectra D,E)

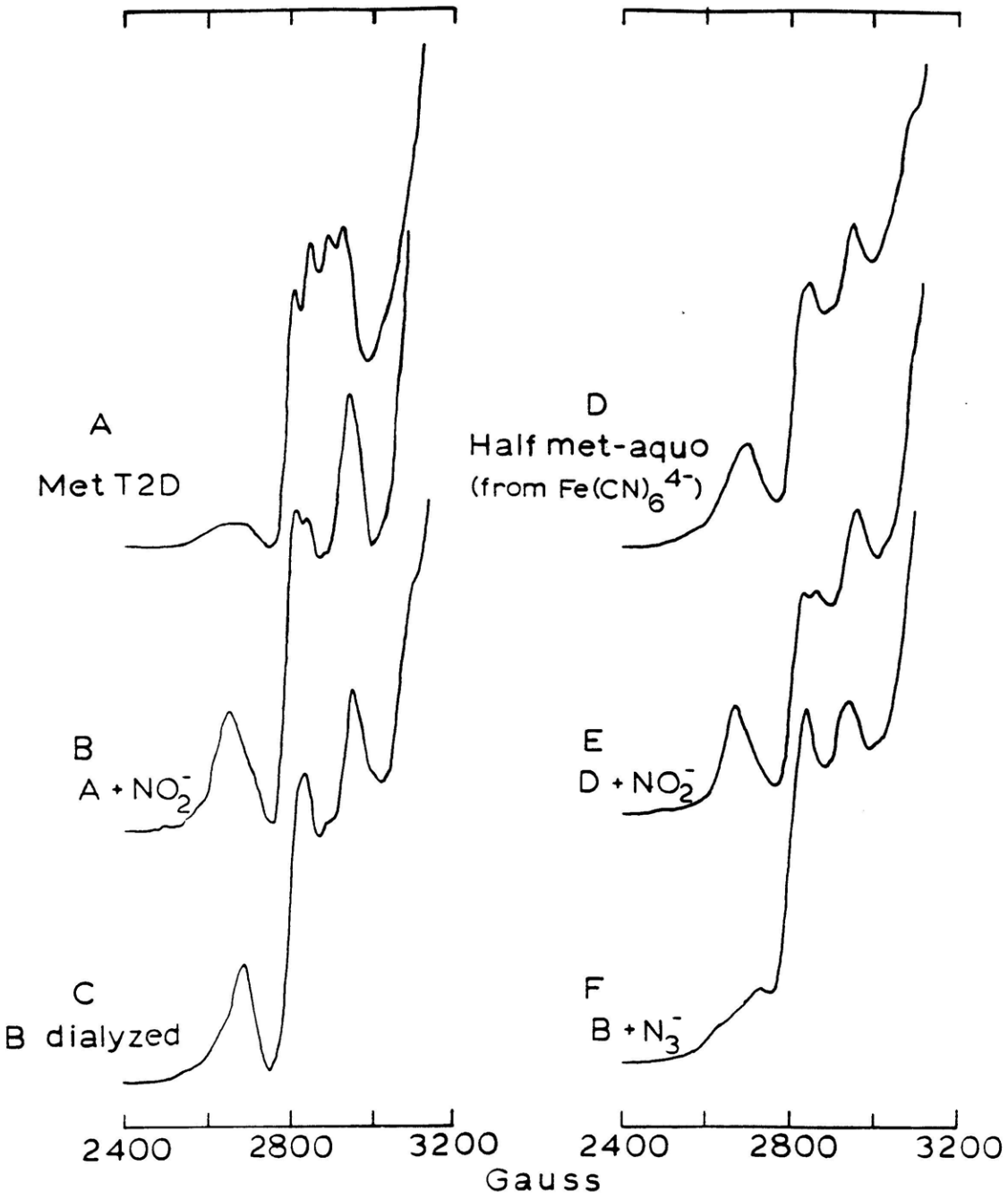
A
Met T2D
B
A + NO_2^-
C
B dialyzed
D
Half met-aquo
(from $Fe(CN)_6^{4-}$)
E
D + NO_2^-
F
B + N_3^-
2400
2800
3200
2400
2800
3200
Gauss

Experiments monitoring the time course of the oxidation state of the T3 site under the action of lower [NO_2^-]'s further evidence both the lack of tight binding of NO_2^- at the mixed valent site and, in the case of deoxy T2D, the generation of an oxidized met intermediate ($2e^-$ oxidation) prior to half met formation ($1e^-$ reduction). In Table 3.2 are summarized the ratios of the absorbance at 330 nm compared to that at 614 nm for deoxy and met T2D (H_2O_2 removed by dialysis) before and after treatment with 10 equivalents of $NaNO_2$. The EPR spectra corresponding to the NO_2^- treated samples after 34 hour and 5 day reaction times are shown in Figure 3.26. After 5 days, 10X NO_2^- reacted with deoxy T2D results in no significant increase in the 330/614 ratio nor T3 contribution to the EPR spectrum (3.26B). While the analogous data for the reaction of 10X NO_2^- on met T2D do indicate significant T3 reduction, it should be noted that Figure 3.26D represents half met-aquo T2D (e.g. $1e^-$ reduction but no NO_2^- coordination), consistent with the weak coordination of the NO_2^- ligand as suggested by its high lability to dialysis. The lack of half met-X formation in deoxy but not met T2D at low [NO_2^-]'s and the observed longer reaction time of deoxy (20 hour) relative to met (6 hour) with 100X NO_2^- (experimental results) further indicate that half met formation from deoxy T2D occurs via an oxidized met intermediate. Finally, while quantitative x-ray

Table 3.2 Nitrite Reactivity of T2D Laccase - Time Dependence

Protein Sample	OD_{330}[a]/OD_{614}		
	10 hours	34 hours	5 days
Deoxy T2D	0.467	0.473	
+ 10X NO_2^-	0.472	0.460	0.504
Met T2D, dialyzed	0.851	0.850	
+ 10X NO_2^-	0.791	0.733	0.648

[a] The absorbance at 330 nm was corrected for $[NO_2^-]_{aq}$

Figure 3.26 EPR spectra at 77 K: time dependence of nitrite reactivity on deoxy and met T2D

$g_{||}$ region of

(A) deoxy T2D after reaction with 10 protein equivalents $NaNO_2$, 34 hours;

(B) sample A after 5 days;

(C) met T2D laccase after reaction with 10 protein equivalents $NaNO_2$, 34 hours

(D) sample C after 5 days.

(9.26 GHz; 0.1 M potassium phosphate, pH 6.0; [protein] = 0.122 mM)

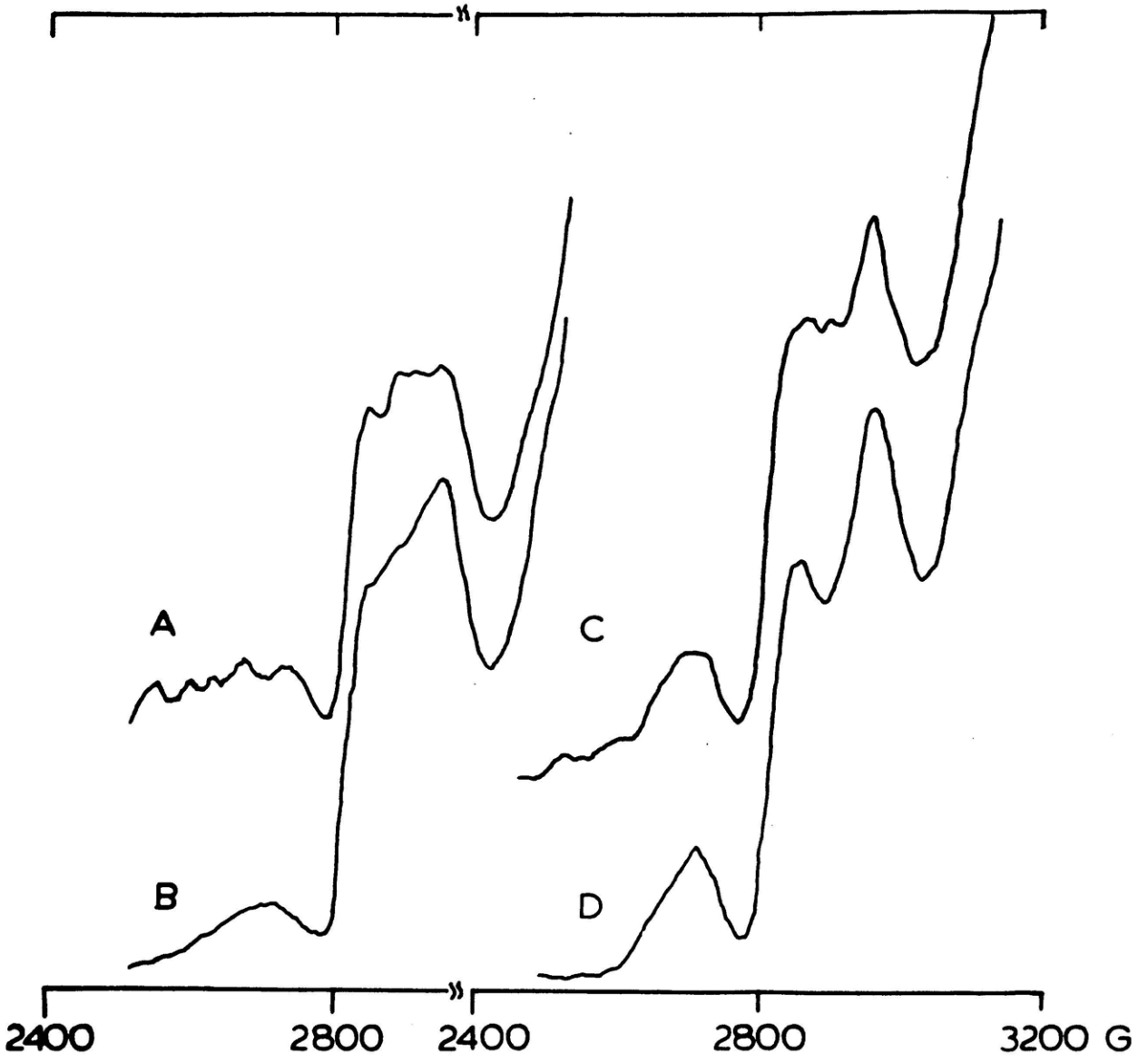
A
B
C
D
2400
2800
2400
2800
3200 G

absorption edge analyses indicate that the met and deoxy T2D proteins differ by 70 ± 15% in their Cu(I) composition, the derived NO_2^--treated edges are essentially superimposable; these studies corroborate both the oxidation of deoxy to met and the assignment of the aforementioned ~11% Cu(I) as being primarily due to half met sites.

The ligand substitution chemistry of this half met T2D laccase has also been pursued. The interconversion of the various half met T2D derivatives indicates $Fe(CN)_6^{4-}$ and NO_2^- reactivity lead to equivalent half met protein forms. Nitrite titration of ferrocyanide-generated half met T2D produces half met-NO_2^- T2D (Figure 3.25 D-E); this further demonstrates that the original products of the NO_2^- preparations contain a coordinated nitrite ligand which is readily removed upon dialysis. Only one NO_2^- is bound, based on half met-aquo T3 EPR perturbation with increasing $[NO_2^-]$. From these 77 K EPR studies, K_{eq} ~300 M^{-1} for NO_2^- binding to the half met-aquo site. Addition of 10X N_3^- to the nitrite-induced half met-NO_2^- (in 100X NO_2^-) decreases $A_{||}$ of the T3 signal and results in half met-N_3^- (Figure 3.25F) identical to that observed upon N_3^- titration of the $Fe(CN)_6^{4-}$-induced half met-aquo T2D (Figure 3.19); this displacement is consistent with the much higher binding affinity for N_3^- (K_{eq} ~6000-8000 M^{-1}) than NO_2^- (K_{eq} ~300 M^{-1}) at the half met site.

Thus, NO_2^- reacts with deoxy and met T2D to form indistinguishable half met-NO_2^- protein forms. Through their spectroscopic and chemical study, it is further clear that these half met derivatives are equivalent to those prepared through the anaerobic ferrocyanide reduction of met T2D. While part II of this chapter concerns the detailed comparison of this reactivity to that of the hemocyanins and tyrosinase, the lack of dimer[20] formation (Equation (iii), page 188)in T2D deserves immediate comment.

To further investigate the possible formation of a dimer-N_xO_y T2D derivative (two cupric centers formally uncoupled and interacting at a short Cu-Cu distance resulting in a broadened g~2 $\Delta m_s = 1$ transition and the appearance of a g~4 $\Delta m_s = 2$ transition), a series of experiments were performed in 0.1 M sodium acetate at pH 5.2. From equation (iv), lowering the pH increases the amount of NO generated, and the latter would increase the probability of further oxidizing and uncoupling the T3 site. In Figure 3.27A and B are shown the EPR spectra of met T2D treated with 100 and 500X $NaNO_2$, respectively, at pH = 5.2. The additional nitrite in spectrum 3.27B leads to no broadening of the four-line localized EPR spectrum in 3.27A. The spectrum does differ slightly from that of Figure 3.24B, however, as the high excess of acetate anion displaces NO_2^- from the half met site. Significantly, at ~10 K and 200 mW microwave power,

Figure 3.27 EPR spectra at 77 and 10 K: met T2D laccase in excess $NaNO_2$ at low pH.

met T2D laccase reacted with

(A) 100 protein equivalents $NaNO_2$;

(B) 500 protein equivalents $NaNO_2$.

(A) is recorded with 10 mW incident power at 77K;

(B) is recorded with 197 mW incident power at ~10K.

Primed spectra were recorded at 8X higher gain.

(9.39 GHz; 0.1 M sodium acetate, pH 5.2; [protein] = 0.141 mM)

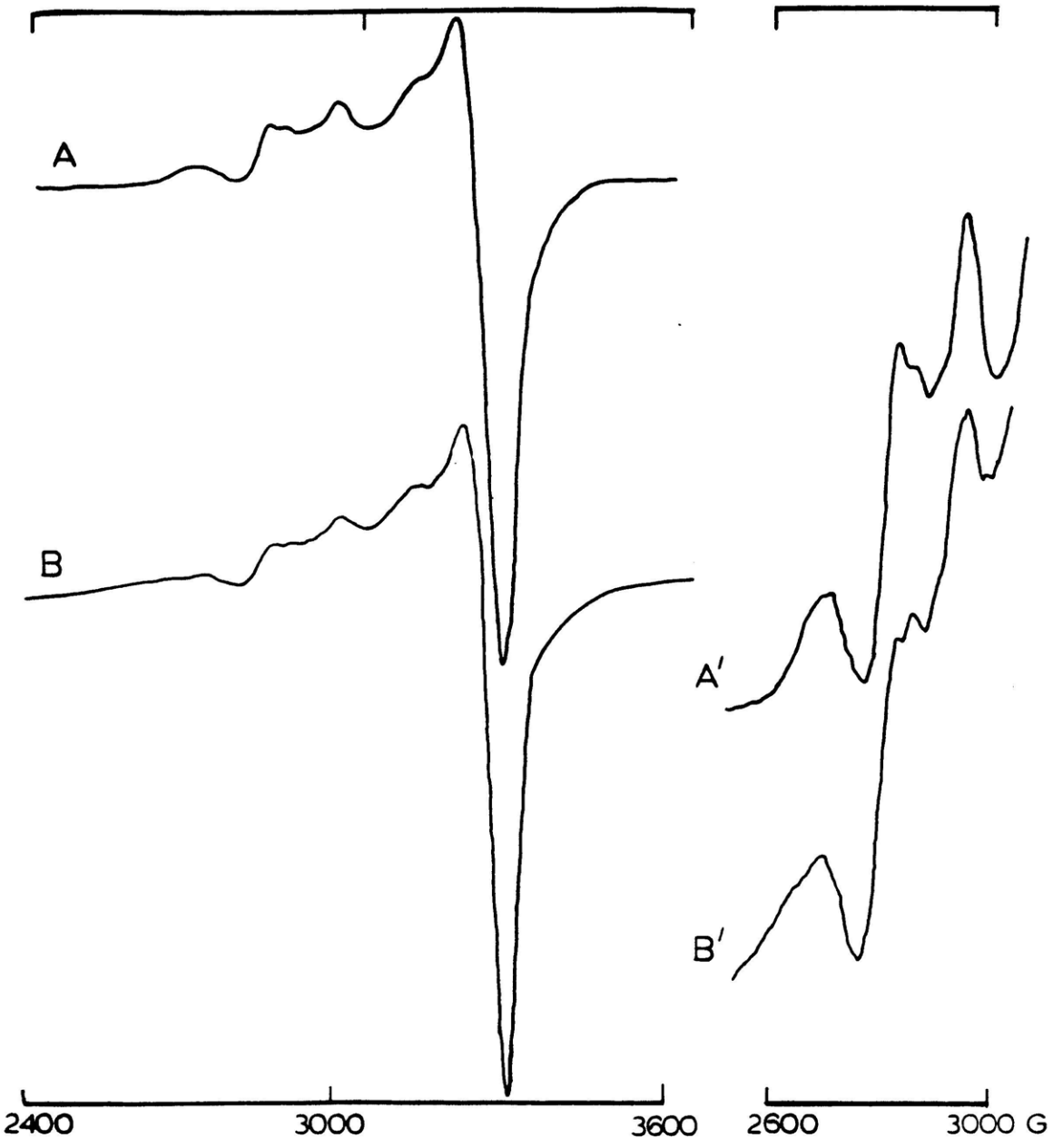
A
B
A′
B′
2400
3000
3600
2600
3000 G

the 500X NO_2^- still shows no evidence for uncoupling of the T3 site (Figure 3.27B).

It should be mentioned that CO at 2 atm does not perturb any of the half met Cu(II)-X EPR spectra. If CO does bind to the Cu(I) at the half met site, it would be reasonable to expect it to affect the electronic and/or geometric structure of the other cupric center at the binuclear copper site, especially in light of its ability in deoxy T2D to perturb the EPR spectrum of the T1 Cu(II). Unfortunately, a perturbation of the underlying T1 Cu(II) EPR signal would be very difficult to see in the various half met derivatives.

C. Met T2D Laccase

i. Spectroscopic Properties

As discussed in Chapter 2, excess peroxide oxidizes the binuclear cuprous site of deoxy T2D to generate met T2D which contains an EPR non-detectable [Cu(II)Cu(II)] T3 site. Thus, only the T1 Cu(II) contributes to the EPR spectra of both deoxy and met T2D (Figure 3.28). While these spectra are very similar, they are not equivalent as $A_{||}$ of the T1 Cu(II) increases from 37.8 to 42.9 X 10^{-4} cm^{-1} upon oxidation of the T3 site, indicating that a concomitant

Figure 3.28 EPR spectra at 77 K: deoxy and met T2D laccase.
(A) deoxy T2D;
(B) met T2D.
Primed spectra were recorded at 8X higher gain.
(0.1 M potassium phosphate, pH 6.0; [protein] = 0.260 mM)

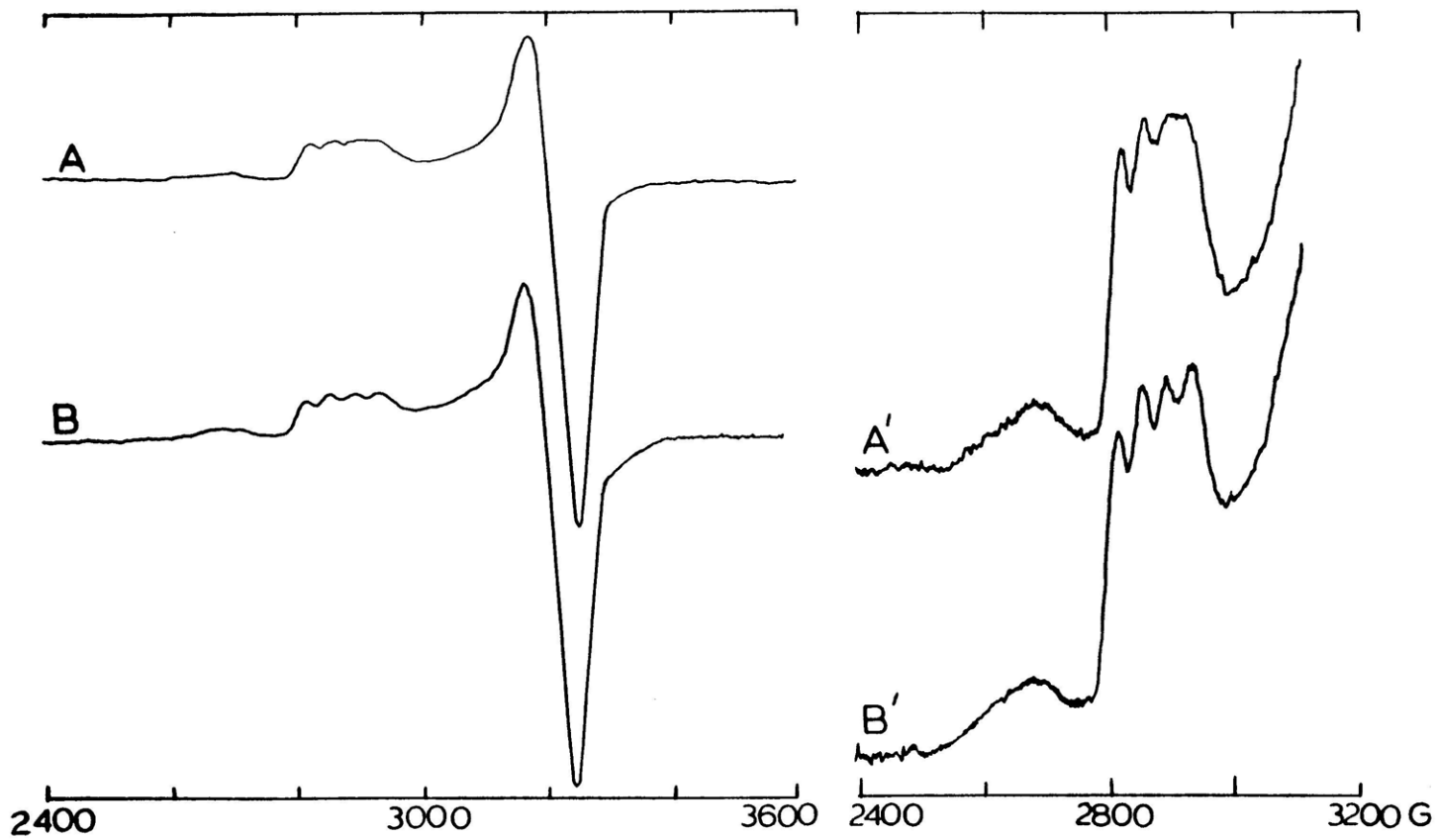
A
B
2400
3000
3600
A′
B′
2400
2800
3200 G

structural change at the T1 center has also occurred (Chapter 4).

Through detailed comparison of met and deoxy T2D, the optical features associated with the oxidized T3 site can be determined. Studies aimed at elucidating and assigning transitions of the T3 pair in the visible spectral region (primarily CT) will first be discussed, followed by somewhat more limited investigations of the near IR (primarily ligand field) spectral region. In Figure 3.29 are shown the 298 K absorption spectra of deoxy and met T2D. The $\Delta\varepsilon_{745} \sim 150$ $M^{-1}cm^{-1}$ has been assigned, by analogy to hemocyanin and tyrosinase, as the d-d transitions of the two tetragonal cupric centers. As demonstrated by the x-ray absorption, visible-UV peroxide titration of T2D (Chapter 2), the broad absorption band which maximizes at 330 nm ($\Delta\varepsilon_{330}$ = 2000 $M^{-1}cm^{-1}$) represents endogenous L ---> Cu(II) CT at the T3 site. A decrease is observed at 614 nm ($\Delta\varepsilon \sim -600$ $M^{-1}cm^{-1}$, as the integrated EPR intensity remains constant) which is interpreted[8] as a structural change of the T1 Cu(II) upon T3 copper oxidation (Chapter 4). As in deoxy T2D, the Blue band sharpens upon cooling to 77 K (Figure 3.30). Additionally in met, however, absorption intensity between 500 and 400 nm is significantly increased. At least two new features are now resolved at ~440 and 400 nm, demonstrating that several bands are indeed contributing to the broad 330 nm absorption

Figure 3.29 Electronic absorption spectra at 298 K: met and deoxy T2D laccase.

(——) deoxy T2D;

(— — —) met T2D, with assignment of spectral features associated with the coupled binuclear cupric site.

(0.1 M potassium phosphate, pH 6.0; [protein] = 0.20 mM)

Figure 3.30 Electronic absorption spectra at 77 and 298 K: met T2D laccase.

(——) 298 K;

(— — —) 77 K.

(1.45 mm pathlength; 50% v/v glycerol/0.1 M potassium phosphate, pH 6.0; [protein] = 1.1 mM)

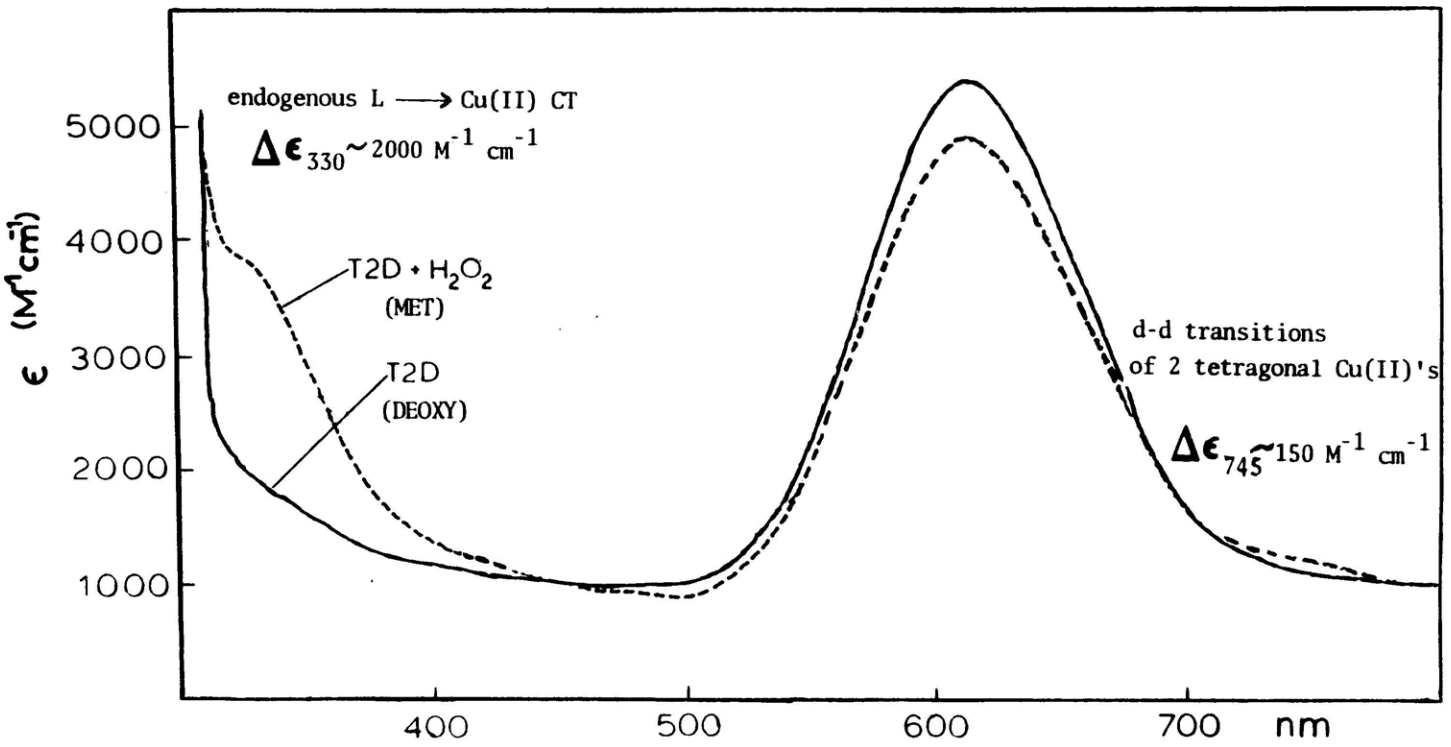
endogenous L ⟶ Cu(II) CT
Δε330~2000 M-1 cm-1
T2D + H2O2
(MET)
T2D
(DEOXY)
d-d transitions
of 2 tetragonal Cu(II)'s
Δε745~150 M-1 cm-1
ε (M-1cm-1)
5000
4000
3000
2000
1000
400
500
600
700
nm

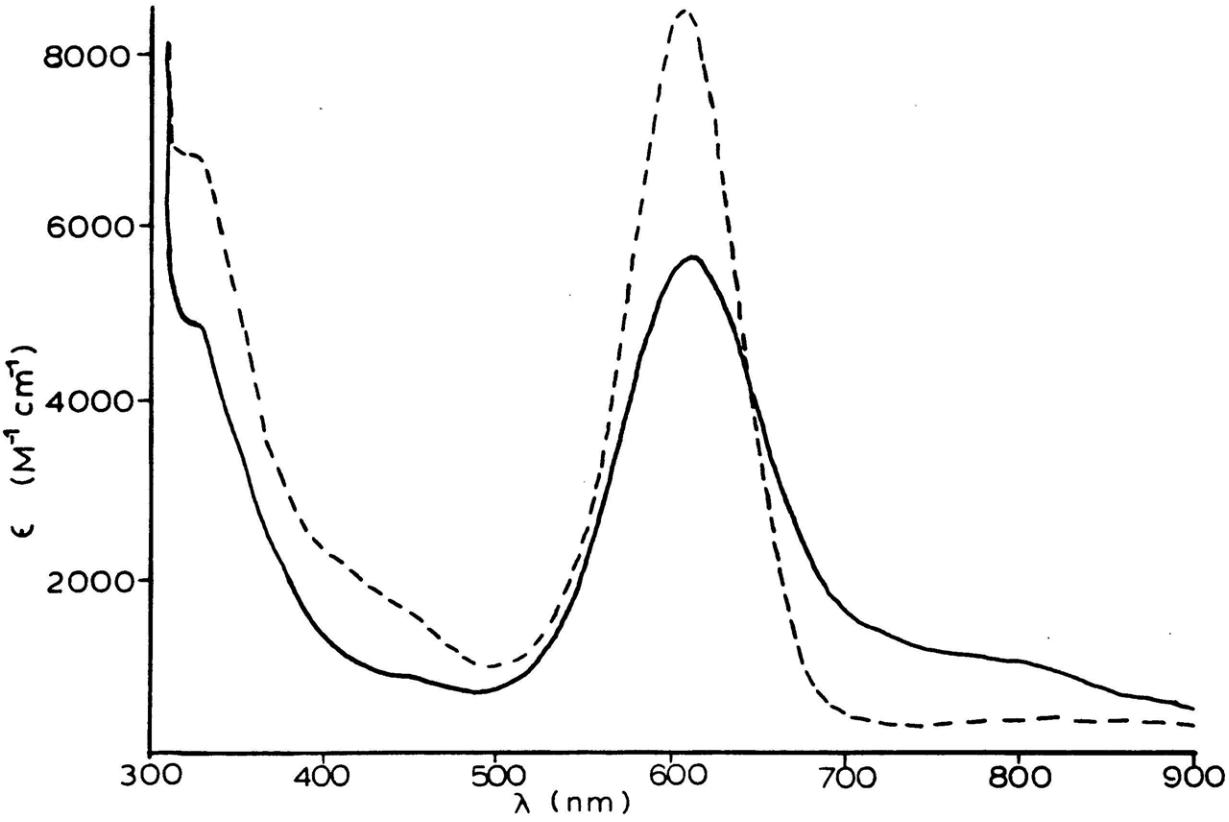
8000
6000
4000
2000
ε (M⁻¹ cm⁻¹)
300
400
500
600
700
800
900
λ (nm)

feature at 298 K. These bands must represent endogenous L ---> Cu(II) charge transfer at the T3 site. The low energy suggests that a phenolate ---> Cu(II) CT transition is a reasonable candidate and may relate to the endogenous bridge. Finally, the "330 nm band" also sharpens upon cooling and now maximizes at 320 nm. In the visible region of the CD spectra of met and deoxy T2D (Figure 3.31) only weak differences are observed: $\Delta(\Delta\varepsilon)_{370} = \leq +0.3\ M^{-1}cm^{-1}$ and $|\Delta(\Delta\varepsilon)_{320}| < 0.2\ M^{-1}cm^{-1}$.

The nature of the ligation at the T3 coppers in laccase and the possible assignment of their resultant 330 nm absorption feature was further investigated through Extended X-ray Absorption Fine Structure (EXAFS) studies of met T2D. In particular, a strong S-Cu bond in a tetragonal cupric site can contribute significant CT intensity in the 300-350 nm spectral region.[24] While no strong sulfur ligand is present in hemocyanin,[25] the 330 nm region is broader and weaker in met hemocyanin[26] than in met laccase; hence, EXAFS studies were pursued in order to ascertain whether sulfur is coordinated at the oxidase T3 site.

The EXAFS data of met T2D laccase and its Fourier Transform are shown in Figure 3.32. As each copper atom generates an EXAFS spectrum which is dependent on the ligands coordinated to it, the EXAFS spectrum of met T2D laccase is

Figure 3.31 Visible-UV CD spectra at 298 K: met and deoxy T2D laccase.

(——) deoxy, and (— — —) met T2D

(0.1 M potassium phosphate, pH 6.0; [protein] = 0.186 mM)

Figure 3.32 Fourier Transform and EXAFS: met T2D laccase.

(top) Fourier transform, K = 4-12 $(Å)^{-1}$, k^3 weighted, and

(bottom) EXAFS at -60°C

(0.1 M potassium phosphate, pH 6.0; [protein] ~2 mM)

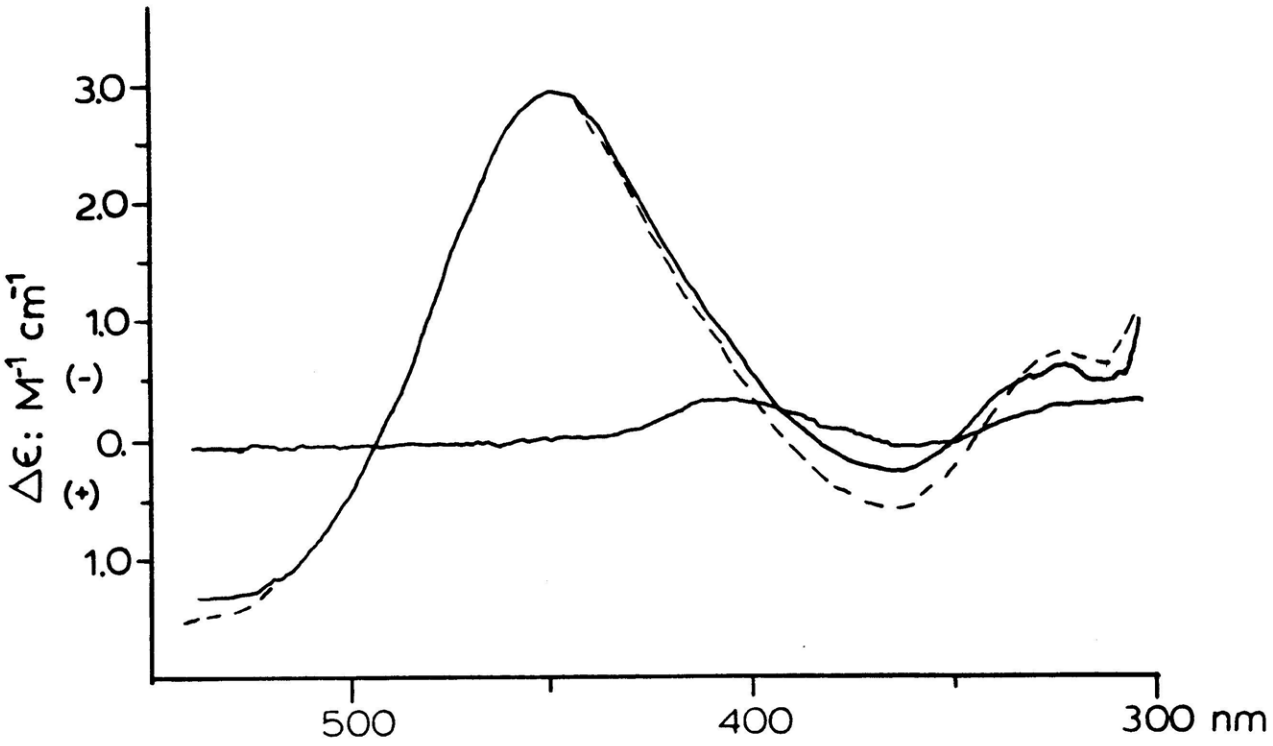
3.0
2.0
1.0
(-)
0.
(+)
1.0
Δε: M⁻¹ cm⁻¹
500
400
300 nm

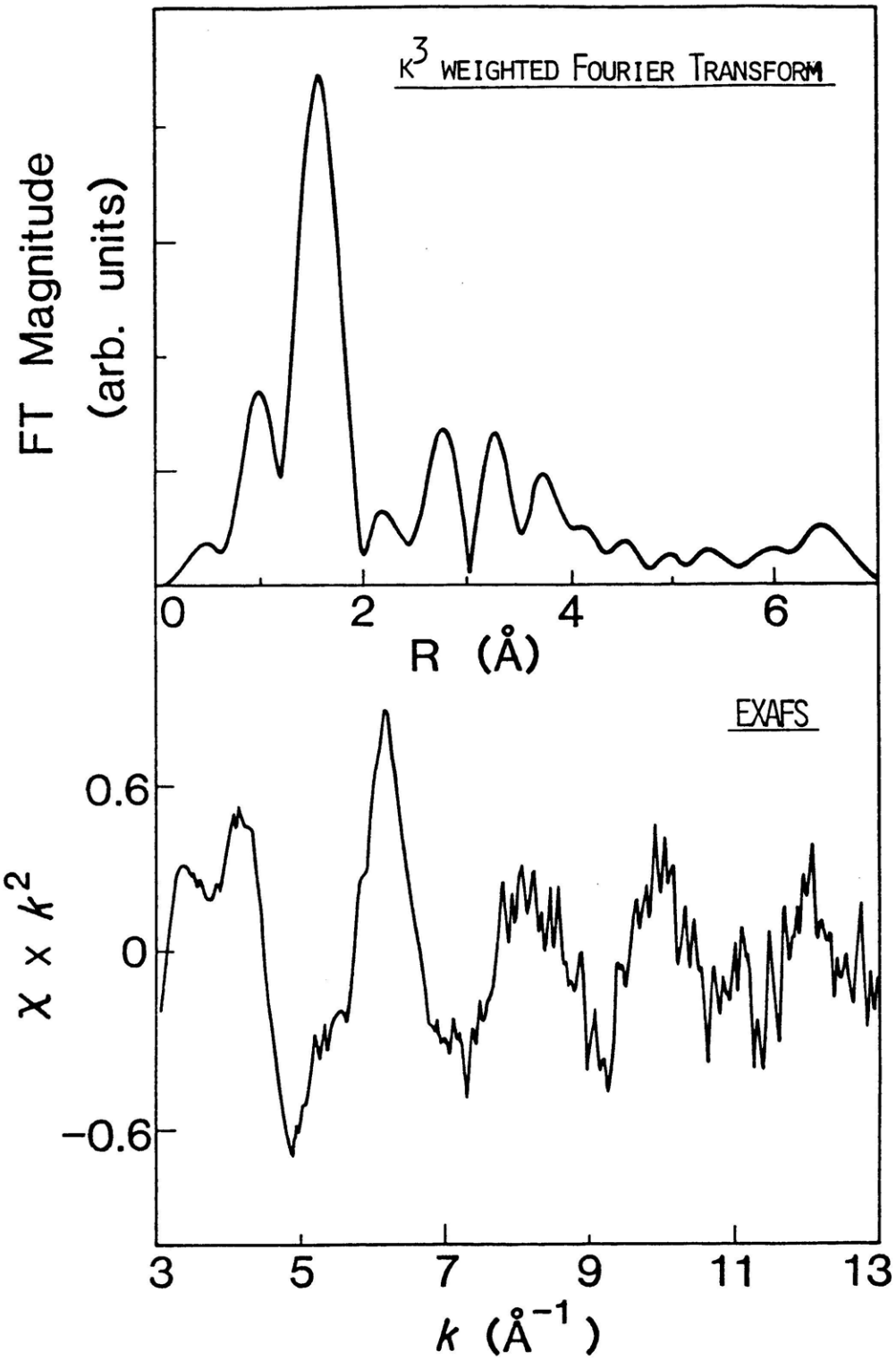
K³ WEIGHTED FOURIER TRANSFORM
FT Magnitude
(arb. units)
0
2
4
6
R (Å)
EXAFS
0.6
0
-0.6
χ x k²
3
5
7
9
11
13
k (Å⁻¹)

an average spectrum of the three absorbing copper atoms.

The major peaks in the transform are filtered and backtransformed to k-space for least-squares curve fitting analysis, as summarized in Table 3.3. In met T2D, the first shell can be fit with a shell of 3.5 nitrogen (or oxygen) atoms at an average Cu-N (or -O) distance of 1.99 Å. Inclusion of an additional shell of sulfur improved the fit significantly, reducing the function value[27] from 0.30 to 0.22. An average of 0.33 sulfur at 2.09 Å and 3.0 nitrogens (or oxygens) at 2.00 Å is obtained in the two shell fit. As the T2D derivative contains three copper atoms, this result suggests that one sulfur atom is coordinated to one of the copper atoms while 3-4 nitrogen (or oxygen) atoms will complete the coordination spheres of all the copper atoms. As all copper atoms are defined to be Cu(II) from the absorption edge studies (Chapter 2) and Cu(II) ions are usually coordinated by 4-6 ligands, the indicated average of 3-4 N (or O) atoms is somewhat low. However, static disorder (as a consequence of averaging heterogeneous copper sites) will cause destructive interference which will lower the prediction of coordination numbers, keeping the Debye-Waller factor constant.

Quantitative chemical and spectroscopic studies have established that T2 copper is ≥90% removed in T2D and that

Table 3.3 EXAFS First Shell Curve Fitting Results - Met T2D Laccase

Copper Centers	Function Values[27]	Cu-N		Cu-S	
		Å	#	Å	#
T1 + T3	0.30	1.99	3.5		
	0.22	2.00	3.0	2.09	0.33
T3	0.20	2.01	3.2		
	0.19	2.01	3.2	2.26	0.06

met T2D laccase contains an oxidized Blue copper center. Further, as shown in Table 3.4, the optical and EPR properties of the laccase T1 Cu(II) closely relate to those of the simpler Blue copper proteins, plastocyanin and azurin (but not stellacyanin).[10,28] Hence, the plastocyanin copper EXAFS spectrum has been used to model that of the T1 site in T2D laccase and generate a difference EXAFS spectrum for the T3 site. Specifically, the average T2D laccase spectrum is multiplied by a factor of three and the Blue copper site (using normalized plastocyanin EXAFS)[29] is subtracted from it; the division of this difference spectrum by two then generates an average spectrum of the two coppers in the T3 site. The major peak in the transform is again filtered and backtransformed for curve fitting analysis. The results (see Table 3.3) indicate 3.2 nitrogen (or oxygen) atoms at 2.01 Å. Sulfur atoms were again included in a two shell fit, but no improvement in function value was obtained and the amplitude of the resulting sulfur atom was no more than the level of noise. The difference EXAFS analysis is thus consistent with the results stated previously that a sulfur atom is coordinated to one copper - in the Type 1 site - and that there is no strong sulfur ligation at the T3 site in laccase. While the Cu-S distance of 2.09 Å for the T1 site in T2D is slightly short for thiolate coordination to Cu(II), a similar distance of 2.11 Å is indicated by EXAFS treatment of plastocyanin, the T1 model system. The average coordination

Table 3.4 Comparison of Laccase T1 Copper(II)[a] to the Blue Copper Proteins[b]

	Rhus met T2D	Plastocyanin[c]	Pseudomonas aeruginosa Azurin	Rhus Stellacyanin
EPR				
$g_{\parallel}$	2.300	2.226	2.26	2.287
$g_{\perp}$	2.054	2.053	2.05	*2.077, 2.025*[d]
$A_{\parallel}$ (cm^{-1})	42.9×10^{-4}	63×10^{-4}	60×10^{-4}	35×10^{-4} (29, 57)
Optical				
λ_{max} (nm)	614	597	625	608
ε ($M^{-1}cm^{-1}$)	~5400	4900	3500	4030
CD[e]				
λ_{max} (cm^{-1}) $\Delta\varepsilon$($M^{-1}cm^{-1}$)		24,000 (+1.26)	24,500 (+0.3)	
	22,100 (-2.8)	21,200 (-1.32)	21,400 (-1.8)	22,400 (*-7.35*)
	18,900 (+1.4)	19,000 (+0.4)	19,000 (+1.2)	19,000 (+0.75)
	16,300 (+1.5)	16,500 (+4.08)	16,100 (+6.5)	16,500 (+3.6)
	~13,600 (-3.0)	12,800 (-3.78)	12,500 (-5.9)	12,800 (-5.0)
rR (cm^{-1})[f]	258	262	262	267
			340 (sh)	
	382	379	372	*350*
	407	407	407	388
	421	426	425	410
			460 (sh)	422, 424
E° (mV)	447	370	300-328	*184*

(a) From LuBien, C.D. et al. (1981) J. Am. Chem. Soc. 103, 7014-7016.
(b) Adapted from Fee, J.A. (1975) Struct. Bonding (Berlin) 23, 4-5.
(c) CD for bean plastocyanin; all other data refers to spinach plastocyanin.
(d) Italicized data most significant in differentiating stellacyanin from the other Blue Copper containing proteins.
(e) All Blue Copper protein CD data from Solomon, E.I. et al. (1980) J. Am. Chem. Soc. 102, 168-177.
(f) All Blue Copper protein rR data from Gray, H.B. and Solomon, E.I. (1981) Copper Proteins, Chapter 1, Academic Press, New York (Spiro, T.G., ed.).

environment of 3-4 nitrogen (or oxygen) atoms at 2.00 Å in met T2D is essentially unaltered by subtraction of the plastocyanin contribution to the EXAFS spectrum.

This calculated (met T2D-T1) difference spectrum can be used to further probe the T3 site in laccase. The outer peak pattern in the transform of the laccase difference spectrum indicates imidazole coordination but there is no evidence of a heavy atom scatterer. Curve fitting analysis of the outer peaks further shows no indication of a copper scatterer at a distance $\leq$ 3.8 Å. Detection of a copper scatterer at $\geq$ 3.8 Å is not possible at this noise level and is further complicated by multiple scattering effects and unknown Debye-Waller factors.

These results depend on how well the T1 site is represented by plastocyanin. Computer simulation and metal complex studies of difference EXAFS techniques have shown that inappropriate subtraction of one site leads to erroneous analysis of the other site.[30] While the lack of x-ray crystallographic data for the T1 site in laccase precludes absolute evaluation of model propriety, the similar spectroscopic properties, as summarized in Table 3.4, would suggest no more appropriate model has been reported.

The exclusion of strong S ligation (to < 2.4 Å) at the

T3 site in laccase indicates that absorption in the 330 nm region, present in native and met but not deoxy T2D, is not S ---> Cu(II) CT. An average of 3-4 N (or O) atoms at a distance of 2.00 Å in met T2D laccase is the only ligation evidenced by EXAFS studies. Based on model studies[31] this feature then likely derives from a composite of His ---> Cu(II) CT transitions with potential contribution of RO^- ---> Cu(II) CT from the endogenous protein bridge.

Lastly, comparison (Figure 3.13) of the 330 nm region in deoxy, half met and met T2D indicates that 330 nm intensity derives only from the fully oxidized T3 site. In a series of experiments monitoring $\Delta\varepsilon_{330}$ as deoxy was oxidized to met (i), reduced to half met (ii) and reoxidized to met (iii), the increase in 330 nm absorption in step (iii) was calculated to be 51 $\pm$ 9% that observed in step (i). As half met T2D contains an approximately equimolar mixture of met and half met sites, this experiment indicates that the mixed valence T3 site contributes essentially no 330 nm absorption intensity. This could indicate that all of the strongest transitions which comprise the met 330 band are associated with the Cu(II) which is reduced in half met, or that the 330 band derives from the entire T3 site, e.g. charge transfer from the non-S endogenous bridge which is no longer active in half met T2D. Alternatively, it may simply be that endogenous L ---> Cu(II) CT occurs to higher energy in half

met and is not spectroscopically accessible. In N_3^- binding studies of both half met and met T2D, the shape and intensity of the 330 nm region are easily perturbed, suggesting that the latter explanation may be the most likely.

To lower energy are the ligand field bands of the tetragonal cupric centers and the CT features of the distorted tetrahedral Blue copper site. In the absorption spectrum (Figure 3.30), the d-d transitions absorb in a broad envelope which maximizes at ~745 nm; no other clear maxima have been observed at 298 or 77 K. In the near-IR CD spectra (Figure 3.33), however, a multitude of features are associated with oxidation of the T3 site: $\Delta(\Delta\varepsilon)_{990}$ --0.47 $M^{-1}cm^{-1}$; $\Delta(\Delta\varepsilon)_{830}$ = +1.03 $M^{-1}cm^{-1}$; $\Delta(\Delta\varepsilon)_{720}$ = +0.90 $M^{-1}cm^{-1}$ and $\Delta(\Delta\varepsilon)_{580}$ = +0.42 $M^{-1}cm^{-1}$. While many of these spectral changes are likely associated with the d-d transitions of the binuclear cupric site, potential structural changes in the T1 site concomitant to oxidation of the T3 site would also be manifested at these wavelengths. Interpretation of these spectral changes is thus quite complex. In the simplest scenario, the CD features of the T1 Cu(II) are unchanged in deoxy and met and the near-IR CD spectrum of met T2D would then be simply a sum of the half met T2D spectrum [Cu(I)met Cu(II)half met] plus the spectral contribution of the additional Cu(II)met center. However, in comparing the met,

Figure 3.33 CD spectra at 298 K: met and deoxy T2D laccase.

(- - -) met T2D laccase;

(——) deoxy T2D laccase.

Digitized spectra have been baseline subtracted by computer and are not smoothed. (0.1 M potassium phosphate, pH 6.0; [protein] = 0.271 mM)

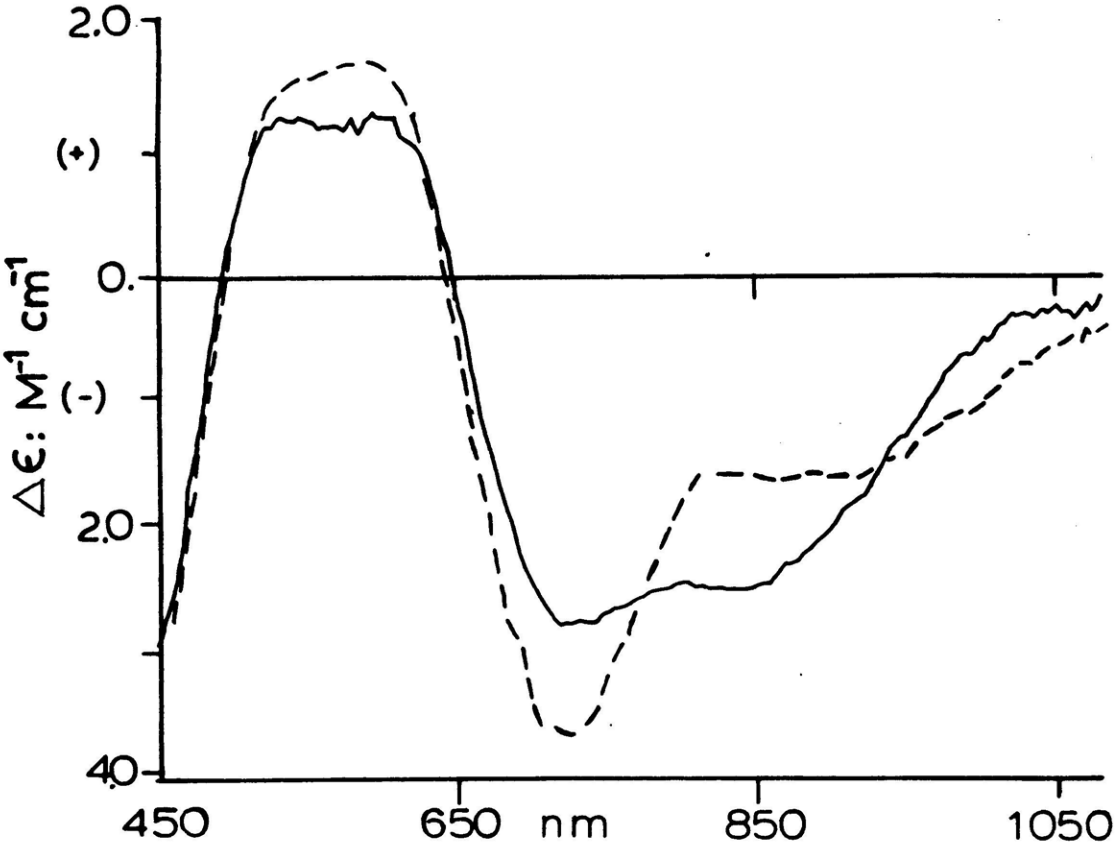
2.0
(+)
0.
(-)
2.0
4.0
Δε: M⁻¹ cm⁻¹
450
650
nm
850
1050

half met (met corrected), and deoxy T2D spectra (Figures 3.33 and 3.16), met and half met would appear to have transitions of opposite sign at similar energies:

Cu(II) Half met Half Met - Deoxy ($M^{-1}cm^{-1}$)	Cu(II) Met Met - Half Met ($M^{-1}cm^{-1}$)
$\Delta(\Delta\varepsilon\ 995) = +1.29$	$\Delta(\Delta\varepsilon\ 995) = -1.66$
$\Delta(\Delta\varepsilon\ 645) = +0.971$	$\Delta(\Delta\varepsilon\ 685) = -1.27$

While this is possible, the gross difference in the overall met and half met spectra provides little evidence that the simplest scenario is correct, and suggests that the spectral properties of the Cu(II) in half met T2D are changing upon further oxidation of the T3 site. CD studies of azide binding to met T2D further support this interpretation (vide infra).

ii. Chemical Properties

The chemical reactivity of the T3 cupric site is accessible to direct probe through optical spectroscopy and as in deoxy T2D, to indirect probe through changes in the T1 Cu(II) EPR spectrum. While fewer ligands bind to the T3 site in met T2D, their studies (especially

N_3^-) have provided significant insight into the T3 site in laccase and its relationship to the hemocyanin and tyrosinase coupled binuclear copper sites.

When 150X F^- is added to met T2D there is change in neither the met T2D near-IR CD spectrum (d-d bands) nor the T1 Cu(II) EPR signal, indicating no evidence for F^- binding to the oxidized T3 sites. While only weak perturbations are observed in analogous Cl^- and I^- studies, Br^- interacts strongly with the oxidized T3 site at 77 K (Figure 3.34). From the increase in the high field hyperfine peak, $K_{eq} \sim 1000$ M^{-1} at 77 K. In half met-Br^- T2D, $K_{eq}(Br^-)$ ~3000 M^{-1} at 77 K, suggesting that Br^- may bind a little more strongly in half met than in met; the similarity of the T1 Cu(II) EPR changes for Br^- binding to met and half met T2D suggest it is binding similarly at these T3 sites.

Reaction with excess SCN^- most significantly alters the T1 Cu(II) EPR features (Figure 3.35); $A_{||}$ increases by a factor of 2, and yet no SCN^- ---> Cu(II) CT features ($\Delta\varepsilon <$ 200 $M^{-1}cm^{-1}$) are observed in the 298 K absorption spectrum. While such transitions are often weak,[18] this data suggests that many of the T1 Cu(II) perturbations may occur only at low temperature; this point will be further discussed in

Figure 3.34 EPR spectra at 77 K: Br^- titration of met T2D laccase.

(A) $g_{||}$ region of original met T2D laccase, in 30X H_2O_2;

(B) after reaction with 25 protein equivalents NaBr;

(C) after reaction with 200 protein equivalents NaBr.

(9.25 GHz; 0.1 M potassium phosphate, pH 6.0; [protein] = 0.155 mM)

Figure 3.35 EPR Spectra at 77 K: SCN^- titration of met T2D laccase.

(A) original met T2D laccase, in 30X H_2O_2;

(B) after reation wtih 10 protein equivalents NaSCN;

(C) after reaction with 200 protein equivalents NaSCN.

Primed spectra were recorded at ~8X higher gain.

(9.26 GHz; 0.1 M potassium phosphate, pH 6.0; [protein] = 0.162 mM)

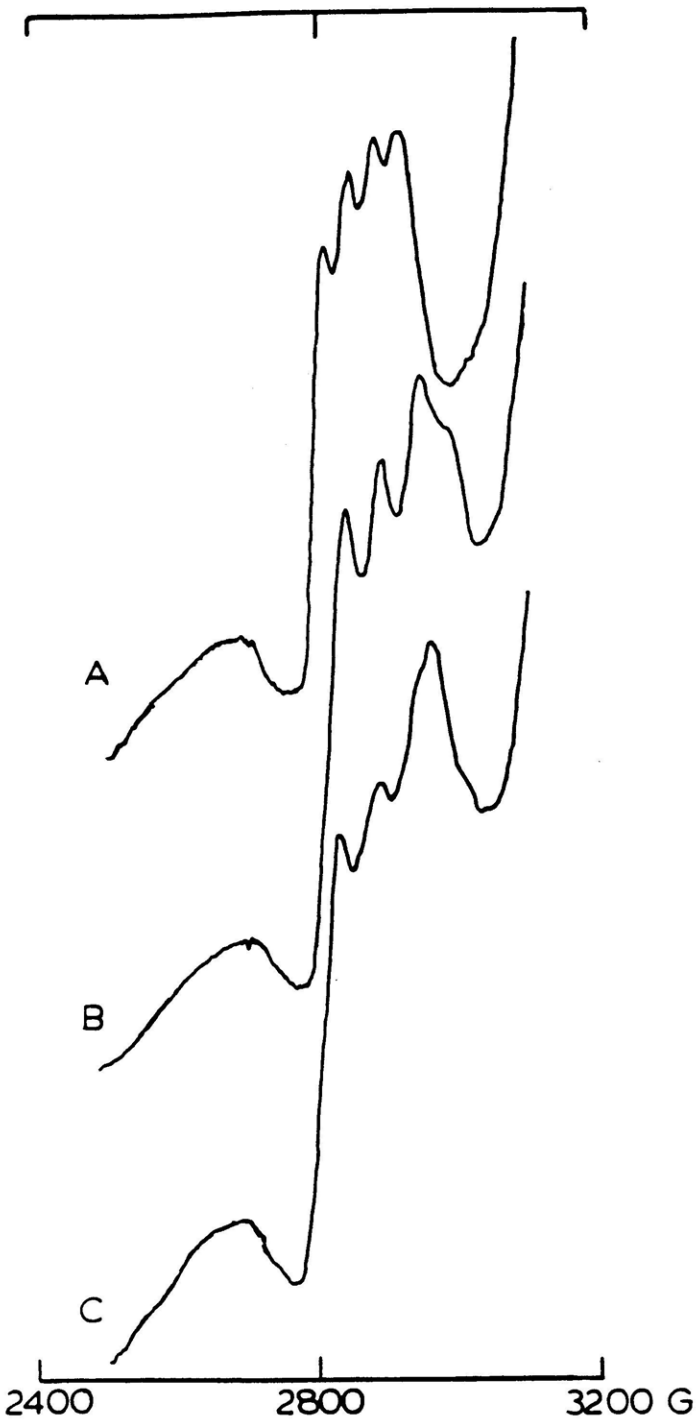
A
B
C
2400
2800
3200 G

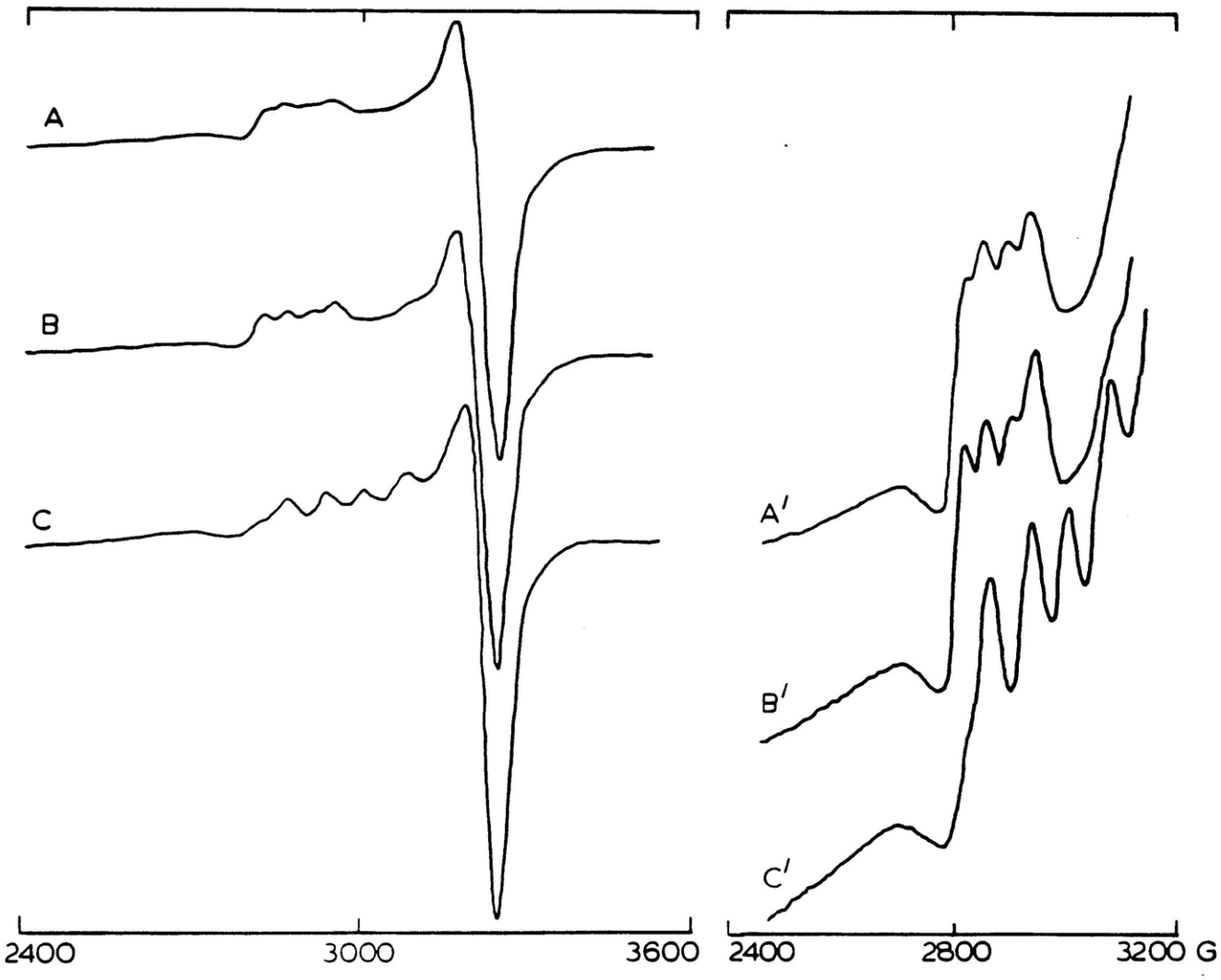
A
B
C
2400
3000
3600
A′
B′
C′
2400
2800
3200 G

Chapter 4. Dialysis readily removes all SCN^- (and Br^-) -related features.

Azide is the only anion which significantly changes the room temperature absorption and CD spectra of met T2D, clearly demonstrating that it is binding to the T3 site at 298 K. The visible-UV absorption spectra of met and met-N_3^-, as first reported by LuBien et al,[8] are shown in Figure 3.36. A broad new feature is centered at ~450 nm ($\Delta\varepsilon \sim 900\ M^{-1}cm^{-1}$) and through resonance Raman studies,[8] it has been assigned as an N_3^- ---> Cu(II) CT transition. The N_3^- binding constant $K_{eq} = 200\ M^{-1}$ is very similar to that of half met-N_3^-. In addition, the intensity of the T3 absorption band is significantly decreased ($\Delta\varepsilon_{614} \sim -600\ M^{-1}cm^{-1}$). In the corresponding CD spectrum in excess N_3^- (Figure 3.37), a positive feature is observed at 450 nm $\Delta(\Delta\varepsilon) = +0.72\ M^{-1}cm^{-1}$), coincident with the N_3^- ---> Cu(II) CT absorption feature.

While only a weak increase, $\Delta\varepsilon_{750} < 100\ M^{-1}cm^{-1}$ is observed in the near-IR of the absorption spectrum (Figure 3.36) it is clear from the near-IR CD spectra (Figure 3.38) that major changes occur in the ligand field upon coordination of N_3^- at the T3 site; at 940 nm, $\Delta(\Delta\varepsilon) = +1.22\ M^{-1}cm^{-1}$ and at 720 nm, $\Delta(\Delta\varepsilon) = +0.51\ M^{-1}cm^{-1}$. From the

Figure 3.36 Electronic absorption spectra at 298 K: N_3^- titration of met T2D laccase.

(——) met T2D laccase; arrows indicate direction of change with 10, 25, 100, and 250 protein equivalents NaN_3. (0.1 M potassium phosphate, pH 6.0; [protein] = 0.228 mM)

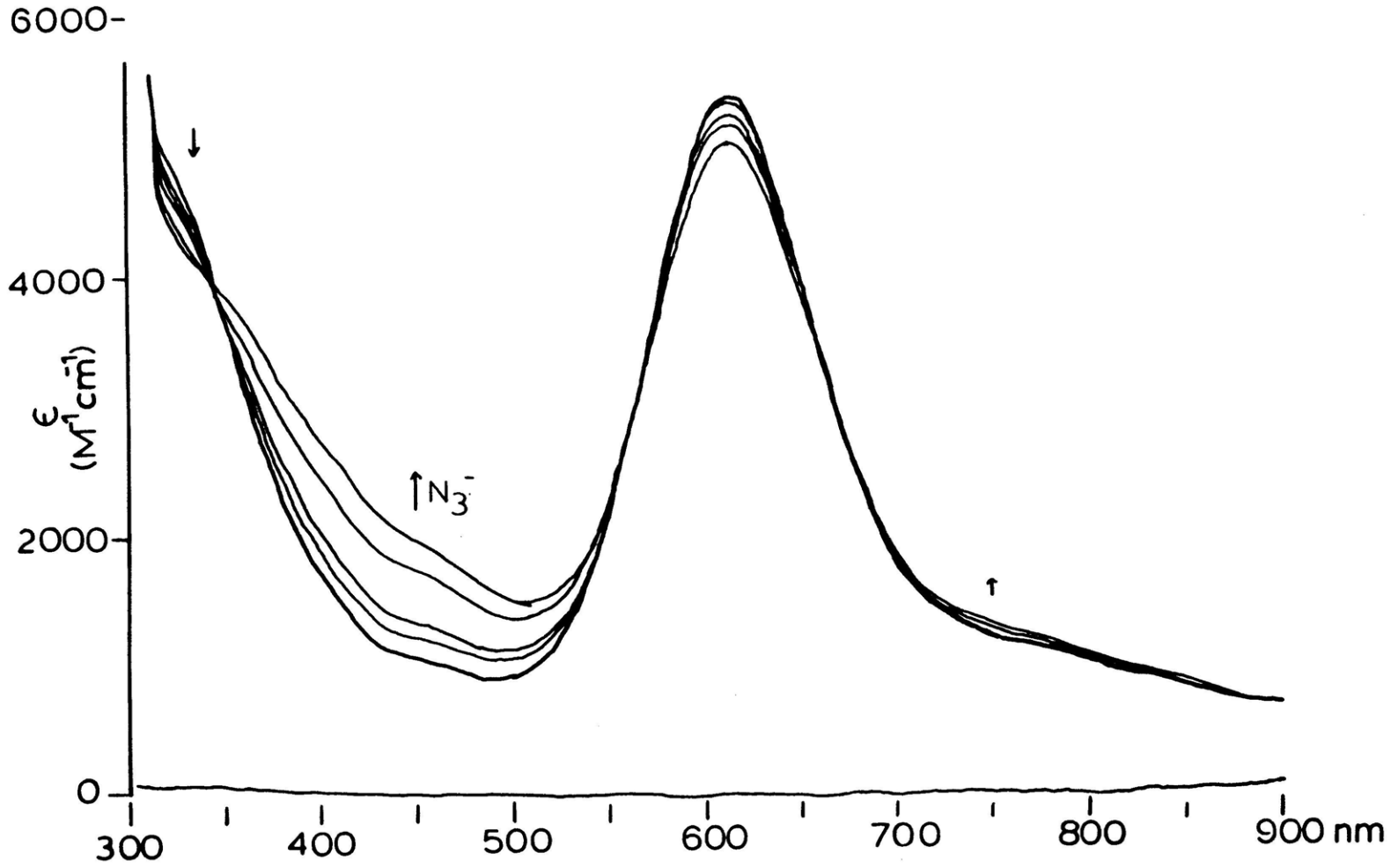
6000
4000
2000
0
ε
(M⁻¹cm⁻¹)
↓
↑N₃⁻
↑
300
400
500
600
700
800
900 nm

Figure 3.37 Visible-UV CD spectra at 298 K: met and met-N_3^- T2D laccase;

(——) met T2D; (▬▬) after reaction with 150 protein equivalents NaN_3. The difference at ~340 nm is due to ~5% T2 Cu(II) and is not associated with met-N_3^- T2D. (0.1 M potassium phosphate, pH 6.0; [protein] = 0.228 mM)

Figure 3.38 Near-IR CD spectra at 298 K: N_3^- titration of met T2D laccase.

(Upper) met T2D laccase; arrows indicate direction of change with 10, 25, 100, and 250 protein equivalents NaN_3. (0.1 M potassium phosphate, pH 6.0; [protein] = 0.228 mM)

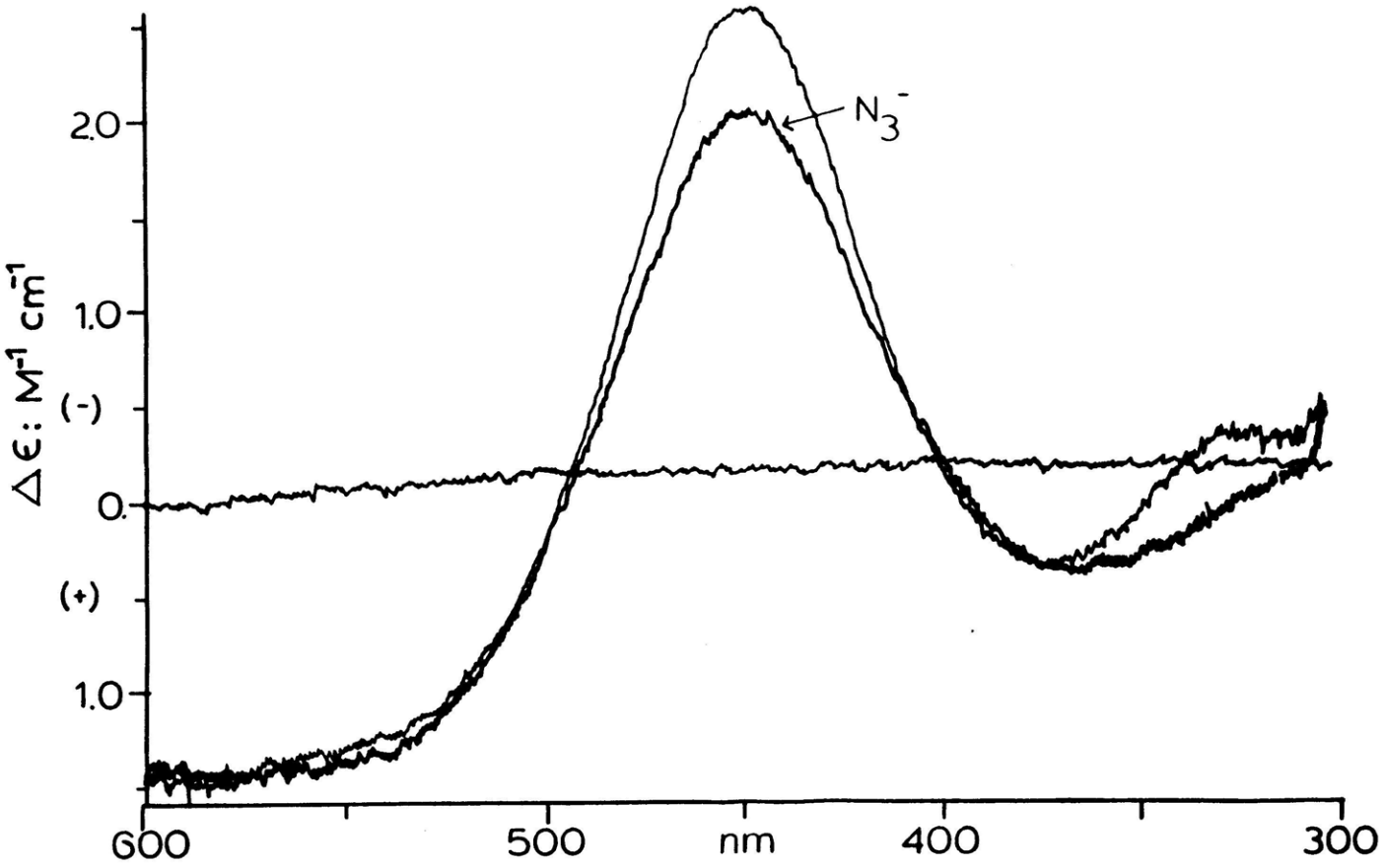
2.0
1.0
(-)
0.
(+)
1.0
Δε : M⁻¹ cm⁻¹
N3⁻
600
500
nm
400
300

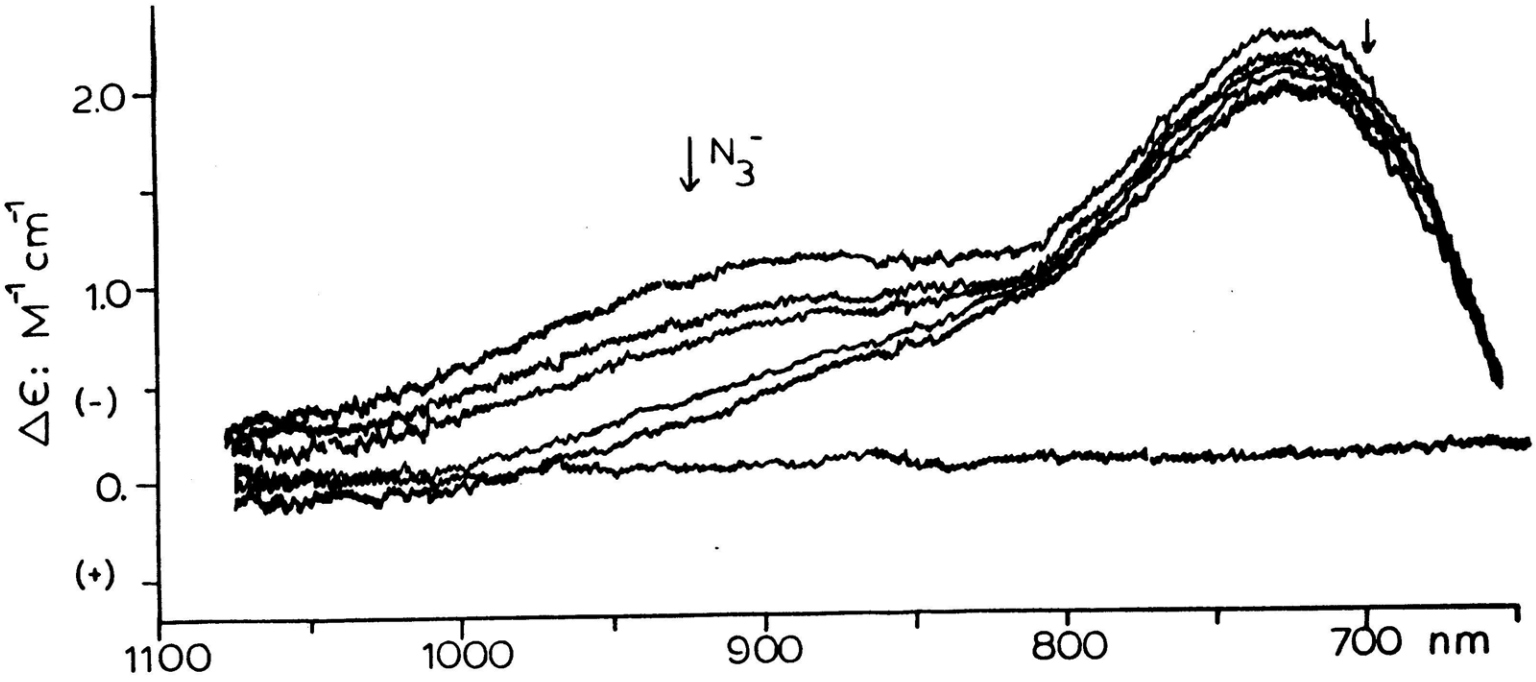
2.0
1.0
(-)
0.
(+)
$\Delta\epsilon$: $M^{-1}cm^{-1}$
N_3^-
1100
1000
900
800
700 nm

titration data at 940 nm K_{eq} = 130 $M^{-1}cm^{-1}$, indicating that these ligand field changes are associated with the new N_3^- ---> Cu(II) CT transition at 450 nm.

In order to determine whether bands are growing in or disappearing, it is necessary to compare met and met-N_3^- to half met and deoxy (cf. Figure 3.16); thus, it appears that in met-N_3^- the ~1000 nm transition in met is shifted to higher energy (~850 nm) and has changed sign, and that the intensity of the negative feature at ~720 nm is greatly decreased. This would require a significant change in the geometric and electronic structure of the T3 site on coordination of N_3^-. Unfortunately, because of changes in the half met Cu(II) concomitant to oxidation of its T3 partner and potential allosteric changes at the T1 Cu(II) related to the redox state of the T3 site, this description is likely invalid (see section bi); similarly, the met-N_3^- and half met-N_3^- spectral features cannot be compared directly. However, a comparison of the (met-N_3^-- met) and (half met-N_3^-- half met) difference spectra (Figure 3.39) can be used to analytically probe the effects of azide coordination at these T3 sites. From these difference spectra, it would appear that N_3^- is interacting very differently at the met and half met T2D sites. This is also supported by differences in their N_3^- ---> Cu(II) CT transitions and will be further discussed in Part 2.

Figure 3.39 CD difference spectra: (half met-N_3^- - half met) and (met-N_3^- - met) T2D laccase.

(———) met-N_3^- - met T2D;

(— — —) half met-N_3^- - half met T2D

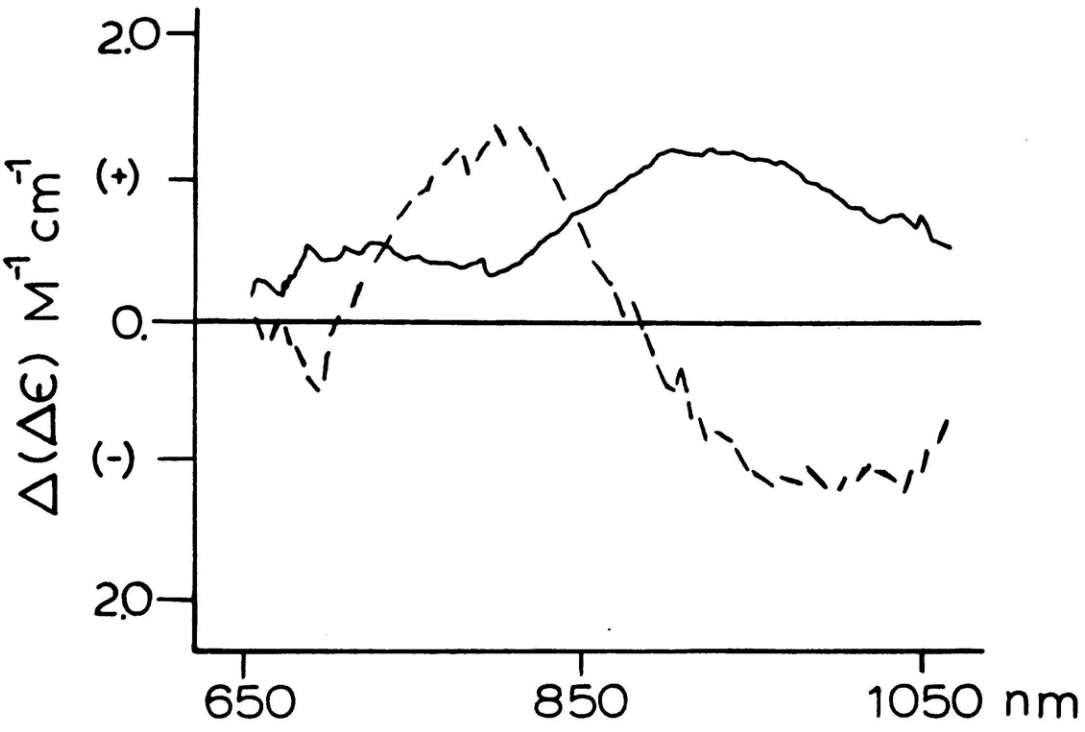
2.0
(+)
0.
(-)
2.0
Δ(Δε) M⁻¹cm⁻¹
650
850
1050 nm

Upon cooling met-N_3^- to 77K (Figure 3.40) the blue band sharpens and absorption intensity increases between 500 and 400 nm, similar to met T2D. The 450 nm feature does not sharpen above its increased absorption background and is barely resolved at 77 K. To higher energy, a new band appears at 350 nm; based on its energy this could represent either a second N_3^- ---> Cu(II) CT transition (two are possible per Cu-N_3^- bond) or the N_3^--perturbed 330 nm feature (Figure 3.36) which may be more clearly resolved at lower temperature.

In the 77 K EPR spectra (Figure 3.41), low [N_3^-]'s only weakly affect the T1 Cu(II). However, if this sample is further cooled to ~10 K, a new broad signal is observed at 3590 G (g = 1.86). At 200 mW microwave power the intensity of the signal is greatly increased relative to that of the T1 Cu(II). This is especially evident at lower pH (Figure 3.42) and demonstrates that the new signal is not associated with the T1 Cu(II). Moreover, through the studies which follow, this signal will be shown to represent a small fraction of T3: [Cu(II)Cu(II)]-N_3^- sites in which the endogenous bridge has been protonated and displaced; in these sites, the cupric centers are therefore no longer antiferromagnetically exchange coupled and are paramagnetic.

Figure 3.40 Electronic absorption spectra at 77 and 298 K: met-N_3^- T2D laccase.

Met T2D laccase after reaction with 20 protein equivalents NaN_3^- (——) at 298 K; (— — —) at 77 K. (1.45 mm pathlength; 50% v/v glycerol/ 0.1 M potassium phosphate, pH 6.0; [protein] = 1.1 mM)

Figure 3.41 EPR spectra at 77 and 8 K: met-N_3^- T2D laccase, pH 6.0.

met T2D laccase after reaction with 10 protein equivalents NaN_3

(A) at 10 mW and 77 K;

(B) at 10 mW and 8 K;

(C) at 200 mW and 8K, primed spectrum was recorded at 6.3X higher gain.

(9.26 GHz (A); 9.39 GHz (B-C); 0.1 M potassium phosphate, pH 6.0; [protein] = 0.201 mM)

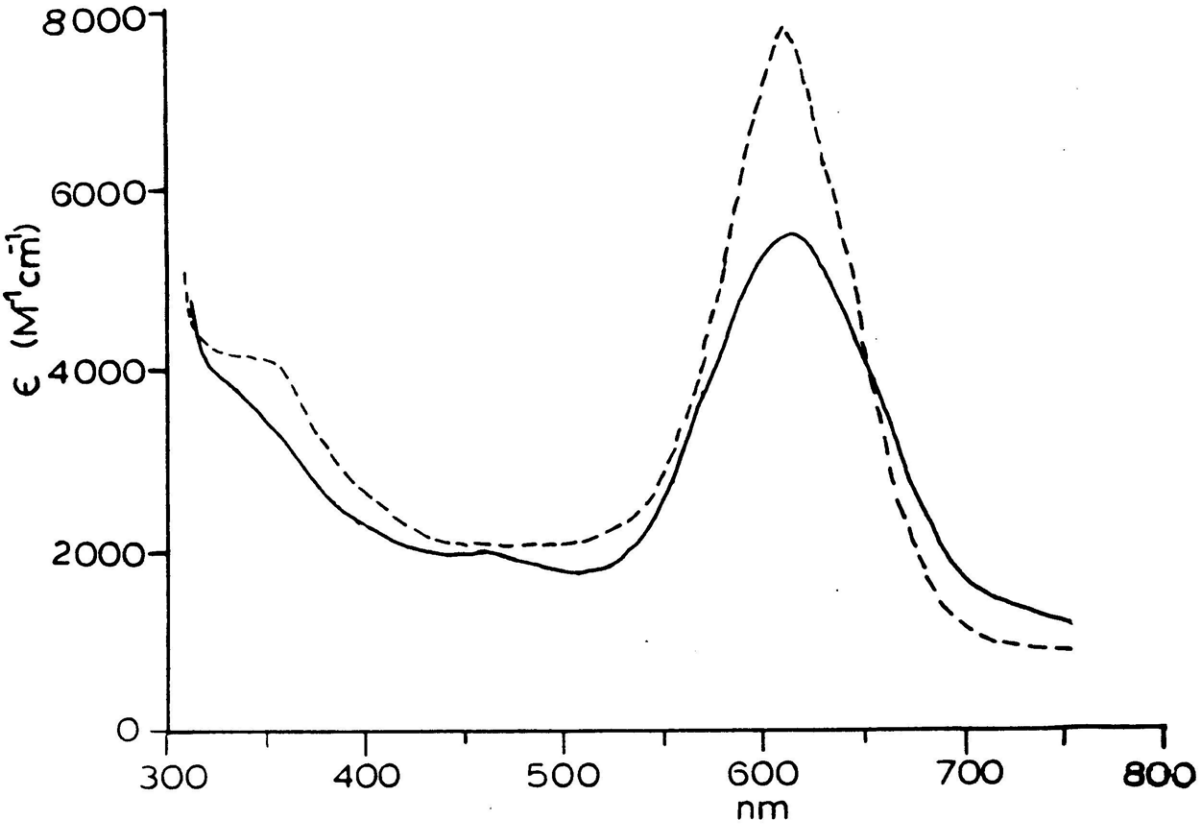
8000
6000
4000
2000
0
ε (M⁻¹cm⁻¹)
300
400
500
600
700
800
nm

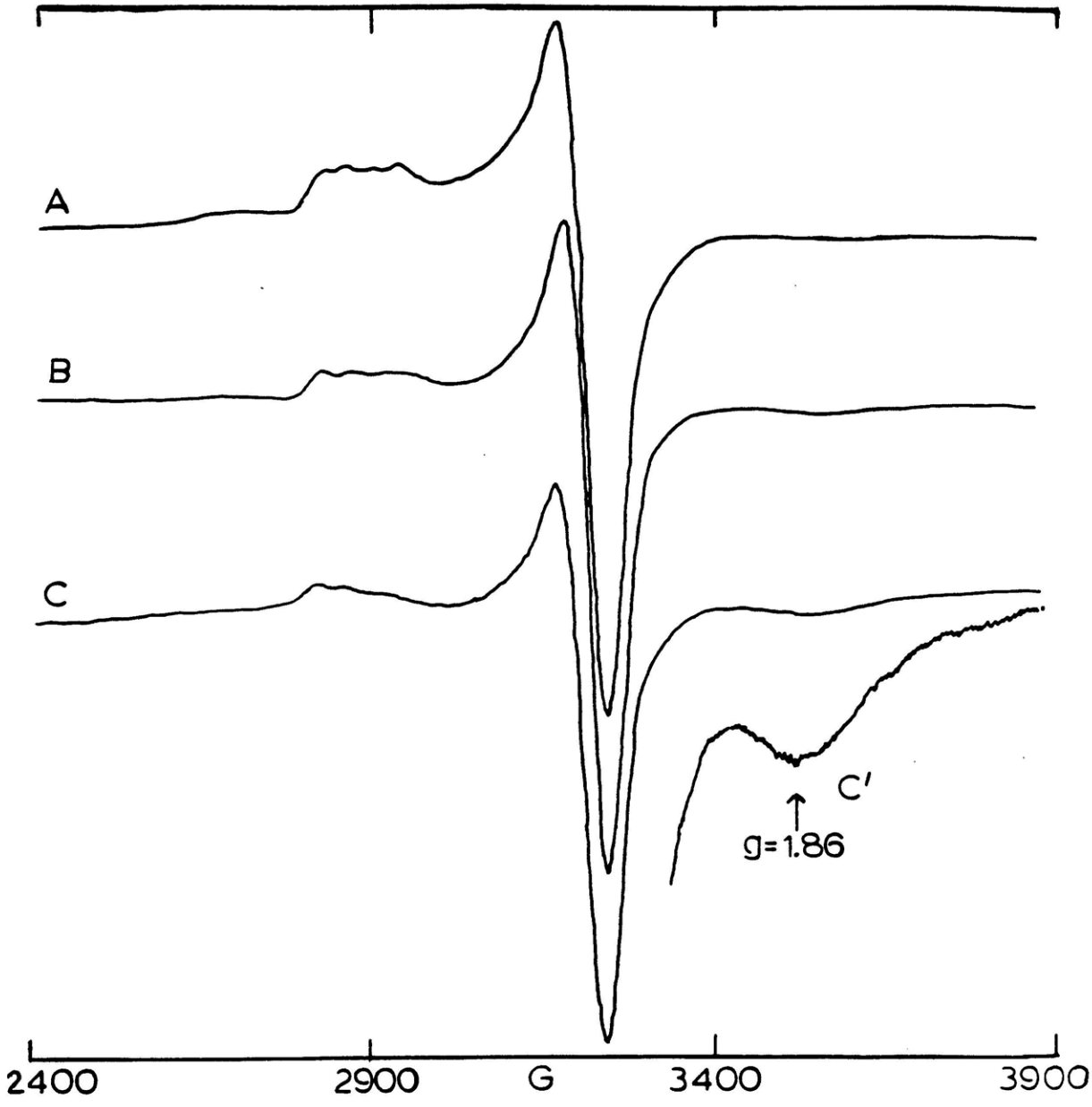
A
B
C
C'
g=1.86
2400
2900
G
3400
3900

Figure 3.42 EPR spectra at 77 and 8 K: met-N_3^- T2D laccase, pH 4.6.

Met T2D laccase after reaction with 3 protein equivalents NaN_3

(A) at 10 mW and 77 K;

(B) at 10 mW and 8 K;

(C) at 200 mW and 8 K, primed spectrum was recorded at 6.3X higher gain.

(9.26 GHz (A), 9.39 GHz (B-C); 0.1 M sodium acetate, pH 4.6; [protein] = 0.20 mM).

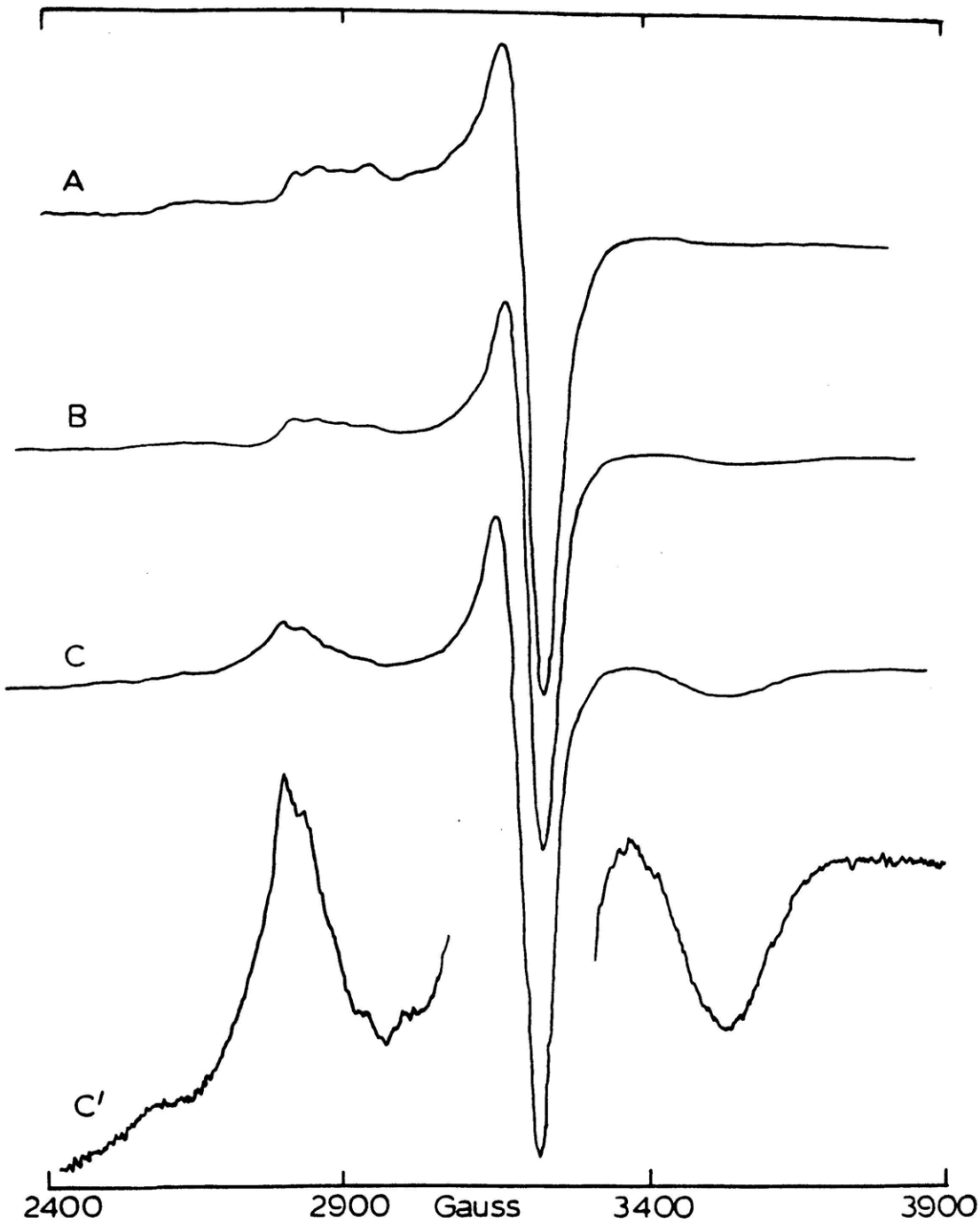
A
B
C
C'
2400
2900
Gauss
3400
3900

EPR examination of met T2D (Figure 3.43A) from pH 4.0 to pH 7.6 shows no unusual signal intensity. However, when N_3^- is added to met T2D at pH 6.0 (Figure 3.43B), a broad derivative shaped signal, characteristic of dipolar coupled cupric centers, appears between 2700 and 3900 G, demonstrating that N_3^- is inducing the signal; no other transitions are observed between 0 and 10,000 G. N_3^- titration of deoxy T2D at 8 K shows no such signal, but if the resultant deoxy-N_3^- is titrated with peroxide, the g = 1.86 signal grows in. Moreover, a plot (Figure 3.44) of the 8 K intensity at 3590 G versus the 298 K increase in 330 nm intensity (which correlates linearly with T3 oxidation, Figure 2.12) shows that there is a direct correlation between these spectral features. This correlation and the fact that no signal is observed in deoxy T2D demonstrates that the new EPR signal is associated with the oxidized T3 sites. Moreover, that the EPR detectable sites are oxidized by H_2O_2 indicates that they are capable of normal T2D chemistry and are not damaged sites. Similarly, dialysis of met-N_3^- restores the original ~10 K met T2D EPR spectrum. No anion other than N_3^- has been found to induce such signals.

The physical properties of the new N_3^- feature further support its binuclear cupric nature. Note that because the low field portion of this signal overlaps the T1 Cu(II), intensity measurements are of the high field component and

Figure 3.43 EPR spectra at 8 K: met and met-N_3^- T2D laccase.

(A) met T2D and

(B) after reaction with 10 protein equivalents N_3^-.

* g~4.3 ubiquitous rhombic iron, 0-6000 Gauss scan, 200 mW incident power and 8 K. (9.39 GHz; 0.1 M sodium acetate, pH 4.6; [protein] = 0.197 mM)

Figure 3.44 Correlation: EPR detectable T3 copper and 330 nm intensity for peroxide titration of deoxy-N_3^- T2D laccase.

Deoxy T2D was pre-incubated with 10 protein equivalents NaN_3, and titrated with H_2O_2; the protein equivalents of H_2O_2 are indicated for each data point.

x-axis: 298 K absorption intensity at 330 nm

y-axis: 8 K EPR intensity at 3590 G

3590 G intensity was measured relative to the EPR baseline extrapolating from 4000 G. (0.1 M potassium phosphate, pH 6.0; [protein] = 0.148 mM)

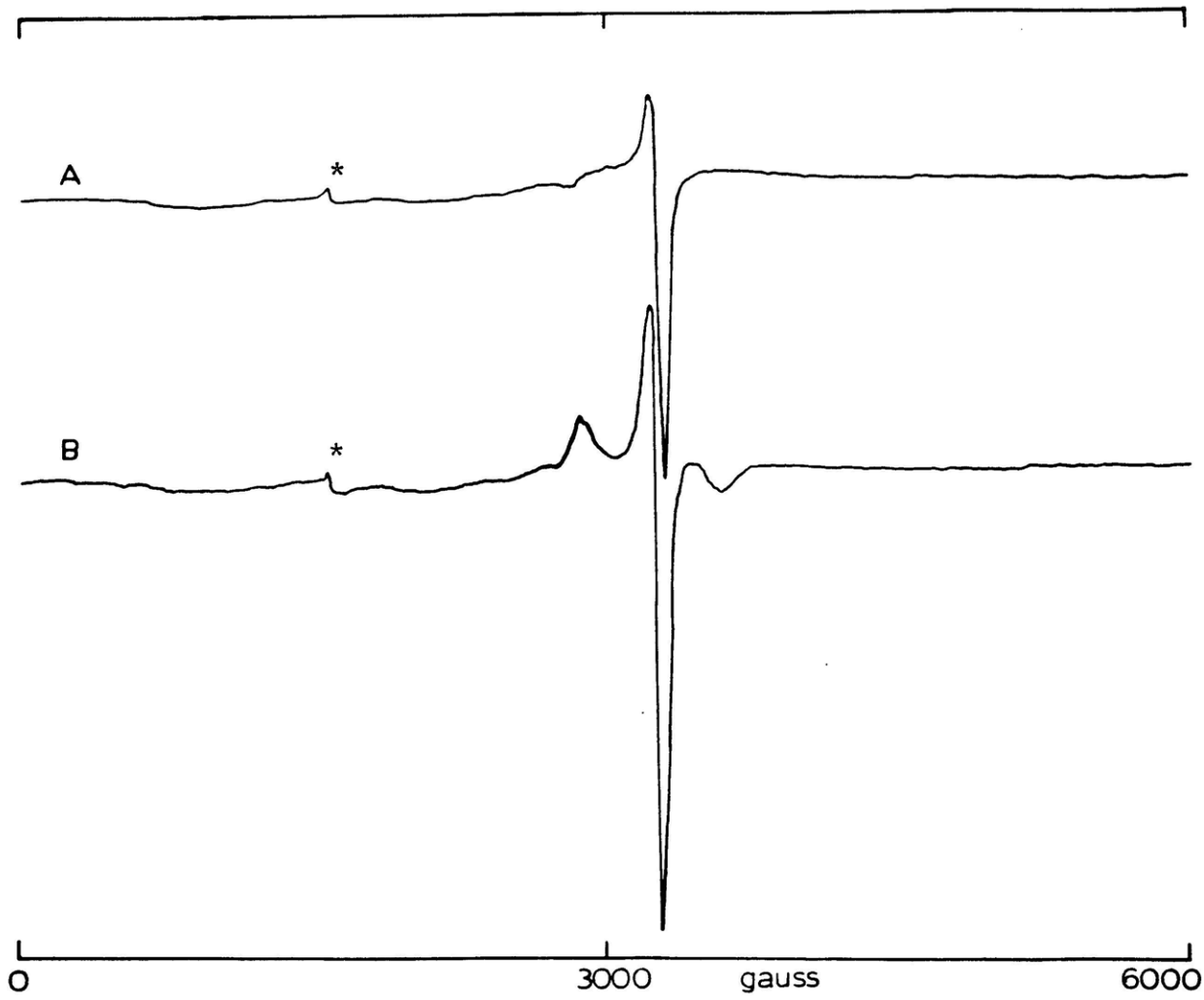
A
*
B
*
0
3000
gauss
6000

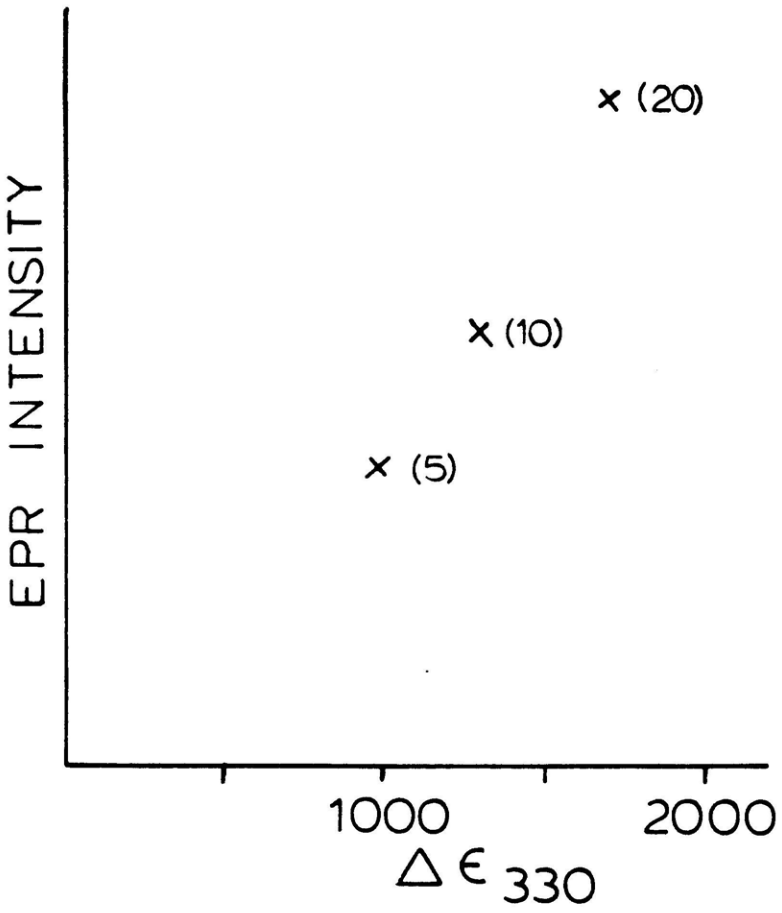
EPR INTENSITY
x (20)
x (10)
x (5)
1000
2000
Δ ϵ 330

the signal is often referred to as "the g = 1.86" signal. At 77 K, essentially no signal intensity is observed. However, as the temperature is lowered, the EPR intensity follows Curie law behavior. From the temperature dependence of the signal intensity, a computer least squares fit of the Bleaney Bowers[32] equation:

$$I = \frac{M}{T(3 + e^{-2J/kT})}$$

established that $-5\ cm^{-1} < 2J < 5\ cm^{-1}$. Since the T3 cupric pair is effectively uncoupled in these sites, N_3^- must interfere with the endogenous protein bridge.

The relaxation[33] of the g = 1.86 signal in met-N_3^- compared to that of the T1 Cu(II) in both met and met-N_3^- is shown in Figure 3.45. Whereas $P_{1/2}$ for the mononuclear T1 Cu(II) signal at 8 K is 1-2 mW, the g = 1.86 signal only begins to saturate at ~50 mW. Comparison of the T1 Cu(II) saturation curves in met and met-N_3^- indicates that the T1 center is slightly harder to saturate in met-N_3^- ($P_{1/2}$ = 2.2 vs. 0.7 mW). As the uncoupled sites represent only a small fraction of T3 sites (vide infra) this effect is more likely associated with a structural change in the T1 Cu(II) on binding N_3^- to the coupled T3 site. It should be noted that from 77 and 8 K EPR studies of half met T2D,

Figure 3.45 Relaxation properties: met-N_3^- and met T2D laccase.

Power saturation curves at 8 K for (*---*) 3590 G signal intensity and (+---+) T1 perpendicular intensity in met-N_3^- T2D; (•– – –•) T1 perpendicular intensity for met T2D is shown for comparison. (0.1 M potassium phosphate, pH 6.0; [protein] = 0.342 mM)

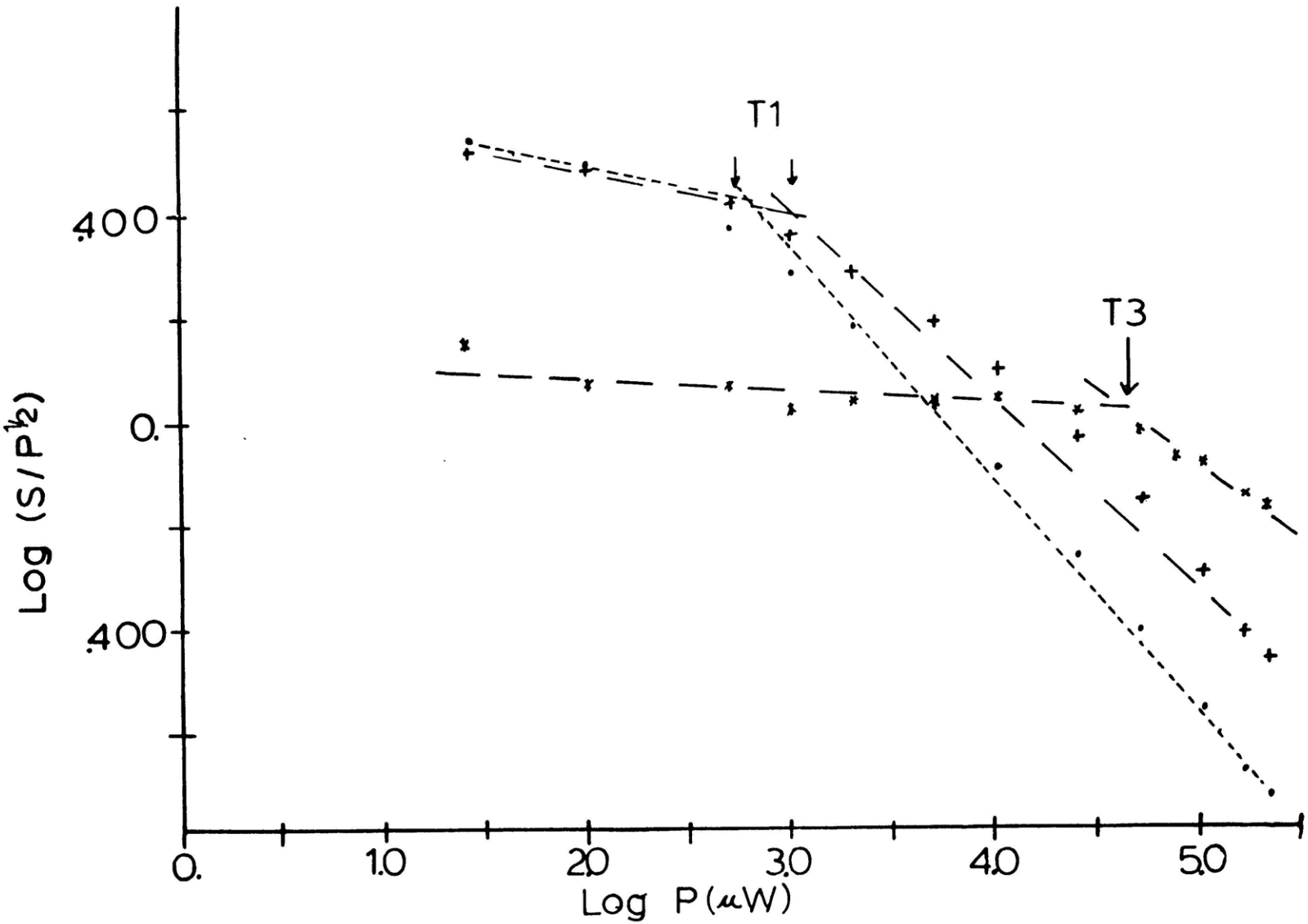
T1
T3
.400
0.
.400
Log (S/P½)
0.
1.0
2.0
3.0
4.0
5.0
Log P (μW)

the T1 and at least one of the T3 Cu(II)'s are not close enough to dipole interact.

Accurate quantitation of the percentage of uncoupled T3 sites requires reasonable T1 and T3 signal intensities under non-saturating conditions. At < 20 K, low microwave powers will saturate the T1 Cu(II), while the uncoupled signal is not accessible at temperatures > 40 K. Double integration of 10 mW spectra at ~35 K using the T1 Cu(II) as a reference suggested that 13 $\pm$ 7% of the T3 sites are EPR detectable under optimum uncoupling conditions (pH 4.6, vide infra). However, from the 298 K binding constant at pH 4.6, approximately three times (or 40%) of the T3 sites should have had normal "coupled" N_3^- bound, and this percentage is likely significantly larger at 10 K. As these spectral changes do not correlate, there must be more than one type of N_3^- interaction at the met T3 site.

Consistent with the quantitation studies, simultaneous 298 K optical and 8 K EPR titrations of N_3^- on met T2D at pH 4.6 indicate that the "normal" met-N_3^- is not the N_3^- which uncouples the T3 site. Figure 3.46 plots intensity at 450 nm (298K) and EPR signal intensity (8 K) against equivalents of N_3^- added. The 450 nm band is well behaved with increasing $[N_3^-]$ while the uncoupled signal starts out normal at low $[N_3^-]$ and then appears to be "back-inhibited" by increased $[N_3^-]$.

Figure 3.46 Correlation: Met-N_3^- charge transfer intensity vs. EPR detectable T3-N_3^-.

N_3^- titration of met T2D laccase -

x-axis: protein equivalents N_3^-

y-axis: (Left, ———) 298 K N_3^- ---> Cu(II) CT intensity at 450 nm

(Right, — — —) 8 K EPR intensity at 3590 G.

(0.1 M sodium acetate, pH 4.6; [protein] = 0.158 mM)

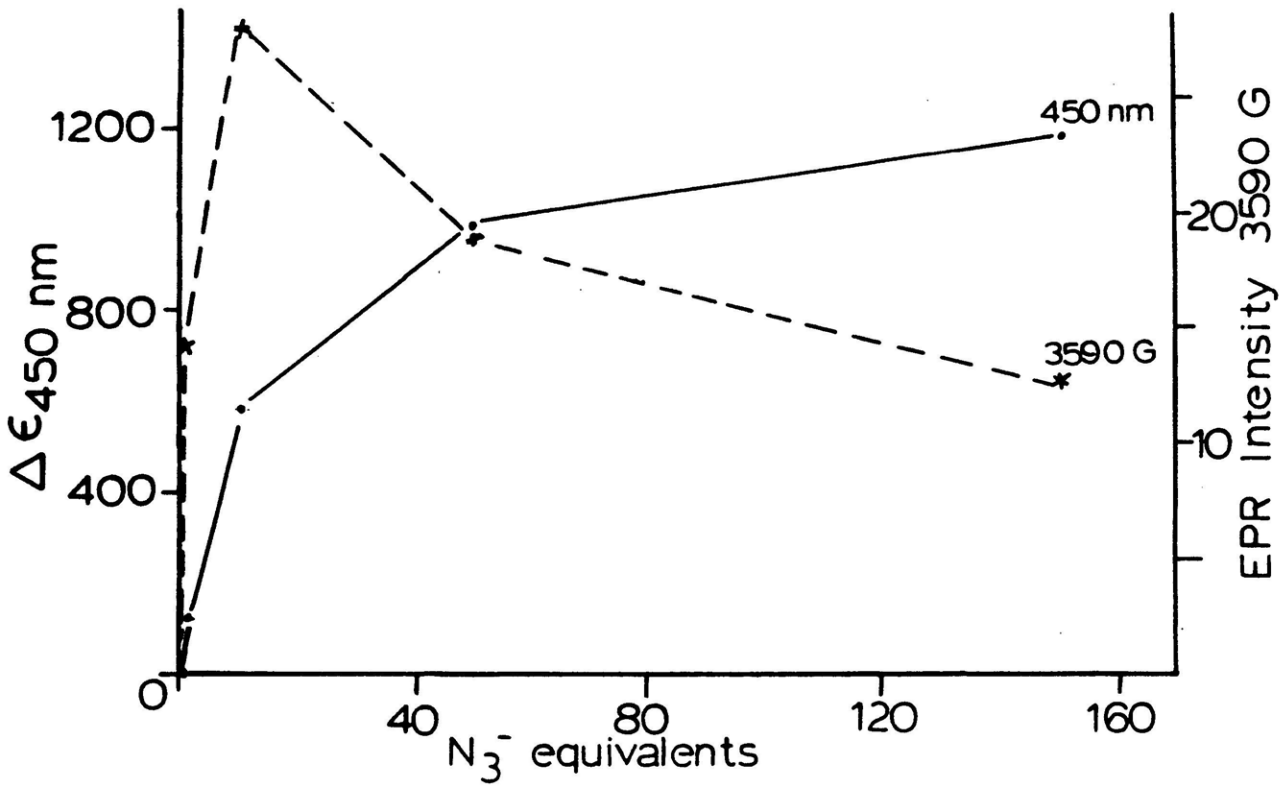
1200
800
400
0
$\Delta\epsilon_{450\ nm}$
40
80
120
160
N_3^- equivalents
450 nm
3590 G
20
10
EPR Intensity 3590 G

The intensity of the T3 EPR signal is dependent on pH as well as the N_3^- concentration. Figure 3.47 plots absolute signal intensity at g = 1.86 of met T2D treated with 0, 3, 10, and 100 protein equivalents of N_3^- over the pH range 7.2 to 4.0. In general, signal intensity increases with increasing $[N_3^-]$, with increasing $[H^+]$, and for a fixed amount of N_3^-, is larger at lower pH. However, at high $[N_3^-]$ and low pH, signal intensity maximizes and then decreases with increasing $[N_3^-]$; this "back-inhibition" by N_3^- is especially evident in Figure 3.48 which plots EPR signal intensity as a function of N_3^- at fixed pH.

Since under most circumstances H^+ and N_3^- uncouple the T3 site, the new EPR signal is interpreted as a competitive displacement by N_3^- of the protonatable exchange-mediating endogenous bridge at a small percentage of the met sites. A similar behavior has been extensively characterized[34] in hemocyanin.

One interpretation of the difference in 450 nm and g = 1.86 behaviors is that the N_3^- which uncouples the site is competing directly for the endogenous bridge position while the N_3^- at 450 nm is simply binding equatorially to an exchangeable coordination position at the T3 site (Scheme 3.2). Thus, it would appear that N_3^- binding in a "normal" equatorial manner ($E \cdot N_3^-$) inductively lowers the pK_a of the

Figure 3.47 Correlation: Met-N_3^- EPR intensity vs. pH.

pH dependence of the 8 K EPR intensity at g = 1.86 for met T2D preincubated with (✕---✕) 0; (•——•) 3; (✕- - -✕) 10; and (•——•) 100 protein equivalents NaN_3. The MES data points (10 and 100X N_3^-) are shown separately (✕—•-•-✕). 0.1 M sodium acetate was used at pH 4.0, 4.6, and 5.3; 0.1 M potassium phosphate at pH 6.3, and 0.1 M (2(N-morpholino) ethanesulfonic acid) (MES) at pH 6.0 and 6.7. [protein], as determined by the 280 nm absorption for each sample, was used to scale the EPR intensities. In general, [protein] ~0.2 mM.

Figure 3.48 Correlation: Met-N_3^- EPR intensity vs. [N_3^-] at fixed pH.

x-axis: protein equivalents of N_3^- added to met T2D laccase

y-axis: EPR intensity at g = 1.86; 200 mW incident power, 8 K.

In 0.1 M sodium acetate, (•——•) pH 4.0; (✕---✕) pH 4.6; (•——•) pH 5.3; (✕-•-•-✕) 0.1 M MES, pH 6.0; (•——•) 0.1 M potassium phosphate, pH 6.3; and (✕—•—•—✕) 0.1 M MES, pH 6.7. [protein] ~0.2 mM.

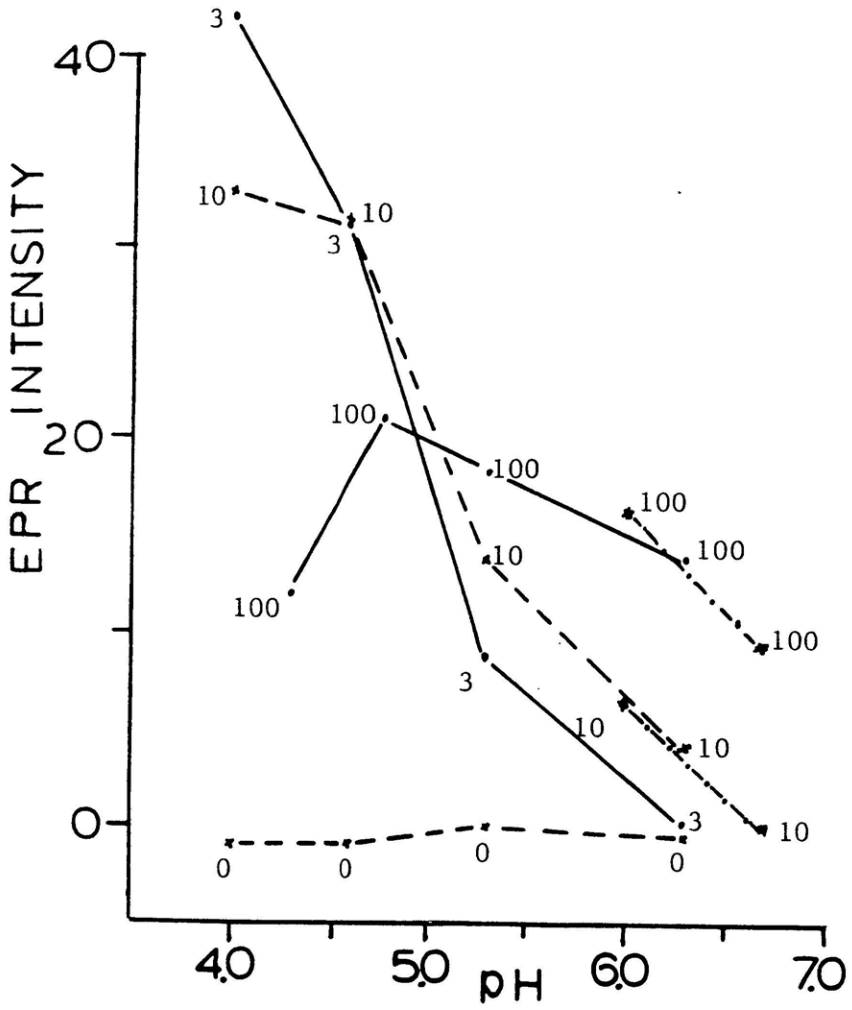
EPR INTENSITY
40
20
0
4.0
5.0
pH
6.0
7.0
3
10
3
10
100
100
100
100
100
10
10
3
10
3
10
0
0
0
0

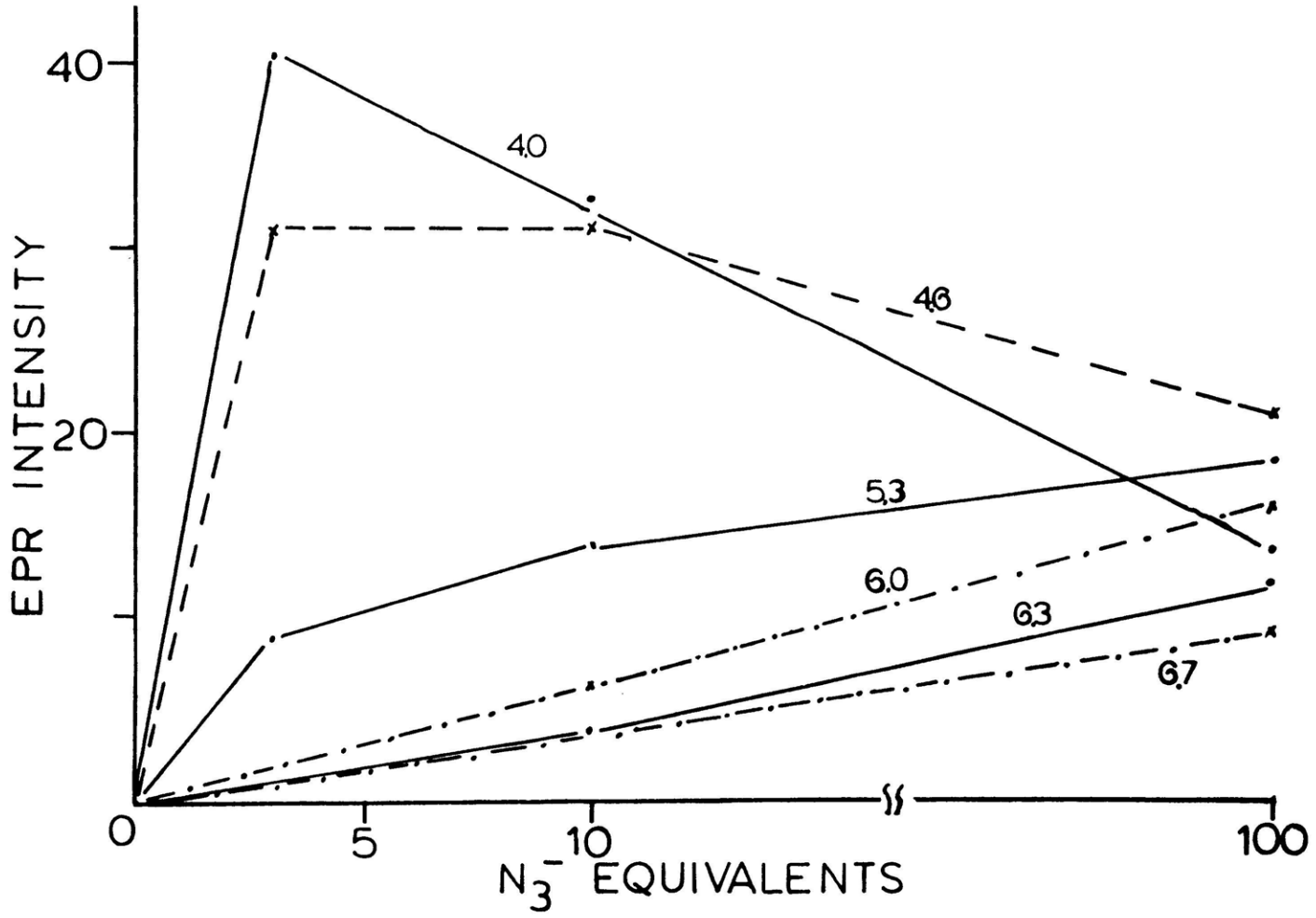
40
20
EPR INTENSITY
4.0
4.6
5.3
6.0
6.3
6.7
0
5
10
100
N3- EQUIVALENTS

SCHEME 3.2. N_3^- INTERACTION AT THE TYPE 3 SITE IN MET T2D LACCASE

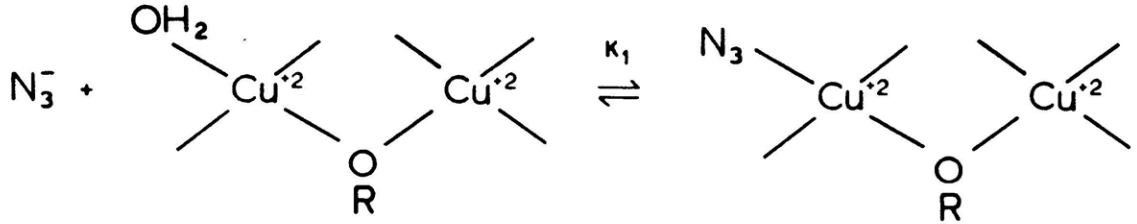

(E) (E·N_3^-)

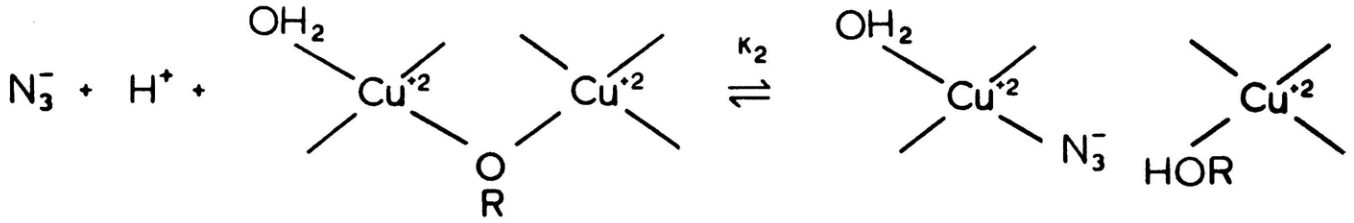

(E'·N_3^-)

endogenous bridge such that no uncoupling ($E'N_3^-$) is observed in the accessible pH range. While no anions other than N_3^- have been observed to uncouple the site, similar inductive effects on signal intensity have been noted with F^- (decrease) and Cl^- (slight enhancement). Calculations to evaluate this model and estimate thermodynamic parameters are currently in progress.

A related EPR signal from T2D laccase has been reported by Reinhammar[35] and is shown in Figure 3.49A. Similar to met-N_3^- T2D, the Reinhammar signal is observed at 10 K but not 77 K, does not saturate as T1 Cu(II) and its high field minimum is at $g < 2.0$. However, the signal in Figure 3.49 would appear to be very different from that of met-N_3^- T2D, as it represents T2D laccase which has been reduced with ascorbate and ferrocyanide under anaerobic conditions and is then exposed to O_2 and frozen after 3 seconds; the signal decays with time to yield the spectra shown in Figure 3.49B and C. Based on earlier studies of native laccase,[36] Figure 3.49A was assigned as a trapped partially reduced oxygen intermediate. While differences do exist between the signal herein described and Figure 3.49, including the full widths of the high field peaks (< 400 vs. 900 G), the high field g values (1.86 vs. 1.75), and the presence vs. lack of intensity in the parallel region, these signals are certainly quite similar and this research would suggest that they might both represent dipolar coupled Cu(II)'s.

Figure 3.49 EPR spectra of T2D laccase: Swedish Intermediate
from reference 35
(A) 3 sec;
(B) 10 sec;
(C) 2 hour after reoxidation of enzyme which had been prior reduced for 20 hours with ascorbate plus $Fe(CN)_6^{4-}$ under anaerobic conditions.

A-C, A'-C' at 20 G modulation, 0.2 mW
A"-C" at 20 G modulation, 20 mW
Primed and double primed spectra recorded at 5X higher gain (at 10 K; 9.27 gHz).

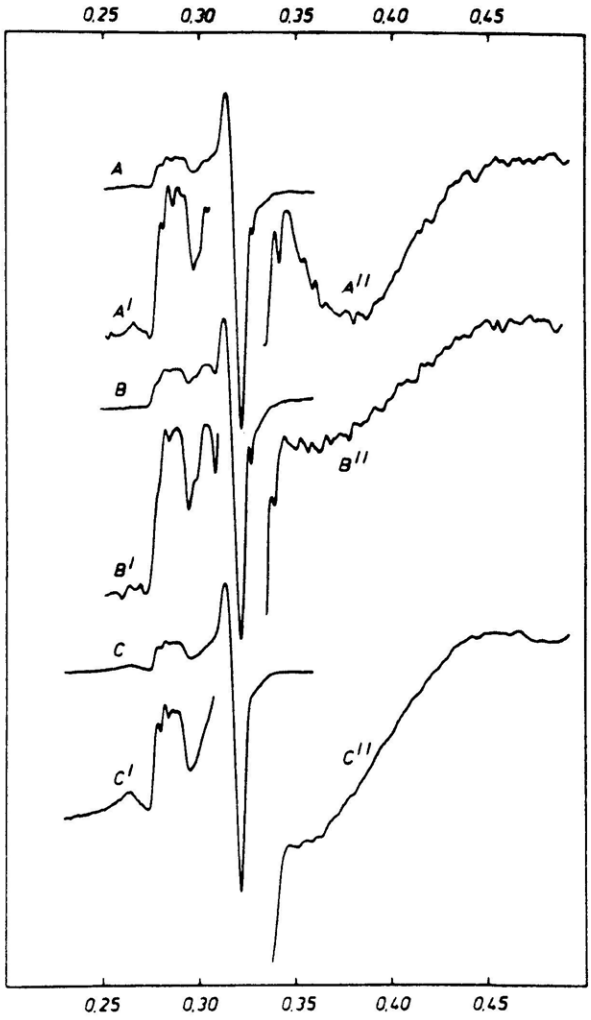
0,25
0,30
0,35
0,40
0,45
A
A'
A''
B
B'
B''
C
C'
C''
0,25
0,30
0,35
0,40
0,45
Magnetic flux density (T)

Finally, the uncoupled signal itself contains significant structural information about the binuclear cupric site. As the temperature dependence has indicated that exchange coupling is negligible, dipolar interaction between the cupric ions is the dominant mechanism leading to zero field splitting (D) of their paramagnetic triplet spin state. To first order, this dipolar zero field splitting is proportional to $1/r^3$, and the shape of the EPR spectrum should therefore reflect the distance between the cupric centers. Dean Wilcox has used an EPR spectral simulation calculation developed by Pilbrow[37] to simulate the triplet signal in met-N_3^- T2D. The met-N_3^- spectrum (including the T1 Cu(II)) and its simulation are shown in Figure 3.50. A good fit is obtained with $g_{||} = 2.30$, $g_{\perp} = 2.06$ and $r = 4.0$ Å. The Cu-Cu distance, r, is dependent essentially only on the separation of the low field maximum and high field minimum and is clearly defined; alternatively, current temperature limitations prevent full saturation of the T1 Cu(II) and so the detailed shape of the signal in this region and the angular information it contains will have to await future studies.

Knowing the Cu-Cu distance, the intensity of the $g = 4$ signal compared to that at $g = 2$ and the zero field splitting can be estimated. The relative intensity of the half field signal in randomly oriented samples is proportional to

Figure 3.50 EPR simulation: met-N_3^- T2D laccase at 8 K.

(———) met T2D laccase after reaction with 3 protein equivalents NaN_3,

(— — —) simulated spectrum of the triplet signal,

(0.1 M sodium acetate, pH 4.6).

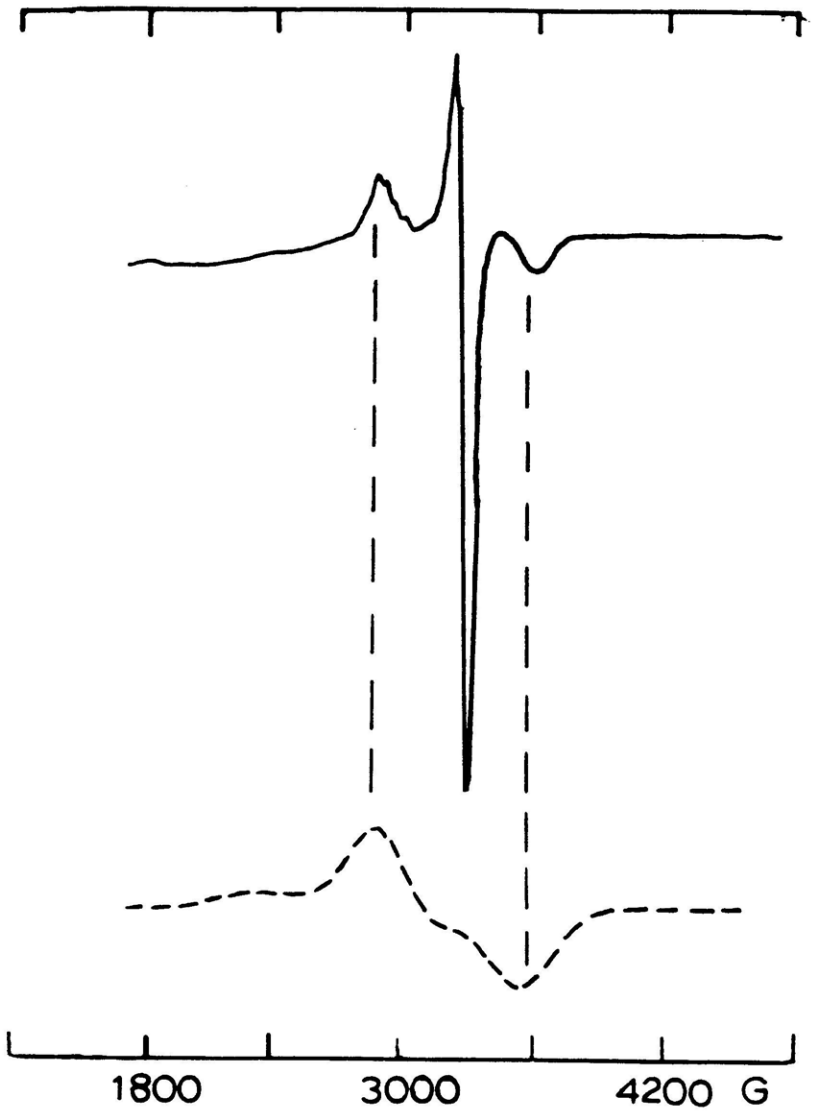
1800
3000
4200 G

$1/r^{6.38}$ For a 4 Å separation, the $\Delta m_s = 2$ signal is then calculated to be ~0.5% the intensity of the $\Delta m_s = 1$ signal. This transition was never observed. Finally, using the parameters in reference 38 and a 4 Å separation, D is estimated to be 0.049 cm^{-1}.

2. COMPARISON TO THE HEMOCYANINS AND TYROSINASE

As indicated in Section 1.3, the hemocyanins and tyrosinase contain only a coupled binuclear copper site which functions to reversibly bind oxygen as peroxide. As summarized in Figure 1.8, deoxy, half met and met derivatives of hemocyanin are accessible and their detailed study has generated the oxyhemocyanin active site[1,26] model shown in Figure 1.9. In Part 1 of this chapter, a series of coupled binuclear copper active site derivatives of T2D laccase were prepared and were the subject of detailed chemical and spectroscopic studies. From these studies, strong similarities - as well as differences - are observed between T2D laccase and the simpler binuclear copper proteins. Thus, through a detailed analysis of the chemistry and spectroscopy of T2D laccase compared to that of the hemocyanins and tyrosinase, a spectroscopically effective model for the T3 site in T2D laccase can be developed.

From x-ray absorption edge studies, deoxy T2D and deoxy hemocyanin[25] (Hc) each contain a [Cu(I)Cu(I)] T3 site and consequently lack characteristic optical and EPR spectral features. Through intramolecular T3-T1 intersite interactions in T2D, however, it has been possible to probe exogenous ligand reactivity at the deoxy site through EPR spectroscopy at 77 K. The halogens, N_3^-, SCN^-, and most importantly, CO, all bind to the binuclear cuprous site. From CO competition studies, there is only one exchangeable position at the reduced T3 site which binds both the anions and CO.

In the hemocyanins, there is, of course, no T1 Cu(II) to probe, but similar exogenous ligand competition studies have been performed through FT-IR spectroscopy.[39] When CO binds to deoxy Hc ($K_{eq} \sim 3.5 \times 10^{-4}$ M^{-1} at 298 K);[39] a peak at 2062 cm^{-1} is observed through difference spectroscopy and has been assigned as the CO stretch.[39,40] By monitoring the 2062 cm^{-1} intensity in the presence of N_3^-, dithiooxamide, I^-, Br^-, and Cl^-, all of these ligands were determined to compete with CO. As for deoxy T2D, only one anion or CO binds per deoxy Hc active site, although in T2D there is no spectroscopic evidence for dithiooxamide binding to the T3 site. Significantly, CO binds considerably less tightly to deoxy T2D than to deoxy hemocyanin and no FT-IR peak has been observed;[41] this may suggest that CO binding to T2D occurs only at low temperature. Moreover, the significantly

decreased CO binding affinity in deoxy T2D suggests that the interaction of the binuclear cuprous site with CO is different in deoxy T2D compared to deoxy hemocyanin.

Whereas deoxy T2D is stable to oxygen, deoxy Hc readily oxidizes to oxy. That CO (and NO) <u>are</u> able to react with deoxy T2D indicates that the lack of O_2 reactivity is not due to an inaccessibility of the binuclear cuprous site to neutral small molecules; that is, if CO can reach the site, it follows that O_2 should as well. Therefore, the lack of O_2 reactivity in T2D would further suggest a major difference in binuclear cuprous active site structure between T2D laccase and deoxy hemocyanin.

Insight into these differences between T2D laccase and hemocyanin is obtained in comparing the chemistry and spectroscopy of their half met derivatives. First, whereas half met hemocyanin[17,18] is accessible only through the action of nitric oxide as can be derived from aqueous nitrite chemistry at pH < 7.0, half met T2D can also be prepared by anaerobic ferrocyanide reduction of met T2D. In hemocyanin, met reduction experiments utilizing ferrocyanide and other one-electron reductants[18] failed to yield one-electron reduced derivatives. Thus, the binuclear copper site in Hc routinely functions as a two-electron acceptor, but under

special conditions (NO_2^- and excess ascorbic acid) will yield a one-electron reduced half met-NO_2^- form. Alternatively, the T3 site in T2D readily undergoes a one- rather than two-electron reduction. As the T3 site in native laccase functions exclusively as a two-electron acceptor,[42] this difference in T3 redox behavior suggests a major role for the T2 Cu(II) in enabling two-electron reduction of the T3 site (see Chapter 5).

Ligand binding to half met T2D laccase has been investigated for a series of anions. N_3^-, SCN^-, NO_2^-, Br^-, and acetate all modify the T3 Cu(II) EPR signal. In each case, four discernable hyperfine lines are observed and suggest that there is no delocalized mixed valence character; this is further observed in the EPR difference spectra half met-X^- - met-X^- (Figure 3.51) which better illustrates the spectral contribution of the T3 Cu(II)-X center. Half met-X T2D is therefore formally a class I mixed valence complex.[43] Further, from both optical and EPR titration studies, only one ligand binds to the half met site and it is readily removed by short term dialysis to restore the original half met-aquo EPR features. To summarize, labile ligand substitution chemistry as found for normal tetragonal Cu(II) complexes and for met apo hemocyanin[17,18] is all that is observed.

Figure 3.51 EPR difference spectra at 77 K: half met-X^- T2D laccase derivatives.

The parallel hyperfine splitting is indicated for each anion. The "splitting" in the $g_{//}$ region is due to T1 complications which arise in subtracting off the met-X^- spectral contribution.

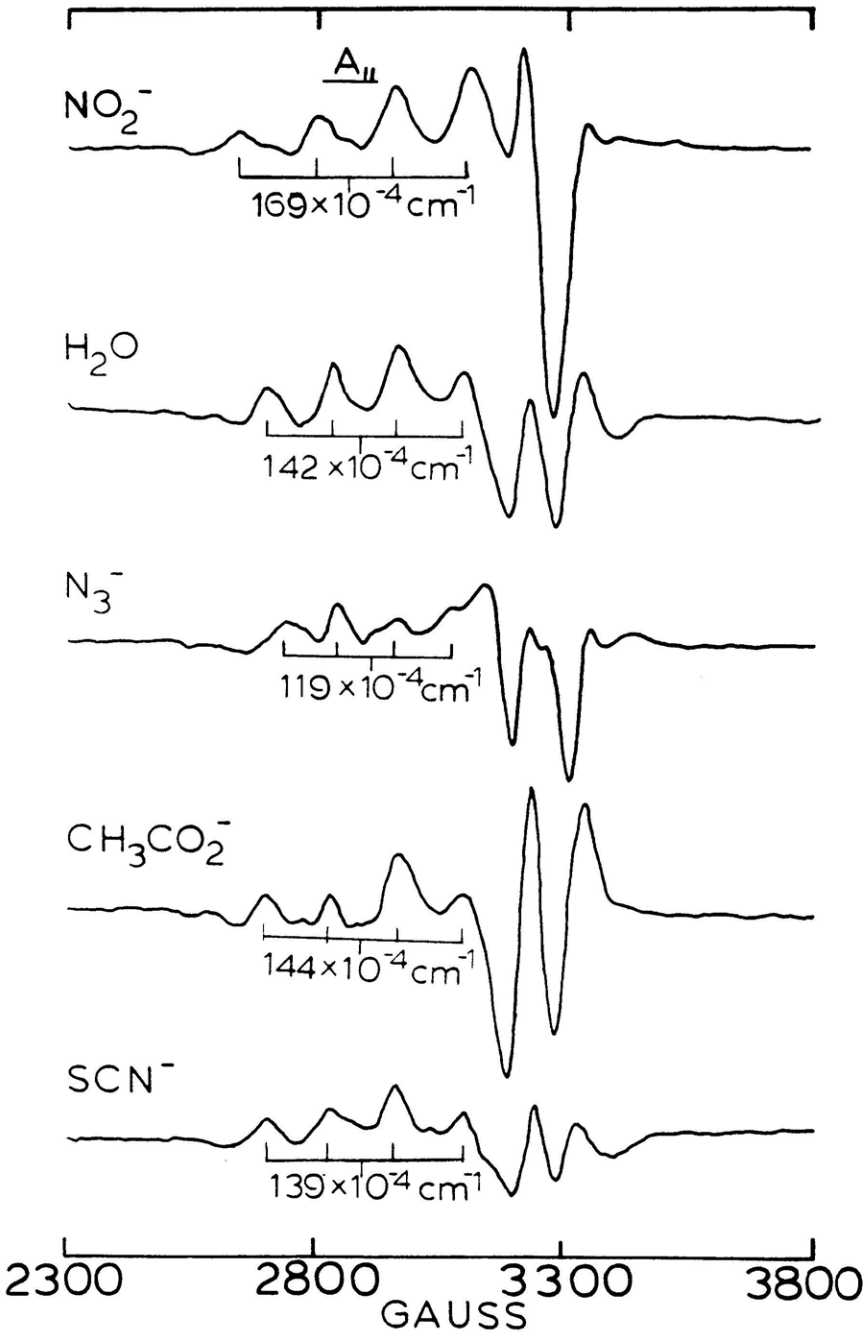
A_{II}
NO_2^-
$169\times10^{-4}cm^{-1}$
H_2O
$142\times10^{-4}cm^{-1}$
N_3^-
$119\times10^{-4}cm^{-1}$
$CH_3CO_2^-$
$144\times10^{-4}cm^{-1}$
SCN^-
$139\times10^{-4}cm^{-1}$
2300
2800
3300
3800
GAUSS

This behavior is in marked contrast to anion binding in half met hemocyanins and tyrosinase.[1,18] In these proteins, exogenous ligands were determined to bridge the cuprous and cupric ions of the binuclear site based on their especially tight binding at this site, and group 1 - group 2 ligand behavior. Group 1 ligands (F^-, Cl^-, Br^-, I^-, OAc^-, NO_2^-) bind tightly to the binuclear coppers with a < 4 Å Cu-Cu distance and produce no change in EPR signal when present in excess concentrations, while group 2 ligands (N_3^-, SCN^-, CN^-) can bridge with a > 5 Å Cu-Cu distance and produce major EPR changes at high excess, indicating that a second group 2 ligand is bound at the cupric center. The increased Cu-Cu separation breaks the endogenous protein bridge, providing the additional coordination position. Upon dialysis, a new EPR signal is observed, indicating that while the second group 2 ligand is removed, the bridging exogenous ligand remains tightly bound. This difference in exogenous ligand reactivity is illustrated in Figure 3.52 for the group 2 ligand, N_3^-. On the left, one N_3^- binds to the laccase T3 site and is readily removed by dialysis to yield the original half met-aquo EPR spectrum. On the right, addition of N_3^- to half met Hc also changes the EPR spectrum. Upon dialysis, however, the EPR spectrum changes again, but even after > 100 hours dialysis time, the original half met aquo signal does not return; one N_3^- remains tightly bound at the half met

Figure 3.52 EPR spectral comparison at 77 K: half met-N_3^- T2D laccase and half met-N_3^- hemocyanin.

(Left) half met T2D laccase and

(Right) half met hemocyanin, reacted with excess N_3^- and dialyzed.

HALF MET COMPARISON

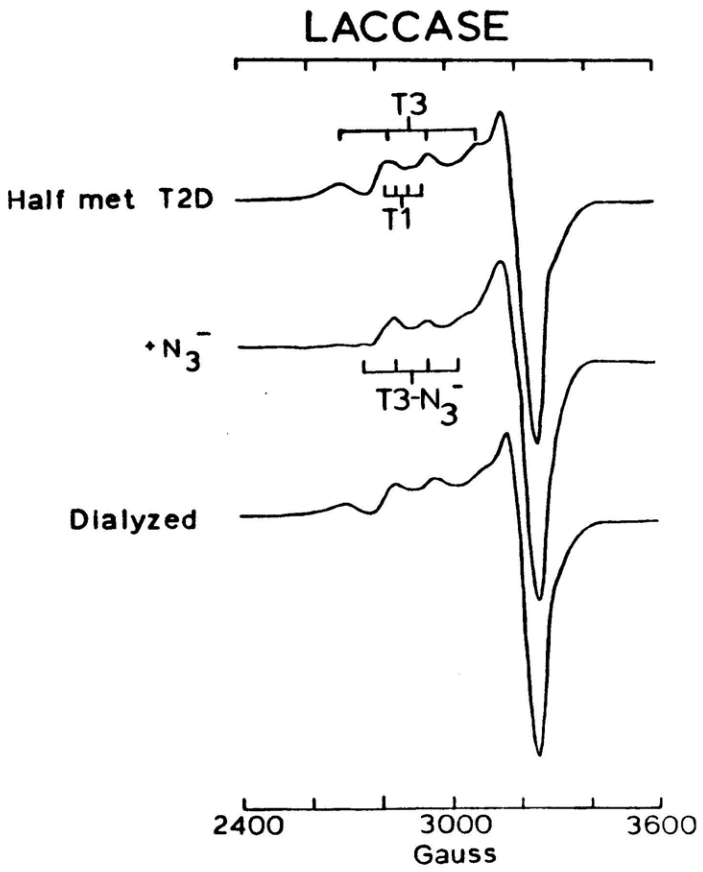

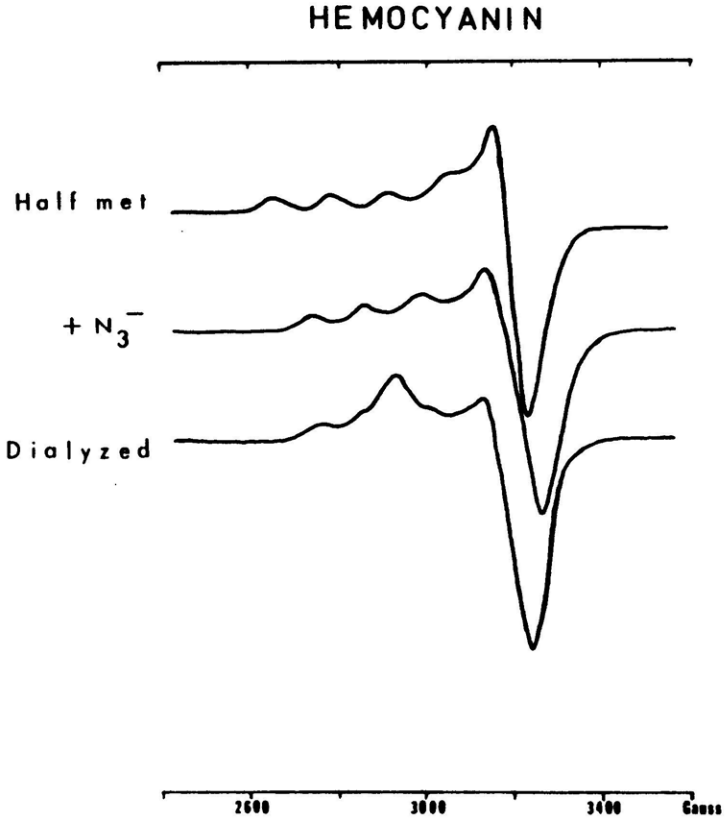

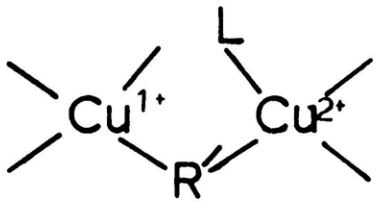

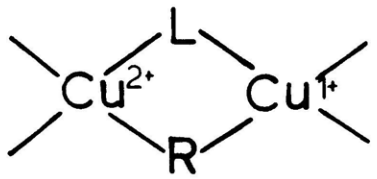

site. The lack of group 1- group 2 behavior, tight binding of anions, or electron delocalization on the EPR time scale in half met T2D laccase indicates that, in contrast to the hemocyanins and tyrosinase, exogenous ligands do not appear to bridge the two coppers.

This lack of exogenous ligand binding in half met T2D laccase is further supported through comparison of the nitrite reactivity of the binuclear copper sites in hemocyanin and T2D laccase. In hemocyanin,[1] deoxy is first oxidized by NO to a half met-NO_2^- intermediate[17] which is then oxidized in trace amounts of oxygen[44] to the uncoupled and EPR detectable dimer $[Cu(II)Cu(II)]N_xO_y$ protein derivative. Oxidation of deoxy by NO to half met-NO_2^- is indirect, proceeding through an EPR non-detectable met intermediate.[20,45] With ascorbic acid, dimer can be reduced to half met-NO_2^-. Similarly, deoxy T2D laccase is oxidized by NO to half met-NO_2^- via an oxidized met intermediate. However, T2D laccase aerobically treated with large excesses of NO_2^- at low pH shows no EPR evidence of dimer formation, even with 200 mW microwave power at 10 K. The inability of exogenous ligands to bridge the T3 site could also account for the apparent lack of dimer[19] formation in T2D (and native[22,46]) laccases. While NO_2^- reacts with both deoxy hemocyanin and deoxy T2D to generate half met-NO_2^- protein derivatives (through a met intermediate), this chemistry

requires only inner sphere electron transfer and exogenous ligand coordination; uncoupling of the site to form dimer hemocyanin, however, is believed[1] to occur through an N_xO_y exogenous ligand bridge which forces Cu-Cu to > 6 Å and ruptures the endogenous protein bridge. If the coordinated exogenous ligand is not able to bridge the binuclear coppers in T2D laccase, the NO_2^- reactivity observed in hemocyanin and tyrosinase, and hence, this route to dimer formation is inaccessible.

With this understanding of exogenous anion interaction at the binuclear copper site in half met T2D, the chemical and spectral properties of the half met-X protein derivatives can be compared in greater detail.

Table 3.5 summarizes the EPR parameters for the aquo (or acetate), nitrite, and azide complexes of half met T2D, half met hemocyanin[18] and met apo hemocyanin.[18] The latter protein derivative represents equatorial coordination to a single Cu(II) ion in hemocyanin and is shown for comparison. It is noted that these half met hemocyanins exhibit the most localized EPR spectra which facilitates comparison to their corresponding half met T2D forms. While the aquo and acetate coordinated cupric centers are fairly similar in these proteins, their perturbations upon binding N_3^- and NO_2^- show no obvious trend. In the corresponding absorption spectra,

Table 3.5. EPR Comparison: Half Met T2D Laccase, Half Met and Met Apo Hemocyanin

	$g_{\|\|}$	$g_{\perp}$	$A_{\|\|}$ ($\times 10^{-4}$ cm^{-1})
Half Met T2D			
Aquo	2.28	2.07	138
NO_2^-	2.31	2.06	160
N_3^-	2.28	2.07	101
Half Met Hc			
Acetate	2.32	2.08	141
NO_2^-	2.30	2.10	125
N_3^- (excess)	2.24	2.06	136
Met Apo Hc			
Acetate	2.31	2.08	131
NO_2^-	2.31	2.10	124
N_3^-	2.24	2.06	152

comparisons can be made only between aquo (or acetate) and azide, due to the intense absorbance of free NO_2^- in solution.

The energies and intensities of the N_3^- ---> Cu(II) CT features for half met-N_3^- T2D, half met-N_3^- (excess N_3^-) Hc[18] and met apo-N_3^-[18] are listed in Table 3.6. The 500 nm band in half met-N_3^- is associated with the bridging of N_3^- while that at 400 nm with the equatorial N_3^-. The low energy of the half met-N_3^- feature likely reflects a steric effect at the Cu(II) which can be induced by bridging the binuclear copper site, but should not be considered as diagnostic of N_3^- bridging Cu(I) and Cu(II) centers, as has been recently suggested.[47] It is further noted that met apo-N_3^- which contains a single copper ion exhibits a weak CD feature at 530 nm. Thus, while the N_3^- ---> Cu(II) CT features are fairly similar, current understanding limits interpretation of the observed similarity.

Finally, while the near IR-CD transitions for met apo and met apo-N_3^- are not known, CD data are available[48] for half met acetate and half met-N_3^- Hc. Figure 3.53 summarizes the energies and intensities of the ligand field and N_3^- ---> Cu(II) CT transitions in half met aquo (acetate) and half met-N_3^- T2D laccase and hemocyanin. In comparing half met-aquo T2D and half met acetate Hc, the d-d bands are at

Table 3.6 298 K N_3^- ---> Cu(II) CT Transitions: Half Met T2D Laccase, Half Met and Met Apo Hemocyanin

		Absorption	CD
	λmax (nm)	Δε ($M^{-1}cm^{-1}$)	Δ(Δε) ($M^{-1}cm^{-1}$)
Half Met-N_3^- T2D	480	~2000	≲-0.2
	?400	~2000	
Half Met-N_3^- Hc[a,b]	500	1000	
(excess N_3^-)	460	<250	-1.0
	380	1200	-0.3
	335	*	0.6
Met Apo-N_3^- Hc[a,b]	530	---	-0.3
	420	2500	-1.2

---

[a] Data is for Busycon Hemocyanin (mollusc)[1,18]

[b] Wilcox, D.E.; Solomon, E.I. to be published

* Obscured by overlap with oxy which may be present

Figure 3.53 Ligand field and N_3^- ---> Cu(II) CT transitions: Half met T2D laccase and half met hemocyanin

Ligand field orbitals are from CD studies; $\Delta(\Delta\varepsilon)$'s ($M^{-1}cm^{-1}$) are indicated and are relative to the respective deoxy derivatives. N_3^- ---> Cu(II) CT energies are from absorption studies; $\Delta\varepsilon$'s ($M^{-1}cm^{-1}$) are indicated for these transitions.

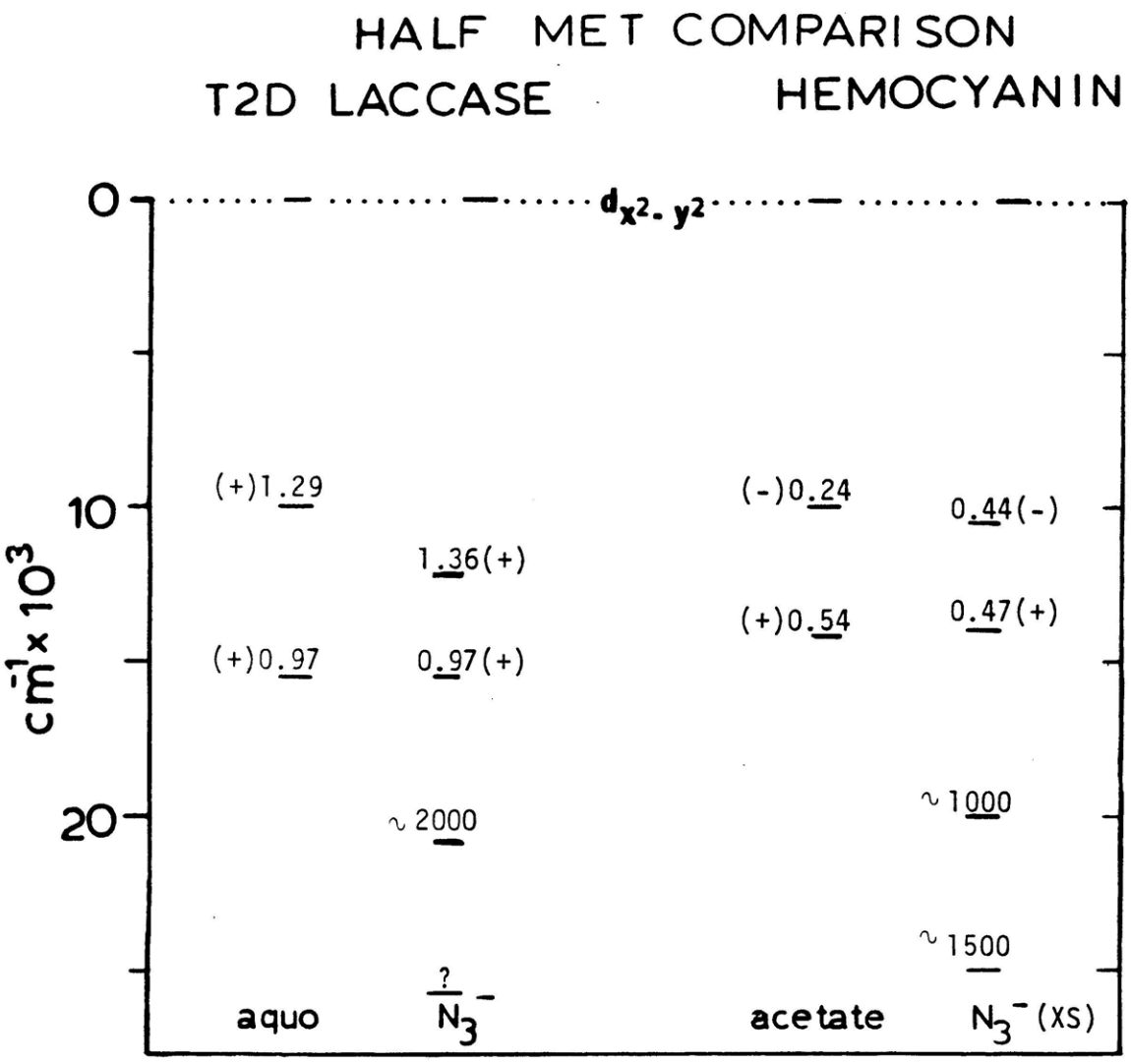
HALF MET COMPARISON
T2D LACCASE
HEMOCYANIN
0
10
20
$cm^{-1} \times 10^3$
$d_{x^2-y^2}$
(+)1.29
(+)0.97
1.36(+)
0.97(+)
~2000
(-)0.24
(+)0.54
0.44(-)
0.47(+)
~1000
~1500
aquo
$\frac{?}{N_3^-}$
acetate
N_3^- (XS)

similar energy, although somewhat more intense in laccase. On binding N_3^-, CT transitions appear at similar energies; however, while the d-d transitions in half met-OAc Hc shift by only a few hundred cm^{-1}'s, the lowest energy feature in half met-aquo T2D shifts by ~2300 cm^{-1}. This demonstrates a major change in the geometric structure of half met T2D but not half met Hc on binding N_3^-. The more significant change in the half met-N_3^- EPR spectrum (Table 3.6) of T2D further supports this conclusion.

In comparing the spectral features of met T2D and met Hc (Figure 3.54) it would appear that the coupled binuclear copper site is basically very similar in hemocyanin and T2D laccase. Both met T2D and met Hc are EPR non-detectable and display a cupric edge spectrum. In the absorption spectra, the d-d transitions are at ~745 nm in each of these proteins and are consistent with tetragonal cupric sites. The simultaneous presence of binuclear cupric centers with d-d transitions and a diamagnetic ground state requires a superexchange mediating endogenous protein bridge in met T2D as has been demonstrated for met Hc. This is confirmed by studies at low pH where, in the presence of N_3^-, the endogenous bridge is competitively displaced and protonated in both laccase and hemocyanin.[34]

The 330 nm region is broader and weaker in met hemocyanin[1] than in met laccase ($\varepsilon_{330} < 1500\ M^{-1}cm^{-1}$ vs. $\varepsilon\sim$

Figure 3.54 Spectroscopic Properties: Met T2D laccase and met hemocyanin.

(upper) electronic absorption spectra at 298 K,

(lower) EXAFS comparison.

OPTICAL FEATURES

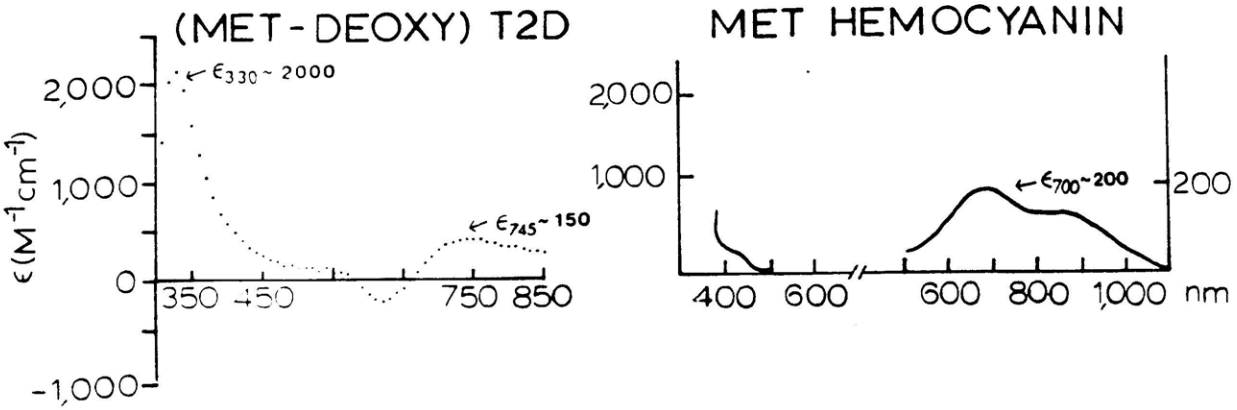

EXAFS

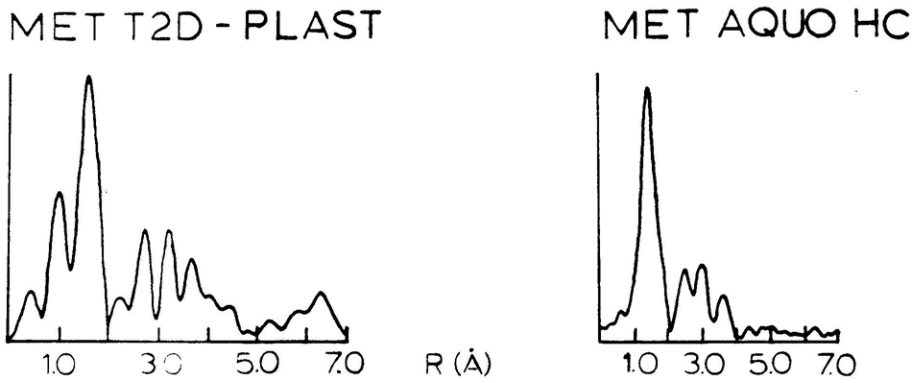

2000 $M^{-1}cm^{-1}$). EXAFS studies have excluded S ligation at the T3 site in T2D laccase, as has also been shown for met Hc.[25,49] An average of 3-4 N (or O) atoms at a distance of 2.00 A in met T2D and 3-5 N (or O) atoms at 1.98-2.02 Å in met aquo Hc[25b] is the only ligation evidenced by EXAFS studies. Thus, the 330 nm transition likely derives from a composite of his ---> Cu(II) CT transitions with potential contribution of CT from the endogenous protein bridge in both laccase and hemocyanin. It may be that the band is broader in Hc because of greater variation in the orientations of the imidazole planes relative to the equatorial plane (hence dx^2-y^2 orbital) of each Cu(II). It is noted that a similar change in the imidazole plane orientation might be responsible for the intensity decrease and broadening at 330 nm which is observed when N_3^- binds to met T2D laccase (Figure 3.36).

To further probe the T3 site in laccase, the calculated (met T2D-T1) difference spectrum (Section 3i) can be compared with the hemocyanin EXAFS spectrum[25b,49] (Figure 3.54). Curve fitting analysis of the outer peak pattern in the transform of the laccase difference spectrum shows no indication of a copper scatterer at a distance ≤3.8 Å. Detection of a copper scatterer at ≥3.8 Å is not possible at this noise level and is further complicated by multiple scattering effects and unknown Debye-Waller factors. While

in oxyhemocyanin[25b,49] a large peak is present at ~3.6 Å and is associated with the second copper, in met Hc which also contains an antiferromagnetically coupled binuclear cupric site at a Cu-Cu distance of < 4 Å , it is less clear whether scattering from a second copper can be observed. Hence, it cannot be concluded whether there is a difference in the Cu-Cu distances of these binuclear copper sites. Thus, EPR, visible-UV absorption, edge, and EXAFS comparison of met T2D and met Hc suggests that the coupled binuclear cupric sites are very similar in these proteins: in both cases, two tetragonal cupric centers are coordinated by simple N,O ligation and are super-exchange coupled through an endogenous protein bridge. This similarity, and in particular the exclusion of strong S ligation (to < 2.4 Å) at the T3 site in laccase indicates that the major differences in the binuclear copper properties of laccase and hemocyanin, e.g. the inability of exogenous ligands to bridge the binuclear coppers and irreversible oxygen binding, are not due to fundamental differences in first shell ligation. These differences can be further probed by comparing F^-, N_3^-, and O_2^{2-} reactivity for the met derivatives.

Where F^- binding to aqueous inorganic cupric complexes is essentially unknown, F^- has been shown to bind with

unusually high affinity ($K \sim 10^3$) to met Hc.[50] As F^- does not bind to half met or deoxy Hc, this binding was associated with the large positive charge at the met site; a hydrophobic active site pocket would further minimize [OH^-] and stabilize F^- binding. In contrast, there is no evidence[51] for F^- binding at the met T2D active site. This could suggest an increased hydrophilicity for the active site pocket of the laccase binuclear cupric site.

Studies of N_3^- binding to met T2D suggest that the absence of bridging behavior in half met T2D extends to this derivative as well. Consistent with equatorial non-bridging N_3^- coordination, absorption, and CD spectra of azide bound to met T2D show only one (isoenergetic) N_3^- ---> Cu(II) CT band (λmax = 450 nm) In contrast, azide on met hemocyanin clearly exhibits three CT peaks in the optical spectra[48,50] (absorption: 500 nm, 380 nm; CD: 460 nm). As only one N_3^- is binding per binuclear cupric site and a single N_3^- ---> Cu(II) bond can have only two CT transitions, the presence of three N_3^- ---> Cu(II) CT transitions indicates that N_3^- must bridge the two coppers.[50,52] This inability of N_3^- to bridge the T3 site in laccase is also observed in the uncoupled T3 sites, even though N_3^- has competitively diplaced the endogenous protein bridge (<u>vide infra</u>)!

In met-N_3^- Hc, as in half met-N_3^- Hc, N_3^- bridges the binuclear copper site. The energies and intensities of the

d-d transitions, determined by IR-CD and the N_3^- ---> Cu(II) CT bands, from absorption and CD studies, in met-aquo T2D and Hc,[48] and their N_3^- bound derivatives are compared in Figure 3.55. As for half met T2D and half met Hc, and consistent with the absorption data, the ligand field bands in met aquo T2D and met aquo Hc are at similar energies. However, whereas N_3^- significantly shifts the energies and signs of the met aquo T2D d-d transitions, only slight energy and intensity changes are observed in going to met-N_3^- Hc. In comparing the met aquo Hc and half met acetate Hc near IR-CD spectra (Figures 3.53 and 3.55), it is clear that in oxidizing half met to met, one is not simply adding the spectral features of the second copper(II) to the original half met spectrum. A similar structural change, although to a much greater extreme, was observed in analogous studies of T2D laccase. Interestingly, whereas the spectral changes associated with N_3^- binding to met and half met T2D are very different form one another (Figure 3.39), in hemocyanin, a very similar set of spectral changes characterize N_3^- binding to each of these binuclear copper derivatives. In both half met and met Hc (Figures 3.53 and 3.55), the low energy CD feature blue shifts by 500-800 cm^{-1} and almost doubles in intensity upon coordination of N_3^-; the higher energy feature only weakly red shifts. The similarity in these ligand

Figure 3.55 Ligand field and N_3^- ---> Cu(II) CT transitions: met T2D laccase and met hemocyanin.

Ligand orbitals are from CD studies; $\Delta(\Delta\varepsilon)$'s ($M^{-1}cm^{-1}$) are indicated and are relative to the respective deoxy derivatives. N_3^- ---> Cu(II) CT energies are from absorption studies; $\Delta\varepsilon$'s ($M^{-1}cm^{-1}$) are indicated for these transitions.

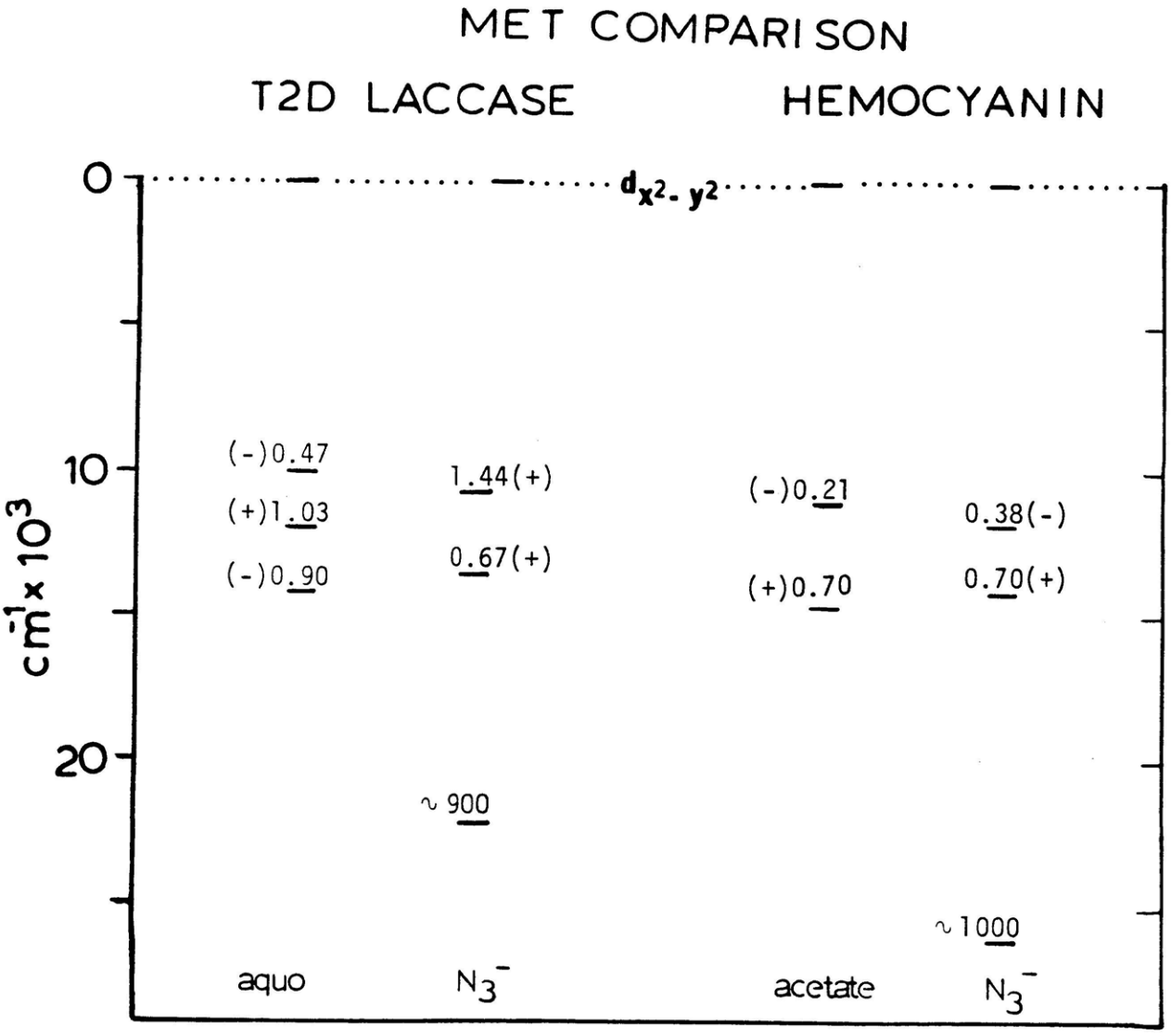
MET COMPARISON
T2D LACCASE
HEMOCYANIN
0
10
20
$cm^{-1} \times 10^3$
$d_{x^2-y^2}$
(-)0.47
(+)1.03
(-)0.90
1.44(+)
0.67(+)
~900
(-)0.21
(+)0.70
0.38(-)
0.70(+)
~1000
aquo
N_3^-
acetate
N_3^-

field perturbations of Hc indicates that the interaction of N_3^- with the binuclear copper site is similar in the met and half met derivatives. Conversely, the extreme dissimilarity which is observed in comparing met and met-N_3^--T2D and half met and half met-N_3^- T2D (Figure 3.39), would then further indicate that the exogenous anion N_3^- is interacting very differently with the T3 site in laccase compared to the binuclear copper site in the hemocyanins and tyrosinase.

The helium EPR studies of the uncoupled T3 site in met-N_3^- T2D probe the endogenous protein bridge as well as exogenous ligation at the T3 site. In part I, it was shown that the broad zero field split triplet EPR signal is characteristic of two dipolar Cu(II)'s interacting at a distance of 4.0 Å and is observed only in the presence of N_3^-. As the exchange coupling for these signals is negligible, it can be concluded that the endogenous superexchange mediating ligand is no longer present.

In met hemocyanin, a related set of signals in the presence of N_3^- or acetate has been extensively characterized. In hemocyanin, these "met EPR signals"[34] have been associated with a small fraction of the binuclear copper sites wherein the endogenous bridge has a lower stability constant and can be uncoupled through competitive anion displacement at low pH. The similiar dependence of signal

intensity on both pH and [N_3^-] in met T2D laccase and met Hc indicates that N_3^- and H^+ also compete with the endogenous bridge in laccase. Comparison of these uncoupled sites in hemocyanin and laccase further demonstrates the inability of exogenous ligands to bridge the T3 site in met T2D. In addition, strong similarities are suggested to exist between the endogenous protein bridges in these proteins. While both N_3^- and acetate compete with the endogenous bridge in met Hc, only the N_3^- studies will herein be discussed so that direct comparison to the analogous T2D signal can be made.

The physical properties of the met-N_3^- Hc and met N_3^- T2D are very similar. Both signals are not observed at > 50 K, follow a Curie Law behavior below 50 K and are much more difficult to saturate than is mononuclear copper(II).

A spectral comparison (Figure 3.56) of the met-N_3^- T2D and met-N_3^- Hc signals at 7 K shows that significant differences also exist in these signals. In met-N_3^- T2D, the peak to peak spacing in the g~2 region is much larger than in met Hc and no g~4 signal is observed. Consistent with these qualitative differences, simulation[34] of the Hc signal indicates r = 5.0 Å in met-N_3^- Hc where it is only 4.0 Å in met-N_3^- T2D. From N_3^- model complexes,[53] N_3^- normally bridges at <3.2 Å in a μ-1,1 geometry and at ≧5.0 Å in a μ-1,3 geometry. Two exceptions to this generalization are binuclear copper chelate complexes by Sorrel[53b] and Reed[53c]

Figure 3.56 Met-N_3^- EPR signals at ~10K: T2D laccase and hemocyanin.

(upper) Met-N_3^- hemocyanin (9.39 GHz, 10 mW) 0.1 M succinate, pH 4.5);

(lower) met-N_3^- T2D laccase (9.39 GHz, 200 mW, 0.1 M sodium acetate, pH 4.6). In hemocyanin, the sharp perpendicular intensity is due to ~3% mononuclear Cu(II) while in laccase, it is the only partially saturated T1 Cu(II).

* ubiquitous rhombic iron at g = 4.3.

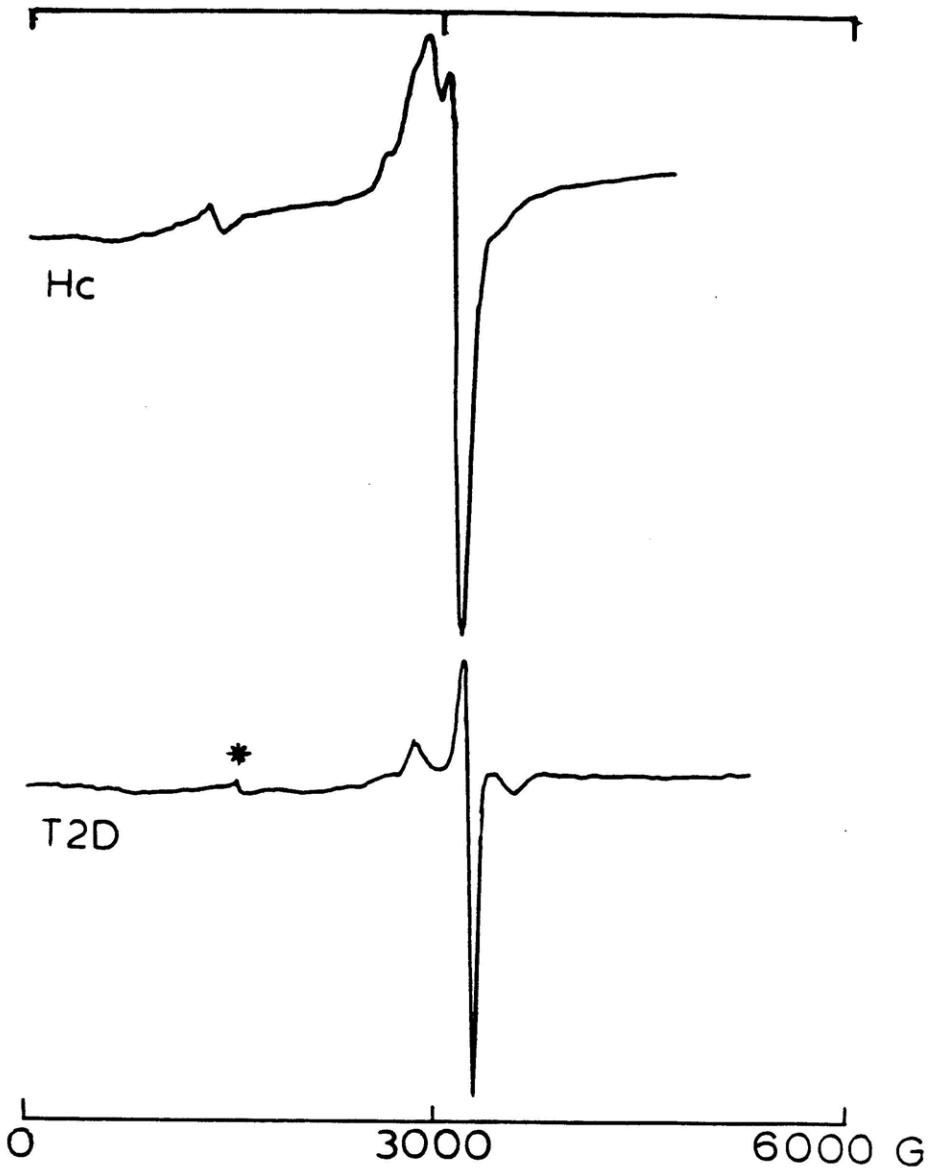
Hc
T2D
*
0
3000
6000 G

in which the N_3^- bridges in a μ-1,3 geometry and the Cu-Cu distances are 3.77 and 3.62 Å, respectively. In these complexes, however, a second bridging ligand (OR^-) is also present and provides a strong superexchange pathway (Sorrel, $2J > -1200\ cm^{-1}$; Reed, $2J > -1100\ cm^{-1}$) which is clearly not present at the uncoupled met-N_3^- T3 site. Thus, while the 5 Å Cu-Cu separation indicates that a u-1,3 N_3^- is bridging the hemocyanin site (consistent with additional studies of inductive effects which show that bridging exogenous ligands determine r_{Cu-Cu} and modify the EPR signals), the 4 Å distance in met T2D indicates that N_3^- is not bridging the uncoupled T3 site; 4.0 Å is too long to sustain a u-1,1 bridging geometry and too short for a u-1,3 N_3^- in the absence of an additional bridging ligand. This data would indicate that even when N_3^- displaces the endogenous bridge from one of the T3 cupric centers, it is still unable to bridge the site. Either the Cu-Cu distance is rigidly fixed by the protein ligand, or the protonated endogenous bridge is relatively strongly coordinated to the second Cu(II) and cannot be further displaced.

Halide ions, when added in the presence of acetate, modify the intensity and shape of the broad EPR signals in Hc; unfortunately, the N_3^- signal is harder to probe in Hc and its analogous halide effects are not known. In met acetate,[34] however, fluoride decreases signal intensity while

chloride and bromide increase it. Further, the signals change in the presence of Cl^- and Br^- indicating that these exogenous anions are in fact binding at the site. These ions are believed to bind to the exogenous ligand bridging position and therefore affect the Cu-Cu distance and the signal shape, as well as the stability constant of the endogenous bridge; the latter is an inductive effect which changes the amount of uncoupling which is observed. In T2D laccase, halide ions do modify signal intensity but have no effect on signal shape. This is completely consistent with both the model proposed in Part 1 and this related data on hemocyanin. That is, in laccase, there is one endogenous bridging coordination position which is where the uncoupling N_3^- binds: thus, anions bind equatorially to the "normal" exchangeable position at the T3 site in met T2D and could easily affect the apparent pKa and stability of the endogenous bridge, but would not be expected to change r_{Cu-Cu} or the shape of the EPR signal. The back inhibition by N_3^- of the uncoupled signal is also an inductive effect, but is observed only in laccase. Finally, it should also be noted that whereas met T2D laccase is a homogeneous protein and these sites represent a small pH dependent fraction of all of the T3 sites, hemocyanin is a heterogeneous protein and the endogenous bridge instability is associated with a small heterogeneous fraction of the active sites.

The ability to reversibly uncouple these Hc and T2D laccase T3 sites under similar $[H^+]$ and $[N_3^-]$, together with the similarity in the physical properties of these signals, strongly suggests that a similar protein residue provides the superexchange pathway in laccase and hemocyanin. In both hemocyanin and laccase, the exchange coupling is large ($2J \geq -550\ cm^{-1}$)[54] such that imidazolate and other N donors do not appear reasonable possibilities. Through EXAFS studies, sulfur ligation has also been eliminated at each of these binuclear copper sites. Finally, thermodynamic analysis[34] of the met-acetate hemocyanin uncoupled signal, utilizing the apparent acetate binding constants at various pH values and their standardized stabilities,[55] determined that the endogenous bridge in the protein site is a protonatable residue with an intrinsic pKa > 7.0, thereby eliminating carboxylate. Similarly in laccase, an analogous thermodynamic treatment of the met-N_3^- T2D signal using the data in Figure 3.48 showed that its endogenous bridge has an intrinsic pKa > 6.7.

Consistent with all of these results, phenolate, alkoxide or hydroxide remain potential candidates for the endogenous bridge. In met hemocyanin, a shoulder at 420 nm ($\varepsilon \sim 250\ M^{-1}cm^{-1}$) has been assigned[1] as a RO^- ---> Cu(II) CT transition, and based on model studies,[31] probably favors a bridging phenolate. In laccase, broad absorption between 500

and 300 nm is associated with endogenous L ---> Cu(II) CT at the coupled binuclear cupric site; spectra at 77 K further indicate the presence of transitions at ~440 and 400 nm, but additional studies are necessary before any potential assignments can be made. Nonetheless, from these chemical and spectral studies of met T2D laccase, direct evidence has been presented for an endogenous protein bridge in laccase. It can further be concluded that a similar bridging ligation, OR^- (where R = phenyl, alkyl, or H), provides the superexchange pathway in laccase and hemocyanin.

Finally, using the chemistry and spectroscopy of the T2D laccase derivatives which have been developed and the results of the analogous studies of the simpler binuclear copper proteins, the lack of exogenous ligand bridging at the binuclear copper site in laccase can now be addressed.

The inability of exogenous ligands to bridge the T3 site was first suggested by the lack of group 1 - group 2 behavior, the lack of tight binding of anions and the lack of electron delocalization in the EPR spectra of half met T2D laccase but not half met Hc protein forms. It was further supported by the lack of dimer-N_xO_y formation in nitrite studies of T2D laccase. The indistinguishable N_3^- ---> Cu(II) CT transition energies in the absorption and CD spectra of met-N_3^- T2D (coupled) also support a non-bridging

N_3^- coordination to one of the antiferromagnetically coupled binuclear cupric centers. This single N_3^- ---> Cu(II) CT transition is in strong contrast to met N_3^- Hc (three N_3^- ---> Cu(II) CT transitions, thereby requiring that N_3^- bridge the binuclear copper site) and indicates that the absence of bridging behavior also extends to the met derivative. Most recently, the lack of exogenous bridging has been observed in the uncoupled met-N_3^- T2D sites where the observed 4.0 Å Cu-Cu distance is not able, based on model studies, to sustain either a u-1,1 or a u-1,3 N_3^- bridge, suggesting that N_3^- is coordinated end-on equatorial in these sites as well.

Thus, from all of these studies, it is concluded that the inability of exogenous ligands to bridge the laccase T3 site is an intrinsic property of the binuclear copper unit in this multicopper oxidase. Possible explanations for this lack of bridging are illustrated in Figure 3.57. In 3.57A, the exchangeable coordination positions on the two Cu(II)'s are spatially separated such that bridging cannot occur. The bridging angle θ may be so large as to prevent overlap between the exogenous ligand valence electrons and the second Cu(II): two exogenous ligands would be expected to coordinate end-on equatorial to T2D laccase. Alternatively, the relative orientation (θ_1 and θ_2) of the exchangeable coordination positions may prevent orbital overlap. Here, two exogenous ligands would again be expected to coordinate

Figure 3.57 Exogenous ligand interaction in T2D laccase: schemes consistent with non-bridging coordination geometries.

A.

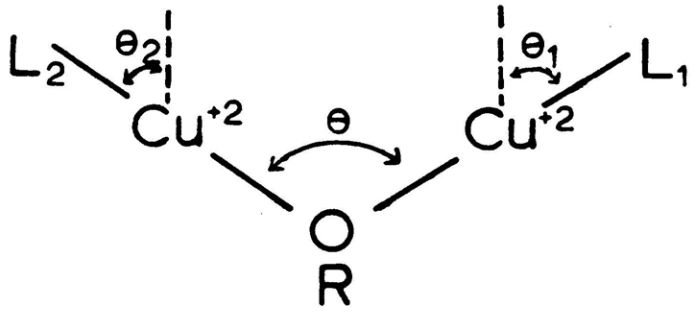

B.

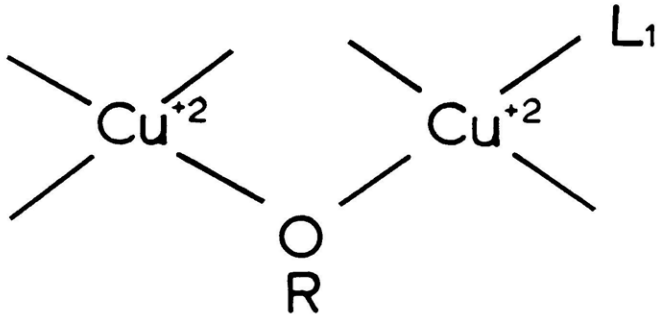

to the T3 site, unless binding of the first ligand sterically prevented binding of the second ligand. As diagrammed in Figure 3.57B, another possibility is that there is only one exchangeable position at the T3 site in laccase, and under these circumstances only one exogenous ligand could coordinate to T2D laccase.

A further examination of the chemical properties of deoxy, half met and met T2D sheds insight into these possibilities. In deoxy T2D, exogenous anions and CO were found to bind at the cuprous site. Through competition experiments, it was further determined that all of these ligands coordinate to the same exchangeable position at the reduced T3 site. In half met T2D, exogenous anions also bind to the T3 site. From optical and EPR titration studies, only one ligand binds per half met site and from competition studies, N_3^-, NO_2^-, and OAc^- all bind to the same exchangeable position at the half met cupric center. This is also true for the halide ions (Cl^-, Br^-, I^-) which are sterically less constrained and should be more flexible in their binding mode. CO studies of half met-aquo and half met-X^- T2D show no apparent perturbation of the T3 Cu(II)-X^- EPR signal and there is no spectral evidence for formation of a half met-X^-/CO ternary complex. Finally, in studies of the met T2D derivative, again only one anion binds per binuclear cupric site. The similarities in the allosterically induced

changes at the met T1 Cu(II) site to those observed in analogous studies of the T1 Cu(II) in deoxy T2D further suggests that exogenous anions are likely binding at the same copper ion site in each of these T2D derivatives.

In view of all these results, it would appear that exogenous ligands cannot bridge the binuclear copper site in laccase because there is only one exchangeable position at the site. In no case[56] are two exogenous ligands spectroscopically observed to bind at the active site in laccase, and indirect evidence would suggest that anions are binding similarly in the various binuclear copper active site derivatives. While the binding of one ligand (Figure 3.57A) could sterically prevent coordination of the second for the larger oriented ligands SCN^- and N_3^-, an extended series of anions has been investigated and in all cases, one exogenous ligand is spectroscopically observed to coordinate. Only the significantly different near-IR CD changes associated with N_3^- binding to met vs. half met T2D might suggest that different Cu(II) binding sites are involved, but alternatively, the major CD changes in the ligand field bands on oxidizing half met to met T2D would suggest that the half met cupric center itself has been greatly modified on oxidation, independent of its interaction with N_3^-.

Thus, we have the spectroscopically effective model for the binuclear copper site in T2D laccase shown in Figure 3.58. The oxyhemocyanin and oxytyrosinase active site[1] is shown for comparison. In both T2D laccase and oxyhemocyanin, two tetragonal Cu(II)'s are antiferromagnetically coupled through an endogenous protein bridge, OR^-. However, whereas two exchangeable coordination positions are oriented so as to allow peroxide to bridge the hydrophobic binuclear copper site in oxyhemocyanin and oxytyrosinase, only one equatorial position at one Cu(II) is available for exogenous coordination at the relatively hydrophilic T3 site in T2D laccase. Imidazole N (or O) ligands complete the first coordination sphere of the copper centers in both T2D laccase and oxyhemocyanin. In T2D laccase, the μ-dioxo bridging mode of O_2^{2-} in oxyhemocyanin and oxytyrosinase is not accessible. This lack of bridging means that only a mono-oxo type binding to one of the T3 coppers is possible.

Together, these differences in hydrophobicity and exogenous ligand binding result in a lack of peroxide binding to met T2D laccase ($K < 100\ M^{-1}$) compared to the high binding affinity ($K \sim 5 \times 10^5\ M^{-1}$) for peroxide binding to met hemocyanin and tyrosinase.[57] These differences in binuclear copper active site structure may further relate to the differences in oxygen reactivity between deoxy T2D laccase and deoxy hemocyanin. Whereas deoxy T2D laccase

Figure 3.58 Spectroscopically effective models: T2D laccase and oxyhemocyanin.

In laccase, the hydroperoxide would bind end-on equatorial but does not form a stable complex and is therefore shown in parentheses at the exchangeable coordination position. OR and OR' represent the endogenous protein bridges in hemocyanin and laccase, respectively.

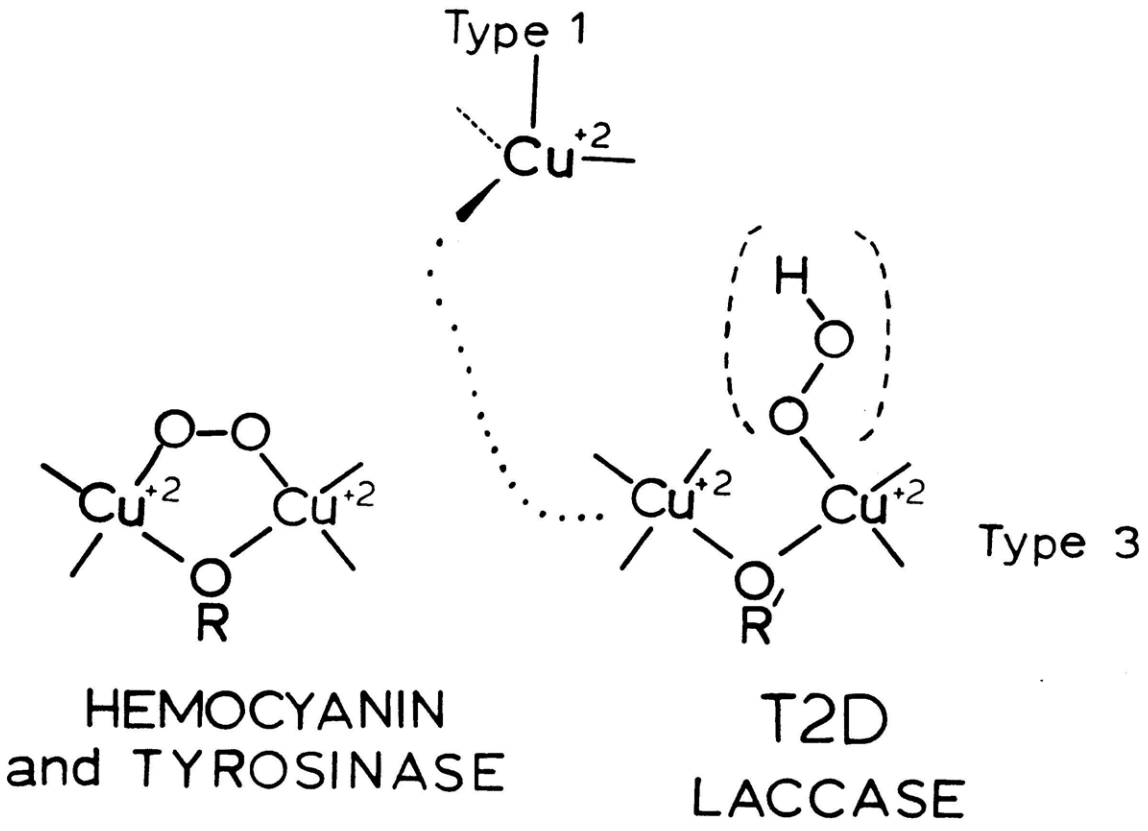
Type 1
Cu+2
H
O
O
O-O
Cu+2
Cu+2
O
R
Cu+2
Cu+2
O
R'
Type 3
HEMOCYANIN
and TYROSINASE
T2D
LACCASE

contains a binuclear cuprous site which is stable in the presence of oxygen, deoxy hemocyanin is readily oxidized to oxyhemocyanin in air. However, native laccase does not react with O_2, and this would appear to indicate a strong involvement of the T2 copper in the oxygen reactivity of the T3 site. This T3-T2 intersite interaction in exogenous ligand binding will be further discussed in Chapter 5.

References and Notes

1. Solomon, E.I. in Copper Proteins **1981**, Spiro, T.G., Ed. (Wiley Interscience: New York) Ch. 2.

2. Himmelwright, R.S.; Eickman, N.C.; LuBien, C.D.; Lerch, K.; Solomon, E.I. J. Am. Chem. Soc. **1980**, 102, 7339-7344.

3. Gordon, A.J.; Ford, R.A. in The Chemist's Companion: A Handbook of Practical Data, Techniques and References **1972** (Wiley Interscience: New York) p. 438.

4. Byers, W.; Curzon, G.; Garbett, K.; Speyer, B.E.; Young, S.N.; Williams, R.J.P. Biochim. Biophys. Acta **1973**, 310, 38-50.

5. Kolthoff, F.M.; Sandell, E.B.; Meehan, E.J.; Bruckenstein, S. Quantitative Chemical Analysis **1969** (MacMillan Co.: New York).

6. Cramer, S.P.; Hodgson, K.O. Prog. Inorg. Chem. **1979**, 25, 1-39.

7. Graziani, M.T.; Morpurgo, L.; Rotilio, G.; Mondovi, B. FEBS Lett. **1976**, 70, 87-90.

8. LuBien, C.D.; Winkler, M.E.; Thamann, T.J.; Scott, R.A.; Co, M.S.; Hodgson, K.O.; Solomon, E.I. J. Am. Chem. Soc. **1981**, 103, 7014-7016.

9. Approximately 0.1 protein equivalent of Fe is determined by AA and is generally accepted in the literature as present in all T2D preparations.[7] And -
Reinhammar, B. J. Inorg. Biochem. **1983**, 18, 113-121.

10. Gray, H.B.; Solomon, E.I. in Copper Proteins **1981**, Spiro, T.G., Ed. (Wiley Interscience: New York) Ch. 1.

11. Desideri, A.; Morpurgo, L.; Rotilio, G.; Mondovi, B. FEBS Lett. **1979**, 98, 339-341.

12. Reinhammar, B.; Malkin, R.; Jensen, P.; Karlsson, B.; Andreasson, L.E.; Aasa, R.; Vanngard, T.; Malmstrom, B.G. J. Biol. Chem. **1980**, 255, 5000-5003.

13. Reinhammar, B. J. Inorg. Biochem. **1981**, 15, 27-39.

14. Potential perturbations of the T1 Cu(II) features would also absorb in this spectral region.

15. Potential absorption at 400 nm due to a small amount of T2 Cu(II) (low affinity N_3^- in native laccase) or $Fe(CN)_6^{3-}$ precludes a definite assignment of this absorption to half met-N_3^-.

16. In a tetragonal ground state, the dominant CD intensity derives from the dxy ---> dx^2y^2 transition, and normally occurs to lower energy than (dxz, dyz) $\dashrightarrow$ dx^2-y^2 which dominate the absorption intensity.

17. Himmelwright, R.S.; Eickman, N.C.; Solomon, E.I. Biochem. Biophys. Res. Comm. **1978**, 81, 237-242.

18. Himmelwright, R.S.; Eickman, N.C.; Solomon, E.I. J. Am. Chem. Soc. **1979**, 101, 1576-1586.

19. Schoot Uiterkamp, A.J.M. FEBS Lett. **1972**, 20, 93-96.

20. Himmelwright, R.S.; Eickman, N.C.; Solomon, E.I. Biochem. Biophys. Res. Comm. **1979**, 86, 628-634.

21. While NO is reported[22] to reduce the T1 copper and to not affect the T3 coppers in three-copper laccase, how this T2D form and its reaction conditions relate to those described herein is not clear (Chapter 2 and reference 23).

22. Martin, C.T.; Morse, R.H.; Kanne, R.M.; Gray, H.B.; Malmstrom, B.G.; Chan, S.I. Biochem. **1981**, 20, 5147-5155.

23. Hahn, J.E.; Co, M.S.; Hodgson, K.O.; Spira, D.J.; Solomon, E.I. Biochem. Biophys. Res. Comm. **1983**, 112, 737-745.

24. a. Miskowski, V.M.; Thich, J.A.; Solomon, R.; Schugar, H.J. J. Am. Chem. Soc. **1976**, 98, 8344-8350.
b. Amundsen, A.R.; Whelan, J.; Bosnich, B. J. Am. Chem. Soc. **1977**, 99, 6730-6739.

25. a. Brown, J.M. J. Am. Chem. Soc. **1980**, 102, 4210-4216.
b. Co, M.S.; Hodgson, K.O.; Eccles, T.; Lontie, R. J. Am. Chem. Soc. **1981**, 103, 984-986.

26. Eickman, N.C.; Himmelwright, R.S.; Solomon, E.I. Proc. Natl. Acad. Sci. USA **1979**, 76, 2094-2098.

27. Fits are done by minimizing the difference between the observed and calculated EXAFS at each point in k space, squared, and then weighted by k^6. The function value F is given by $F^2 = \sum\{k^6(\text{data-fit})^2\}/N$.

28. Fee, J.A. Struct. Bonding (Berlin) **1975**, 23, 1-60.

29. Tullius, T.D. Ph.D. Dissertation, Stanford University, Stanford, California, **1980**.

30. Hahn, J.E.; Smith, T.A.; Scott, R.A.; Hodgson, K.O. unpublished results.

31. Solomon, E.I.; Penfield, K.P.; Wilcox, D.E. Struct. Bonding (Berlin) **1982**, 53, 1-57.

32. Bleaney, B.; Bowers, K.D. Proc. R. Soc. (London) Ser. A **1952**, 214, 451-465.

33. Beinert, H.; Orme-Johnson, W.H. in Magnetic Resonance in Biological Systems **1967**, Ehrenberg, A.; Malmstrom, B.G.; Vanngard, T., Eds. (Pergamon: Oxford) pp. 221-247.

34. Wilcox, D.E.; Long, J.R.; Solomon, E.I. J. Am. Chem. Soc. **1984**, 106, 2186-2194.

35. Reinhammar, B.; Oda, Y. J. Inorg. Biochim. **1979**, 11, 115-127.

36. a. Aasa, R.; Branden, R.; Deinum, J.; Malmstrom, B.G.; Reinhammar, B.; Vanngard, T. FEBS Lett. **1976**, 61, 115-119.

b. Branden, R.; Deinum, J.; Biochim. Biophys. Acta **1978**, 524, 297-304.

37. Smith, T.D.; Pilbrow, J.R. Coord. Chem. Rev. **1974**, 13, 173-278.

38. Eaton, S.S.; More, K.M.; Sawant, B.M.; Eaton, G.R. J. Am. Chem. Soc. **1983**, 105, 6560-6567.

39. a. Hwang, Y.T., Ph.D. Thesis, Massachusetts Institute of Technology, Cambridge, Massachusetts, **1983**.

b. Hwang, Y.T.; Kau, L.S.; Solomon, E.I. to be published.

40. a. Fagen, L.Y.; Alben, J.O. Biochem. **1972**, 11, 4786-4792.

b. van der Deen, H.; Hoving, H. Biophys. Chem. **1979**, 9, 169-179.

41. Experimentally, protein solutions of laccase will not concentrate nearly as high as will those of hemocyanin, further decreasing the ability to observe a weak FT-IR signal.

42. Reinhammar, B. Biochim. Biophys. Acta **1972**, 275, 245-259.

43. Robin, M.B.; Day, P. Adv. Inorg. Chem. Radiochem. **1967**, 10, 245.

44. van der Deen, H.; Hoving, H. Biochem. **1977**, 16, 3519-3525.

45. Verplaetse, J.; Van Tournot, P.; Defreyn, G.; Witters, R.; Lontie, R. Eur. J. Biochem. **1979**, 95, 327-331.

46. Rotilio, g.; Morpurgo, L.; Graziani, M.T.; Brunori, M. FEBS Lett. **1975**, 54, 163-166.

47. Morpurgo, L.; Desideri, A.; Rotilio, G. Biochem. J. **1982**, 207, 625-627.

48. Wilcox, D.E.; Solomon, E.I. to be published.

49. Woolery, G.L.; Spiro, T.G.; Powers, L.; Winkler, M.E.; Solomon, E.I. J. Am. Chem. Soc. **1984**, 106, 86-92.

50. Himmelwright, R.S.; Eickman, N.C.; LuBien, C.D.; Solomon, E.I. J. Am. Chem. Soc. **1980**, 102, 5378-5388.

51. It should be noted that inductive effects of F^- on the uncoupled met-N_3^- sites at 10 K have been noted, but F^- does not compete with the coupled N_3^- binding at 298 K.

52. Thamann, T.J.; Solomon, E.I. to be published.

53. a. Karlin, K.D.; Hayes, J.C.; Hutchinson, J.P.; Zubieta, J. J.C.S. Chem. Comm. **1983**, 376-378.

b. Sorrel, T. personal communication.

c. McKee, V.; Dagdigian, J.V.; Bau, R.; Reed, C.A. J. Am. Chem. Soc. **1981**, 103, 7000-7001.

54. a. Solomon, E.I.; Dooley, D.M.; Wang, R.H.; Gray, H.B.; Cerdonio, M.; Mogno, F.; Romani, G.L. J. Am. Chem. Soc. **1976**, 98, 1029-1031.

b. Dooley, D.M.; Scott, R.A.; Ellinghaus, J.; Solomon, E.I.; Gray, H.B. Proc. Natl. Acad. Sci. USA **1978**, 75, 3019-3022.

55. Sigel, H.; McCormick, D.B. Accts. Chem. Res. **1970**, 3, 201-209.

56. The inductive effects noted at the met-N_3^- uncoupled site require two binding positions, but here, the additional coordination position has been provided through protonation and displacement of the endogenous bridge.

57. Jolley, R.L., Jr.; Evans, L.H.; Makino, N.; Mason, H.S. J. Biol. Chem. **1974**, 249, 335-345.

IV. TYPE 3 - TYPE 1 INTERSITE INTERACTIONS IN TYPE 2 DEPLETED AND NATIVE LACCASE

A. Introduction

In Chapter 3, T3-T1 allosteric interactions were used analytically to probe exogenous ligand reactivity at the deoxy and met T2D binuclear copper sites. In this chapter, the changes induced in the T1 Cu(II) by perturbation of the T3 copper site will be further studied. By systematically varying the T3 copper oxidation and ligation states and applying appropriate spectroscopic techniques, preliminary insight into the physical properties and biological activity of the laccase T1 Cu(II) is accessible. T2D laccase is the ideal derivative for directly probing T3-T1 intersite interactions in the multicopper oxidases, and when possible, these studies are being extended to the native enzyme, where the additional T2 copper center can further complicate the interpretation of spectral changes at the T1 Cu(II) site.

It should be noted that these studies are also important for their potential insight into the unique properties of the Blue copper site, that is, its intense blue color, small parallel hyperfine coupling constant, and unusually high redox potential. In the simpler Blue copper proteins, this site is not perturbed by exogenous anions, and only endogenous perturbations (i.e., isotope enrichment and substitution) can be used as spectroscopic probes.

Alternatively, a variety of changes are allosterically induced in the laccase T1 copper site by modification of the T3 (and T2) copper centers which are also present at the active site, and these interactions enable a systematic study of how specific changes in the geometric and electronic structure of the T1 site are manifested in their biological function.

B. Experimental

Native and T2D laccase were prepared as described in Chapter 2. EPR spectra of frozen solution samples at 77 K were collected on a Bruker ER 220D-SRC EPR spectrophotometer operating at 100 KHz modulation frequency, 10 mW incident power, 20 G modulation amplitude and ~9.27 GHz microwave frequency. All protein solutions are in 0.1 M potassium phosphate, pH 6.0 and utilized reagent grade chemicals without further purification. NaSCN(s) was added directly to the protein solutions. For the 298 K resonance Raman studies, protein samples were concentrated to ~0.6 mM by an Amicon concentrator (Amicon Corporation, Lexington, MA) with either a PM-10 or YM-10 membrane; a Micro-ProDicon concentrator (Biomolecular Dynamics, Beaverton, Oregon) further concentrated these samples to ~1.5 mM for the rR experiments at 10K. Protein integrity after laser irradiation was monitored by EPR spectroscopy.

All resonance Raman studies were performed by Dr. Arturo G. Porras. Protein samples in either the liquid or frozen states were irradiated with 50-100 mW of the 5682 A line of an Innova 90 Krypton laser (Coherent, Palo Alto, CA). The scattered light was collected with a Spex double monochromator (Spex Industries, Metuden, NJ) with slits set to a spectral band width of 2.5 cm^{-1}. The signals' intensities were determined by a Spex DPC2 photometer interfaced to a Nicolet 1180E computer (Nicolet Instruments, Madison, Wisconsin). Multiple scans (16-80) were collected for each spectrum and stored on disc.

Experiments at room temperature were run using 90° angle scattering with a spinning cell. Experiments at low temperature (15-77 K) were also performed using 90° angle scattering. The sample was held in a LTR liquid transfer Heli-tran refrigerator equipped with a specially designed[1] sample holder.

C. Results and Discussion

As first reported by LuBien et al,[2] the spectral features of the T1 copper change on oxidation of the T3 copper in T2D laccase. In the 298 K absorption spectrum, peroxide oxidation of the binuclear cuprous site in deoxy T2D results in a decrease of $\Delta \varepsilon \sim -600\ M^{-1}cm^{-1}$ in the 614 nm band

(ε = 5700 $M^{-1}cm^{-1}$), as the integrated EPR intensity remains constant. In the EPR (Figure 4.1), $A_{||}$ of the T1 Cu(II) increases from 37.8 to 42.9 X 10^{-4} cm^{-1} when deoxy is oxidized to met T2D, where the $A_{||}$ in met T2D is essentially indistinguishable from the $A_{||}$ -43 X 10^{-4} cm^{-1} observed in native laccase. These spectral changes indicate a structural change in the T1 Cu(II) site concomitant to the change in the oxidation state of the T3 copper site.

In collaboration with Dr. Arturo G. Porras, these changes have been further investigated through resonance Raman (rR) spectroscopy. By tuning the excitation laser wavelength into the intense blue copper absorption feature, only those vibrational modes associated with distortion of the excited electronic state relative to the ground state geometry are resonance enhanced. Resonance Raman spectroscopy is therefore a very sensitive and useful technique for selectively probing the vibrations directly associated with the T1 Cu(II) site. While detailed band assignments of the Blue copper site remains a subject of great controversy,[3] changes in these bands can be used to analytically probe structural changes in the T1 Cu(II) over a series of laccase derivatives.

In Figure 4.2 are shown the 298 K resonance Raman spectra of native, deoxy T2D and met T2D laccase forms. Upon

Figure 4.1 EPR spectra at 77 K: native, deoxy, and met T2D laccase.

The parallel hyperfine splittings are indicated.

Figure 4.2 Resonance Raman spectra at 298 K: native, deoxy, and met T2D laccase.

5682 Å excitation wavelength; 50-100 mW power, and 2.5 cm^{-1} spectral band width. (64 scans/ sample; [protein] ~0.6 mM)

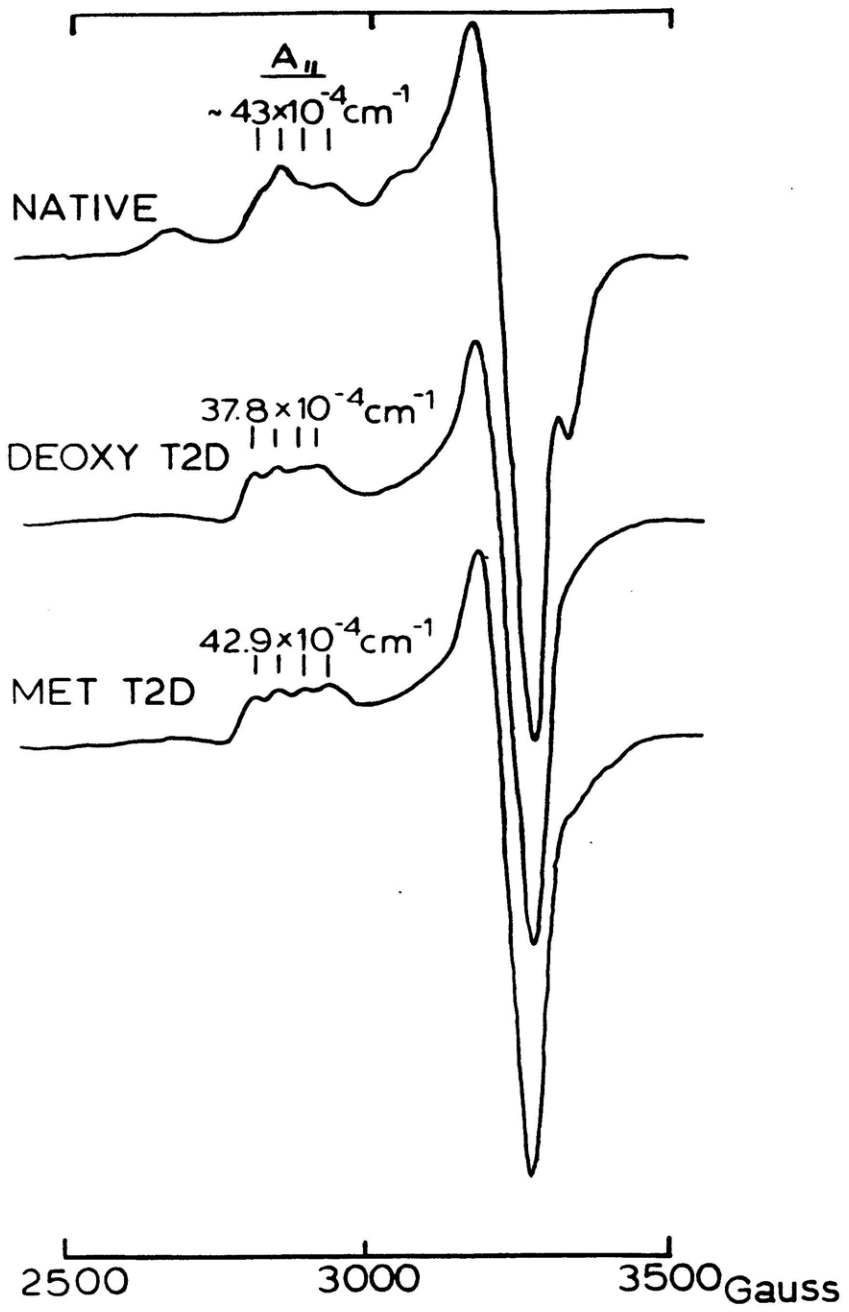
$A_{\parallel}$
~ 43x10^{-4}cm^{-1}
NATIVE
37.8x10^{-4}cm^{-1}
DEOXY T2D
42.9x10^{-4}cm^{-1}
MET T2D
2500
3000
3500 Gauss

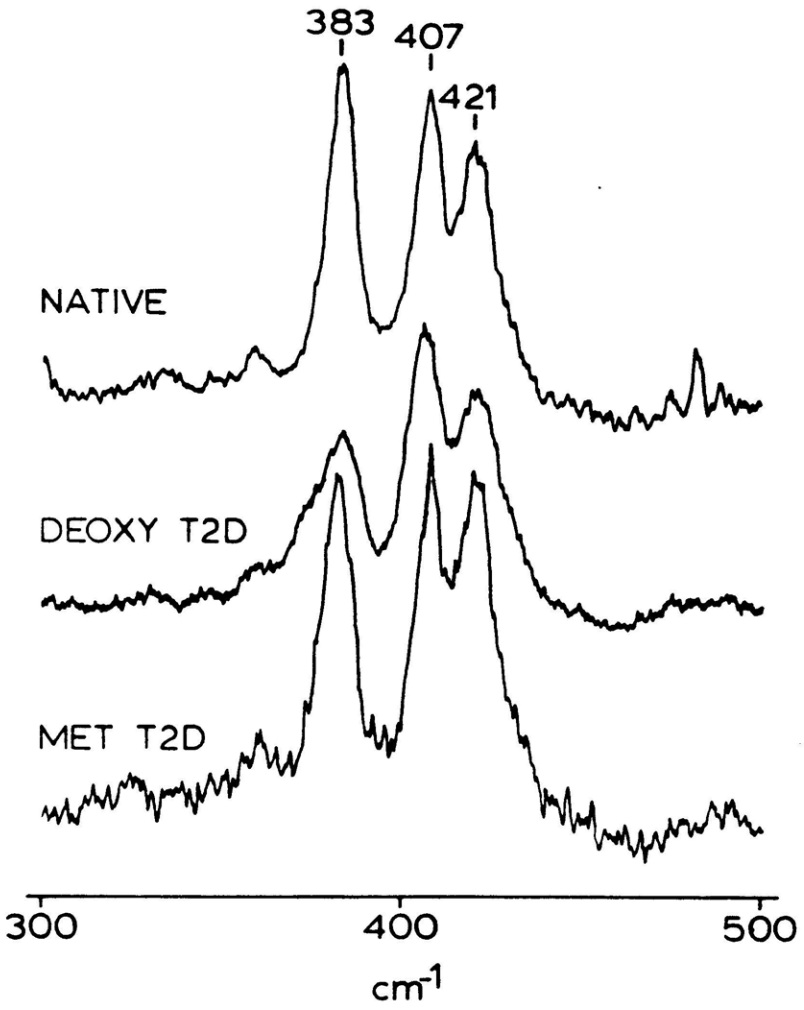
383
407
421
NATIVE
DEOXY T2D
MET T2D
300
400
500
cm-1

removal of the T2 Cu(II), the intensity of the 383 cm^{-1} peak decreases by ~60% relative to that of native laccase and a new shoulder appears to lower energy. However, peroxide oxidation of deoxy T2D results in a spectrum very similar to that of native laccase. Consistent with the related EPR data, Figure 4.2 would suggest that the change in the 383 cm^{-1} vibration is associated with the reduction of the T3 site rather than the absence of the T2 Cu(II). This data and its interpretation are in strong contrast with reports[4] of another research laboratory which claim that "three copper laccase may be heterogeneous with respect to the structure of the T1 site, where the 370 and 382 cm^{-1} vibrations would be due to two populations of enzyme molecules that are influenced in different ways by removal of the T2 copper".

As previous x-ray absorption edge data had demonstrated that native laccase contains 12% $\pm$ 3% reduced T3 sites (Chapter 2), these studies were extended to the peroxide-oxidized native laccase to determine whether analogous changes in the 383 cm^{-1} vibration would result from oxidation of the native T3 site. Similar to H_2O_2 reaction of deoxy T2D laccase, when H_2O_2 is added to native laccase a small decrease ($\Delta\varepsilon_{614}$ ~-300 $M^{-1}cm^{-1}$) is observed in the 614 nm feature.[5] As shown in the rR spectra in Figure 4.3, H_2O_2

Figure 4.3 Resonance Raman spectra at 298 K: peroxide reaction of native laccase.

(A) native;

(B) A, after reaction with 30 protein equivalents H_2O_2.

5682 Å excitation wavelength; 50-100 mW power, and 2.5 cm^{-1} spectral band width. (native, 64 scans/sample; native + H_2O_2, 80 scans/sample; [protein] ~0.6 mM)

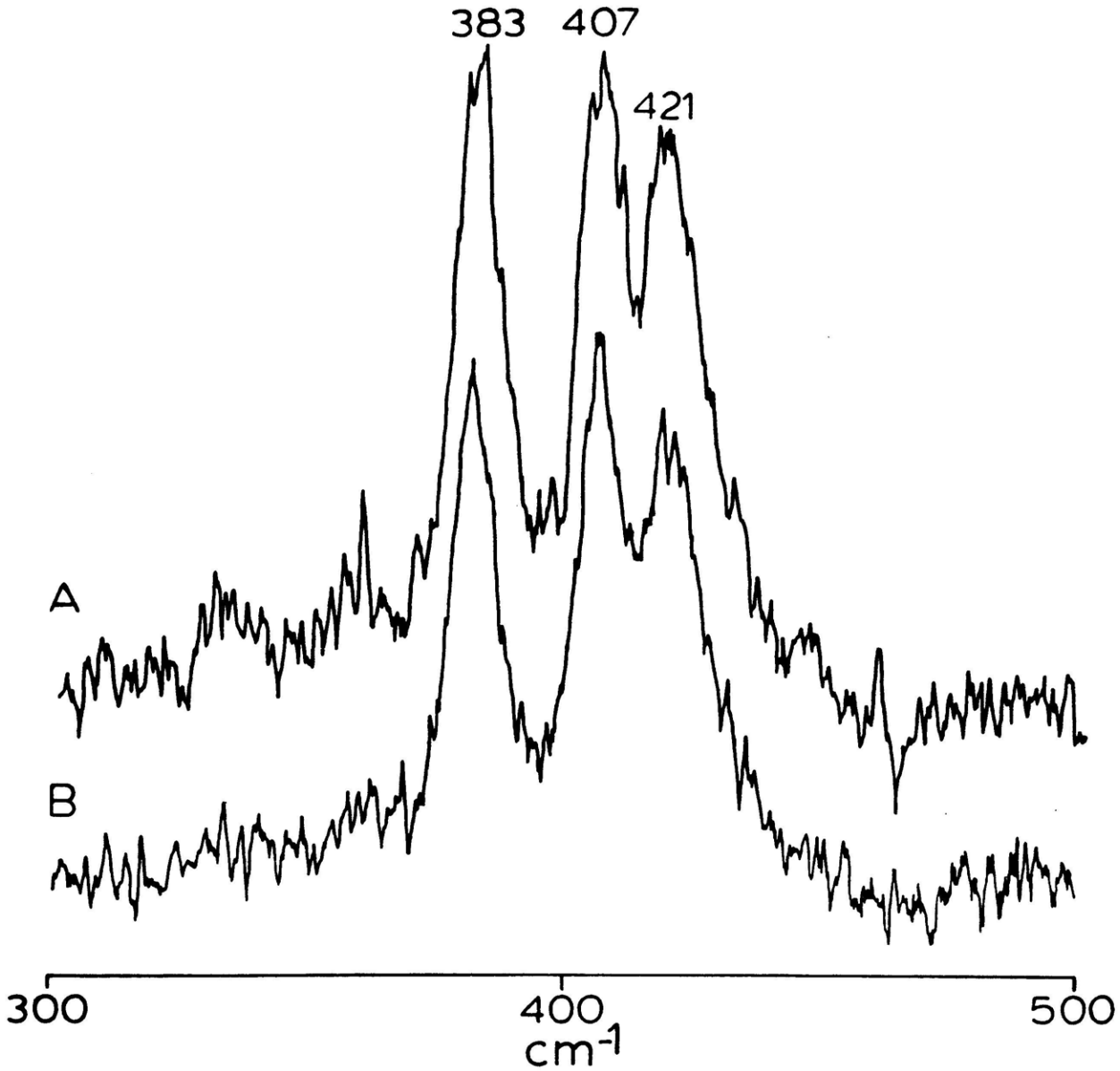
383
407
421
A
B
300
400
500
cm-1

does not further increase but rather decreases the relative 383 cm^{-1} peak intensity; this suggests that a peak is disappearing from the 383 cm^{-1} region with T3 oxidation. Interestingly, the resultant native + H_2O_2 spectrum is extremely similar to that of met T2D laccase (Figure 4.2). As H_2O_2 does not bind to native laccase, this change solely represents oxidative changes in ~12% of the native laccase active sites. That is, a theoretical spectrum for laccase molecules containing a reduced T3 site and oxidized T1 and T2 copper centers would exhibit a 383 cm^{-1} vibration which is significantly more intense than is the 407 cm^{-1} vibration. In this spectrum, the 383 cm^{-1} region would be very unlike that observed in deoxy T2D {T1:[Cu(II)]; T3:Cu(I)Cu(I)]} (Figure 4.2).

Thus, comparison of the deoxy T2D rR spectrum and the theoretical T3-reduced native spectrum indicates that the 383 cm^{-1} peak is composed of several overlapping vibrations. The observed changes in these vibrations may further suggest a major role for the T2 Cu(II) in modifying geometric and electronic structure at the T1 Cu(II) site when the T3 pair is reduced. Alternately, the similarity of the rR and EPR spectral features of the T1 Cu(II) in Native + H_2O_2 and met T2D would suggest that when the T3 pair is oxidized, it allosterically determines the structure of the T1 cupric site, essentially independent of the T2 center. It should be

noted that these studies of the native enzyme are in conflict with another literature report[4] which claims that H_2O_2 has no effect on the native laccase resonance Raman spectrum.

The ability to study the rR spectrum at both 298 K and 15 K has made rR spectroscopy an especially valuable link for the comparison of 298 K optical and low temperature EPR data. The 15 K rR spectra of deoxy and met T2D are shown in Figure 4.4. In both deoxy and met, a new shoulder is resolved at ~428 cm^{-1} and the relative 407/421 peak intensity increases, suggesting that a similar conformational change in the T1 site occurs upon cooling each of these derivatives. In addition, the peak and shoulder at 383 cm^{-1} in the 298 K data seem to coalesce at low temperature. The resulting deoxy and met spectra are much more similar to one another at 15 K than at 298 K. Consistent with these changes in the T1 site on cooling, a temperature dependence of the T1 Cu(II) EPR parameters in both T2D and native laccase has also been reported.[6] In these studies, the $A_{||}$ = 38 X 10^{-4} cm^{-1} at 77 K increases to 60 X 10^{-4} cm^{-1} at 298 K. Related resonance Raman studies[4] confirm that this change is associated with the absolute temperature range and not simply the act of freezing at 0°C.

A number of T1 Cu(II) perturbations have also been noted in exogenous ligand binding studies of T2D laccase (see

Figure 4.4 Resonance Raman spectra at 15 K: deoxy and met T2D laccase.

5682 Å excitation wavelength; 50-100 mW power, and 2.5 cm^{-1} spectral band width. (deoxy, 64 scans/sample; met, 46 scans/sample; [protein] ~1.5 mM)

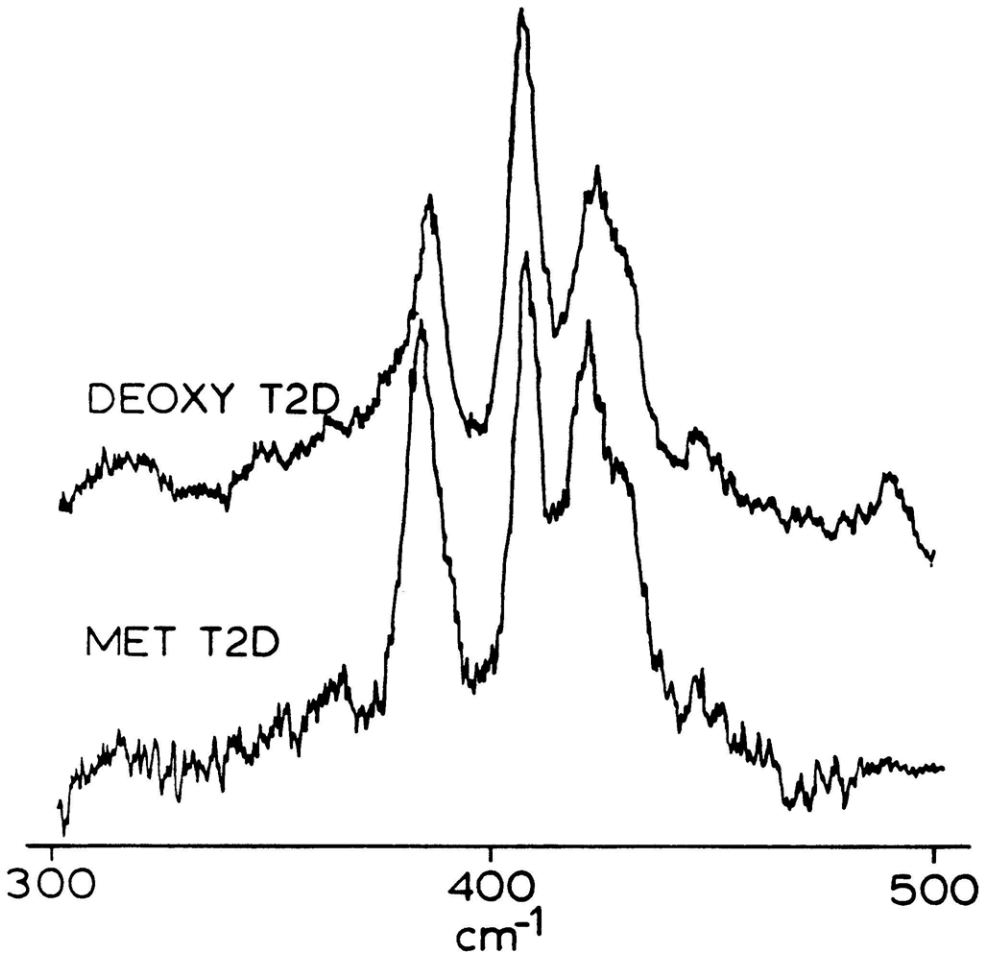
DEOXY T2D
MET T2D
300
400
500
cm-1

Chapter 3). In particular, NaSCN was noted to increase $A_{||}$ of the T1 Cu(II) to ~83 X 10^{-4} cm^{-1} at 77 K and to result in a more axial EPR spectrum for each of the T2D derivatives (Figure 4.5B and C). A similar change (Figure 4.5A) has been observed in the 77 K EPR spectrum of native laccase with no perturbation of the T2 Cu(II), suggesting that SCN^- was binding at the T3 site; the similarity of the spectral changes in T2D and native laccase further supports this interpretation. While a SCN^- ---> Cu(II) CT transition is observed in native laccase (Chapter 5) and assures that SCN^- is binding to a T3 (or T2) cupric center at 298 K, no such transitions are observed in met T2D laccase and only very weak changes are observed in the ligand field region of the corresponding CD spectrum. This suggested that SCN^- might be binding only at low temperature to T2D laccase derivatives.

In support of this interpretation, the 298 resonance Raman spectrum of met T2D shows no perturbation after treatment with excess SCN^-. However, upon cooling to 10 K (Figure 4.6), major changes are observed in the 400-430 cm^{-1} region relative to met T2D at the same temperature (Figure 4.4). At lower temperature, binding constants do increase, but in addition there appears to be a conformational change at the active site (Figure 4.2 vs. Figure 4.4) which may change the dielectric or accessibility of the T3 site so as to increase its affinity for exogenous ligands. While 15 K

Figure 4.5 EPR spectra at 77 K: SCN^- reactivity of native, deoxy and met T2D laccase.

All reactions are with ~150 protein equivalents NaSCN. The increased parallel hyperfine splittings are indicated. (9.26 GHz; [protein] ~0.6 mM)

Figure 4.6 Resonance Raman spectrum at 15 K: met-SCN^- T2D laccase.

5682 Å excitation wavelength; 50-100 mW power, and 2.5 cm^{-1} spectral band width. (64 scans/ sample; [protein] ~1.5 mM)

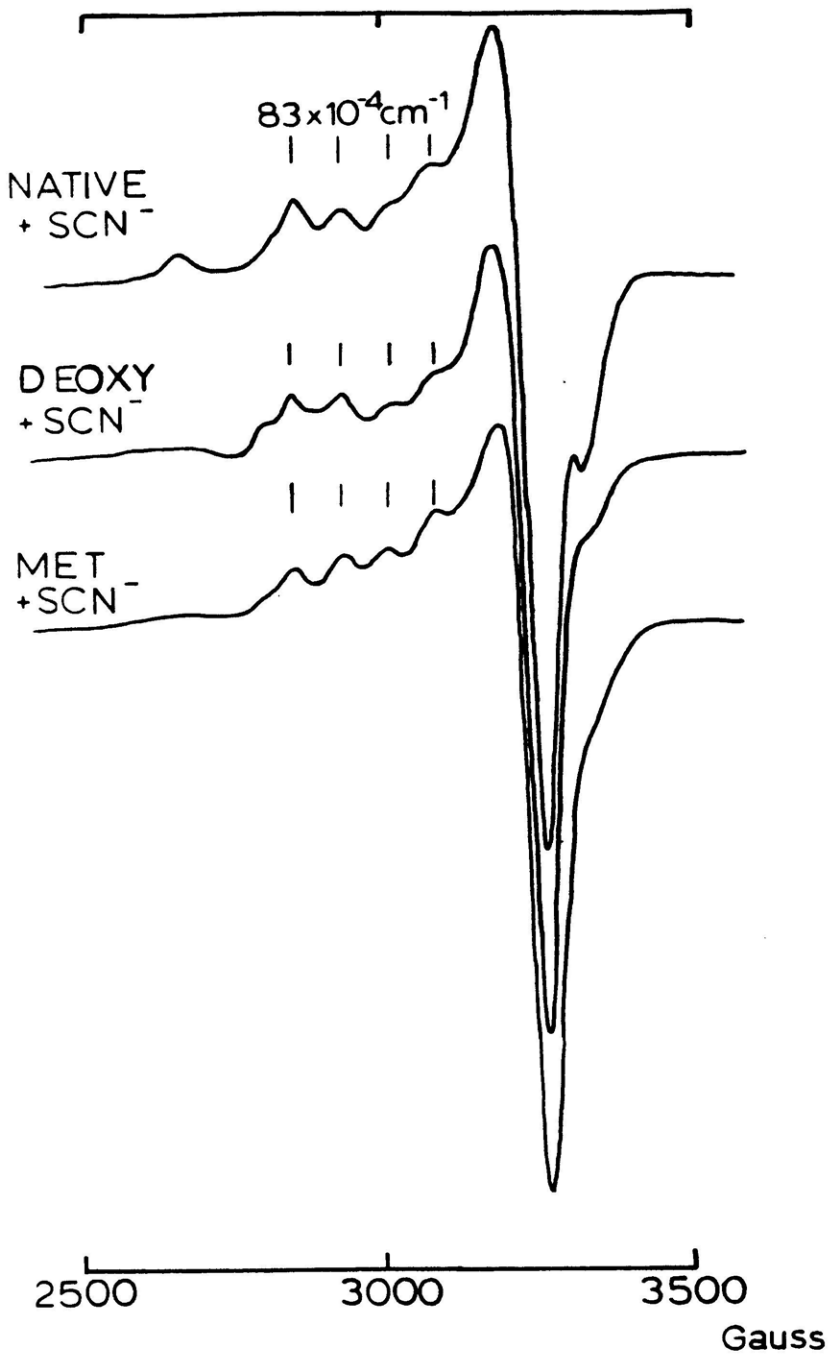
83x10⁻⁴cm⁻¹
NATIVE
+ SCN⁻
DEOXY
+ SCN⁻
MET
+ SCN⁻
2500
3000
3500
Gauss

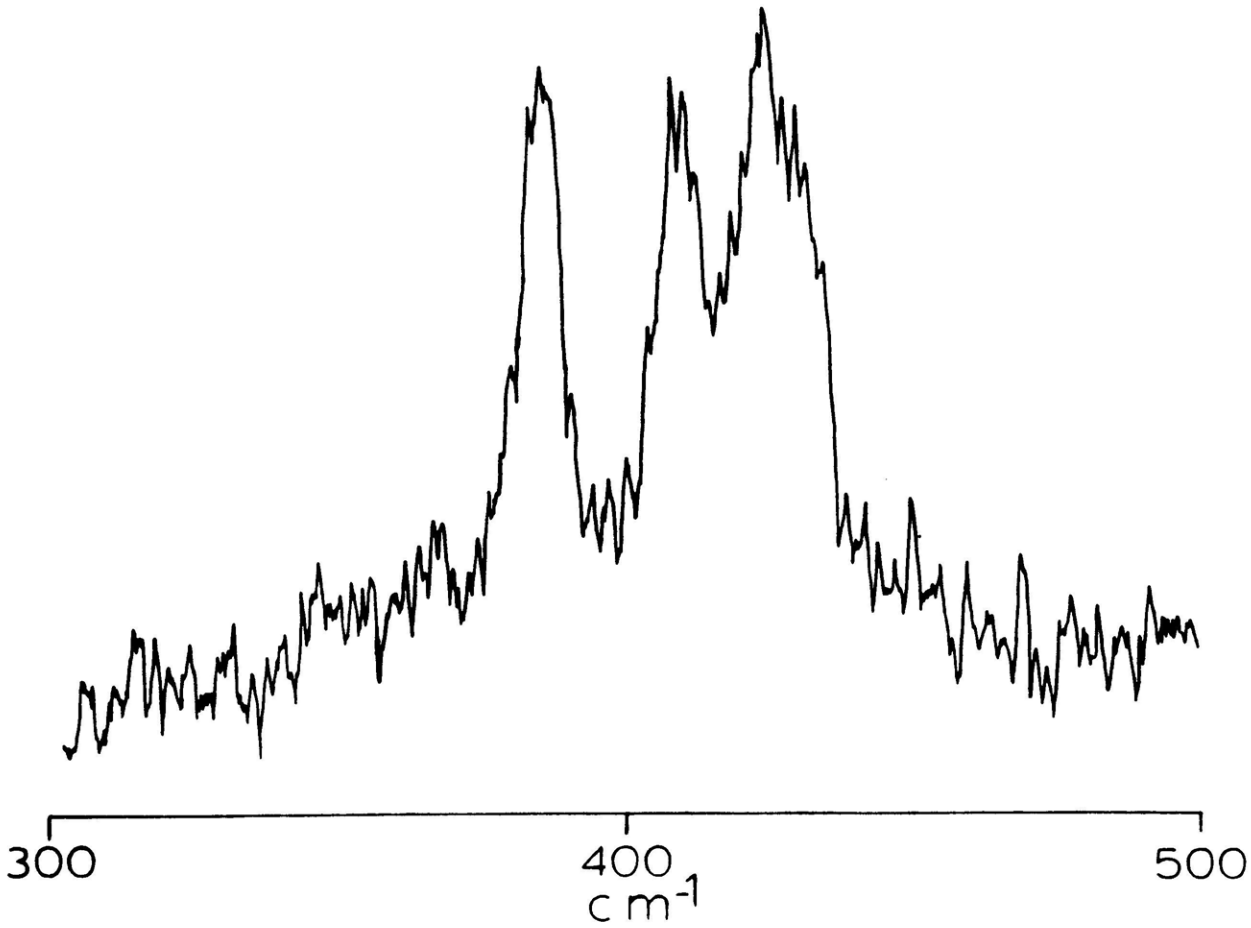
300
400
500
cm-1

data is not yet available for native laccase, SCN^- does bind to native laccase at 298 K and this resonance Raman data are shown in Figure 4.7. In comparison to the native laccase spectrum in Figure 4.2, the intensity of the 407 cm^{-1} peak is significantly increased relative to that at 383 and 421 cm^{-1}, and these changes are consistent with the observation of a SCN^- ---> Cu(II) CT feature at 298 K. While this Native + SCN^- spectrum is very different from the met SCN^- spectrum in Figure 4.6, the temperature variable prevents any direct comparison. It is interesting to note, however, that perturbations of the 407 cm^{-1} and higher energy peaks seem to be associated with exogenous ligand binding at the T3 site whereas the 383 cm^{-1} vibration appears most sensitive to oxidation state changes. Additional studies of the exogenous ligand perturbations described in Chapter 3 are clearly necessary before the electronic and geometric structural information contained in these T1 spectral changes can be realized.

In summary, however, from these preliminary studies of T2D laccase, it is clear that structural changes in the T1 Cu(II) are associated with changes in the oxidation and ligation states of the binuclear copper site. The resonance Raman studies indicate that the changes in the T1 site which are induced by oxidation of the T3 site are different from those induced by exogenous ligand interaction at that site.

Figure 4.7 Resonance Raman spectrum at 298 K: native + SCN^-.

5682 Å excitation wavelength; 50-100 mW power, and 2.5 cm^{-1} spectral band width. (64 scans/ sample; [protein] ~0.6 mM)

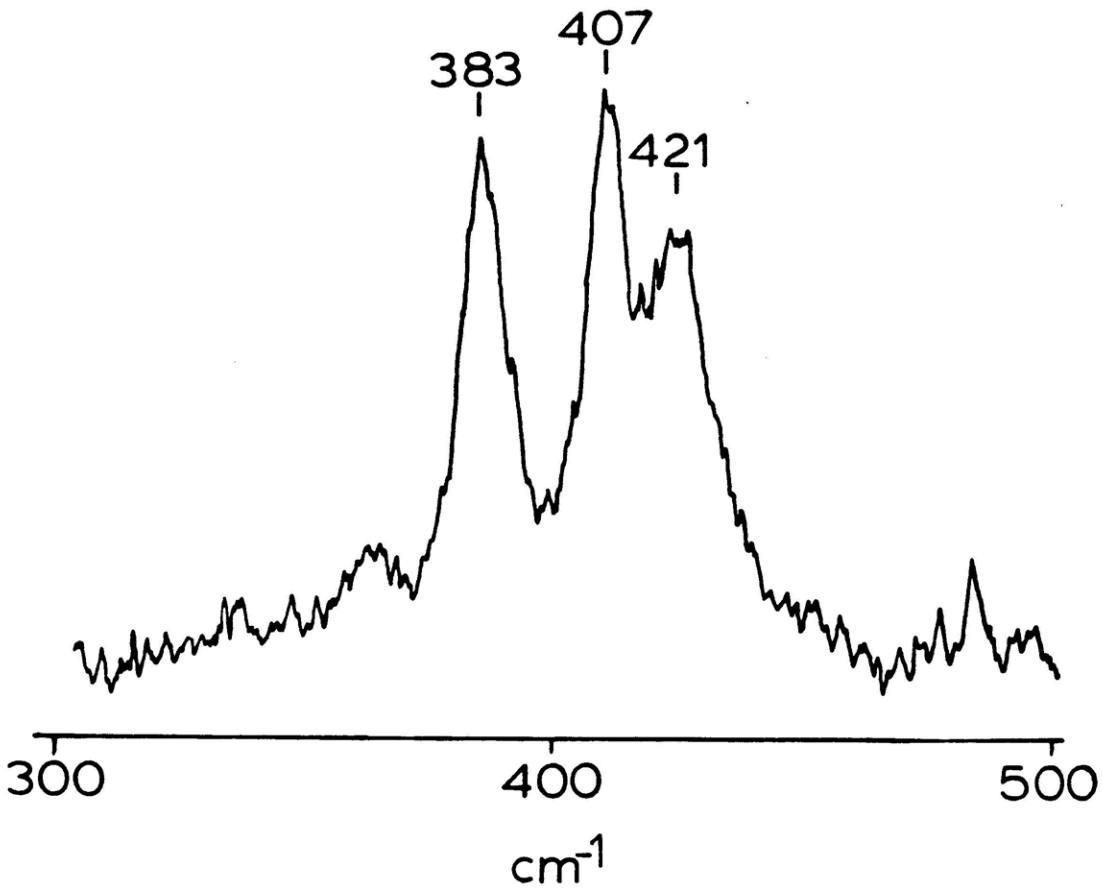
383
407
421
300
400
500
cm-1

Extensions to the native enzyme may further suggest a strong T2-T1 interaction when the T3 pair is reduced. These intersite interactions are important to the four-electron transfer which is necessary to catalytic function and require further study. Ultimately, these distortions may correlate to changes in T1 electrochemical potential as it relates both to the simple Blue copper proteins and intramolecular electron transfer in laccase.

References and Notes

1. Porras, A.G.; Solomon, E.I. to be published.
2. LuBien, C.D.; Winkler, M.E.; Thamann, T.J.; Scott, R.A.; Co, M.S.; Hodgson, K.O.; Solomon, E.I. J. Am. Chem. Soc. **1981**, 103, 7014-7016.
3. a. Siiman, O.; Young, N.M.; Carey, P.R. J. Am. Chem. Soc. **1974**, 96, 5583-5587.
   b. Miskowski, V.M.; Tang, S.P.W.; Spiro, T.G.; Shapiro, E.; Moss, T.H. Biochemistry **1975**, 14, 1244-1250.
   c. Siiman, O.; Young, N.M.; Carey, P.R. J. Am. Chem. Soc. **1976**, 98, 744-748.
   d. Ferris, N.S.; Woodruff, W.H.; Tennent, D.L.; McMillan, D.R. Biochem. Biophys. Res. Comm. **1979**, 88, 288-296.
   e. Thamann, T.J.; Frank, P.; Willis, L.J.; Loehr, T.M. Proc. Natl. Acad. Sci. USA **1982**, 79, 6396-6400.
   f. Woodruff, W.H.; Norton, K.A.; Swanson, B.I.; Fry, H.A. J. Am. Chem. Soc. **1983**, 105, 657-658.
   g. Nestor, L.; Larrabee, J.A.; Woolery, G.; Reinhammar, B.; Spiro, T.G. Biochem. **1984**, 23, 1084-1093.
4. Blair, D.F.; Campbell, G.W.; Lum, V.; Martin, C.T.; Gray, H.B.; Malmstrom, B.G.; Chan, S.I. J. Inorg. Biochem. **1983**, 19, 65-73.

5. In the native enzyme, it has not been shown whether this change is due to slight protein degradation with H_2O_2 or a reversible intramolecular intersite interaction.

6. Musci, G.; Desideri, A.; Morpurgo, L.; Garnier-Suillerot, A.; Tosi, L. Biochem. J. **1983**, 216, 503-506.

7. Morpurgo, L.; Calabrese, L.; Desideri, A.; Rotilio, G. Biochem. J. **1981**, 193, 639-642.

V. TYPE 3 - TYPE 2 ACTIVE SITE INTERACTION IN NATIVE LACCASE

A. Introduction

In preliminary studies of azide, peroxide, and fluoride binding to native laccase, a number of interesting spectral perturbations were observed. Titration studies indicated that each of these anions binds with unusually high affinity ($K_{eq} \geq 10^4\ M^{-1}$) at the laccase active site, and that both the T3 and T2 cupric centers are capable of binding exogenous ligands. A series of anion competition studies were pursued, and while the observed spectral changes were generally too complicated for interpretation, these extensive studies did suggest that ligands bound at the T2[Cu(II)] site could affect those supposedly bound at the T3[Cu(II)Cu(II)] site, and visa versa. Since these studies, native laccase has been demonstrated to contain ~25% reduced T3 sites (see Chapter 2) and this research would indicate that these partially reduced sites {T2:[Cu(II)]; T3:[Cu(I)Cu(I)]}, as well as the fully oxidized sites {T2: [Cu(II)]; T3: [Cu(II)Cu(II)]}, are capable of binding exogenous anions. Thus, having characterized the oxidation state composition of native laccase and its peroxide reactivity, many of the spectral perturbations observed in the ligand binding and competition studies are now understood (Part 1). Further, a combination of variable temperature Magnetic Circular Dichroism (MCD), 77 K absorption and 10 K EPR studies have defined the detailed nature of N_3^- interaction at the laccase

active site (Part 2). These studies indicate that it is inadequate to describe laccase as containing separate T3 and T2 copper sites, but rather a newly defined "three copper active site" which binds exogenous ligands.

B. Experimental

Native laccase was purified as described in Chapter 2. Many of the experiments in Part 1 of this chapter were originally performed by Dr. Cynthia LuBien in 1981.[1] Optical spectra were recorded on either a Cary 14 or Cary 17 spectrophotometer, and EPR spectra at 77 K were recorded using a Varian E-9 EPR spectrophotometer.

All of the studies in Part 2 of this chapter are of frozen glycerol glasses. At pH 6.0, the buffer was 50% v/v glycerol/0.1 M potassium phosphate and at pH 4.6, 50% v/v glycerol/0.1 M sodium acetate. Routinely, the protein solutions were concentrated to ~0.4 mM by Amicon (Amicon Corporation, Lexington, MA) using a YM-10 or PM-10 membrane. This protein was then dialyzed 12-16 hours into the appropriate 50% glycerol buffer, which further concentrated the sample to ≥1 mM. For a given titration experiment, this protein was divided into 300-400 μL aliquots, and 5μL of N_3^- solution (of appropriate N_3^- concentration in pure buffer) was added to each sample. These solutions were then

incubated for a minimum of 16 hours at 4°C at which point 298 K and 77 K optical spectra were recorded.

Each sample was injected between two quartz disks spaced by a rubber gasket; a micrometer measured the exact pathlength (generally 1.4-1.5 mm) of each sample for accurate spectral comparisons. The sample was mounted on the sample holder of an Air Products LT-3-110 Heli-tran liquid helium transfer cryotip sample holder. The cryotip was then fixed in the sample compartment of a Cary 17 spectrophotometer. It was evacuated to a pressure of ~9 X 10^{-6} torr using either a Pfeiffer turbomolecular or Edwards High Vacuum, Inc. (Grand Island, NY) pumping system. A Lakeshore Cryotonics, Inc. Cryogenic Model DTC-500 allowed variation of the sample temperature from 300-80 K. While a room temperature glycerol baseline was recorded in the cryotip sample holder and indicates the baseline shape, absorption due to random cracks in the glycerol glass shift the 80 K baseline and prevent its absolute determination. In order to approximate the baseline position (the shape was generally independent of freezing), the cryotip spectra were recorded out to 1200 nm at both 298 K and 80 K, and compared to their analogous spectra recorded in 2 mm quartz cells for which the relative baseline position is known. The cryotip baseline position was then floated until absorbance ratios throughout the cryotip spectra best mimicked those observed in the 2 mm

cells. Finally, as the 80 K spectra show little N_3^- dependence between 1000 and 1200 nm, these spectra were qualitatively aligned at these wavelengths which then resulted in "reasonable" spectral changes in the visible spectral region. Expanded scale absorption measurements were obtained on a Varian 2300 spectrophotometer. All gaussian band simulations were performed on a Nicolet 1180E computer.

EPR spectra were recorded on a Bruker ER 220 D-SRC spectrometer operating at ~9.39 GHz. An Air Products LTD-3-110 Helitran liquid helium transfer refrigerator and the Lakeshore temperature controller maintained samples at 8 K.

In collaboration with Mark D. Allendorf, MCD spectra were recorded on a Jasco J-500 C spectropolarimeter utilizing an Oxford Instruments SM4 superconducting magnet/cryostat, which produces fields up to 60 kg. Samples were mounted in cells consisting of a rubber gasket (1.5 mm thick) sandwiched between two quartz disks (0.75 mm thick, each). Solutions were injected into the cell using a hypodermic syringe (an additional needle was inserted in order to provide an air vent). Path lengths were determined using a micrometer. Glasses were formed by insertion of the sample rod into the sample bore of the cryostat, containing 1-2" of liquid helium. Lowering of the sample into the helium at a rate

such that the temperature dropped ~1 K/second gave the best glasses (this generally required about 2 1/2 - 3 minutes).

Depolarization due to mechanical strain in the glass was measured and corrected for by recording the CD of nickel tartrate placed before and after the sample (zero magnetic field). Sample temperatures were measured with a carbon glass resistor, calibrated from 1.5-300 K by Cryogenic Calibrations, Pitchcott, Aylesburg, Bucks., U.K. This sensor was placed as close to the sample as possible, being about 4 mm above it in the copper sample block. The temperature was maintained by an Oxford Instruments DTC-2 temperature controller connected to a Rh/Fe resistance thermometer. All spectra were digitized using a Houston Instruments Hipad digitizer and entered into a DEC PDP-1124 computer for baseline subtraction and conversion of intensities to $\Delta\varepsilon$ ($M^{-1}cm^{-1}Kg^{-1}$) from millidegree values obtained from the spectrometer. Positive $\Delta\varepsilon$ values correspond to left-right circularly polarized light.

C. Results and Discussion

1. Anion Binding and Competition Studies of Native Laccase

Peroxide addition to native laccase at pH 6.0 (Figure 2.10) causes a limited increase in the absorption and

CD spectra at ~330 nm ($\Delta\varepsilon$ 800 M^{-1}, $\Delta(\Delta\varepsilon) < |0.7| M^{-1}cm^{-1}$) and small changes in the optical spectra at 614 nm; the EPR spectrum is not perturbed.[2] Through difference x-ray absorption edge analysis of native laccase and native laccase treated with H_2O_2, the native enzyme was demonstrated to contain ~25% reduced T3 sites (Figure 2.13). Oxidation of these reduced sites accounts for essentially all of the aforementioned optical changes, leaving no evidence for peroxide binding to native laccase ($K_{eq} < 10^2 M^{-1}$). Prior to the XAS edge studies and based on numerous research reports by Farver, et al.[3] it was believed that peroxide bound to the laccase T3 site ($K_{eq} > 10^8 M^{-1}$ at pH 7.0) and formed a μ-1,2 peroxylaccase complex, similar to oxyhemocyanin.[4] Thus, with this demonstration that peroxide is acting as an oxidant but not a ligand at the T3 site, many of the previous chemical and spectral studies of native laccase can be clarified.

At pH 6.0, fluoride reacts with native laccase[1,5] (Figure 5.1) as characterized by an increase in absorbance at 320 nm ($\Delta\varepsilon \sim 1000 M^{-1}cm^{-1}$) with a concomitant decrease at 390 nm ($\Delta\varepsilon \sim -400 M^{-1}cm^{-1}$); the isosbestic point occurs at 345 nm. From the intensity increase at 320 nm, two fluorides bind with high affinity ($K_1 \sim 40{,}000 M^{-1}$, $K_2 \sim 5000 M^{-1}$) and coordinate equatorially to the T2 Cu(II), as evidenced by triplet superhyperfine splitting (^{19}F: I = 1/2) of the T2 EPR signal (Figure 5.2). Both fluoride ions bind with much

Figure 5.1 Electronic absorption spectra[1] at 298 K: F^- titration of native laccase.

The protein equivalents of F^- are indicated for each spectrum. ([protein] ~0.16 mM)

Figure 5.2 EPR spectra[1] at 77 K: F^- titration of native laccase.

(A) original native laccase at pH 6.0;

(B) after reaction with 10 and

(C) 150 protein equivalents KF.

The primed spectra were recorded at ~4X higher gain. ([protein] ~0.16 mM)

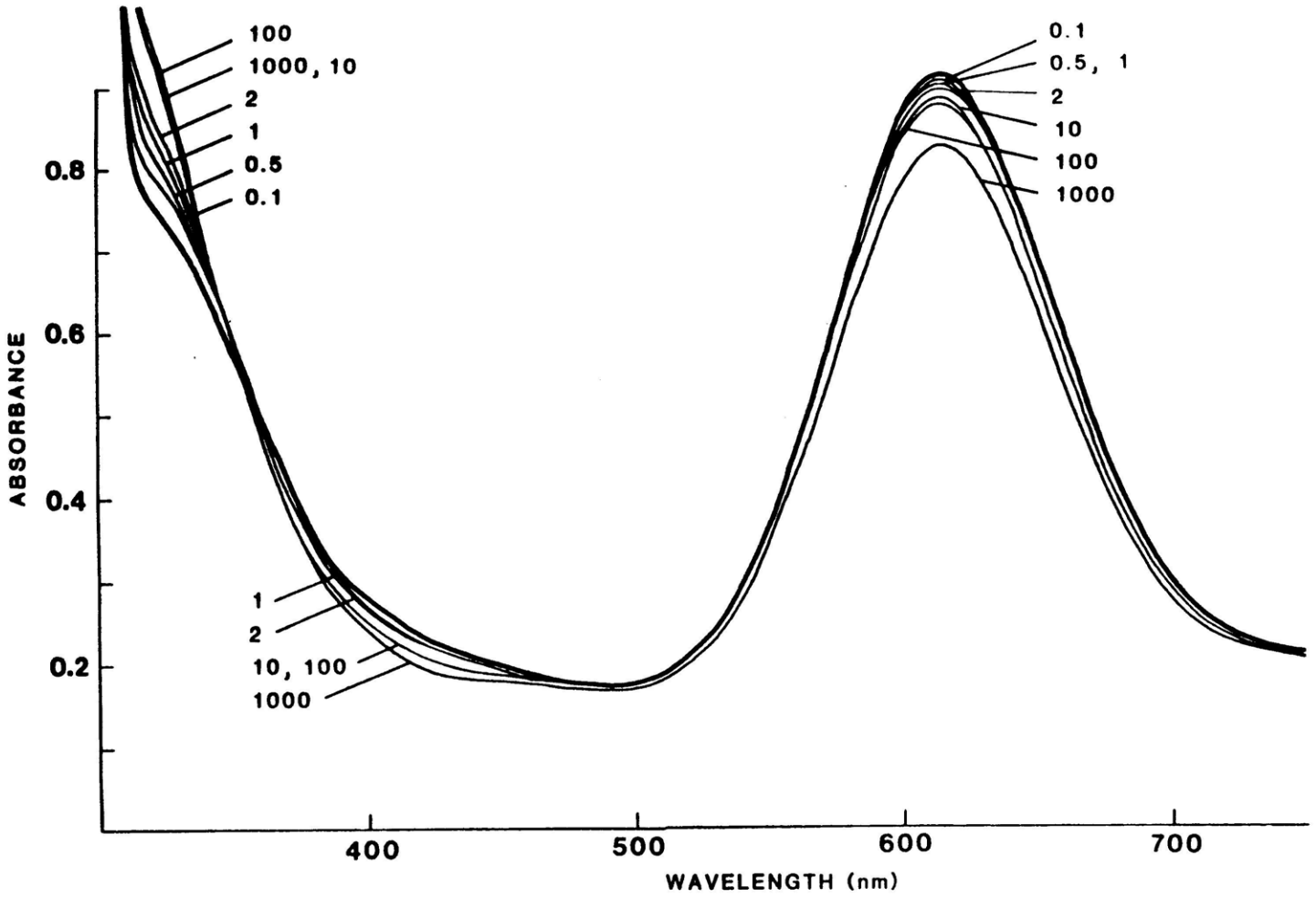
100
1000, 10
2
1
0.5
0.1
0.1
0.5, 1
2
10
100
1000
1
2
10, 100
1000
0.8
0.6
0.4
0.2
ABSORBANCE
400
500
600
700
WAVELENGTH (nm)

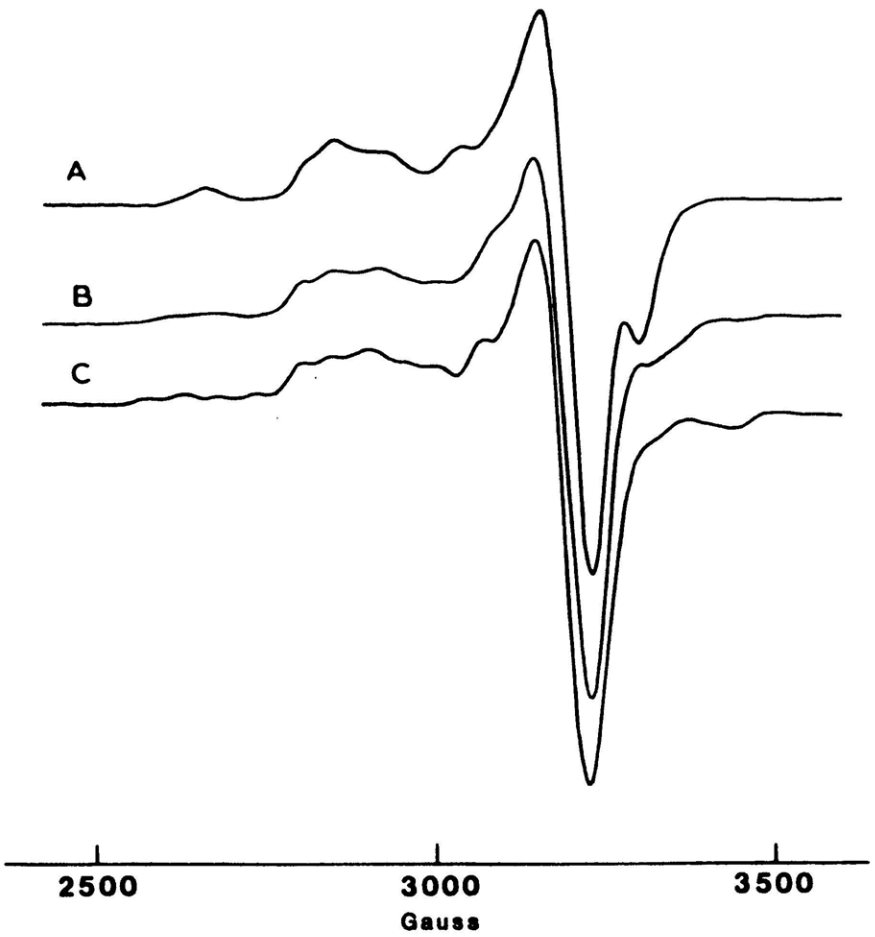
A
B
C
2500
3000
3500
Gauss

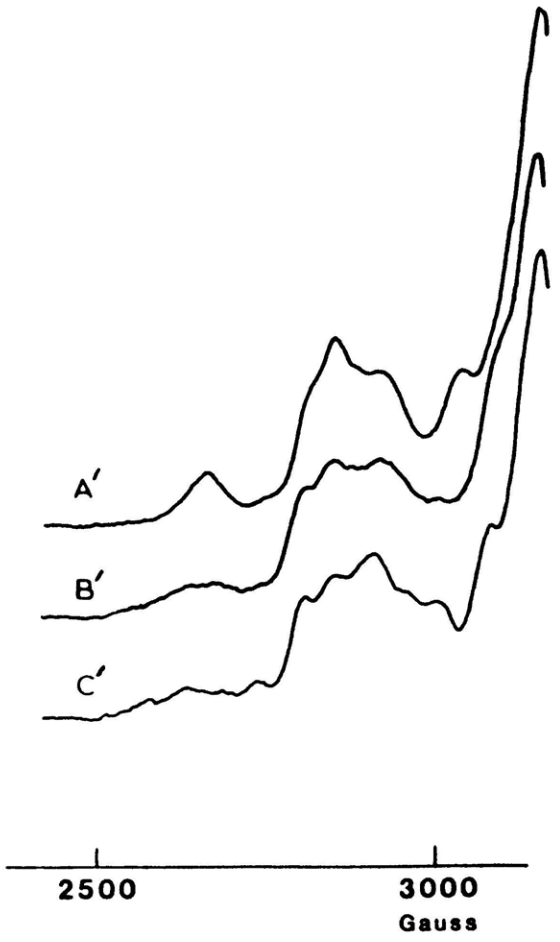
A′
B′
C′
2500
3000
Gauss

higher affinity to laccase than to galactose oxidase[6] or aqueous Cu(II) model complexes ($K < 10\ M^{-1}$). F^- does not appear to bind to met T2D laccase. While two F^-'s bind to the T2 site, the apparent "sharpening" of the T3 optical feature suggests that the T3 site may also be affected by F^-.[7]

When fluoride reacts with peroxide-oxidized laccase, triplets are still observed in the EPR spectrum and are more clearly defined, demonstrating that the T2 Cu(II) in the fully oxidized site is binding two fluorides; that is, the changes observed for fluoride reaction with native laccase are not due to F^- binding singly to the inequivalent T2 Cu(II)'s in the presence of reduced and oxidized T3 sites, respectively. From N_3^-/F^- competition studies (vide infra), F^- does not appear to bind to T2 Cu(II) in the presence of reduced T3 sites.

The highly resolved EPR features associated with fluoride binding to peroxide oxidized native laccase are shown in Figure 5.3. From the superhyperfine splitting, the average covalency of the Cu-F bonds and their relative F^- 2s/2p character can be estimated.[8] Fermi contact, dipolar coupling, and indirect dipolar coupling all contribute to the superhyperfine coupling constant:

Figure 5.3 EPR spectra at 77 K: F^- superhyperfine in native laccase.

(A) native laccase after reaction with 30 protein equivalents H_2O_2, dialyzed;

(B) after reaction with 150 protein equivalents KF. The superhyperfine splittings are indicated.

(9.27 GHz,; [protein] = 0.352 mM)

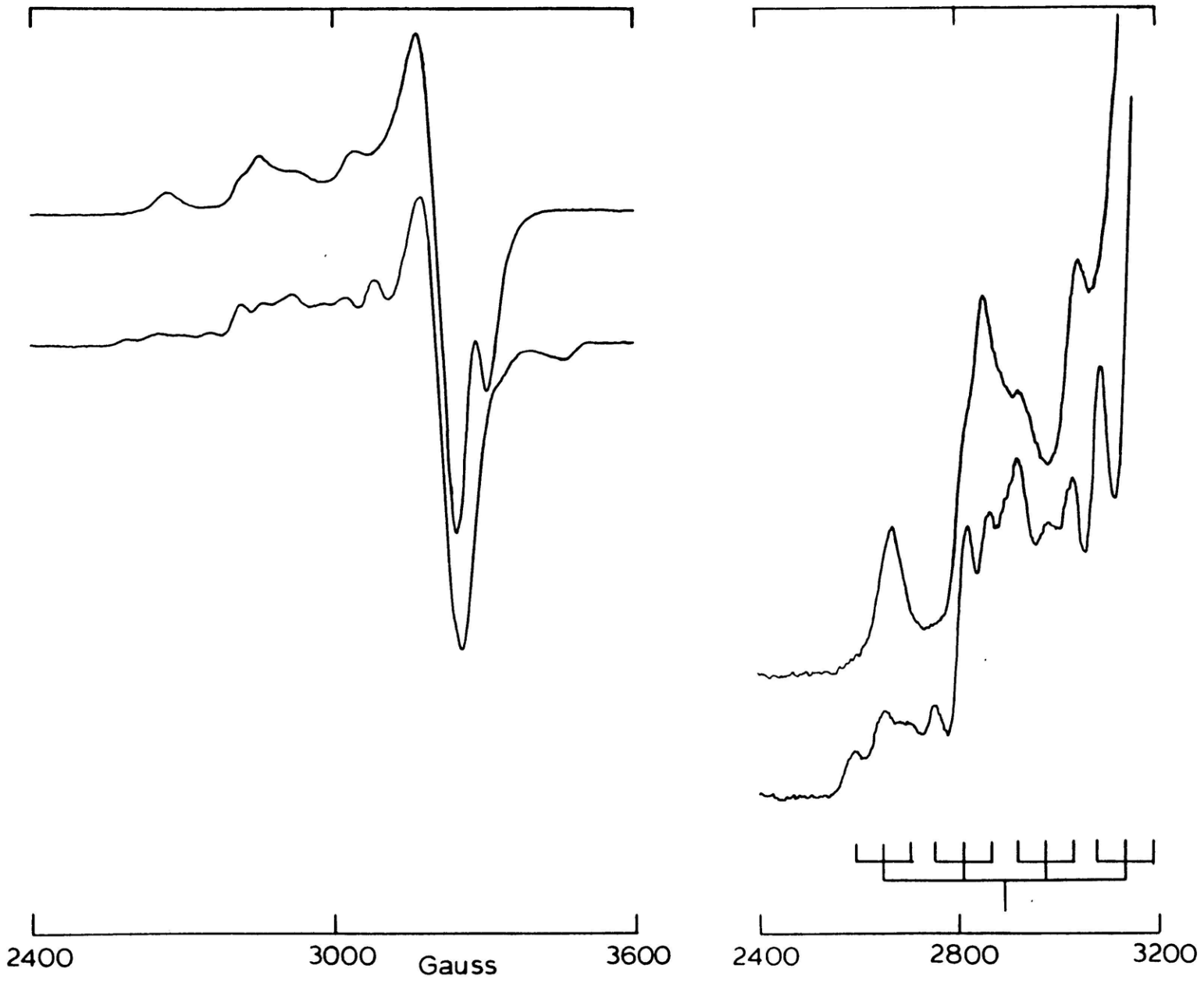
2400
3000
Gauss
3600
2400
2800
3200

$$A_{SHF} = A_{FC} + A_{DIP} + A_{ID}.$$

Fermi contact interaction is purely isotropic and proportional to the unpaired electron density at the nucleus. Direct Fermi contact can therefore only occur for an electron in an s orbital, although indirect Fermi contact hyperfine contribution can also arise from the exchange interaction between valence and core electrons. That is, the unpaired electron in the dx^2-y^2 orbital can polarize the spin of the $(1s)^2$, $(2s)^2$, and $(3s)^2$ core electrons. The dipolar interaction term is due to the classical interaction of the dipoles associated with the electron and nuclear spins ($\vec{\mu}_e = g_e\beta_e\vec{s}$, $\vec{\mu}_N = g_N\beta_N\vec{I}$) interacting at a distance r and is purely anisotropic. Finally, the nuclear spin of the metal can also dipole couple with the orbital angular momentum of the electron. This indirect dipole term has both anisotropic and isotropic components, and is a function of the experimental g values.

These three interactions determine the superhyperfine coupling constant for an unpaired electron in a dx^2-y^2 orbital. However, covalent delocalization of the unpaired electron onto the F^- ligands must also be considered. While the indirect dipolar term already includes covalency in that it is based on the experimental g values, both the Fermi contact and dipolar terms assume that the electron occupies a

pure Cu(II) dx^2-y^2 orbital. In reality, the dx^2-y^2 orbital is mixed with the ligand s and p orbitals such that the molecular orbital for the half occupied $^2B_{1g}$ ground state is of the form

$$\Phi(b_{1g}) = C_M\Phi(dx^2-y^2) + C_L\Phi(L);$$

therefore, the observed F^- superhyperfine coupling constant can provide an estimate of electron delocalization onto the ligands.

The superhyperfine coupling constant is generally anisotropic, where the z axis for each ligand refers to the specific M-L axis and not the molecular axis of the complex. Hence, $A_{||}^F$ is the superhyperfine splitting observed when the magnetic field is along the Cu-F axis and $A_{\perp}^F$ is the splitting observed due to the fluoride nucleus when the magnetic field is perpendicular to the Cu-F bond. As described by Goodman and Raynor,[9] the point dipole approximation can be used to calculate the dipolar contribution to the superhyperfine coupling constant

$$A_{DIP} = \frac{g_e\beta_e g_N\beta_N(3\cos^2\theta-1)}{r^3}$$

When H is parallel to the Cu-F bond, $\theta = 0°$ and

$$A_{DIP,||} = 2\,\frac{g_e \beta_e g_N \beta_N}{r^3};$$

likewise, when H is perpendicular to the Cu-F bond, $\theta = 90°$ and

$$A_{DIP,\perp} = -\,\frac{g_e \beta_e g_N \beta_N}{r^3}$$

where g_e = free electron g value, β_e = the Bohr magneton and β_N = nuclear Bohr magneton. For the F^- ion, $\mu_N = g_N \beta_N I = 2.63\ \beta_N$ and $I = 1/2$, so $g_N \beta_N = 5.26\ \beta_N$. Using the equatorial Cu-F bond distance = 2.0 Å determined by the crystal structure of copper hexafluoride[10] as an estimate for the T2 Cu-F distance in laccase, $A_{DIP,||} = 6.2 \times 10^{-4}\ cm^{-1}$ and $A_{DIP,\perp} = -3.1 \times 10^{-4}\ cm^{-1}$. This contribution will be subtracted from the experimental superhyperfine coupling constants to obtain the overlap-related contributions to the superhyperfine constant.

As previously mentioned, bonding interactions with the fluoride ligands produce a molecular orbital

$$\Phi(b_{1g}) = C_{Cu}\,\phi(dx^2\text{-}y^2) + C_F\,\phi(F^-).$$

C_M and C_F are related by the normalization condition $(C_{Cu})^2$ +

$(C_F)^2 + 2(C_{Cu})(C_F)S_{(\phi dx^2-y^2, \phi)^F} = 1$. With two equatorial F^-'s bound, covalent interactions result in unpaired electron density equal to $C_F^2(1/\sqrt{2})^2$ in each F^- 2pz orbital. Further, sigma bonding to the copper will result in a small fraction (n^2) of F^- 2s mixed into the F^- 2pz such that the $F^-\sigma$ 2pz is actually equal to $(1-n^2)F^-2pz + (n^2)F^-2s$. One unpaired electron in a $F^-\sigma 2pz$ orbital will then have two contributions to its hyperfine splitting: $(n^2)A^F iso$ due to direct Fermi contact associated with the 3s mixing, and $(1-n^2)A^F aniso$ $(3\cos^2\theta-1)/2$ due to dipolar coupling of the F^- nuclear spin with the unpaired electron averaged over the F^- 2pz orbital. Thus, the total covalent contributions to the superhyperfine coupling constants for the tetragonal $^2B_{1g}$ ground state are given by[8]

$$A_{||}^F = (C_F)^2(1/2)[n^2 A^F iso + (1-n^2)A^F aniso].$$

$$A_{\perp}^F = (C_F)^2(1/2)[n^2 A^F iso - 1/2(1-n^2)A^F aniso]$$

For F^-, $A^F iso \approx 1.57$ cm^{-1} and $A^F aniso \approx 0.088$ cm^{-1}.[11] From Figure 5.3, $A_{||}^F$ and $A_{\perp}^F$ are experimentally determined to be $|129| \times 10^{-4}$ cm^{-1} and $|59| \times 10^{-4}$ cm^{-1}, respectively. Subtraction of the calculated dipolar contribution gives

$$A_{||}^F = 0.0123 \text{ cm}^{-1} = C_F^2/2[(n^2 \cdot 1.57) + (1-n^2)(0.088)] \text{ cm}^{-1}$$

$A_{\perp}^{F} = 0.0056\ cm^{-1} = C_F^2/2[(n^2\ 1.57) - 1/2(1-n^2)(0.088)]\ cm^{-1}$.

Simultaneously solving these equations, the experimental superhyperfine splitting gives $C_F^2 = 0.112$, $n^2 = 0.0895$ and $(1-n^2) = 0.9105$. That is, each Cu-F bond is ~5.6% covalent, and there is $n^2/1-n^2 = 9.8\%$ s character contributing to each of the Fσ 2pz orbitals. Qualitatively, this significant an amount of covalency requires that the equivalent F^-'s both coordinate equatorially at the T2 Cu(II) site. A quantitative evaluation of this covalency and s/p mixing, calibrated by structurally defined copper model complexes, may further provide a probe of the interaction of the F^- bound to the T2 Cu(II) with the T3 [Cu(II)Cu(II)] site, and the relative contribution of this interaction to the observed high affinity binding constant (Part 2).

As first reported by Morpurgo et al. in 1974,[12] azide binds to native laccase producing N_3^- ---> Cu(II) CT bands at ~400 and 500 nm at low $[N_3^-]$ and an additional feature at 410 nm with excess N_3^-. These CT features (Figure 5.4) were further characterized at pH 6.0 by LuBien[1] and Winkler[13] who determined that $K_1 = 60{,}000\ M^{-1}$ at 500 nm, $\Delta\varepsilon = 500\ M^{-1}cm^{-1}$ and $\Delta\varepsilon_{410} = 630\ M^{-1}\ cm^{-1}$, and $K_2 = 60\ M^{-1}cm^{-1}$ at 400 nm, $\Delta\varepsilon = 1900\ M^{-1}cm^{-1}$. The high affinity binding constant is extremely large and very unusual for N_3^- binding to Cu(II). In both met T2D laccase and met mollusc hemocyanin, $K_{N_3^-} \sim 200\ M^{-1}$ (Chapter 3). As the T2 Cu(II) EPR spectrum was reported

Figure 5.4 Electronic absorption spectra at 298 K: high and low affinity N_3^-.

(———) native laccase;

(– – – –) high affinity N_3^- (8 protein equivalents);

(—·—·—) low affinity N_3^- (165 protein equivalents).

([protein] = 0.202 mM)

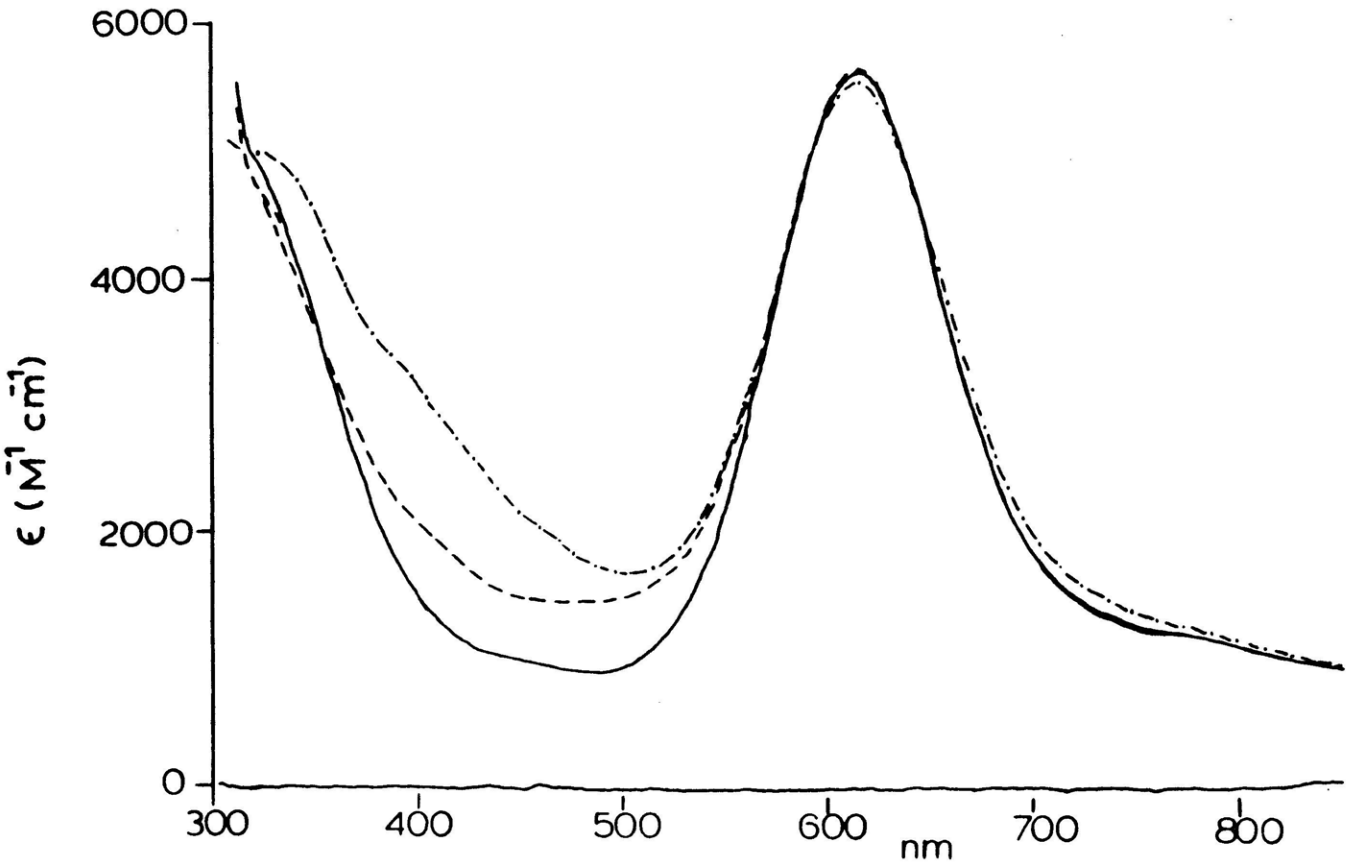
6000
4000
2000
0
ε (M⁻¹ cm⁻¹)
300
400
500
600
700
800
nm

to change only on binding the second N_3^-, it was suggested that the higher affinity N_3^- was binding at the T3 site while the lower affinity N_3^- was bindng to the T2 site. While detailed studies of these N_3^- ---> Cu(II) CT transitions comprise part 2 of this chapter, the complicated spectral features observed[1] in "N_3^-/O_2^{2-} competition studies" can now be readdressed.

When a small excess of N_3^- ($\leq$10X at $\leq$0.2 mM protein) is added to oxidized native laccase (in 30X H_2O_2), the resulting spectral features are very different from those of high affinity N_3^- bound to native laccase. As shown in Figure 5.5, the absorption band at ~500 nm is greatly enhanced (K = 6600 M^{-1}), $\Delta\varepsilon \sim 1300\ M^{-1}cm^{-1}$) with an accompanying decrease at 330 nm (K ~6100 M^{-1}, $\Delta\varepsilon \sim 1200\ M^{-1}cm^{-1}$). In addition, significant change in the T2 Cu(II) EPR signal is observed (Figure 5.6), also in contrast to the reaction of < 10X N_3^- on native laccase. These unique spectral changes were originally thought to represent a ternary complex wherein N_3^- and O_2^{2-} were both bound to the active site with high affinity; moreover, this chemistry was interpreted as strong evidence that peroxide <u>did</u> indeed bind to the laccase active site, despite the dissimilarity of the associated optical changes for peroxide reaction of native laccase compared to oxyhemocyanin and oxytyrosinase (see Figure 2.10). The lack of peroxide binding to native laccase in the absence of N_3^-

Figure 5.5 Electronic absorption spectra[1] at 298 K: N_3^-/O_2^{2-} chemistry.
(——) native laccase pre-incubated with 30 protein equivalents. The protein equivalents of N_3^- are indicated for each spectrum.
([protein] ~0.17 mM)

Figure 5.6 EPR spectra at 77 K: N_3^-/O_2^{2-} chemistry.
(A) native laccase pre-incubated with 30 protein equivalents H_2O_2;
(B) after reaction with 8 equivalents NaN_3, 50 minutes.

Primed spectra were recorded at 8X higher gain. (9.30 GHz; [protein] = 0.272 mM)

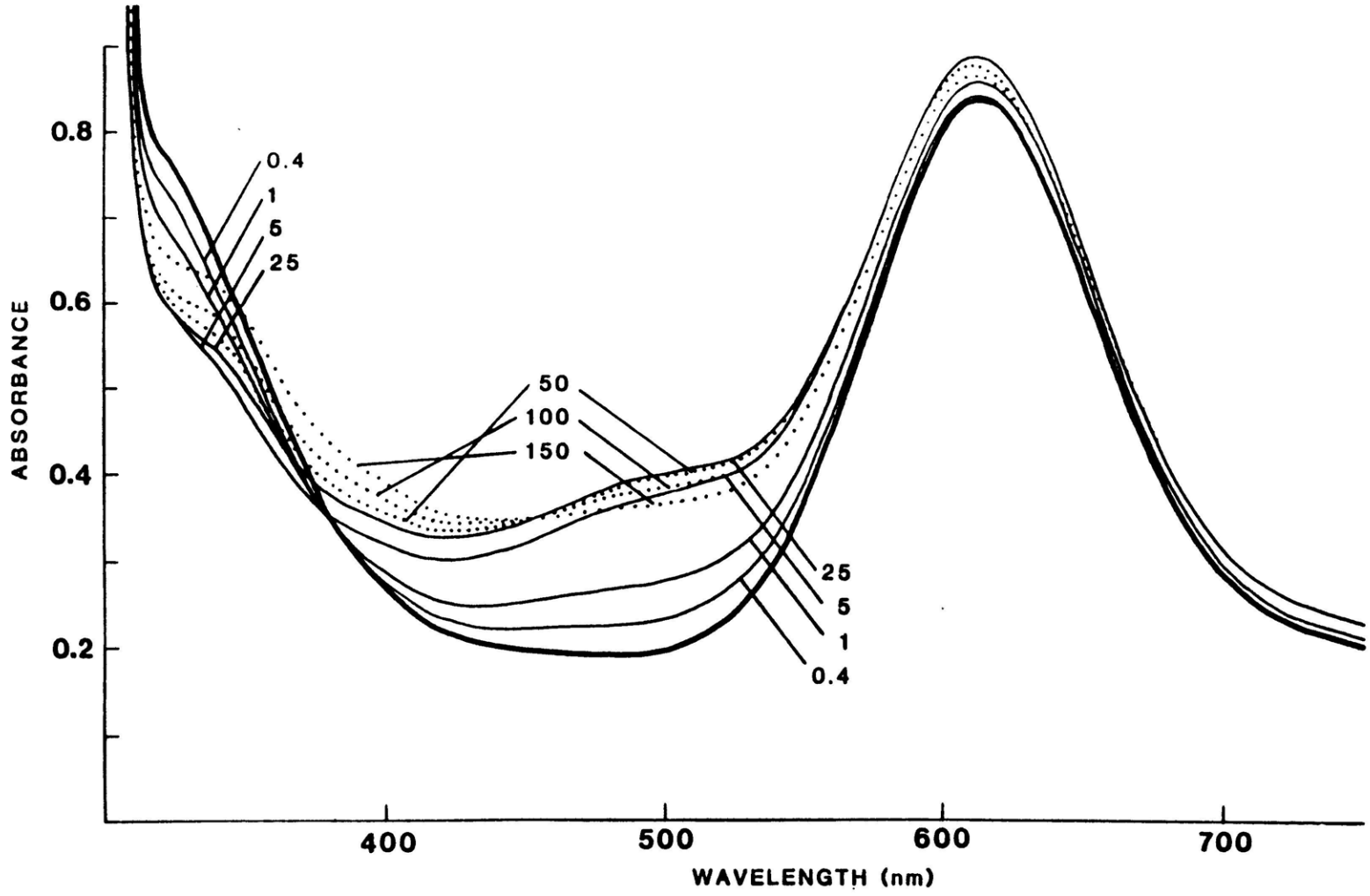
ABSORBANCE
0.8
0.6
0.4
0.2
0.4
1
5
25
50
100
150
25
5
1
0.4
400
500
600
700
WAVELENGTH (nm)

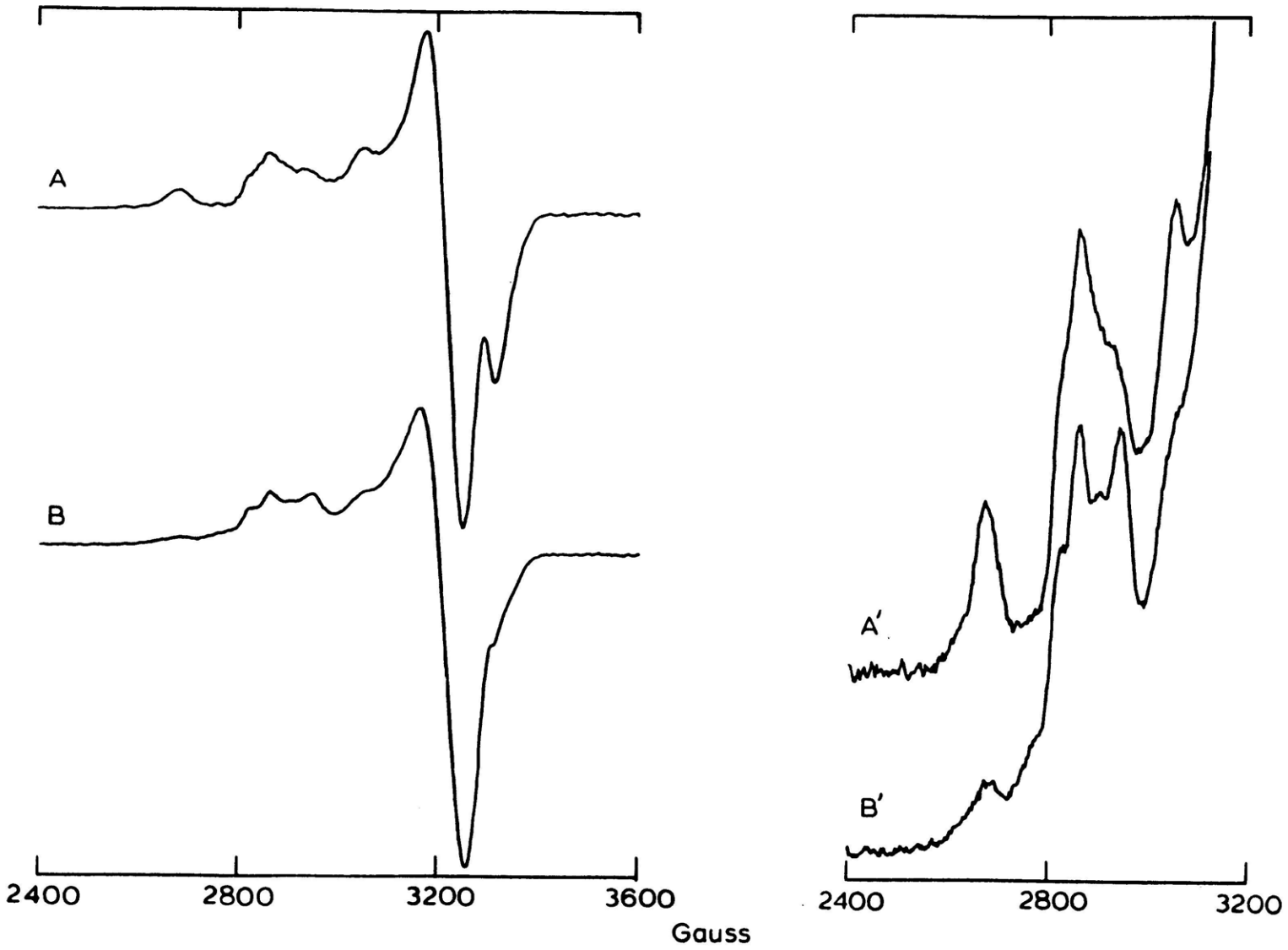
A
B
2400
2800
3200
3600
Gauss
A'
B'
2400
2800
3200

suggested that these spectral features should be further examined.

X-ray absorption edge studies of native laccase treated with 30X H_2O_2, in the presence and absence of 2.5X N_3^- are shown in Figure 5.7. Difference edge analysis indicates that the azide sample contains approximately 25% Cu(I), or twice the amount of Cu(I) which is routinely observed in native laccase. As the T1 and T2 copper ions are fully oxidized by optical (T1) and EPR (T1,T2) spectroscopies, the T3 sites must be partially reduced in this protein form. Thus, whereas in all previous studies of T2D and native laccase, peroxide has functioned as an oxidant, in the presence of N_3^-, it acts as a reductant for the native T3 sites.

500 nm is an extremely low energy for an N_3^- ---> Cu(II) CT transition, and yet a similar feature is observed for high affinity N_3^- bound to native laccase. Further, it would appear that 500 nm N_3^- ---> Cu(II) CT intensity correlates with Cu(I) present (high affinity N_3^-: $\Delta\varepsilon_{500}$ = 630 $M^{-1}cm^{-1}$ and ~12% Cu(I); N_3^-/O_2^{2-} : $\Delta\varepsilon_{500}$ = 1300 $M^{-1}cm^{-1}$ and ~25% Cu(I)). These studies therefore suggest that high affinity N_3^- is associated with N_3^- ---> T2 Cu(II) CT in the presence of the reduced T3 sites. Upon further examination of the EPR spectra of high affinity N_3^- and N_3^-/O_2^{2-} on native laccase, one observes that in both cases,

Figure 5.7 X-ray absorption difference edge spectra at 210 K: N_3^-/O_2^{2-} chemistry.

(———) [native laccase + 25X H_2O_2, + 2.5X N_3^-) -(native + 25X H_2O_2)]

(••••) [native laccase - (native + 30X H_2O_2)] is shown for comparison.

([protein] ~1.1 mM)

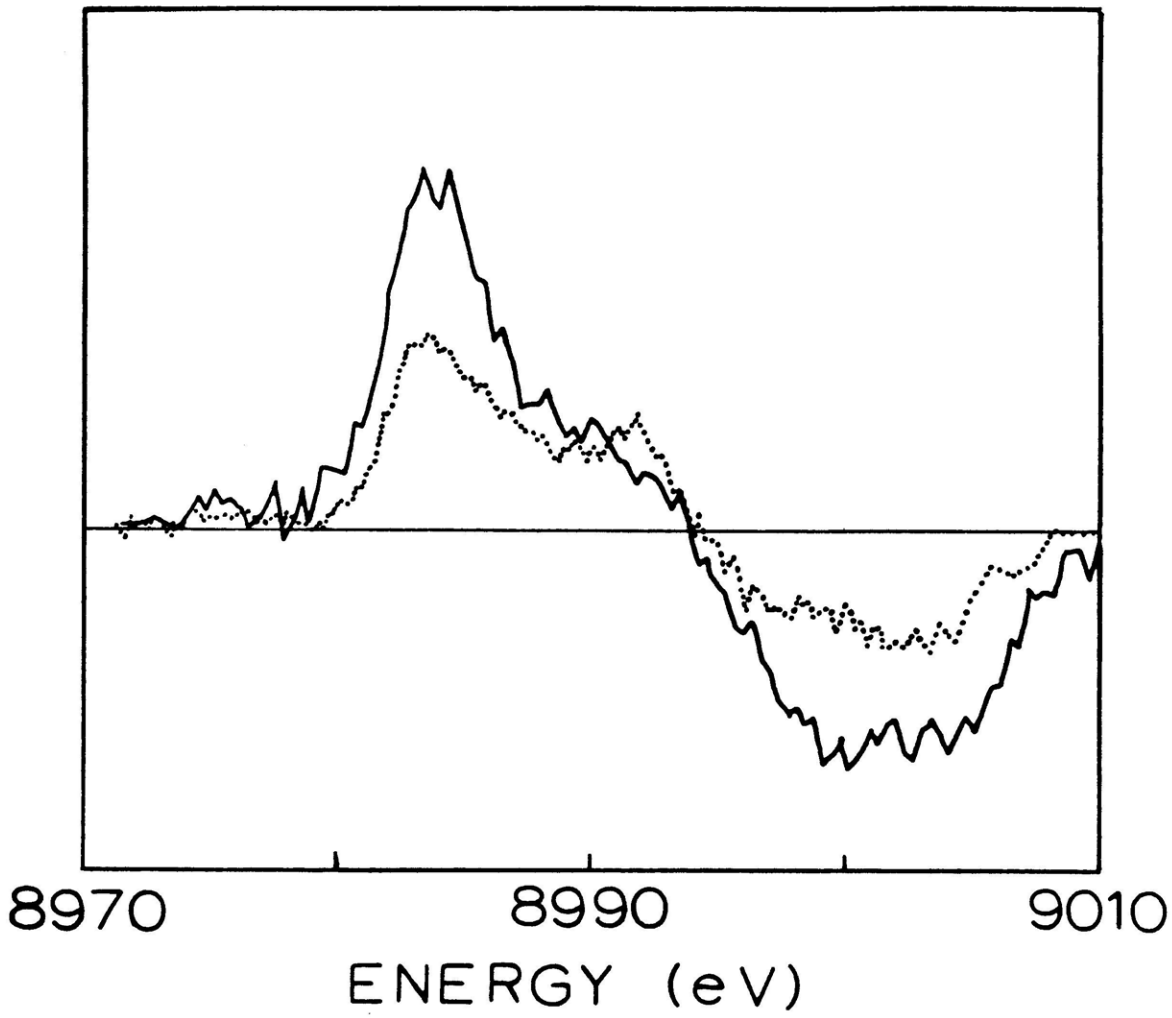
8970
8990
9010
ENERGY (eV)

$A_{||}$ of the T2 Cu(II) decrease from 200 X 10^{-4} cm^{-1} to 100 $\pm$ 5 X 10^{-4} cm^{-1} and $g_{||}$ shifts from 2.22 to 2.28, further indicating the equivalent nature of these optical changes. Redox titration studies[14] of N_3^- treated native laccase further support this assignment.

It is noted that while a 400 nm band has been associated with high affinity N_3^- in native laccase, a corresponding feature is not observed in the N_3^-/O_2^{2-} optical spectrum. This 400 nm absorption intensity is addressed in Part 2.

Finally, studies of the time dependence of N_3^-/O_2^{2-} reactions in varying anion concentrations have generated numerous optical spectra similar but not identical to Figure 5.5. While the detailed nature of these perturbations depends on the free N_3^- and O_2^{2-} in solution, all of these intermediate spectral states would appear to relate to changes in electron distribution at the laccase active site.

In competitive anion binding studies between N_3^- and F^-, spectral features indicative of both N_3^- and F^- coordination are observed. The presence of partially reduced as well as fully oxidized active sites clarifies many earlier spectral observations. As shown in Figure 5.8, when only 0.4X N_3^- is added to native laccase which has been

Figure 5.8 Electronic absorption spectra at 298 K: F^- and high affinity N_3^-.

(a) native laccase pre-incubated with 150 protein equivalents NaF;

(b) after reaction with 0.4 and

(c) 10 protein equivalents NaN_3.

([protein] = 0.132 mM)

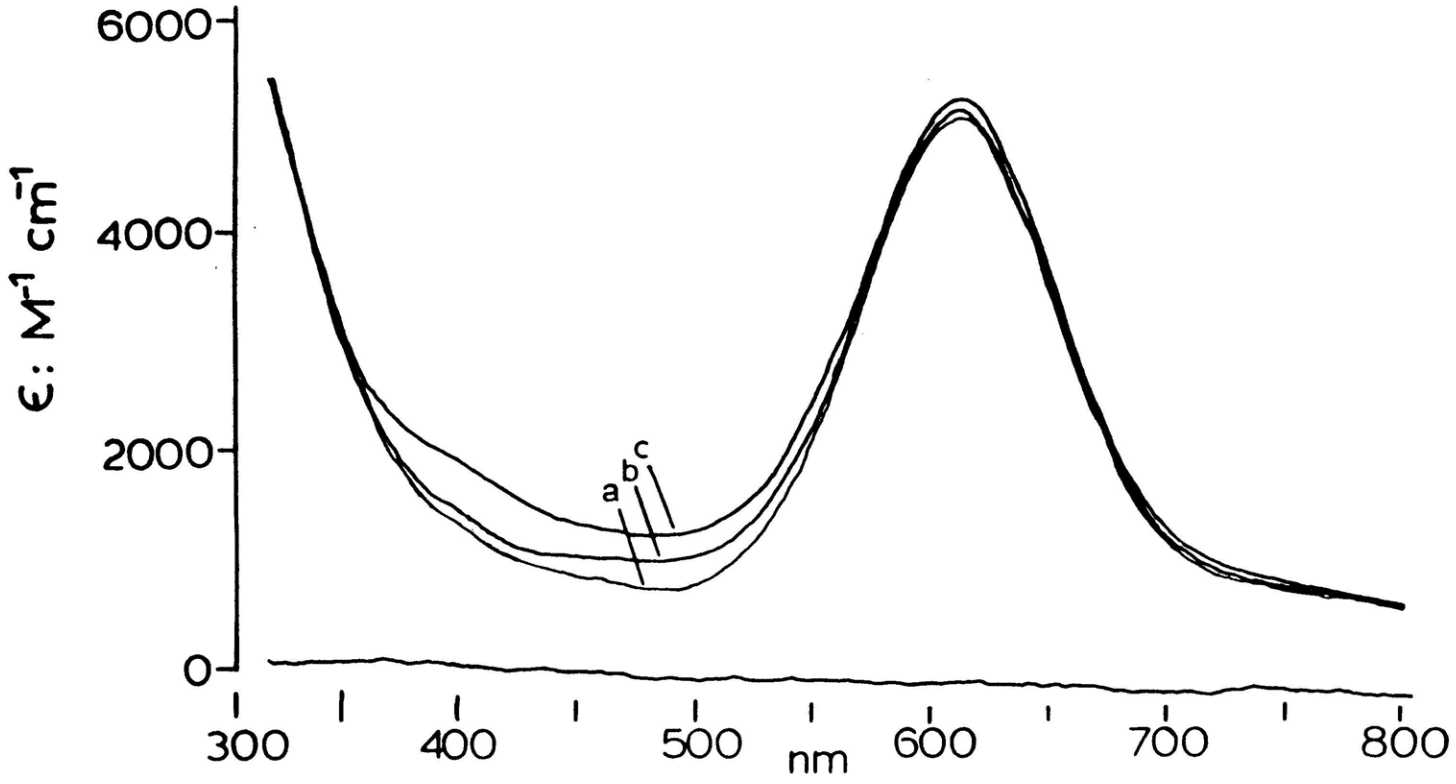
6000
4000
2000
0
ε: M⁻¹ cm⁻¹
a
b
c
300
400
500
nm
600
700
800

pre-incubated with 150X F^- at pH 6.0, significant charge transfer intensity is observed at 500 nm. In the corresponding EPR spectrum (Figure 5.9) two fluorides remain bound at the T2 Cu(II) and careful analysis of the $g_{||}$ region (~2750 G) shows the presence of high affinity N_3^- as well. Similarly, when laccase which has been preincubated with 10X N_3^- is titrated with F^- (data not shown) 2 F^-'s bind (EPR triplet) and the N_3^- does not decrease their binding affinity at the site; there is also essentially no decrease at 500 nm in the absorption spectrum. Thus, high affinity N_3^- and F^- do not compete for the same binding site. This is not surprising since N_3^- is binding at the partially reduced copper sites while F^- is binding at those which are fully oxidized.

Alternatively, low affinity N_3^- and F^- do compete with one another. In native laccase, the higher affinity F^- is essentially 100% bound with only 2X F^-, but as shown in the EPR spectrum in Figure 5.10, 150X N_3^- significantly decreases fluoride affinity at the T2 Cu(II). Essentially no F^- is bound with 2X F^-, but as the [F^-] is increased, doublets and triplets become evident in both the parallel and perpendicular region. In the corresponding absorption spectra, there is a concomitant decrease at 400 nm, indicating that low affinity N_3^- is being displaced. The final EPR spectrum in the presence of 150X F^- is very similar

Figure 5.9 EPR spectra at 77 K: F^- and high affinity N_3^-.

(A) native laccase pre-incubated with 150 protein equivalents NaF;

(B) after reaction with 0.4 and

(C) 10 protein equivalents NaN_3.

Arrow indicates increased absorbance due to high affinity N_3^-. Primed spectra were recorded at ~8X higher gain. ([protein] = 0.149 mM)

Figure 5.10 EPR spectra at 77 K: F^- and low affinity N_3^-.

(A) native laccase pre-incubated with 150X N_3^-;

(B) after reaction with 2 and

(C) 150 protein equivalents NaF;

(D) native laccase pre-incubated with 50 protein equivalents NaF is shown for comparison.

Primed spectra were recorded at 5X higher gain. ([protein] ≈0.16 mM)

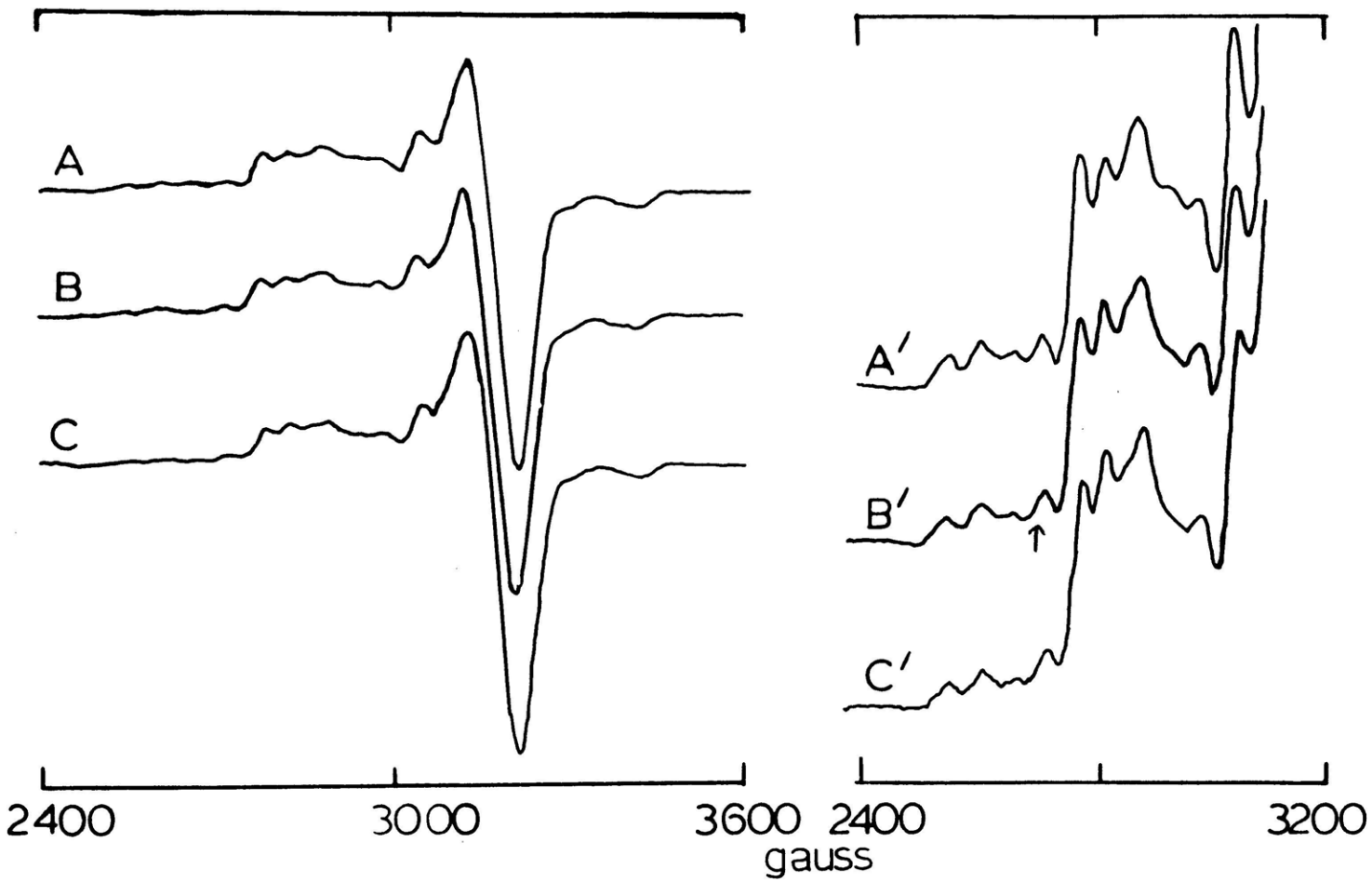
A
B
C
A′
B′
C′
2400
3000
3600
2400
3200
gauss

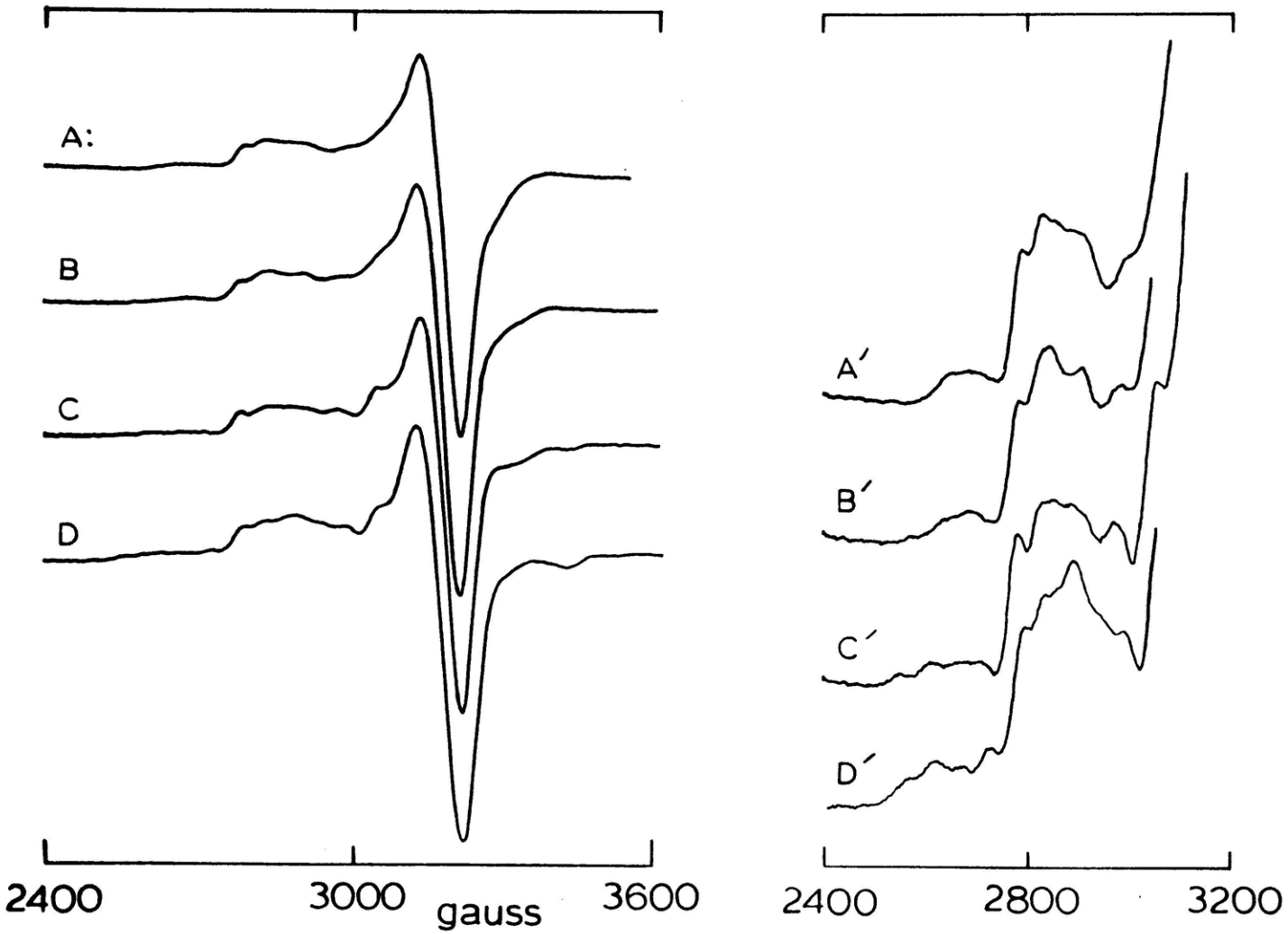
A:
B
C
D
2400
3000
gauss
3600
A′
B′
C′
D′
2400
2800
3200

to that of native laccase treated with 50X F^- in the absence of N_3^-, suggesting that most of the low affinity N_3^- is no longer bound. The lack of new spectral features throughout the titration indicates that a ternary complex does not form, despite the presence of two exchangeable positions of the T2 Cu(II) site. N_3^- titration studies of native laccase preincubated with 150X F^- are consistent with these spectral changes.

Finally, these binding and competition studies have been extended to SCN^-, which also binds with high and low affinity to native laccase (Figure 5.11). From the absorption increases at 410 and 320 nm: ($K_1 \sim 5000\ M^{-1}$, $\Delta\varepsilon_{410} = 150\ M^{-1}cm^{-1}$, $\Delta\varepsilon_{320} = 400\ M^{-1}cm^{-1}$ and $K_2 \sim 100\ M^{-1}$, $\Delta\varepsilon_{410} = 800\ M^{-1}cm^{-1}$, $\Delta\varepsilon_{320} = 950\ M^{-1}cm^{-1}$. SCN^- significantly alters the T1 Cu(II) EPR spectrum but does not affect that of the T2 Cu(II) (Figure 4.5) suggesting that it may be binding to the T3 site. In competition studies, it would appear that both F^- and SCN^- can bind simultaneously to laccase. As shown in the EPR spectra in Figure 5.12, when native laccase is preincubated with 150X SCN^- and titrated with F^- at pH 6.0, the T1 hyperfine remains large at $83 \times 10^{-4}\ cm^{-1}$ and the T2 Cu(II) hyperfine peaks are split into doublets, indicating that both F^- and SCN^- are bound. Importantly, at 150X F^-, only one F^- binds and demonstrates that SCN^- inhibits binding of the second F^-. Similarly, when SCN^- is added to native

Figure 5.11 Electronic absorption spectra at 298 K: SCN^- titration of native laccase.

Arrows indicate direction of change with 0, 1, 10, 25, 50, and 150 protein equivalents NaSCN. (0.1 M potassium phosphate, pH 6.0; [protein] = 0.132 mM)

Figure 5.12 EPR spectra at 77 K: low affinity SCN^- and F^-.

(A) native laccase pre-incubated with 150 protein equivalents NaSCN;

(B) after reaction with 25 and

(C) 150 protein equivalents NaF.

Primed spectra were recorded at 8X higher gain. ([protein] = 0.123 mM)

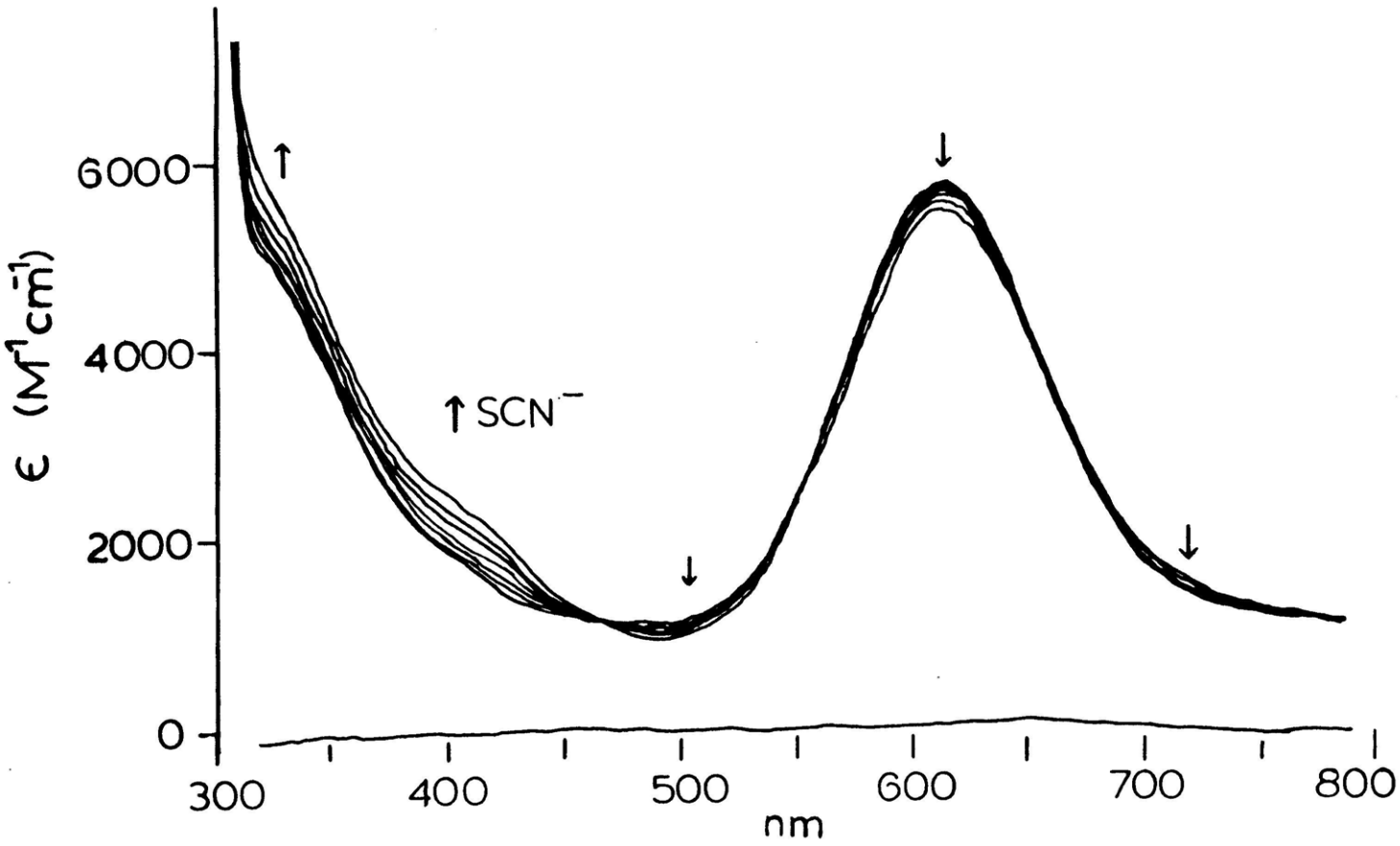
6000
4000
2000
0
ε (M⁻¹cm⁻¹)
↑
↑ SCN⁻
↓
↓
↓
300
400
500
600
700
800
nm

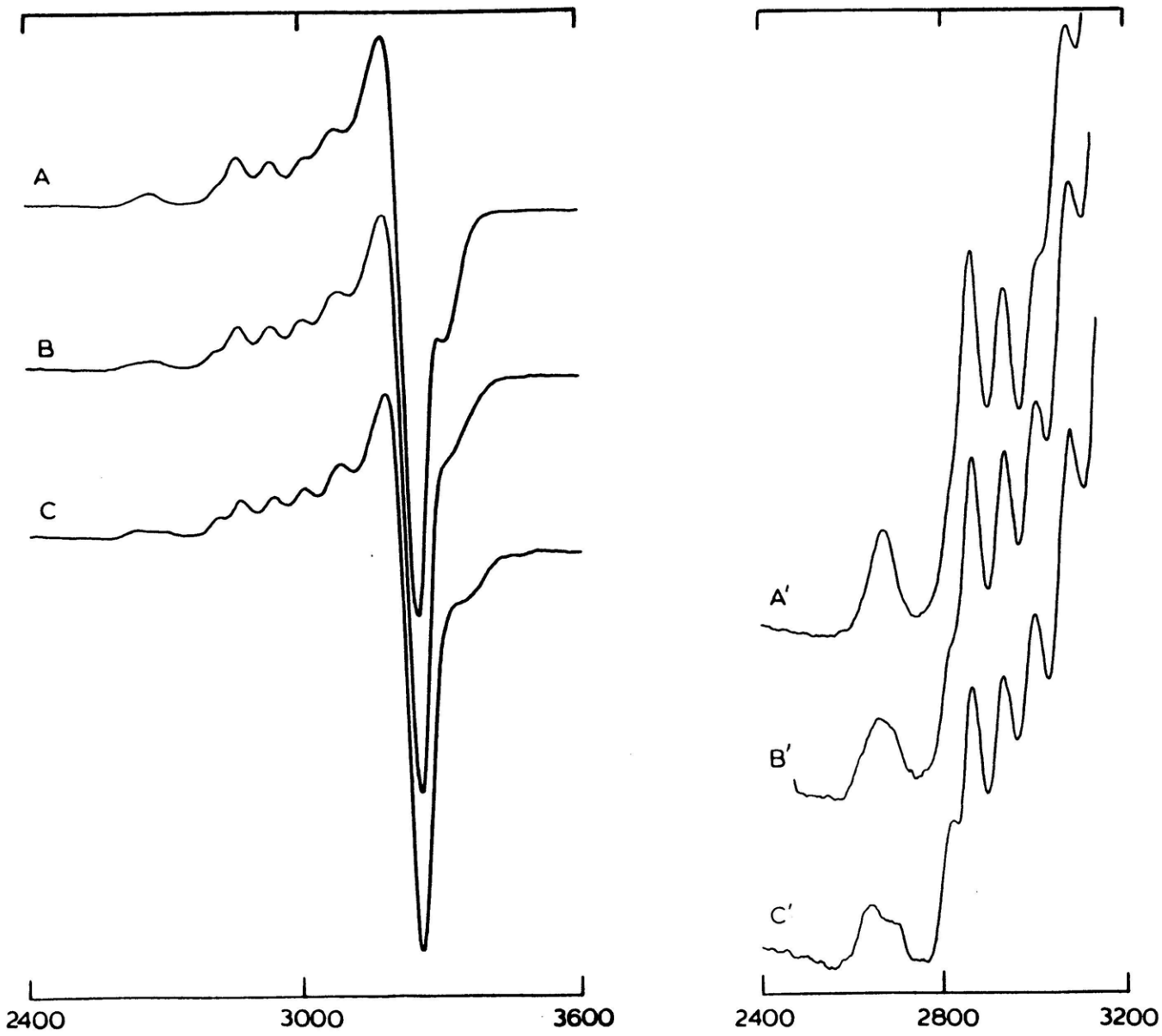
A
B
C
A'
B'
C'
2400
3000
3600
2400
2800
3200
gauss

laccase bound by two F^-'s, the EPR triplets are converted to doublets and the T1 hyperfine increases to 83 X 10^{-4} cm^{-1}.

Thus, while O_2^{2-} does not bind to native laccase, N_3^-, F^- and to a lesser degree SCN^-, bind with remarkably high affinity. X-ray absorption edge studies indicate that in the case of N_3^-, this high affinity binding is associated with laccase molecules in which the binuclear copper sites are reduced. F^- binds only to the fully oxidized sites and therefore binds independently of high affinity N_3^- but in competition with low affinity N_3^-. Alternatively, EPR studies indicate that SCN^- and F^- can bind together at the active site.

2. Magnetic Circular Dichroism Studies of Anion Binding to Native Laccase: The Three Copper Exogenous Ligand Binding Site

Through a series of variable temperature MCD studies (in collaboration with Mark D. Allendorf), low temperature optical and liquid helium EPR experiments, it has been possible to determine how these exogenous anions, and in particular N_3^-, the small molecule analog of peroxide, bind at the laccase active site. Variable temperature MCD allows correlation of ground state paramagnetic centers with excited state electronic spectral features through temperature

dependence and saturation curves. As the MCD intensity associated with electronic transitions can be of negative as well as positive sign, MCD further allows identification and resolution of broad, overlapping absorption transitions. It has thus been the ideal complement to the aforementioned spectroscopies for assigning the optical features generated in reactions with N_3^-, and moreover, for probing site-site interactions in exogenous ligand binding.

Through the dispersion and temperature dependence of the MCD spectrum of a given electronic transition, the parameters A_1, B_o and C_o are obtained.

A terms: indicative of degenerate ground or excited state; shape is as first derivative of an absorption band and temperature independent.

B terms: associated with magnetic field mixing all the excited states; absorption band dispersion and temperature-independent.

C terms: indicative of ground state degeneracy; absorption band shape and temperature-dependent. At high temperature, $kT >> g\beta H$ and intensity $\propto 1/T$, while at low temperature, one observes saturation

magnetization behavior which directly relates to the ground state Zeeman and zero field energy splittings.

For tetragonal copper (II), the magnetic field splits the ground and excited states as diagrammed in Figure 5.13. As the temperature is changed, the Boltzmann population of these states and consequently, the relative transition intensities vary.

Since the T1 and T2 copper in laccase are paramagnetic and EPR detectable, only these centers should exhibit optical features with significantly temperature-dependent MCD behavior. Transitions of the antiferromagnetically exchange coupled T3 site will be temperature independent and observed only (if at all) at higher temperatures (e.g. > 100 K) where the paramagnetic C_o terms ($I \propto 1/T$) no longer dominate the MCD spectrum. This is extremely important in associating optical spectral features with specific copper sites. As MCD intensity must be correlated with absorption intensity and all MCD studies are at < 100 K, low temperature absorption spectroscopy was necessary for accurate spectral comparison. Finally, N_3^- uncouples a small percentage of T3 sites in native as well as met T2D laccase (Chapter 3). From the MCD intensity associated with these uncoupled T3 coppers, it has been possible to further define the optical features

Figure 5.13 MCD C terms for tetragonal Cu(II).

(upper) transitions between the Zeeman split degenerate $^2B_{1g}$ ground state and ^2X excited states for tetragonal Cu(II) (^2X = $^2A_{1g}$, $^2B_{2g}$, ^2E_g); $\Delta m_{LCP} = +1$, $\Delta m_{RCP} = -1$.

(lower) the effect of varying temperature on the MCD C term[15]

(a) 14.4 K;

(b) 28.8 K;

(c) 72.0 K.

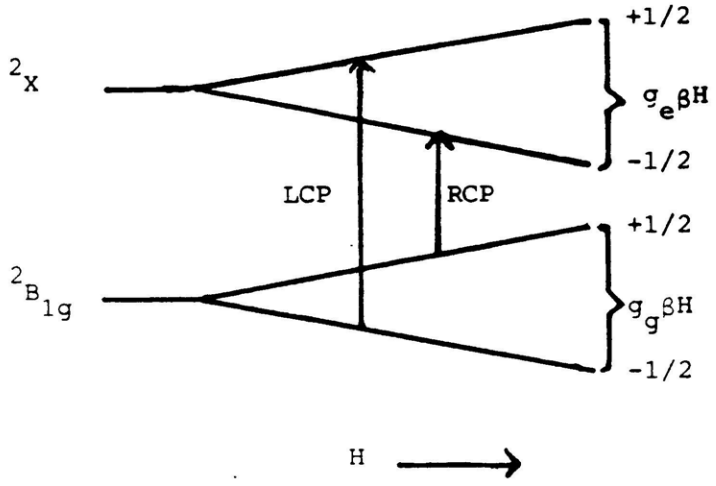
+1/2
^2X
$g_e\beta H$
-1/2
LCP
RCP
+1/2
$^2B_{1g}$
$g_g\beta H$
-1/2
H

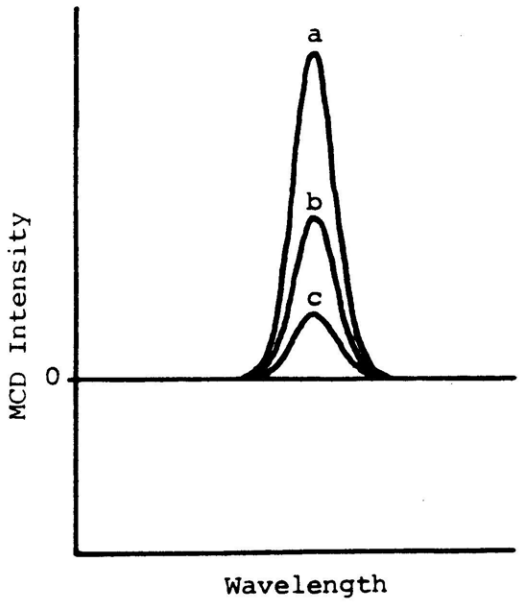
a
b
c
MCD Intensity
0
Wavelength

associated with the binuclear cupric site. Therefore, EPR studies at liquid helium temperatures were necessary to monitor their potential MCD spectral contributions.

In Figures 5.14 and 5.15 are shown the 298 K and 77 K absorption spectra of native laccase titrated with N_3^- in 50% v/v glycerol/0.1 M potassium phosphate at pH 6.0. In the room temperature spectrum, N_3^- binds with high affinity and results in a broad absorption increase between 500 and 400 nm ($\Delta\varepsilon_{500}$ = 500 $M^{-1}cm^{-1}$, $\Delta\varepsilon_{400}$ = 370 $M^{-1}cm^{-1}$); these changes maximize with ~0.5X N_3^-. With additional N_3^-, intensity at 400 nm continues to increase ($\Delta\varepsilon_{400}$ = 1790 $M^{-1}cm^{-1}$) and a weak shoulder is evident at 450 nm; the 330 nm region is decreased in intensity and broadened. Upon cooling to 77 K, the Blue band and 330 nm region sharpen, as was observed in met T2D laccase. In addition, the low affinity ~400 nm feature shifts to 385 nm and is significantly sharpened ($\Delta\varepsilon$ = 2600 $M^{-1}cm^{-1}$). Figure 5.15 indicates that low affinity N_3^- is weakly contributing even to the 0.5X N_3^- sample. The 450 nm feature is better resolved at 77 K ($\Delta\varepsilon_{450}$ = 720 $M^{-1}cm^{-1}$) and is clearly also associated with the low affinity N_3^- binding. Pseudo first order binding constant analyses[16] indicate that at 77 K, $K_1 \sim 6 \times 10^4$ M^{-1} at 510, 450 and 385 nm; a second binding constant $K_2 \sim 170$ M^{-1} is calculated at 450 and 385 nm.

Figure 5.14 Electronic absorption spectra at 298 K: N_3^- titration of native laccase, pH 6.0.
(——) native laccase; after reaction with
(—·—·—) 0.25; (— — —) 0.5; (— — —) 2.5;
(····) 9; and (——) 38 protein equivalents NaN_3. 50% v/v glycerol/0.1 M potassium phosphate, pH 6.0; pathlength ~1.45 mm [protein] = 0.95 mM)

Figure 5.15 Electronic absorption spectra at 77 K: N_3^- titration of native laccase, pH 6.0.

Samples in Figure 5.14 at 77 K.

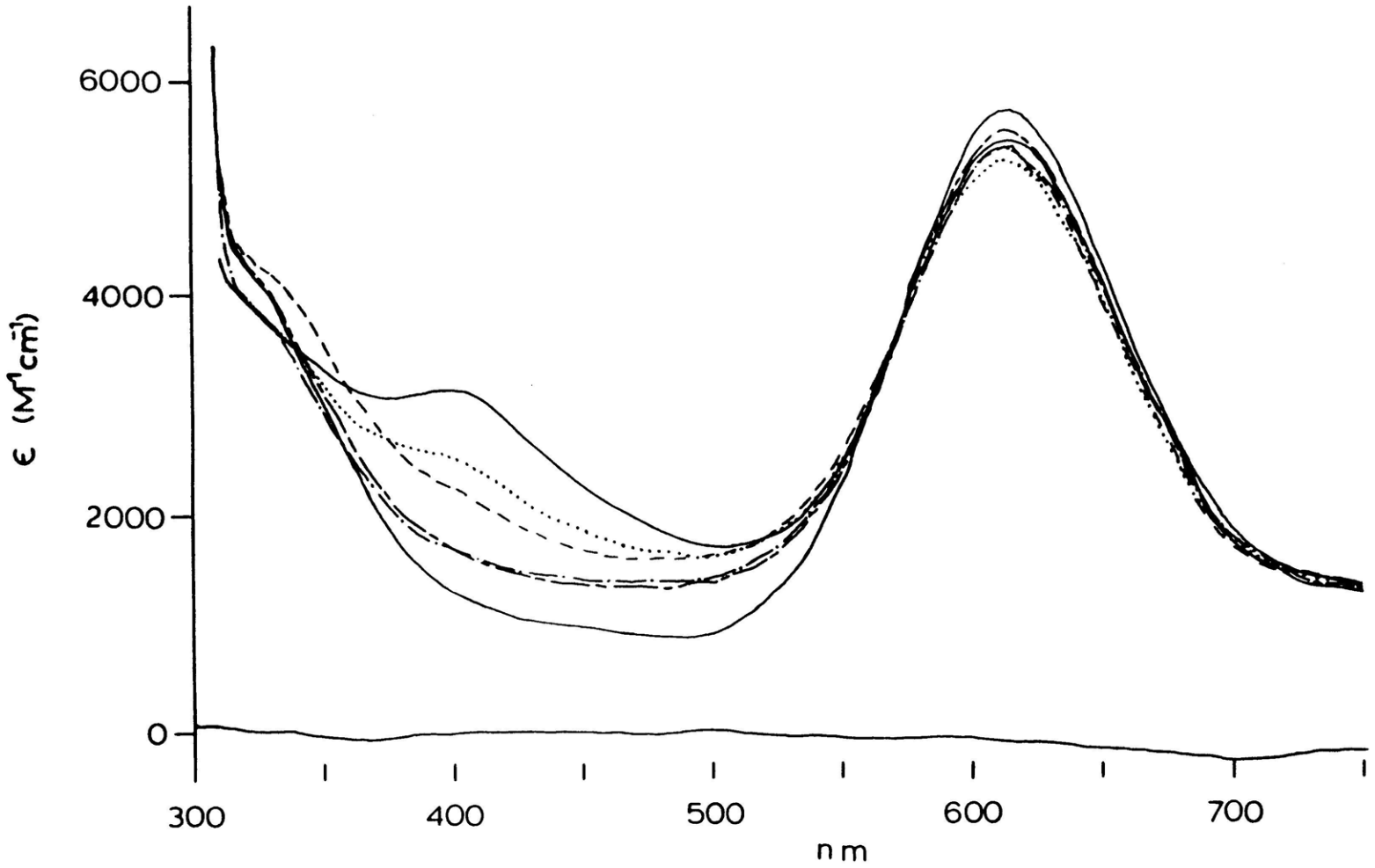
6000
4000
2000
0
ε (M⁻¹cm⁻¹)
300
400
500
600
700
nm

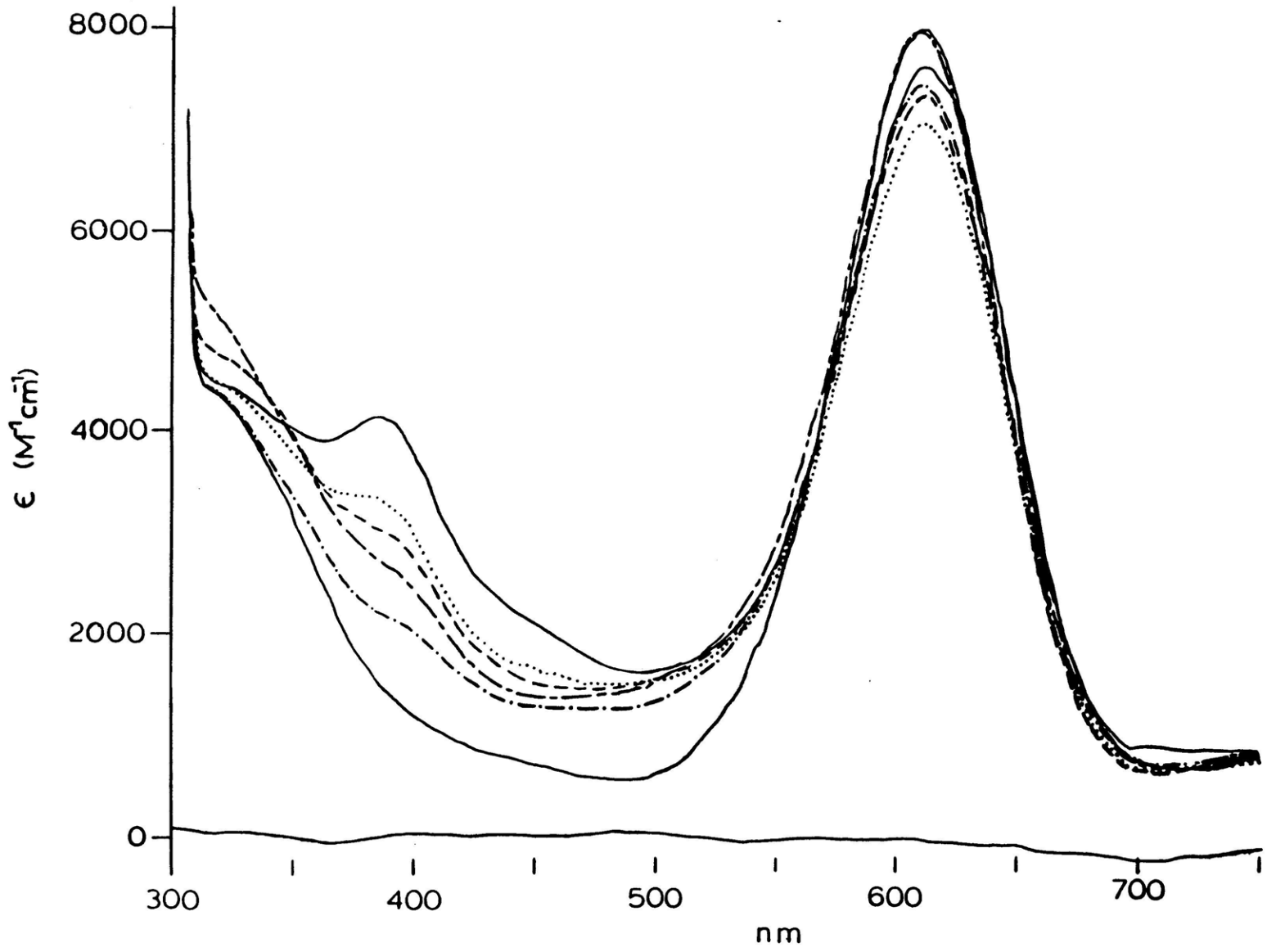
8000
6000
4000
2000
0
ε (M⁻¹cm⁻¹)
300
400
500
600
700
nm

In Figure 5.16 are shown the (A) near-IR and (B) visible-UV MCD spectra of native laccase at 4.7 K. Several overlapping spectral features are observed, and as the entire spectrum is temperature-dependent (data not shown), these features must all represent transitions at the paramagnetic T1 and T2 cupric centers. At higher temperatures, temperature-independent transitions of the antiferromagnetically coupled T3 site must also be present. These transitions are undoubtedly quite weak and have not been resolved.

When native laccase is titrated with N_3^-, major changes are observed in its 900-300 nm MCD spectrum. However, the detailed nature of N_3^- interaction at the laccase active site is contained primarily in its charge transfer spectrum, and therefore, only the relevant 550-300 nm MCD spectral region (Figure 5.17) will henceforth be reported. With $\leq$0.5X N_3^-, a strong negative feature at ~510 nm and a positive feature centered at ~440 nm appear in the MCD spectrum. Weak broad positive intensity continues into the UV and is also associated with high affinity N_3^-. With increased [N_3^-], two negative features at ~485 and 450 nm and two very intense features at ~385 and 340 nm are observed. Significantly, the 38X N_3^- sample does not titrate with the lower N_3^- samples. All of these spectral changes are temperature dependent and are therefore associated with paramagnetic cupric centers.

Figure 5.16 MCD spectrum at 4.2 K: native laccase.
(A) near-IR and
(B) visible-UV spectral regions.

(50 KG; 50% v/v glycerol/0.1 M potassium phosphate, pH 6.0; [protein] ~0.84 mM)

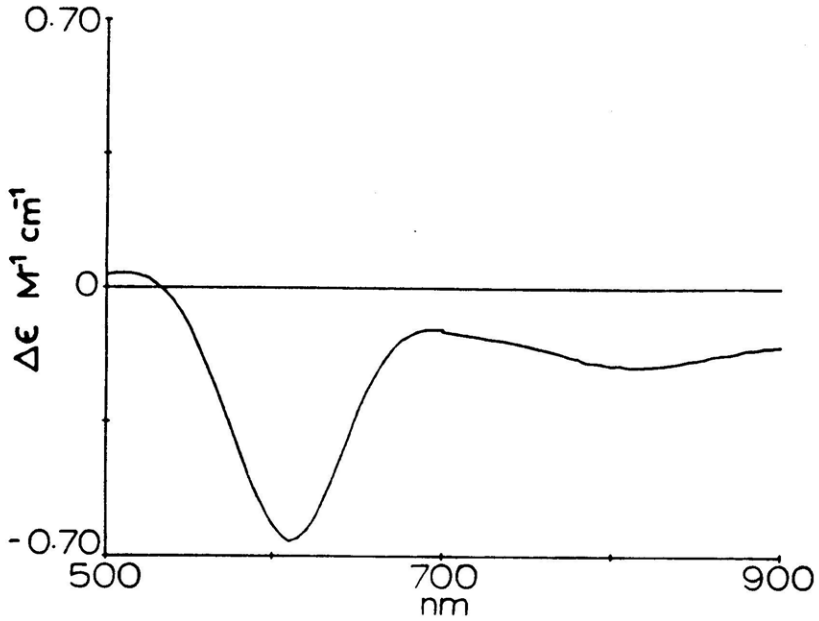
0.70
0
-0.70
Δε M⁻¹ cm⁻¹
500
700
900
nm

A

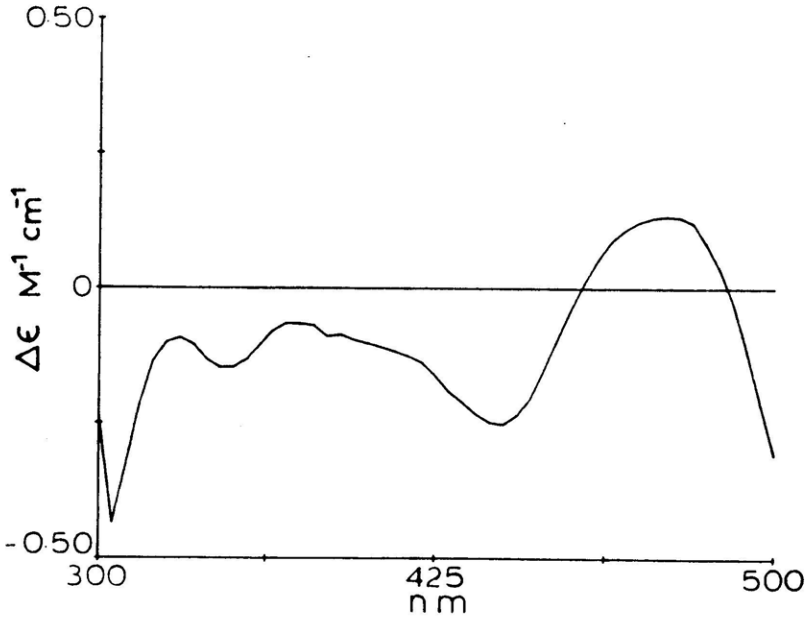
0.50
0
-0.50
Δε M⁻¹ cm⁻¹
300
425
500
nm

B

Figure 5.17 MCD spectra at 4.2 K: N_3^- titration of native laccase, pH 6.0.

(———) native laccase; after reaction with

(– – —) 0.25;

(—– – —) 0.5;

(— — —) 2.5;

(—•—) 9; and

(—– – —) 38 protein equivalents NaN_3.

(50 kG; 50% v/v glycerol/0.1 M potassium phosphate, pH 6.0; [protein] = 0.95 mM)

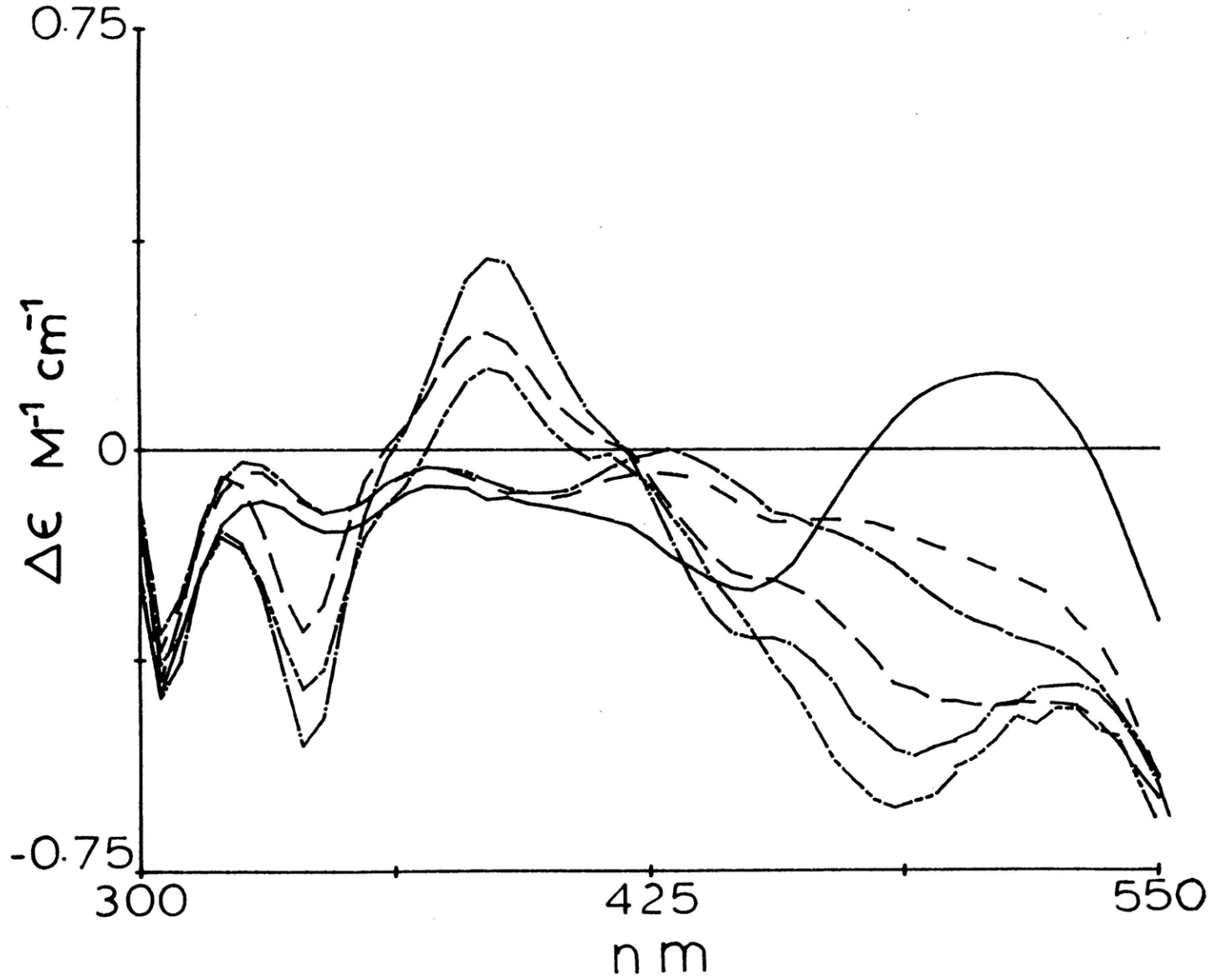
0.75
0
-0.75
Δε M⁻¹ cm⁻¹
300
425
550
nm

Binding constants for the MCD data (up to 9X N_3^-) have been fit at 515, 485, 450, 385, and 340 nm and are summarized in Table 5.1. From these pseudo first order calculations, it would appear that in general, the high and low affinity N_3^- spectral features observed in the 77 K absorption spectra have corresponding temperature dependent MCD transitions.

In order to further probe these spectral features, appropriate difference spectra of these optical changes have been calculated and gaussian analyzed. The (0.5X N_3^--native) and (9X - 0.5X N_3^-) laccase difference MCD spectra are shown in Figure 5.18 and represent the spectral features associated with the binding of high and low affinity N_3^-, respectively. The peak maxima and their relative intensities are summarized in Table 5.2. While baseline uncertainties in the 77 K absorption data limit the accuracy to which the analogous difference absorption spectra could be gaussian fit, analysis of the 298 K absorption data in Figure 5.14 is also summarized in Table 5.2. In general, peak maxima are predicted to shift to slightly higher energy upon cooling to 77 K.

In comparing the high affinity absorption and MCD spectral features, the 500 and 450 nm absorption features have corresponding temperature-dependent MCD transitions; therefore, these features are unambiguously assigned as N_3^-

Table 5.1 4.7 K MCD Binding Constants, pH 6.0

High Affinity N_3^-	K_1 (M-1)	$\Delta\varepsilon_1$ ($M^{-1}cm^{-1}$)
515 nm	5.3×10^4	-0.505
450 nm	6.5×10^4	+0.182

Low Affinity N_3^-	K_2 (M^{-1})	$\Delta\varepsilon_2 - \Delta\varepsilon_1$ ($M^{-1}cm^{-1}$)
485 nm	800	-0.461
450 nm	170	-0.551
385 nm	510	+0.553
340 nm	200	-0.688

Figure 5.18 MCD difference spectra: high and low affinity N_3^-.

From 5.17,

(———) high affinity N_3^- = [(native + 0.5X N_3^-)-native laccase];

(—•—•—) low affinity N_3^- = [(native + 9X N_3^-)-(native + 0.5X N_3^-)]

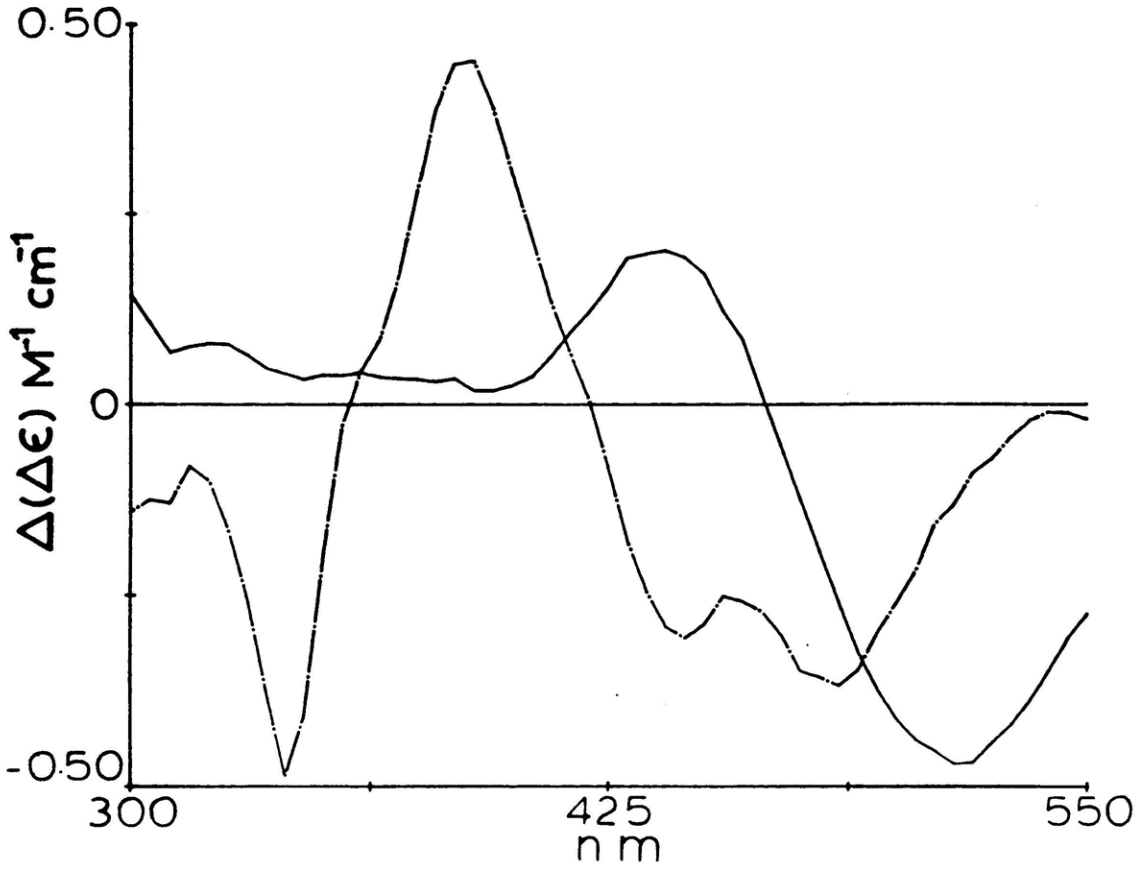
0·50
0
-0·50
Δ(Δε) M⁻¹ cm⁻¹
300
425
550
nm

Table 5.2 Gaussian Resolution of Optical Data

MCD (4.7 K)		Absorption (298 K)	
λmax (nm)	Relative Intensity	λmax (nm)	Relative Intensity
<u>High Affinity</u> N_3^-			
513	-1.0	506	1.0
442	0.46	448	0.52
360	0.08	406	0.54
322	0.14		
295	0.34		
<u>Low Affinity</u> N_3^-			
480	-0.80	498	0.83
447	-0.68	447	0.51
		420	1.1
385	0.83	393	1.3
341	-1.0	366	1.0

---> T2 Cu(II) CT transitions. Their temperature dependence, as well as their maximization with less than stoichiometric [N_3^-], are consistent with high affinity N_3^- binding at the T2 Cu(II) in the partially reduced laccase molecules. Due to the lack of spectroscopic probes for Cu(I), it has not been possible to determine whether a direct Cu(I)-N_3^- interaction stabilizes high affinity N_3^- at these partially reduced site. Whereas all previous studies[1,12,14] had associated CT transitions centered at 500 and 410 nm with high affinity N_3^- binding, this research indicates the additional presence of a band at 450 nm. While an absorption transition is also observed at ~400 nm with intensity comparable to that at 450 nm, no corresponding MCD intensity is observed which suggests that the 400 nm absorption derives from N_3^- ---> T3 Cu(II) CT intensity; this point will be further addressed later. Finally, the three weak MCD features to higher energy likely relate to changes in endogenous coordination at the T2 (or T1) cupric site concomitant to binding N_3^-.

Comparison of the low affinity N_3^- spectral features is somewhat more complicated. While Table 5.2 suggests that the energies of the absorption and MCD features are fairly well correlated, reexamination of the MCD titration in Figure 5.17 shows that whereas the 485 nm intensity increases with increasing [N_3^-], that at 385 nm maximizes with 9X N_3^- and is then significantly decreased with 38X N_3^-; similar, although

less dramatic, N_3^- titration anomalies are observed at 442 and 341 nm. Importantly, in the 77 K absorption titration (Figure 5.15), the 385 nm feature increases monotonically with increasing $[N_3^-]$. Thus, whereas the essentially indistinguishable energies of these MCD and absorption features strongly suggest that they originate from the same N_3^- ---> Cu(II) CT transition, their dissimilar intensities with increasing $[N_3^-]$ suggest otherwise. The presence of absorption intensity in the absence of MCD intensity indicates that the 385 nm absorption must have diamagnetic as well as paramagnetic contributions. Alternately, the 485 nm MCD and 385 nm absorption features do titrate together and therefore, it would appear that these two different paramagnetic and diamagnetic transitions are associated with the same mode of N_3^- interaction.

Examination of these N_3^- titrated samples by EPR spectroscopy at liquid helium temperatures provides further insight into the temperature dependent features. As shown in Figure 5.19, when N_3^- is added to native laccase, a broad new paramagnetic feature grows in at ~3600 G. Based on its physical properties, pH dependence, and chemistry, this signal, which is qualitatively very similar but not identical to that of met-N_3^- T2D (Chapter 3, section c), has been associated with uncoupled and therefore paramagnetic T3 cupric pairs. In these sites, N_3^- (and H^+) competitively

Figure 5.19 EPR spectra at 8 K: N_3^--uncoupled T3 sites in native laccase.

(A) native laccase;

(B) after reaction with 9 protein equivalents NaN_3.

* due to ubiquitous rhombic iron impurity at g = 4.3. (190 mW; 9.39 GHz; 50% v/v glycerol/ 0.1 M potassium phosphate, pH 6.0; [protein] ~0.9 mM)

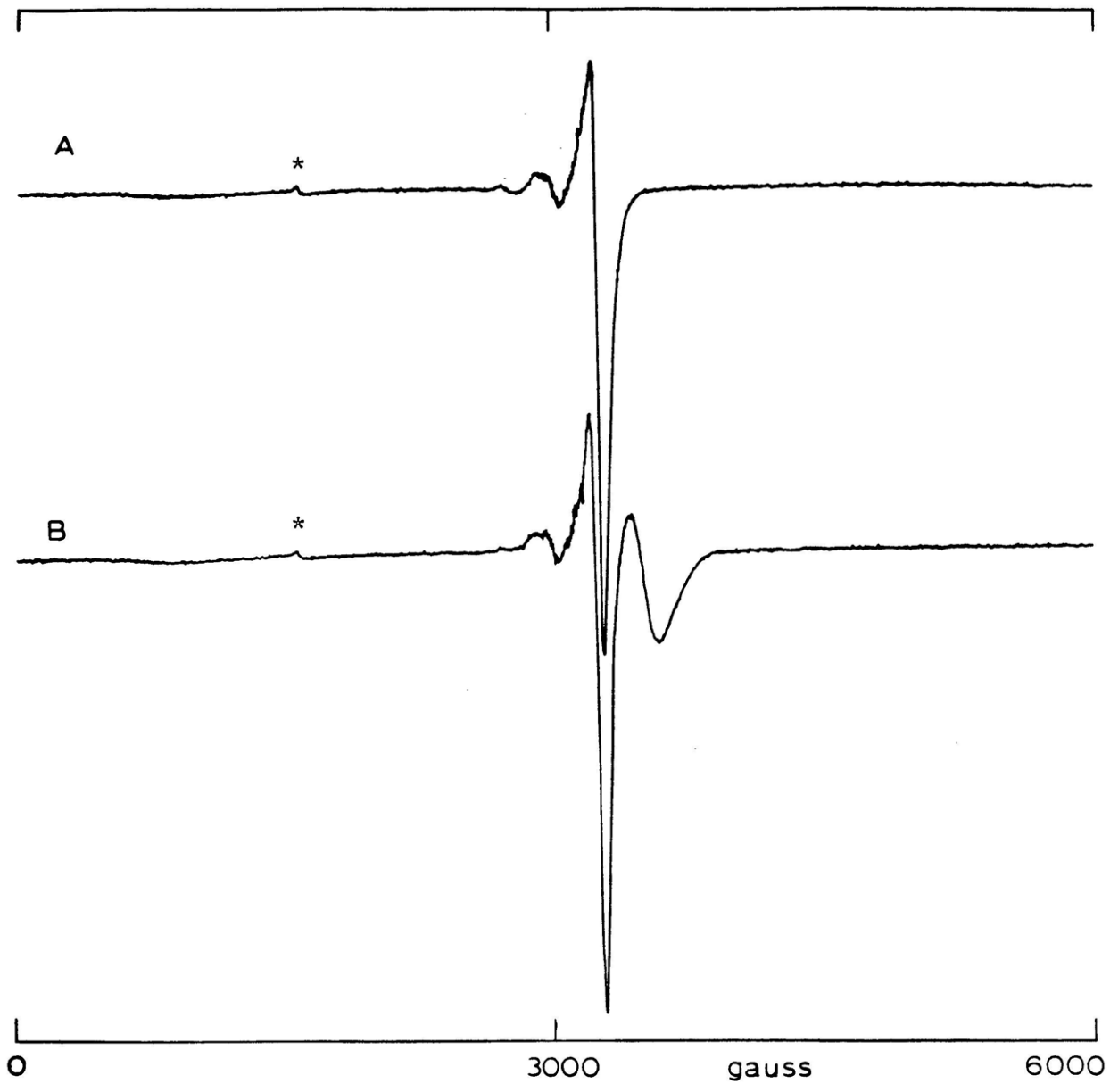
A
*
B
*
0
3000
gauss
6000

displace (and protonate) the endogenous protein bridge, turning off the superexchange pathway to generate EPR detectable dipolar interacting Cu(II)'s. Thus, these signals can be used to further probe N_3^- interaction at the binuclear copper sites.

At pH 6.0, no uncoupling could be detected with 0.5X N_3^-, indicating that these sites do not contribute to the aforementioned temperature dependent high affinity N_3^- MCD spectral features. However, with ≥2.5X N_3^-, uncoupling is observed (data not shown) and increases with increasing $[N_3^-]$, but like the 385 nm MCD feature, its intensity does not follow the 385 nm absorption intensity. This correlation would suggest that N_3^- ---> Cu(II) CT transitions at both the uncoupled and coupled T3 sites absorb at 385 nm. That is, low affinity N_3^- binds to the T3 sites in native laccase with $K_{eq} \sim 200\ M^{-1}$, and generates absorption intensity at 385 nm. However, a small fraction of these sites are uncoupled by N_3^- in a mechanism which is dependent upon both pH and $[N_3^-]$, but only these paramagnetic sites are observed in the EPR and MCD spectra of low affinity N_3^-.

To investigate further this correlation and also, to potentially associate these temperature-dependent MCD features with N_3^- binding to T2 Cu(II) (low affinity N_3^-) versus uncoupled T3 cupric sites, these N_3^- titration studies

Figure 5.20 Electronic absorption spectra at 77 K: N_3^- titration of native laccase, pH 4.6.

(———) native laccase; after reaction with

(—•—•—) 0.2;

(—— - ——) 0.5;

(— — — —) 1.0;

(• • • • •) 2.5; and

(———) 9 protein equivalents NaN_3.

(50% v/v glycerol/0.1 M sodium acetate, pH 4.6; pathlength ~1.5 mm; [protein] =0.83 mM)

Figure 5.21 MCD spectra at 4.7 K: N_3^- titration of native laccase, pH 4.6.

(———) native laccase; after reaction with

(— — —) 0.2;

(—— - ——) 0.5;

(— — —) 1.0;

(—•—•—) 2.5; and

(— - - — - - —) 9 protein equivalents NaN_3.

(50 kG; 50% v/v glycerol/0.1 M potassium phosphate, pH 6.0; [protein] = 0.83 mM)

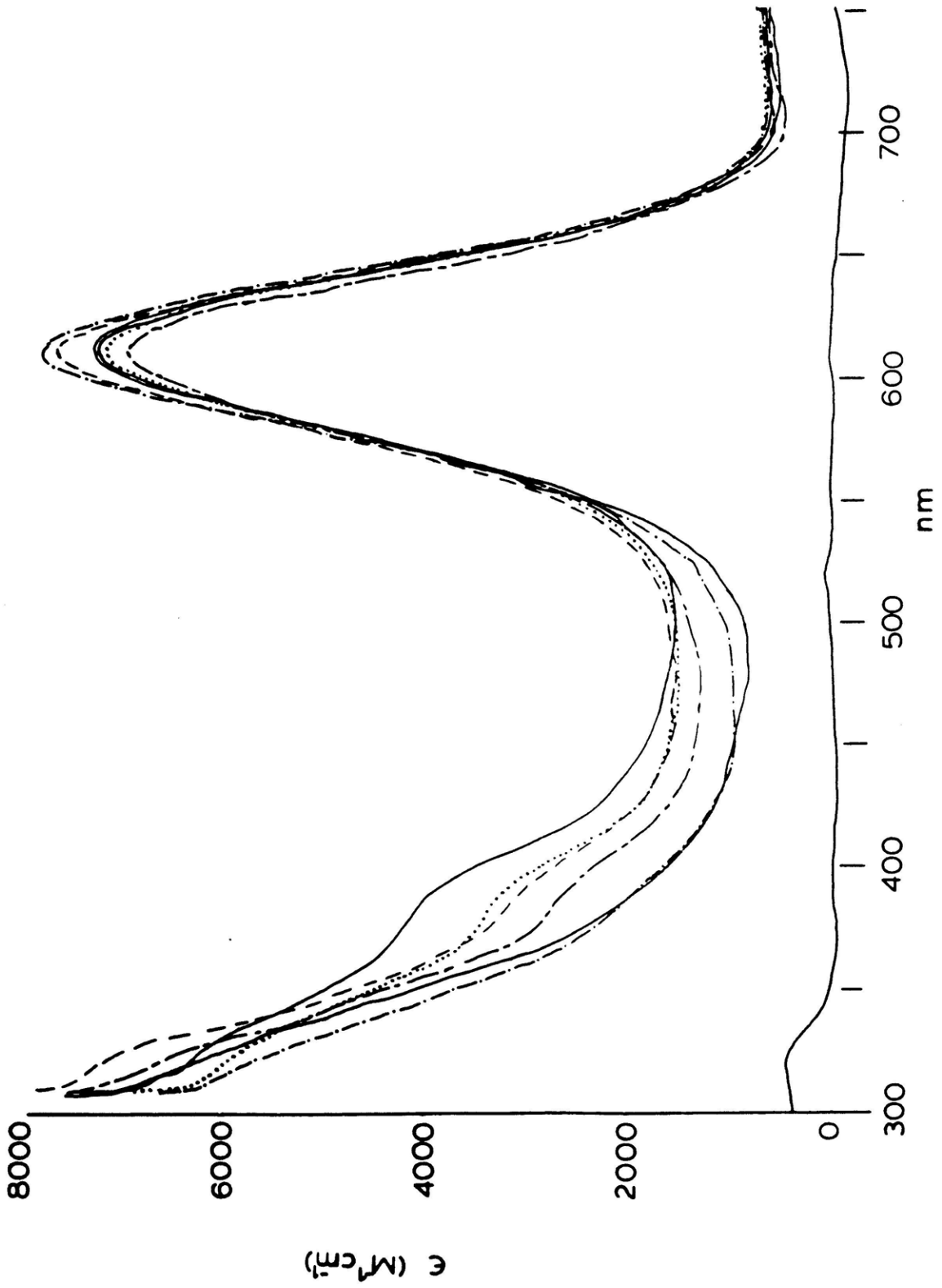
8000
6000
4000
2000
0
ε (M⁻¹cm⁻¹)
300
400
500
600
700
nm

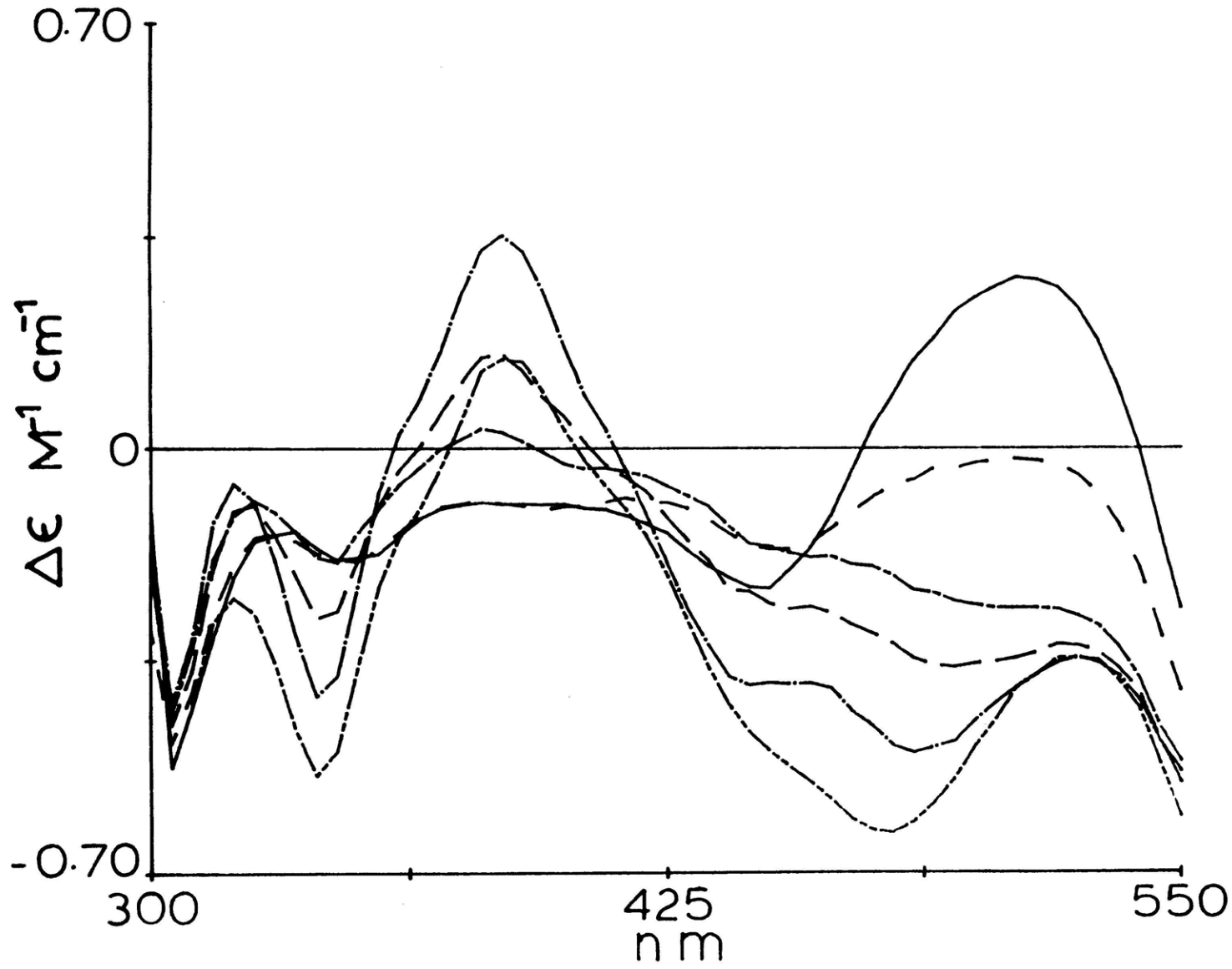
0.70
0
-0.70
Δε M⁻¹ cm⁻¹
300
425
550
nm

Figure 5.22 EPR spectra at 8 K: N_3^- titration of native laccase, pH 4.6.

The equivalents of added NaN_3 are indicated. (200 mW; 9.39 GHz; 50% v/v glycerol/0.1 M sodium acetate, pH 4.6; [protein] = 0.83 mM)

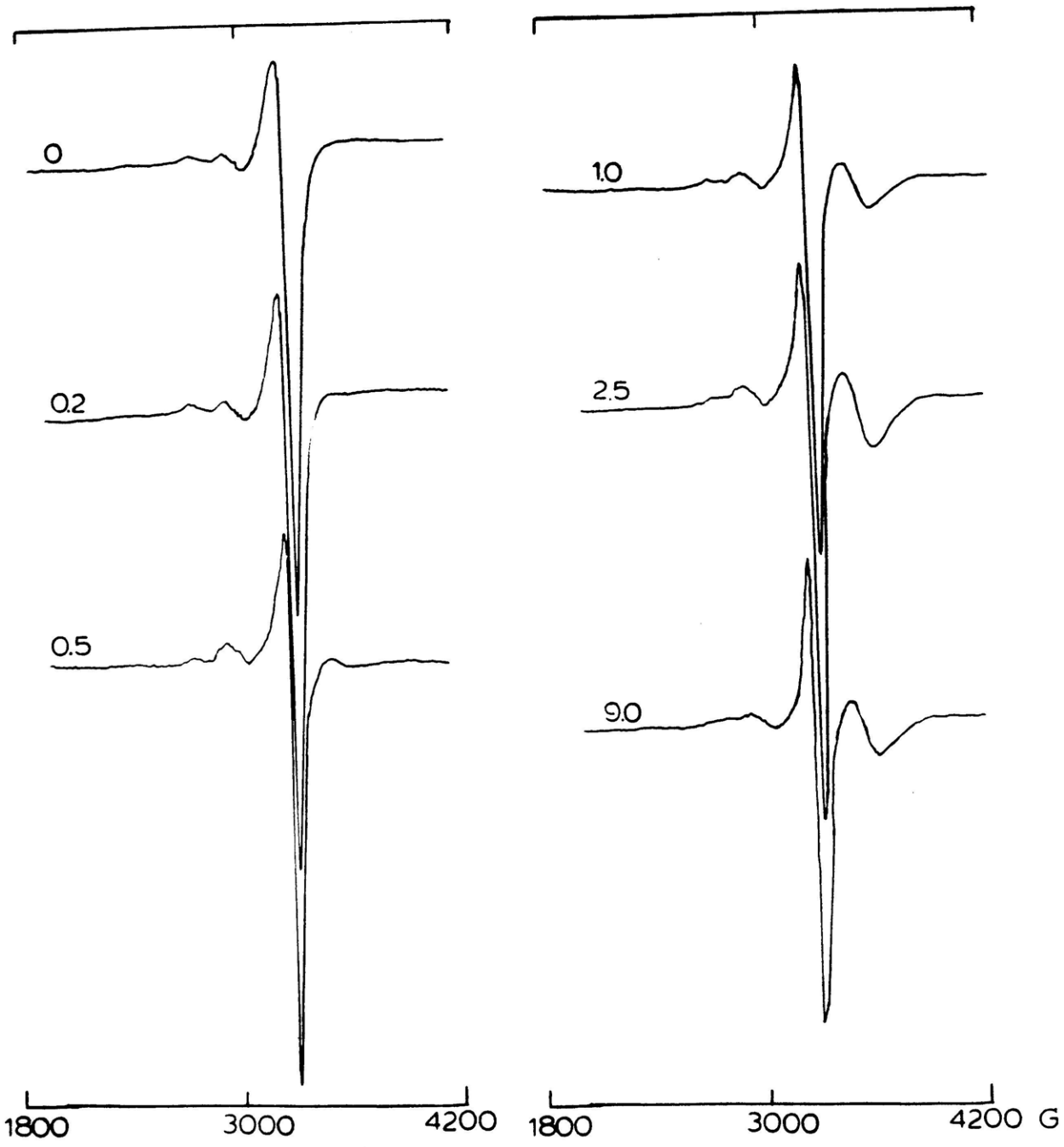
0
0.2
0.5
1.0
2.5
9.0
1800
3000
4200
1800
3000
4200 G

were extended to pH 4.6. As the uncoupling involves protonation of the endogenous bridge, it was anticipated that the lower pH would favor the relative distribution of uncoupled compared to "normal" low affinity N_3^- bound T3 sites. In the 77 K absorption spectra (Figure 5.20), N_3^- ---> Cu(II) CT transitions grow in at pH 4.6 as at pH 6.0. Unfortunately, however, in view of the original experimental intentions, the low affinity N_3^- binding affinity is also significantly increased at low pH. In general, at pH 4.6, $K_1 > 5.0 \times 10^4\ M^{-1}$ and $K_2 \sim 5 \times 10^3\ M^{-1}$; therefore, lower $[N_3^-]$'s lead to more extensive spectral perturbations than in the corresponding spectra at pH 6.0.

In the MCD spectra, (Figure 5.21), the 385 nm band is observed with only 0.5X N_3^-, maximizes with 2.5X N_3^-, and is now significantly decreased in the presence of only 9X N_3^-. The 485 nm feature is again "well-behaved" and follows the absorption intensity at 385 nm (and 450 nm).

In the 8 K EPR spectra (Figure 5.22), the uncoupled sites are also apparent with 0.5 X N_3^- and grow in with increasing $[N_3^-]$; however, in the presence of 9X N_3^-, the EPR intensity is significantly less than is observed with 2.5X N_3^-. As shown in Figure 5.23, this behavior is similar to that of the 385 nm MCD feature but again, neither the MCD nor EPR spectral features follow the 385 nm absorption intensity.

Figure 5.23 Correlation: T3-N_3^- spectral features; coupled and uncoupled sites.

(———) 77 K absorption intensity at 385 nm;

(— - — -) 4.7 K MCD intensity at 385 nm;

(—•—•—) 8 K EPR intensity at 3590 G.

(50% v/v glycerol/0.1 M sodium acetate, pH 4.6; [protein] = 0.83 mM)

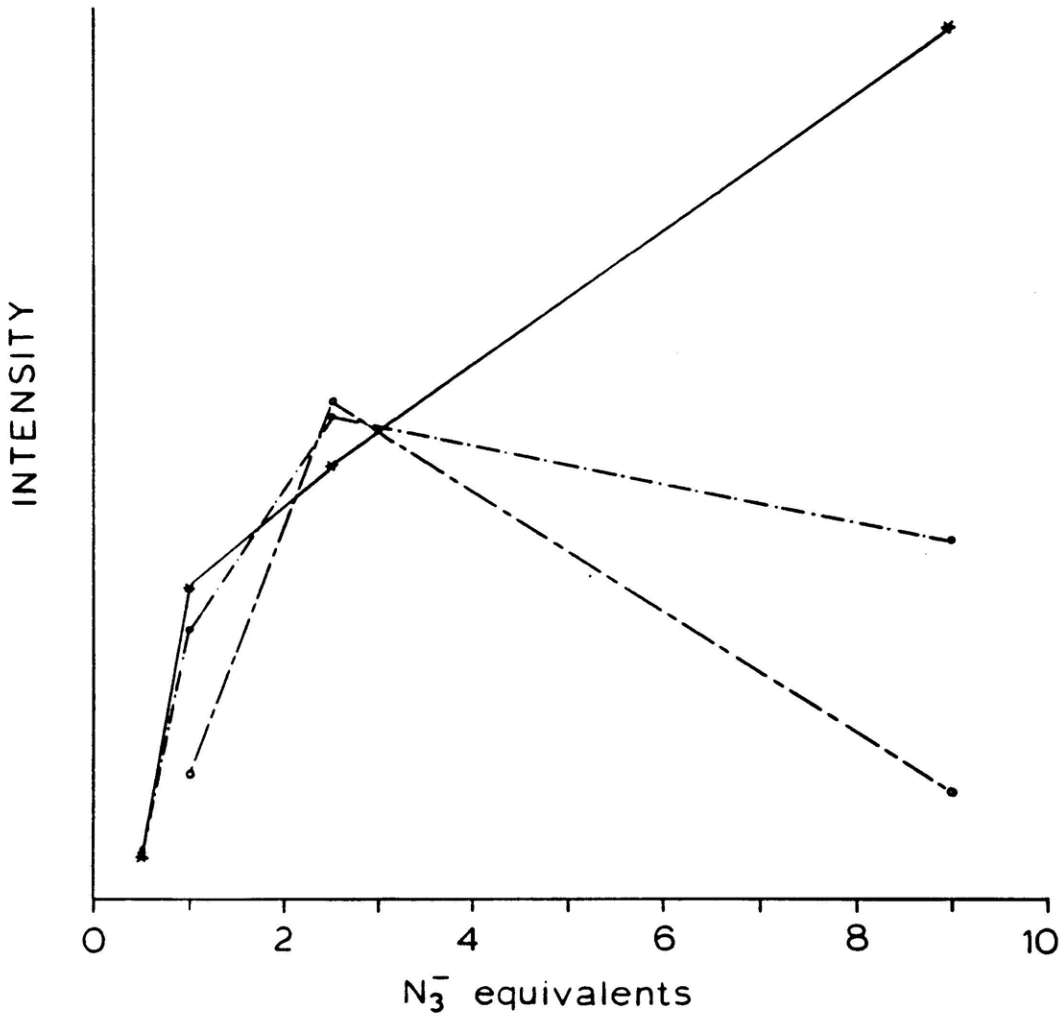
INTENSITY
0
2
4
6
8
10
N_3^- equivalents

These spectroscopic studies therefore confirm the proposed assignment of the 385 nm MCD intensity as an N_3^- ---> T3 Cu(II),uncoupled CT transition. Alternatively, the intensity of the 385 nm absorption feature always increases with increasing $[N_3^-]$. It therefore must contain a component which is not related to the 385 nm MCD transition and hence, it must be associated with N_3^- ---> Cu(II) CT at the coupled binuclear cupric site. Moreover, from the correlation of 385 nm absorption intensity and 485 nm MCD intensity, low affinity binding must also involve N_3^- ---> T2 Cu(II) CT intensity; that is, the well behaved paramagnetic 485 nm transition is associated with the diamagnetic 385 nm transition. These spectral features require that N_3^- bridge the T2 and T3 cupric ions.

The intensities of the 442 and 341 nm MCD features generally increase with $[N_3^-]$ as at 485 nm, suggesting that these features are associated with the T2 Cu(II). However, they are not totally well-behaved, and T2 or T3 charge transfer from the uncoupled active sites may also contribute at these wavelengths. That is, the spectral features of the T2 Cu(II) may change in the presence of the uncoupled T3 sites. In addition, the weak MCD intensity of the 442 nm transition relative to the 448 nm absorption intensity may suggest that N_3^- ---> T3 Cu(II),coupled CT contributes at this wavelength; the overlapping and opposing optical changes

in this region preclude any definite assignment, however. Finally, while the 340 nm transition could represent N_3^- ---> Cu(II) CT, its relatively high energy would suggest that it more likely derives from the appearance (or disappearance, based on the decrease in absorption intensity (Figure 5.20)) of endogenous (or OH^-) charge transfer at a paramagnetic cupric center.

At this point, the 400 nm transition associated with high affinity N_3^- can be further addressed. While this transition is routinely observed in the absorption spectrum ($\Delta\varepsilon$ $\sim$500 $M^{-1}cm^{-1}$), no corresponding MCD intensity has been observed suggesting that it involves charge transfer at the antiferromagnetically coupled binuclear cupric site. However, all other spectral studies indicate that high affinity N_3^- is bound to the partially reduced active sites, and a Cu(I) ---> N_3^- CT transition is predicted to occur at much higher energy. Interestingly, no additional 400 nm absorption intensity was observed (Figure 5.5) in the high affinity enhanced N_3^-/O_2^{2-} chemistry in Part 1 of this chapter. These observations suggest that the 400 nm absorption is not associated with the 450 and 500 nm high affinity N_3^- CT features. Based on the low affinity binding constants at pH 6.0 and at pH 4.6, some low affinity N_3^- is contributing at 400 nm even at very low $[N_3^-]$. This binding would not be observed by MCD spectroscopy.[17] Expanded

absorbance scale titrations of native laccase with 0.05 - 0.5X N_3^- and their gaussian analyses further indicate that while there is some overlap from the high affinity 448 nm feature, a relatively weak third band at 406 nm is necessary for spectral simulation. Based on its unusually high affinity, this transition may represent N_3^- binding to the oxidized T3 in the presence of a reduced T2 copper center. A 5-10% reoxidation of the T2 Cu(II) EPR signal has been indicated by H_2O_2 oxidation studies of native laccase and is within the uncertainty of EPR double integration. In theory, it is also possible that a second high affinity N_3^- binds to the oxidized T3 site, but the $\Delta \varepsilon_{400}$ $\sim$300 $M^{-1}cm^{-1}$ is too low an extinction coefficient for a CT transition resulting from 75% of the protein sites. The presence of only weak ligand field perturbations in the near-IR CD spectrum of native laccase reacted with low (but not high) concentrations of N_3^- further supports the proposal that only a total of 20-25% of the active sites are involved in high affinity N_3^- coordination.

3. Summary

These studies have confirmed that high affinity N_3^- binds to the T2 Cu(II) in the presence of reduced T3 sites. The unusually high affinity of these sites for N_3^- might suggest that N_3^- is binding in a very special geometry, e.g.

bridging the oxidized T2 and reduced T3 sites, although this has not been spectroscopically determined. Low affinity N_3^- has been demonstrated to bridge the oxidized T2 and oxidized T3 copper sites, thereby requiring a distance of ≤5.5 Å between the T2 and one of the T3 Cu(II) ions. Thus, in laccase there is a T3-T2, or more appropriately, a new type of "three copper active site" for binding exogenous anions. Consistent with these results, other studies[13] have suggested that the T2 and T3 copper sites are in close proximity at the active site pocket in native laccase; however, no previous studies have demonstrated a direct involvement of the T2 copper in T3 reactivity.

In view of these results, the ligand binding and competition studies in Part 1 of this chapter can be further addressed. Since low affinity N_3^- bridges the T2 and T3 Cu(II)'s, it is not surprising that it competes with F^-. F^- may be too small to bridge the three copper site, but near-IR MCD studies[18] will further define F^- interaction. SCN^- also binds to native laccase, but its ability to bind in the presence of F^- would suggest that it binds only to the T3 site; the relative S affinity at the T2 Cu(II) may not be strong enough for SCN^- to bridge the site.

It is not clear why the partially reduced active sites display such an unusually high affinity for N_3^-. Moreover,

the binding constant at these sites is $\sim 10^2$-10^3 greater than for N_3^- binding to the fully oxidized three copper sites. F^- also binds with remarkably high affinity, but only to the oxidized sites, suggesting that the high F^- affinity may be associated with the large positive charge of the fully oxidized three copper site.

Finally, the presence of a three copper binding site in laccase which is capable of binding small molecules suggests that oxygen reduction may occur via a three-electron rather than a two-electron reduced dioxygen intermediate. While there have been a number of reports of peroxide level intermediates observed in laccase, the two stable forms, peroxy laccase[3] and peroxy T2D[19] laccase have been shown through x-ray absorption studies to involve oxidation but not binding by peroxide, and it is likely that the other reported spectral intermediates also involve changes in T3 oxidation state. Alternatively, in reactions of anaerobically reduced laccase with molecular oxygen, a paramagnetic intermediate has been observed[20] which, based on its kinetics of formation and decay, appears[21] to represent an O^- radical bound to the active site. In this three copper oxygen site, a three-electron transfer could take place as a normal step in catalysis; that is, an O^- radical could readily form without prior stabilization of a two-electron reduced peroxide intermediate. In addition, this asymmetric binding geometry

should stabilize the irreversible binding and reduction of oxygen at the oxidase active site.

Thus, it is clear that the interaction of exogenous ligands at the coupled binuclear copper site in native laccase is very different compared to the hemocyanins and tyrosinase. Further, the inability of exogenous ligands to bridge the binuclear copper site in laccase is consistent with the T3 site instead being structurally defined for exogenous ligand bridging to the T2 copper of the three copper active site.

References and Notes

1. LuBien, C.D., Ph.D. Dissertation, Massachusetts Institute of Technology, 1982.
2. ≤10% T2 reoxidation by H_2O_2 has been observed in 1984 laccase preparations.
3. a. Farver, O.; Goldberg, M.; Lancet, D.; Pecht, I. Biochem. Biophys. Res. Comm. **1976**, 73, 494-500.
   b. Farver, O.; Goldberg, M.; Pecht, I. Eur. J. Biochem. **1980**, 104, 71-77.
   c. Farver, O.; Pecht, I. in Copper Proteins **1981**, Spiro, T.G., Ed. (Wiley Interscience: New York) Ch. 4.
4. Solomon, E.I. in Copper Proteins **1981**, Spiro, T.G., Ed. (Wiley Interscience: New York) Ch. 2.
5. Malkin, R.; Malmstrom, B.G.; Vanngard, T. FEBS Lett. **1968**, 1, 50-54.
6. a. Bereman, R.D.; Kosman, D.J. J. Am. Chem. Soc. **1977**, 99, 7322-7325.
   b. Kurland, R.J.; Marwedel, B.J. J. Phys. Chem. **1979**, 83, 1422-1427.
7. The difference in 330 nm extinction coefficient between met T2D and native laccase suggests the T2 Cu(II) may also absorb in this spectral region.
8. Solomon, E.I. Comments Inorg. Chem. **1984**, Sutin, N.S.; Gutlich, P., Eds. (Gordon and Breach Science) in press.

9. Goodman, B.A.; Raynor, J.B. Adv. Inorg. Chem. Radiochem. **1970**, 13, 171.

10. Billy, C.; Haendler, H.M. J. Am. Chem. Soc. **1957**, 79, 1049-1051.

11. Hall, T.P.P.; Hayes, W.; Stevenson, R.W.H.; Wilkens, J. J. Chem. Phys. **1963**, 38, 1977-1984.

12. Morpurgo, L.; Rotilio, G.; Finazzi-Agro, A.; Mondovi, B. Biochim. Biophys. Acta **1974**, 336, 324-328.

13. Winkler, M.E.; Spira, D.J.; LuBien, C.D.; Thamann, T.J.; Solomon, E.I. Biochem. Biophys. Res. Comm. **1982**, 107, 727-734.

14. Morpurgo, L.; Desideri, A.; Rotilio, G. Biochem. J. **1982**, 207, 625-627.

15. Stephens, P.J. Adv. Chem. Phys. **1976**, 35, 197.

16. Byers, W.; Curzon, G.; Garbett, K.; Speyer, B.E.; Young, S.N.; Williams, R.J.P. Biochim. Biophys. Acta **1973**, 310, 38-50. Pseudo first-order calculations assume $K_1 = 10^5\ M^{-1}$ and a 20%/80% distribution of T3 sites.

17. A small amount of low affinity N_3^- at the T2-T3 coupled sites would show MCD intensity only in the 450-500 nm region which would be masked by the overlapping (and opposite at 440 nm) high affinity N_3^- peaks.

18. Allendorf, M.A.; Spira, D.J.; Solomon, E.I. to be published.

19. a. Farver, O.; Frank, P.; Pecht, I. Biochem. Biophys. Res. Comm. **1982**, 108, 273-278.

b. Frank, P.; Farver, O.; Pecht, I. Inorg. Chim. Acta **1984**, 91, 81-88.

20. a. Andreasson, L.E.; Branden, R.; Reinhammar, B. Biochim. Biophys. Acta **1976**, 438, 370-379.

b. Aasa, R.; Branden, R.; Deinum, J.; Malmstrom, B.G.; Reinhammar, B.; Vanngard, T. FEBS Lett. **1976**, 61, 115-119.

c. Andreasson, L.E.; Reinhammar, B. Biochim. Biophys. Acta **1979**, 568, 145-156.

21. The presence of a related signal in T2D laccase[22] is inconsistent with this assignment.

22. Reinhammar, B.; Oda, Y.J. J. Inorg. Biochem. **1979**, 11, 115-127.

ACKNOWLEDGEMENT

Many individuals have contributed to the scientific results which have been presented, as well as to the extremely enjoyable graduate career which I have had.

First, I'd like to express my strongest appreciation to my research advisor, Professor Edward I. Solomon, for teaching me how to most reasonably approach a complex scientific problem, the right way to evaluate scientific results, and the realization that one is rarely limited in what one can spectroscopically learn.

Mark D. Allendorf and Dr. James E. Penner-Hahn are specially acknowledged for their scientific contributions, without which the MCD and x-ray experiments would not have been possible. The all-night experiments, and the intense valuable scientific discussions will always be appreciated.

Dr. Arturo Porras, not only for the resonance Raman experiments but also for numerous helpful and entertaining scientific discussions - regardless how diverse.

Dean Wilcox and Joe Deaton, for all of their cryogenic assistance and useful discussions, but more importantly, for their continual support and good friendship.

Professor Keith Hodgson, for generously providing all of the beam time at SSRL, but moreover, Keith is responsible for having introduced me to academic research, and in particular, the field of bioinorganic chemistry.

Dr. Marjorie Winkler, for teaching me how to "handle" a protein, how to anticipate the "right" experiment before Ed could ask for it, and for being a great friend.

Dr. Cynthia LuBien, for her initial studies of T2D and native laccase, and also Dr. Richard S. Himmelwright, Dr. Nancy C. Eickman, Dr. Yeong Hwang, and Dr. (almost) Dean E. Wilcox for "solving" hemocyanin so that I had something with which to compare laccase.

Dr. Man Sung Co, for his collaboration on the EXAFS studies, and Dr. Britt Hedman for her many all-night runs at SSRL collecting data that "all looked the same".

In addition, Richard Reem and Dr. James Whittaker (as well as Joe, Mark, and Dean) for always being around when I needed a spare hand. I'd further like to thank the other members of the Solomon group Sue Cohen, Dr. Sylvie Desjardins, Mark Fletcher, Lung Shan Kau, Jim Pate, Dr. Kevin Penfield and our secretary Ms. Margaret Helton for their contributions and good times over the past four years.

Kristie, for her amazing support and friendship, and Dr. Britt Hedman (Figures) and Ms. Michelle Pallas (word processing) for their energy and perseverance without which this thesis would not have been submitted on time.

Finally, but most importantly, my fiance Ed, for the love, commitment, and understanding which we will always share.